MAGNETOSTRATIGRAPHY OF EARLY PALAEOGENE SEDIMENTS FROM N.W. EUROPE

by

Jason Richard Ali

A thesis submitted to the University of Southampton for the degree of Doctor of Philosophy

Department of Oceanography
The University
SOUTHAMPTON

December 1988

List of contents

UNIVERSITY OF SOUTHAMPTON

Abstract

FACULTY OF SCIENCE

OCEANOGRAPHY

Doctor of Philosophy

MAGNETOSTRATIGRAPHY OF EARLY PALAEOGENE SEDIMENTS FROM N.W. EUROPE

by Jason Richard Ali

This study presents the results of a detailed magneto-stratigraphic investigation of Early Palaeogene sediments from the NW European Tertiary Basin. Many of the classic sections, including the internationally recognised strato-types for both the Thanetian and Ypresian Stages have been studied. Most of the work has been carried out on the deposits in the London and Belgium Basins, from which the best record of geomagnetic polarity history has been obtained. Work on the succession in the Hampshire Basin has concentrated on clarifying the results from the Whitecliff Bay section, which was proposed by Townsend and Hailwood (1985) as the southern UK Early Eocene magnetostratigraphic type-section.

Preliminary magnetostratigraphic investigations have been carried out on the deposits in the Paris and Danish Basins. Although further work on these deposits is required, the palaeomagnetic results, when combined with the existing biostratigraphic data, enable the sequences to be correlated with the geomagnetic polarity time-scale.

The work of Steurbaut and Nolf (1986) on the calcareous nannoplankton zonation of the Ieper Clay Formation of Belgium has enabled a high resolution definition of the magnetostratigraphy of the Ypresian Stage. From these data, adjustments to the magneto- biostratigraphic time-scale for the Early Eocene may have to be considered.

Acknowledgements

I am particularly grateful to Chris King for his invaluable help with fieldwork, and for the extremely useful discussions as the work progressed. Also to Ernie Hailwood for his supervision and encouragement during this studentship. Claus Heilmann-Clausen was of great help with the fieldwork in Denmark and has kindly allowed me to present unpublished biostratigraphic data. Robert Knox helped with access to the British Geological Survey's borehole material.

Nick Johnston must be thanked for his "on the spot" advice in the palaeomagnetic laboratory, and for his help with proof reading in the final stages of the preparation of this thesis. I would also like to thank the technical staff in the Department of Oceanography for their support.

Norman Hamilton kindly allowed use of facilities in the Geology Department and offered advice at various times during the last three years.

Special mention must be made of Beth Savage who during the last three months has provided support and encouragement which has been "above and beyond the call of duty".

I express my thanks to NERC who funded this research through their PhD studentship scheme.

List of figures

List of tables

Chapter 1 Introduction

1.1 Magnetostratigraphy: an introduction

A sedimentary rock may acquire a magnetic remanence at, or shortly after, deposition due to the detrital grains' magnetic moments aligning parallel to the ambient geomagnetic field. Continued deposition and consolidation traps the remanence; thus a sedimentary sequence may accurately record any variations of the Earth's magnetic field with time. As a consequence of geomagnetic field reversals, which are considered to be instantaneous events occurring synchronously across the globe, the succession may contain a number of normal and reversely magnetised stratigraphic units. (A stratigraphic interval with a uniform polarity is called a magnetozone. The polarity is termed normal if the remanence is directed in the same sense as the present-day Earth's field; reverse if it is in the opposite sense.) In magnetostratigraphic studies it is assumed that the primary remanence was acquired at the time of the rock's formation.

Magnetozone boundaries are important stratigraphic markers since they represent absolute time-planes within a sequence. They provide a stratigraphic framework which is independent of the depositional environment (whereas biostratigraphic correlation schemes may be environmentally dependent). Palaeomagnetic information combined with biostratigraphic data can vastly improve stratigraphic resolution, using magnetozone boundaries as tie-points between two, or more, age-related successions.

1.2 The Earth's magnetic field

Over 99.5% of the Earth's magnetic field is of internal origin (Tarling, 1971). The simplest model of the Earth's magnetic field is a uniformly magnetised sphere with the dipole axis aligned parallel to the Earth's axis of rotation. The present-day field approximates to a geocentric dipole inclined at about 11.5^{o} to the geographic axis (Fig 1.1). This model accounts for 80% of the Earth's total

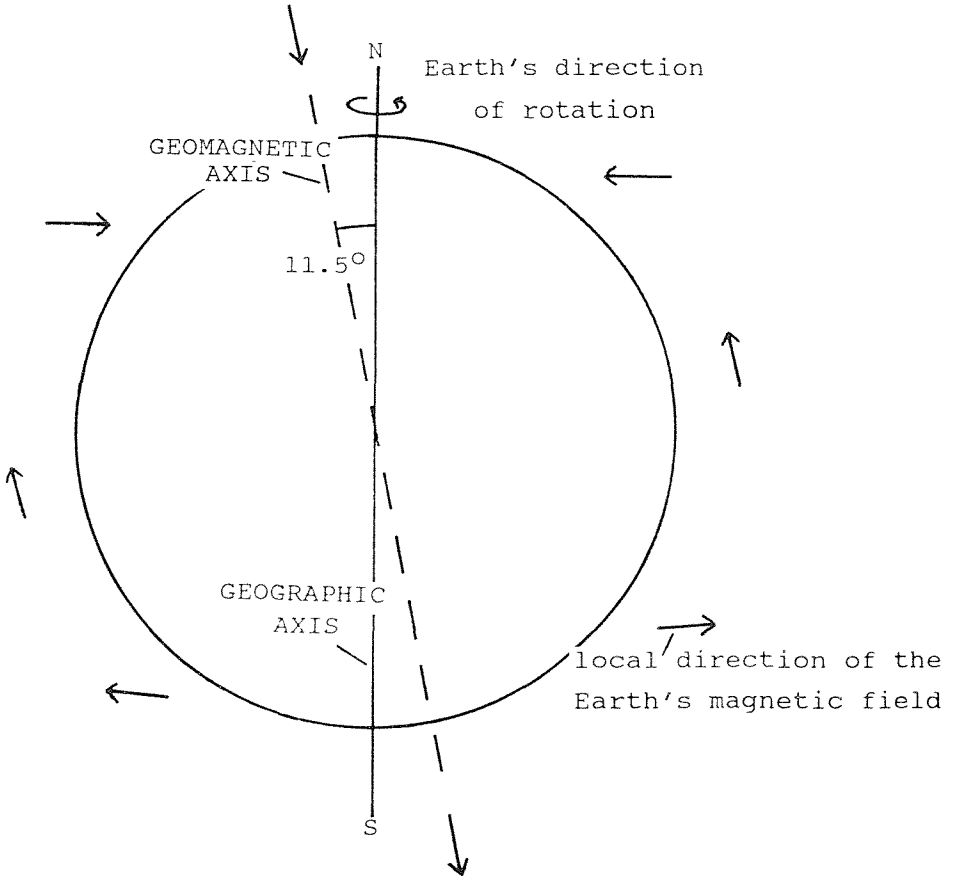

Fig 1.1 Model of the present-day Earth's Magnetic Field.

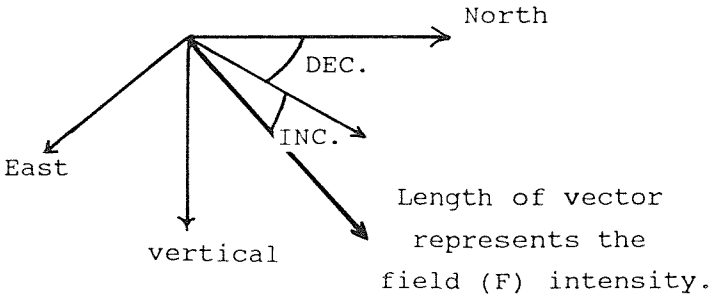

Fig 1.2 Elements of the geomagnetic field.

field; the remaining 20% being attributed to the weaker non-dipole field.

The orientation of the dipole axis varies with time, but when averaged over periods of 10^4 to 10^5 years it is believed to coincide with the axis of rotation (Opdyke and Henry, 1969). With such a model, the inclination of the magnetic field (I) is related to the latitude of the site (L) by the equation:

$$\tan I = 2 \tan L.$$

Apparent shallowing of the magnetic inclination for rocks of Quaternary and Late Tertiary age in the northern hemisphere, resulting in the mean pole position plotting on the opposite side of the geographic pole, was first reported by Wilson and Ade-Hall (1970). This property, termed "far-sidedness", could be conveniently modelled by an offset of the magnetic dipole axis some 300km northwards from the centre of the Earth along the axis of rotation (Wilson, 1971).

Wilson and McElhinny (1974) demonstrated a tendency for increased offset with geological age (c. 550km offset averaged between 7 and 25 Ma). Hailwood (1977) looked in detail at results from Early Tertiary sites as far apart as North America and the central Soviet Union. Correcting for plate motions, using DSDP palaeoequator determinations and the Icelandic Hot-Spot as fixed reference points, a possible offset of around 1000km was postulated. However, for magnetostratigraphic studies a simple time-averaged geocentric dipole model is assumed.

1.3 Elements of the geomagnetic field

The direction and strength of the Earth's magnetic field may be expressed in terms of the declination, inclination and intensity (Fig 1.2). The declination (D) is the angular deviation from true North measured clockwise in a horizontal plane. The inclination (I) is the dip of the total field vector measured from the horizontal plane, with a downward dip having a positive sign, and an upward dip having a negative sign.

S.I. units are used throughout this study. The intensity of the Earth's field is expressed in tesla (T) and commonly has a value of about $50*10^{-6}$T. The magnetisation of a rock is expressed in terms of declination (D), inclination (I) and intensity (J), where J is measured in A/m, with typical values of 1-10mA/m.

1.4 Variations in the Earth's magnetic field with time

Periodic changes in the direction and strength of the Earth's magnetic field occur on a variety of scales from seconds (micropulsations) to 10^7 years. Two types of behaviour are of particular importance to the palaeomagnetist, namely secular variations and polarity reversals.

1.4.1 Secular variation

At any one time, the Earth's dipole axis may be aligned at some angle (no more than about 20^{o}) to the Earth's rotation axis. The dipole axis may also "drift" relative to the rotational axis through time. This behaviour, called Geomagnetic Secular Variation, typically occurs on a timescale of about 10^2 to 10^3 years. Evidence is based on observatory measurements over the last few centuries, archaeomagnetic studies (for the last 8000 years) and palaeomagnetic data (up to the last 15000 years). The secular variation pattern is rather complex with no obvious long-term cyclic pattern; however stable remanence data can be used for archaeo-palaeomagnetic correlations. This is achieved by matching the large swings in the declination and inclination in, say, a borehole core through lake sediments with swings observed in similar cores elsewhere (see Tarling, 1983:p 175). Cox (1970) proposed a model in which secular variation was caused by "dipole-wobble" combined with non-dipole fluctuations. (Palaeomagnetic data from Tertiary and pre-Tertiary igneous rocks were used to test the model, for example by Brock (1971).)

Most palaeomagnetic studies aim to average-out the effects of secular variation by combining data from

specimens magnetised over a sufficient period of time for the geocentric axial dipole model to be valid.

1.4.2 Magnetic polarity reversals

The geological record contains overwhelming evidence that the geomagnetic field has periodically reversed its polarity. The best evidence comes from the patterns of marine magnetic anomalies, which were used by Vine and Matthews (1963) to support the theory of sea-floor spreading from ocean-ridge axes. Polarity reversals occur globally and because the field transition is thought to take about 1000 years (Ninkovitch et al 1966) they can be considered as geologically "instantaneous" events. It is thought that the field intensity decreases for about 10^4 years prior to the reversal before increasing over a similar period afterwards (reviewed by Tarling, 1983). After a reversal the polarity commonly remains constant for a period varying from 10^5 to 10^6 years. The duration between polarity changes during the last 80 Ma has been extremely varied, and at present it is not posssible to predict future field reversal behaviour.

1.5 The magnetic polarity time-scale

Geomagnetic polarity history is recorded in two independent mediums. The first is the pattern of marine magnetic anomalies imprinted onto laterally accreted oceanic crust (Vine and Matthews, 1963). The second is vertically accreted sedimentary and volcanic rocks (during the early 1960's work on Late Neogene volcanic sequences first established correlateable magnetozones). Utilising the biostratigraphic record it is possible to correlate the two records, and to define absolute ages by correlation with radiometrically dated rocks.

Heirtzler et al (1968) constructed the first "standard" polarity time-scale which extended back from the present to the Upper Cretaceous (Fig 1.3). The scale was based on the pattern of marine magnetic anomalies in the South Atlantic (Vema track V-20). The older boundary of anomaly 2A was

used as the calibration point and dated at 3.35 Ma (based on the radiometrically dated anomaly scale of Cox et al (1965). A constant spreading rate of 1.9 cm/year was used to extrapolate the scale back to Chron C32N. (A magnetic chron represents the period of time between the younger ends of successive normal polarity intervals. Chron C32N therefore represents the normal polarity portion of Chron 32; which is associated with anomaly 32 in the marine magnetic anomaly profile). Although based on a single tie-point the older anomalies were dated with a maximum error of some 20% when compared with more recent studies (Tarling (1983).

Since the work of Heirtzler et al (1968), numerous revisions have been made to the Cenozoic polarity time-scale. The more recent studies date a number of anomalies and interpolate the age of intermediate anomalies, assuming a constant rate of ocean-floor spreading between successive dated anomalies. The polarity time-scale used in this study was presented by Berggren et al (1985). It is similar to that of La Brecque et al (1977) and uses six tie-points to date the younger ends of Chrons C2.1N, C5N, C12N, C13N, C21N and C34N. This polarity timescale is discussed in more detail in Chapter 3.

It must be noted, however, that other workers such as Curry (1985) and Odin and Curry (1985), have questioned the reliabilty of magnetostratigraphic scales based on inter-polations between so few tie-points. They argue that the time-scale should be based on the full use of all available radiometric data (both high and low temperature) and that magnetostratigraphic data be used only for smaller inter-polations. However, Hailwood (in press) presents a very strong case supporting the idea that ocean spreading has been effectively constant between the dated anomalies for the transect lines on which the magnetostratigraphic scales are based. Arguments concerning the validity of the assumption of a constant rate of sea-floor spreading for periods of the order of 10 m.y. will certainly continue.

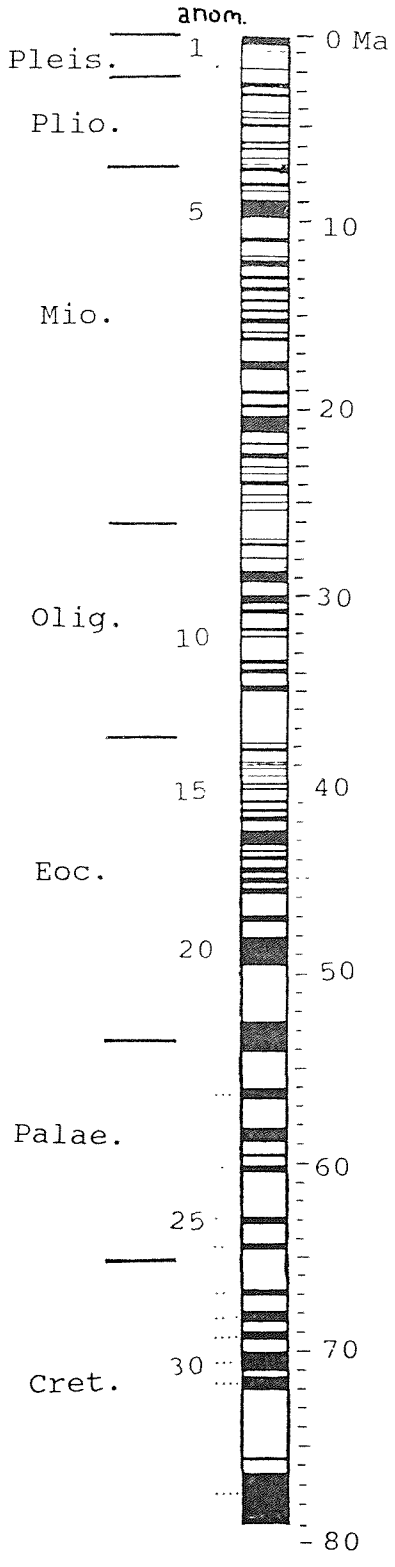

Fig 1.3 The geomagnetic polarity time-scale of Heirtzler et al (1968).

1.6 Magnetisation of sediments

Virtually all rocks exhibit ferromagnetic properties due to the presence of magnetic minerals. In the case of sediments, they should be regarded as a weak "solution" of ferromagnetic particles dispersed within a predominantly paramagnetic matrix. Tarling (1983) and O'Reilly (1984) discuss in detail the various magnetic minerals found in most rocks. The most important ferromagnetic minerals in rocks are the iron-titanium oxides of which there are two principal series.

1.6.1 The titanomagnetite series

The titanomagnetites form a solid-solution series with magnetite (Fe_3O_4) and ulvospinel (Fe_2TiO_4) as end-members. The magnetic properties are strongly dependent on grain-size, composition, and crystal lattice impurities; but this series becomes strongly magnetic towards the magnetite end-member. Maghemite (Fe_2O_3) has a cubic structure and properties similar to magnetite, but has the chemical composition of hematite. Maghemitisation may occur as result of the low temperature oxidation of magnetite (Tarling, 1983).

1.6.2 The titanohematite series

The titanohematites form a solid solution series with hematite (Fe_2O_3) and ilmenite ($FeTiO_3$) as end-members. The series has a rhombohedral (corundum) structure. Again the magnetic properties are dependent on grain-size, composition and crystal lattice impurities, but are weak when compared with those of magnetite and maghemite.

Other important magnetic minerals include the iron-sulphides (pyrrhotite), iron-hydroxides (goethite and lepidocrocite), and iron-carbonates (siderite). These minerals are either paramagnetic or only very weakly magnetic. However, they may provide an important source of iron oxides if they are broken-down through weathering, diagenesis or metamorphism.

1.6.3 Detrital Remanent Magnetism

Sedimentary rocks are commonly formed from detrital particles, which may include magnetic minerals, derived from pre-existing igneous, metamorphic or sedimentary rocks. The particles may possess a magnetic moment and rotationally align parallel to the geomagnetic field as they pass down through the water-column. Preservation of this alignment after deposition results in a Depositional Detrital Remanent Magnetisation (DDRM). Laboratory studies have shown that such a remanence may be subject to three different types of "error":

1. "Inclination errors", which cause a shallowing of the inclination from that of the ambient field due to a gravitational couple acting on the magnetic grains during deposition (King, 1955). This "error" may be as great as 20^{o}.

2. "Bedding errors" occur when magnetic grains are deposited on an inclined surface. These may be as great as 25^{o} (King, 1955; Rees, 1966).

3. "Rotation errors" arise from hydrodynamic couples acting when magnetic grains are deposited in a moving fluid (Rees, 1961).

The observed values of depositional magnetisation "errors" for natural sediments appear to be much less than for laboratory deposited sediments. This is attributed to the acquisition of a Post-Depositional Remanent Magnetisation (PDRM) by the natural sediments due to the realignment of interstitial magnetic grains within water-filled pore spaces. Irving and Major (1964) first reported PDRM in laboratory deposited sands. Lovlie (1974) suggests that the acquisition of a PDRM may be dependent upon the consolidation rate, which in turn is a function of the accumulation rate. The time-lag between initial deposition and the acquisition of the PDRM is uncertain. Estimates vary between days (Barton et al, 1980) and tens of years (Suttill, 1980). Geologically this represents a very short time period; consequently it corresponds with only a short interval in a sedimentary column.

1.6.4 Chemical remanent magnetism

A sedimentary rock may also acquire a Chemical Remanent Magnetisation (CRM). As a magnetic crystal grows after its nucleation, it behaves initially in a paramagnetic fashion. Beyond a critical blocking diameter it retains a remanence parallel to the ambient field vector. Continued crystal growth results in an increased relaxation time, until it reaches dimensions where multi-domain behaviour commences. The critical dimensions for the various physical states of the main magnetic minerals are discussed by O'Reilly (1976).

CRM's can be produced during the formation of red beds (Collinson, 1965 and 1967). They can also be produced during the consolidation of other sediments, e.g. the dehydration of iron-hydroxides to hematite (Strangway et al, 1968). Chemical changes may occur in a sedimentary rock any time after deposition and so the Natural Remanent Magnetisation (NRM) may be the combination of a DRM and a CRM. (The NRM represents the vector sum of all magnetisations within a rock.)

If a specimen contains a high proportion of low coercivity grains, the NRM may be dominated by a Viscous Remanent Magnetisation (VRM). With such specimens, the magnetic moments of the low coercivity grains rapidly relax parallel to the ambient field vector at the sampling locality. However, the VRM is readily removed in low demagnetising fields.

Most palaeomagnetic studies are concerned with identifying the primary remanence component acquired by a rock at, or shortly after, the time of formation. Under favourable circumstances, secondary components can be systematically removed from a specimen, thus revealing the primary remanence. The basic theory and techniques used to achieve this objective are discussed in the following chapter.

Chapter 2 Sampling procedures and palaeomagnetic techniques

2.1 Sampling Techniques

Samples were obtained using the technique described by Townsend (1982). Almost all of the sections were sampled at approximately 1m intervals (except some of the Danish sections which were sampled at 0.15m intervals) with normally two samples being taken from each stratigraphic level (site). The outcrop was first excavated to remove any weathered surface material. Thin-walled copper tubes, with an internal diameter of 2.5cm were then carefully hammered into the outcrop (to protect the end of the tube during insertion a wooden block was held over the "hammer-end"). The tubes could then be oriented (azimuth and "plunge") by mounting a compass/dipmeter table to the upper end of the copper tube (Fig 2.1). An orientation line was then marked onto the tube before removal from the outcrop. Clay mini-cores were removed from the copper tubing in the laboratory and the orientation line on the tube was then transferred to the sample. Standard cylindrical specimens, 2.3cm in length, were then cut from each sample, and sealed in "Clingfilm" to prevent drying-out during subsequent laboratory analysis.

Two methods were employed to sample the borehole cores. C. King sampled two boreholes from Sheppey, Kent, by inserting copper tubes into the split core as shown in Fig 2.2. A horizontal line (parallel to the bedding-plane) was then marked onto the tube. The samples were then extruded from the copper tube and the reference line was transferred to the sample before it was cut down to specimen size. The specimen "X-axis" was drawn perpendicular to the horizontal line, across the end of the cylinder in an uphole direction.

The second method made use of non-magnetic, thin-walled palaeomagnetic sampling boxes (cubes; with an internal volume of $8cm^3$). Each box has an arrow marked onto it, which acts as the specimen's orientation line ("X-axis").

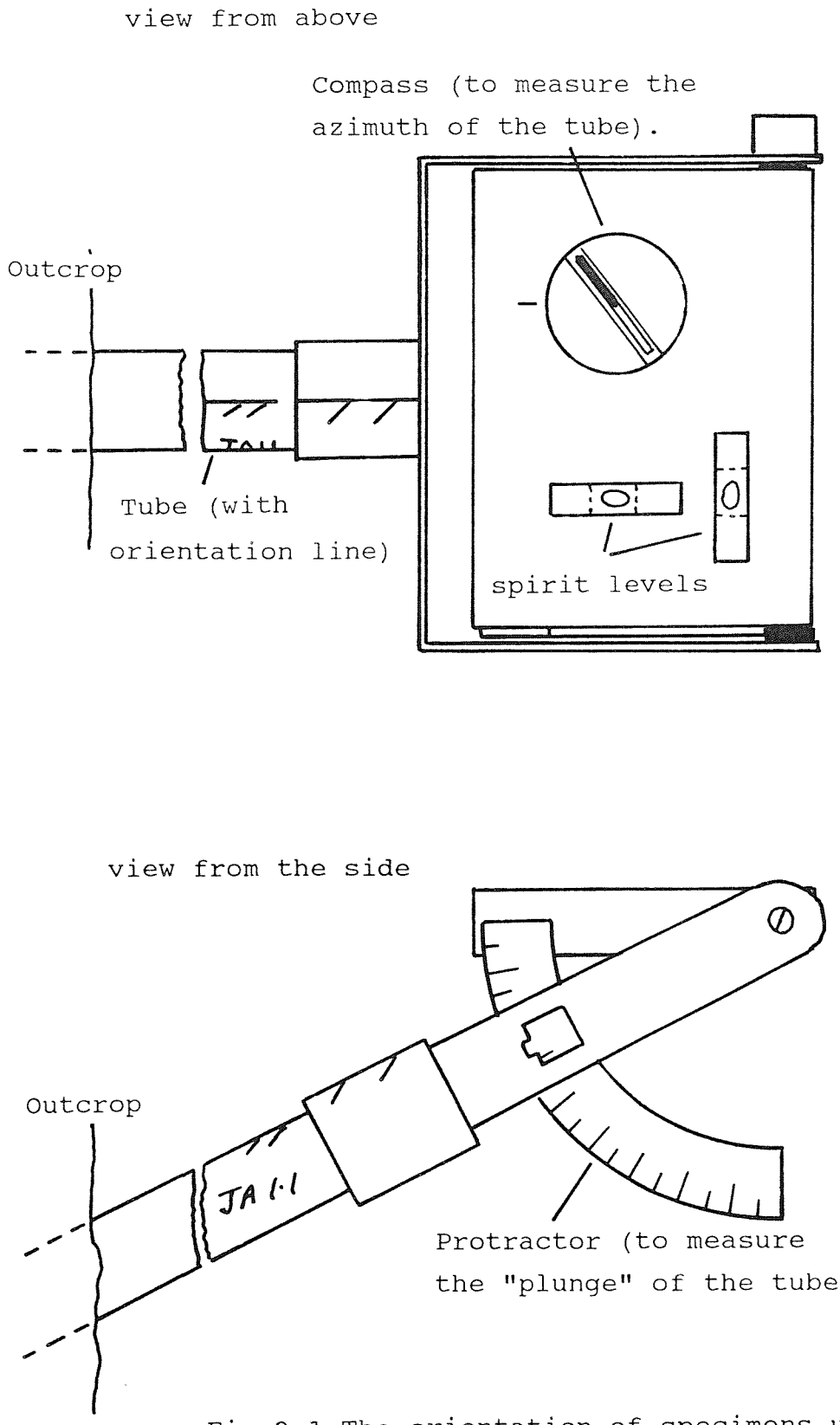

Fig 2.1 The orientation of specimens using the copper tube method of sampling.

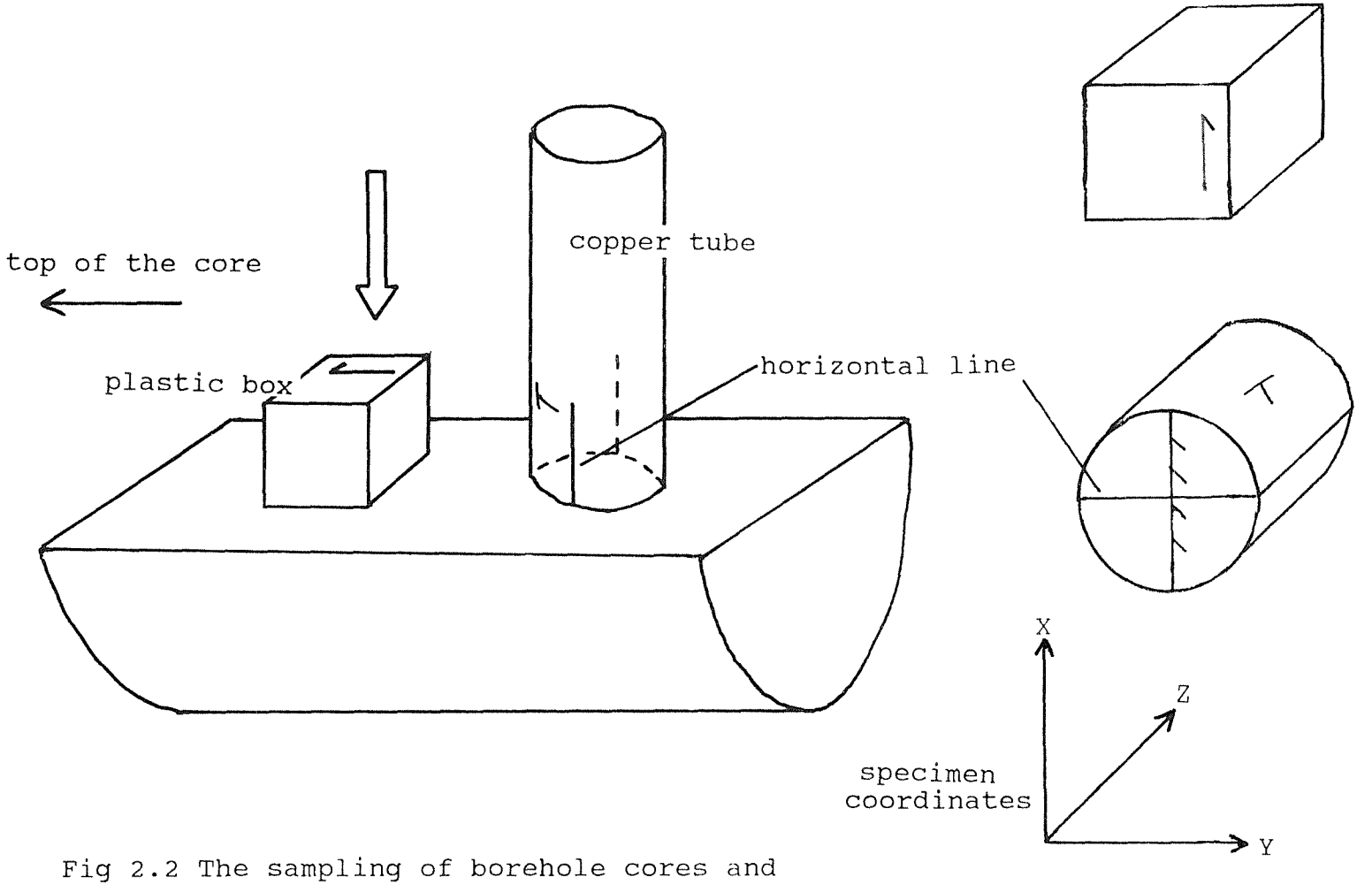

Fig 2.2 The sampling of borehole cores and the specimen coordinate framework.

The box is laid onto the split core surface with the arrow pointing "up-hole", and is then carefully pressed into the core. The box (full of sediment) is then removed from the core using scalpels and spatulas. A lid is then fitted to the box, which is then sealed using non-magnetic tape to prevent the sediment from drying out.

2.2 Remanence measurement

The direction and intensity of the magnetic remanence of each specimen was measured using one of two types of magnetometer. Approximately 85% of the specimens were measured using a "Molspin" spinner magnetometer similar to that described by Molyneux (1971), linked to a BBC micro-computer. The magnetometer had a noise level typically in the range 0.02-0.045mA/m, and was used for specimens with intensities >0.3mA/m. Specimens were measured between one and four times in order to accurately determine the magnetisation. The Fisher-mean direction (Fisher, 1955) and average intensity were recorded.

The cryogenic magnetometer was used for the more weakly magnetic specimens (about 15% of the total). The instrument can be reliably used for specimens with intensities greater than 0.03mA/m. The basic principles involved in the use of this instrument to measure the magnetic remanence of a specimen is described by Collinson (1983). Two sense coils are used to detect the specimen's magnetisation. One coil is used to measure the vertical component of the specimen's magnetisation, whilst a second coil detects the horizontal component. In order to measure the components along all three orthogonal axes, the specimen is rotated through 90^{o} increments in the horizontal plane within the sense region to measure the "X" and "Y" axes (both positive and negative), as well as measuring the "Z" axis four times in a positive sense. This method is thought to be fairly reliable, although it assumes that specimens are magnetically homogeneous. There is an option on the system that allows one to manually invert the specimen (so as to measure the "Z-axis" in a negative sense), but is rarely

utilised as the system is really designed to keep specimens in field free space once the measurement/demagnetisation cycle begins. A Hewlett Packard microcomputer controls the operation of the cryogenic magnetometer, the demagnetising system (see Section 2.5) and data acquisition.

The remanence direction, specified in terms of declination (D), and inclination (I) is measured relative to the specimen (Fig 2.2) as follows:

$$D = \tan^{-1}(Y/X) \text{ and } I = \tan^{-1}(Z/H)$$

$$(\text{where } H = (X^2+Y^2)^{0.5})$$

The intensity of magnetisation (J) is given by:

$$J = (X^2+Y^2+Z^2)^{0.5}$$

where X, Y and Z are the components of the magnetisation along the three principal orthogonal axes.

2.3 The demagnetisation of specimens

Magnetostratigraphy (and indeed most other sub-branches of palaeomagnetism) requires the identification of the primary (at the time of formation) remanence direction. A specimen may acquire secondary magnetisations any time after formation; for example a VRM, CRM, or both. Incremental demagnetisation allows the detailed investigation of the specimen's magnetisation history. The process aims to progressively remove less stable components of magnetisation and to isolate the component of stable remanence (assumed to be of primary origin). The basic principle behind the demagnetisation process is illustrated in Fig 2.3.

2.4 Alternating field demagnetisation

One technique used to remove less stable magnetisations is to subject a specimen to progressive alternating field (AF) demagnetisation. The technique, originally developed for palaeomagnetic work by As and Zidjerveld (1958), is now routine to most studies. The process effectively randomises the magnetisation of all grains with coercivities less than the peak applied field. After the NRM measurement, a specimen is demagnetised at, say, 5mT and the remanence is

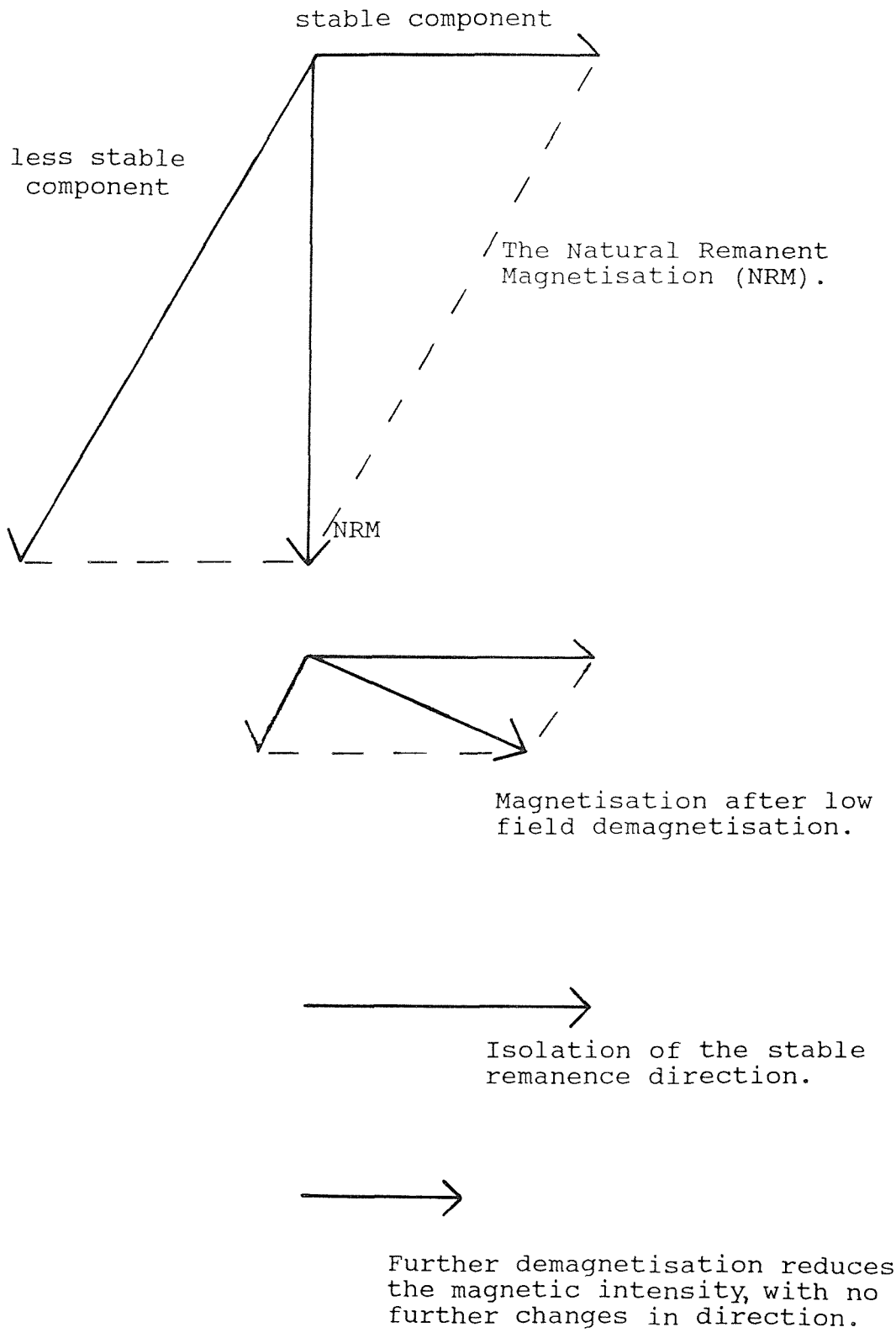

Fig 2.3 The principle of demagnetisation in isolating the stable remanence of a rock specimen.

then remeasured. (For this study the process was repeated in fields of 10, 15, 20, 25, 30, 40, and occasionally 50 and 60mT.) The resulting changes in direction and intensity of the magnetisation vector allow, under favourable circumstances, unequivocal determination of the polarity of the stable magnetisation of the specimen.

Thermal demagnetisation (see Collinson, 1983) could not be used, due to the drying-out and subsequent disaggregation of the specimen.

2.5 AF demagnetisation systems

2.5.1 "3-axis stationary" system

The "3-axis stationary" system is mounted above the cryogenic magnetometer. Two pairs of demagnetising coils surrounded by a double mu-metal shield form the basic system (Fig 2.4). The whole operation is controlled by a Hewlett Packard microcomputer linked to a power amplifier, and two stepper-motors, used to position the specimen in the demagnetising coils.

The specimen is lowered, in a holder (Mylar), into the the upper AF coil and the "X-axis" is demagnetised (the field is ramped up to the required setting before smoothly decaying back to zero). The stepper-motors then rotate the specimen through 90^{o} about the "Z-axis", and the "Y-axis" is then demagnetised in the same way. The stepper motors then rotate the specimen through 270^{o}, and lower the specimen so that it is positioned in the centre of the lower AF coil, and the "Z-axis" is then demagnetised. The specimen is then lowered into the cryogenic magnetometer where the remanence is measured. The system can theoretically operate up to about 40mT, but increasing "magnetic noise" means that the system is used to a maximum of between 30 and 35mT. Further work is required on the system to enable "clean" demagnetisations up to at least 50mT.

2.5.2 Rotating field system

The rotating field system, first developed by Noel and Molyneux (1975), is described by Collinson (1983). A

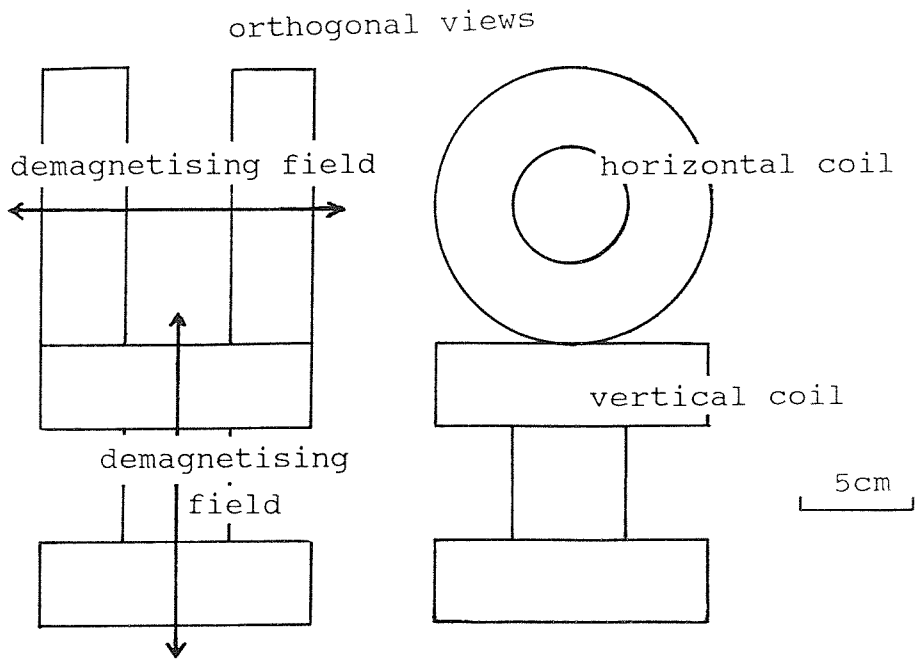

Fig 2.4 The "3-axis stationary" demagnetisation system.

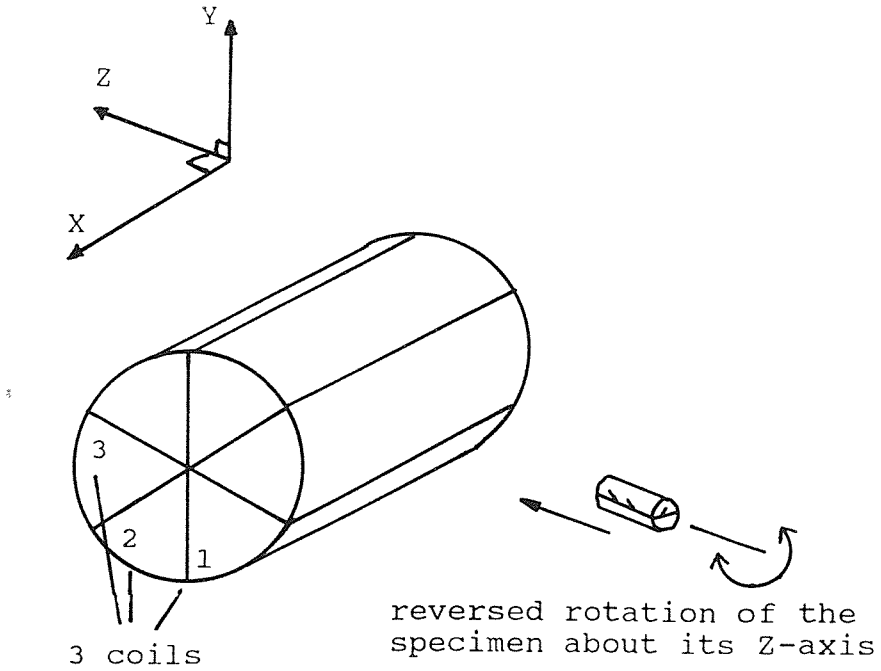

Fig 2.5 The rotating field demagnetisation system.

rotating magnetic field is generated in a 3 coil system (Fig 2.5) by feeding each coil with an alternating current of relative phase difference of $2\pi/3$. A specimen in the centre of the coil will experience a demagnetising field rotating within the "Z-X plane". Rotating the specimen from 0^{o} to 360^{o} and back to 0^{o} about the "Z-axis" demagnetises all directions in the specimen. To avoid generating spurious components, the magnetic field and specimen are rotated at 50 and 1Hz respectively. The field is set manually using a hand variac and smoothly ramped down by a motor-driven three-phase variac. The demagnetisation coil system is contained within a double mu-metal shield which reduces the ambient field to around $0.2*10^{-6}$T

The system proved useful in demagnetising specimens up to 30mT, utilising "double demagnetisation" (Section 2.6) for fields of 20mT and above. Above 30mT the demagnetisation behaviour became increasingly erratic. Mechanical problems involved in designing a clutch system to smoothly reverse the rotation of the specimen probably account for this. The system was used on about 3-4% of specimens during the early part of this study, but has since been dismantled to make space for a commercially built tumbler demagnetiser.

2.5.3 Tumbling systems

The most widely used AF demagnetisation technique is to tumble a specimen at the centre of a demagnetising coil. The alternating field is generated along the axis of the coil and the specimen is tumbled about two or more perpendicular axes. Tumbling presents the specimen in as many different orientations as possible to the demagnetising field, and in doing so also reduces the effects of a residual field acting on the specimen. Two different sytems have been used in this study

2.5.3.1 The "Highmoor" system

The "Highmoor" tumbler system in the Geology Department at Southampton University has been operated reliably for many years now. About 25 to 30% of the specimens in this study were demagnetised on this system. Residual fields are cancelled using three pairs of mutually perpendicular Helmholtz coils surrounding the demagnetising coil. Reliable results were obtained in fields up to 50mT, however, Rotational Remanent Magnetisations (Section 2.6) were generated above 20mT.

2.5.3.2 The "Molspin" system

The "Molspin" system was installed in the Oceanography Department at Southampton University in the summer of 1987. It has proved to be the best system used in this study for the following reasons:

1. Rapid demagnetisation (because the AF signal is 800Hz allowing a very fast decay rate).
2. It avoids generating RRM's by reversing (very smoothly) the tumbling direction every 2 rotations about the vertical axis.
3. It produces "clean" fields up to at least 70mT (and probably up to 100mT, although it has not been tested to these levels).

Over 30% of the specimens in this study were processed on this system.

2.6 Rotational Remanent Magnetism (RRM)

Wilson and Lomax (1972) reported that a spurious magnetisation (RRM) could be introduced into a specimen if it were rotated during the decay of an alternating field. More recent investigations have been carried out by Brock and Iles (1974), R.W. Stephenson (1976) and A.Stephenson (1980a and b). The RRM is generated along the innermost rotation axis (usually anti-parallel to the rotation vector) of the tumbler (Fig 2.6).

The effects of RRM can be removed by repeating each demagnetising run at the same peak AF, but with the

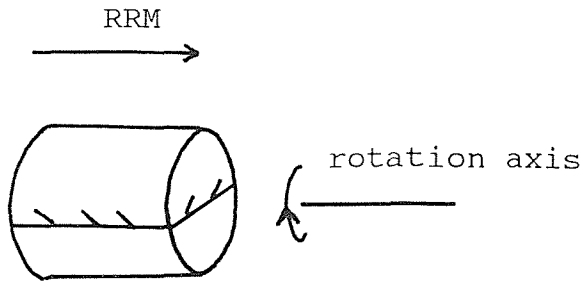

The generation of a RRM.

first demagnetisation generates RRM

second demagnetisation (at the same field, but with the specimen inverted) generates RRM in opposite sense

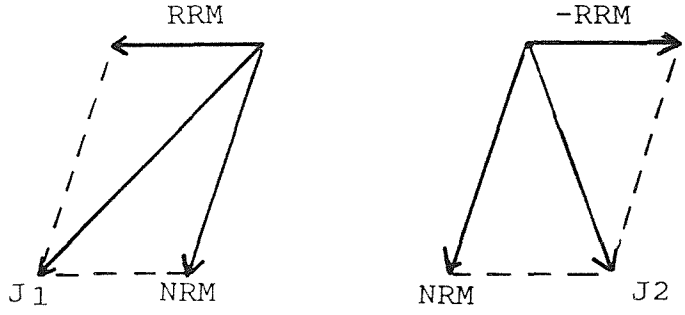

J1=(NRM+RRM)

J2=(NRM-RRM)

J1+J2=2NRM

The removal of the RRM using "double demagnetisation".

Fig 2.6 Rotational Remanent Magnetisation (RRM).

specimen in the reverse orientation. The RRM generated in the second run is thus equal and opposite to that in the first, and can be subtracted out by averaging the two palaeomagnetic vectors.

The effect is not present in all specimens, nor all tumbler sytems, although it does occur when using the "Highmoor" system.

2.7 Presentation of demagnetisation data

Before the remanence data are analysed, field and/or bedding corrections are applied to the specimen's declination and inclination values in order to relate the magnetisation to the palaeo-North and -vertical. None of the borehole cores that were sampled for this study were oriented relative to North during drilling, and so polarity determinations from these specimens are based on the magnetic inclination angles only. All of the borehole specimens were sampled in the manner described in Section 2.1, and so the standard Strike=270^{o} and Dip=90^{o} bedding correction has been applied.

For each specimen, data for each demagnetisation step are entered into an HP86 microcomputer, which processes the results and produces a three diagram graphic output, e.g. Fig 2.7.

A stereographic projection (Schmidt equal area net) is shown in the upper left-hand side of the diagram. The direction of magnetisation is plotted in the conventional way, with solid and open circles representing positive and negative inclination angles respectively. A line joins the different step directions, tracing out the progressive changes in the remanence with the applied field.

A plot of intensity decrease versus demagnetisation field is shown in the lower left-hand corner. The intensities are normalised against the NRM value.

A vector-end point plot is shown on the right-hand side of the diagram. This form of diagram, which is used to examine vector data, was first applied to palaeomagnetic studies by As (1960). It represents the direction and

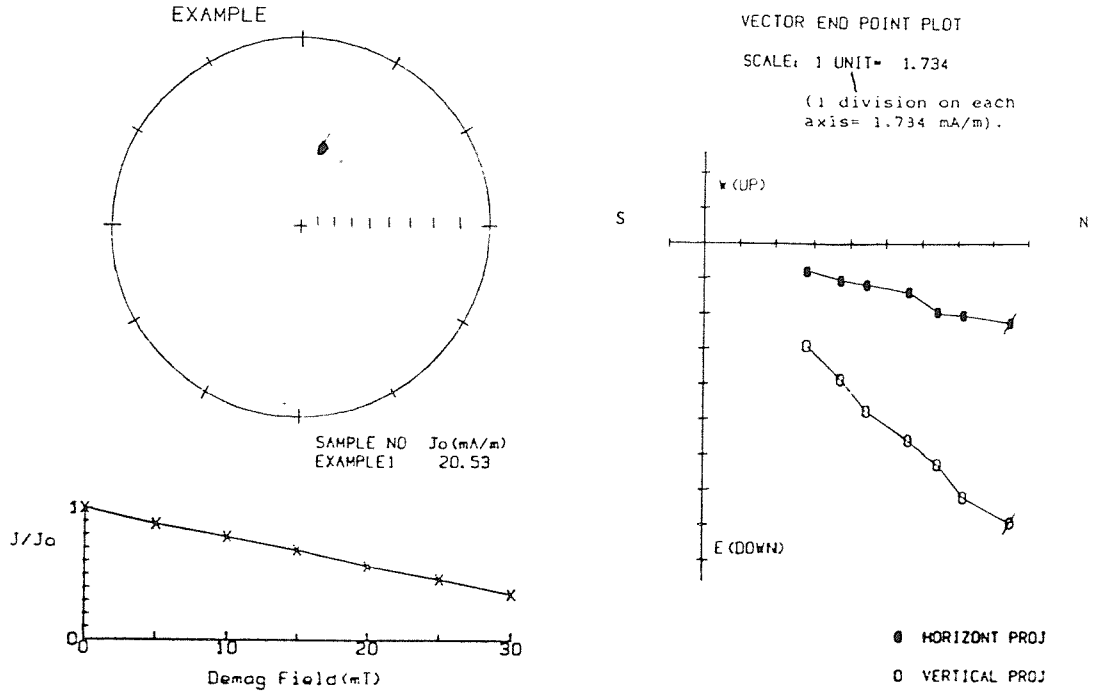

Fig 2.7 A standard demagnetisation plot. A stereographic projection is shown at the upper left hand side of the diagram (North is at "twelve O'clock"). The direction of magnetisation, for each demagnetisation step, is plotted in the conventional way, with solid and open circles representing positive and negative inclination angles respectively. A line joins the different step directions, tracing out the progressive changes in the remanence with the applied field. The NRM direction is marked by a slash.

A plot of intensity versus demagnetisation field is shown at the lower left-hand corner. The intensities (J) are normalised against the NRM value (J_o).

A vector-end point plot is shown at the right-hand side of the diagram. It represents the direction and intensity, projected on to the horizontal and vertical planes, of the magnetisation component which has been removed between successive demagnetisation steps. When the effects of low coercivity (? secondary) magnetisations have been totally "cleaned" from a specimen, the components removed at higher fields will trace a straight-line path towards the origin of the plot in both planes.

intensity, in both the horizontal and vertical planes, of the magnetisation component which has been removed between successive demagnetisation steps.

2.8 The classification of demagnetisation data

The demagnetisation data for each specimen (based on the computer plots described in the preceding Section) are assigned a reliability index. (The reliability index for each specimen is included in the Appendix.) Specimens are classified in the following way:

2.8.1 Stable end point directions

A stable end point (SEP) direction is obtained during the demagnetisation process, when the effects of any low coercivity magnetisations are completely removed from the specimen (e.g Fig 2.8). The specimen's remanence direction remains unchanged above a particular demagnetisation step. Beyond this step, the only property affected by the continued demagnetisation is the steady decay of the intensity.

2.8.2 "Trend" directions

Specimens included in this class do not show an SEP, indicating that the effects of low coercivity magnetisations have not been completely removed from the specimen. The data from "trending" specimens can still be reliably used in polarity determinations (if the "trend" is toward a normal or reverse polarity direction). However, with "trending" specimens it is not possible to use the direction for, say, evaluating palaeomagnetic pole positions. Fig 2.9 shows a specimen trending towards a reverse polarity.

2.8.3 "Erratic" directions

The term "Erratic" direction is used to classify the remanence data which show great swings in both the direction and intensity. This is most commonly encountered when the specimens are weakly magnetic, and the signal from the specimen measured by the magnetometer is greatly

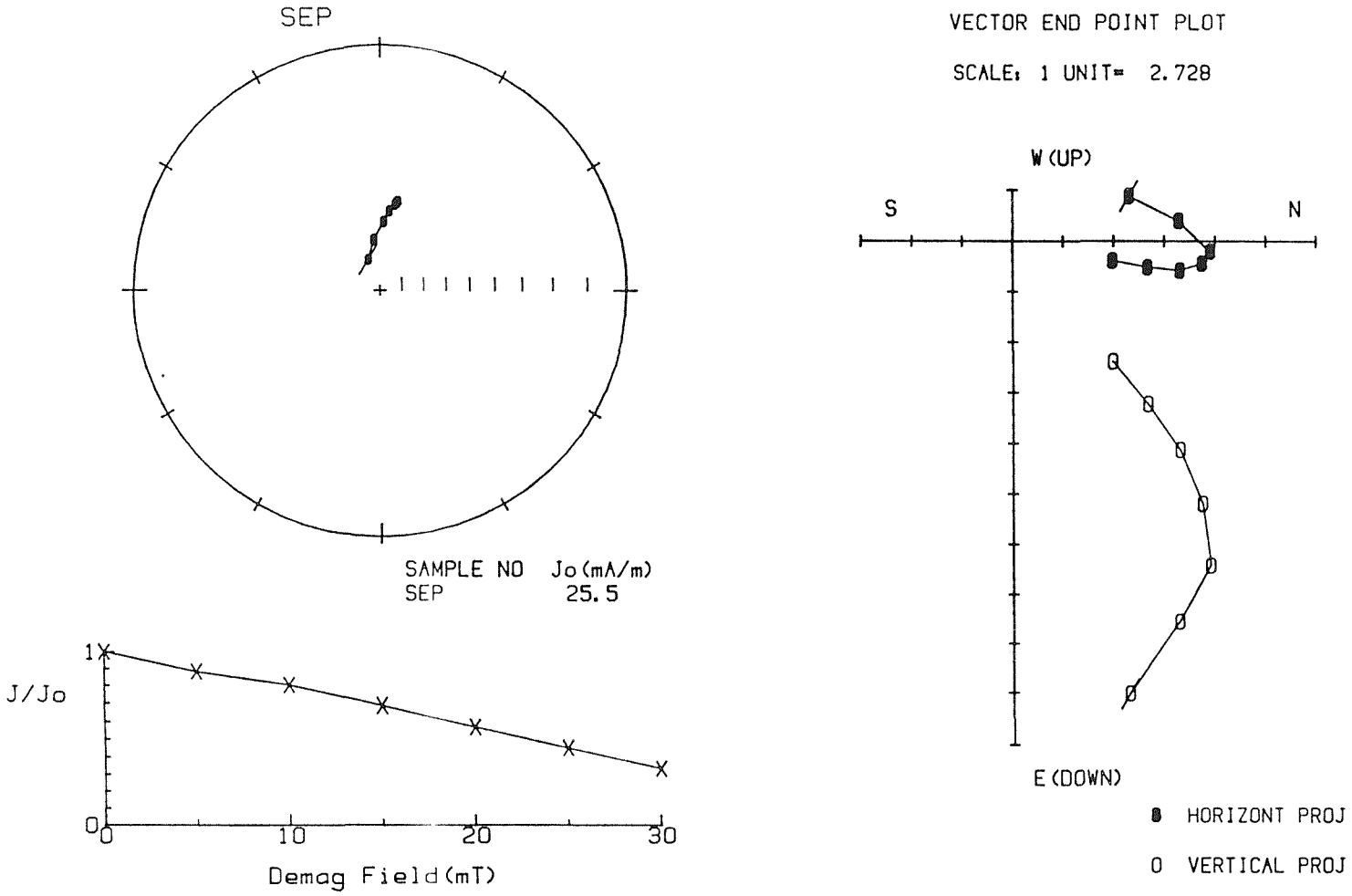

Fig 2.8 A demagnetisation plot illustrating a normal polarity SEP. At the 25mT step the effects of all low coercivity magnetisations have been removed, and the remanence direction (Dec.= 11^{o} Inc.= 50.0^{o}) remains unchanged with further demagnetisation.

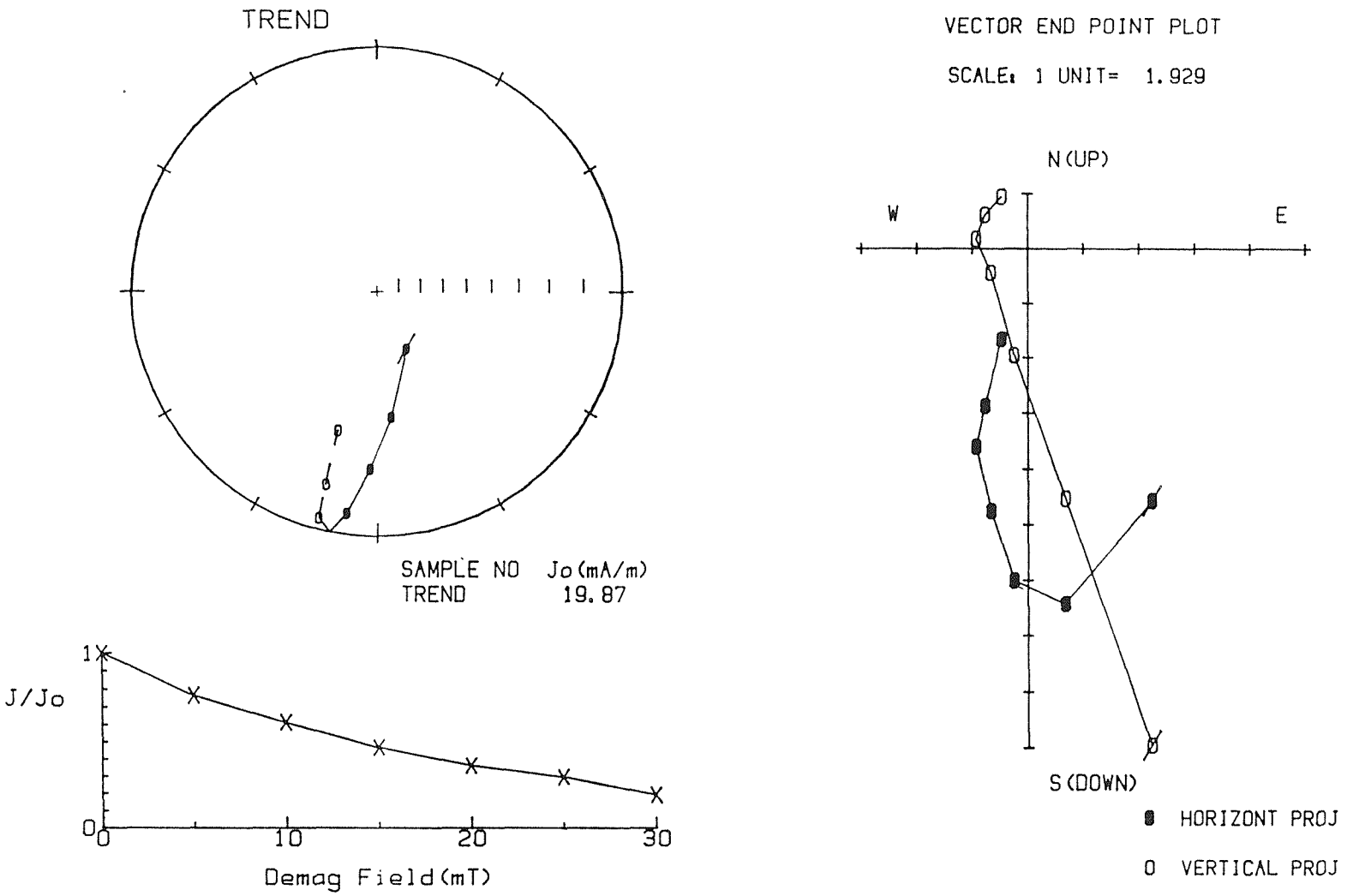

Fig 2.9 A demagnetisation plot illustrating a reverse polarity "trend". Although the specimen's intensity has fallen to one-third of the NRM at 30mT, an SEP is not reached. However, the data on this plot can be reliably used to define a reverse polarity "trend" direction.

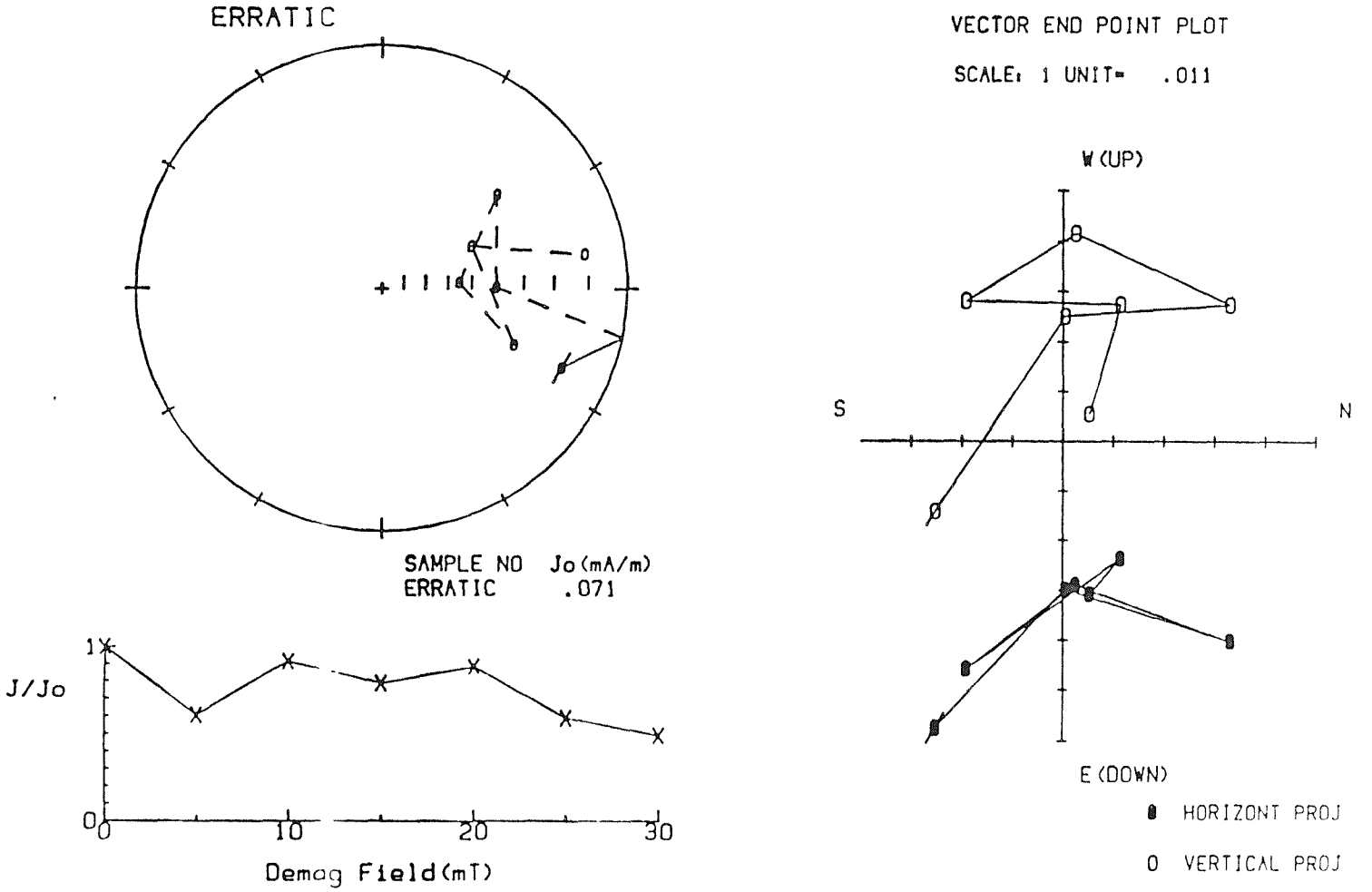

Fig 2.10 A demagnetisation plot illustrating "erratic" behaviour. The specimen is very weakly magnetic, and so the large jumps in direction between succesive steps probably represent the effects of instrumental noise superimposed on the palaeomagnetic signal. It is possible to use the directions from "erratic" specimens for polarity evaluations, however in most cases these specimens are classified as "indeterminate" polarity.

influenced by instrumental "noise". Fig 2.10 is an example of a specimen with an "erratic" demagnetisation.

2.9 Classification of polarities

A normal polarity direction is one which has a northerly declination and positive (downward) inclination. A reverse polarity direction has a southerly declination and a negative (upward) inclination. Indeterminate polarities also occur, but are rather infrequent (in some cases they may represent anomalous excursions of the magnetic field over very short periods of geological time).

Specimens may have a normal (or reverse, or indeterminate) polarity based on a SEP, "trend" or "erratic" direction. However, virtually all of the specimens in this study produced normal or reverse polarities based on SEP or "trend" directions.

2.10 Techniques used to examine the magnetic mineralogy

Extra information concerned with the magnetic mineralogy can be extracted from specimens using a number of non-desructive magnetic techniques. Important stratigraphic/magnetic relationships may become apparent when data for each parameter are drawn as downhole plots. The effects of recent weathering and the development of a CRM can often be recognised, thereby improving the quality of the data used in the magnetostratigraphic data set.

2.10.1 NRM intensity

The first step in any remanence carrier analysis study is to produce a stratigraphic plot of the NRM intensity values. The NRM intensity sometimes is a good indicator of the relative proportion of ferromagnetic grains in a specimen.

2.10.2 The Median Destructive Field

The Median Destructive Field (MDF) is the field value at which a specimen's intensity is reduced during demagnetisation to 50% of the NRM value. It is a particularly

useful parameter for quickly assesssing the stability of a specimen's magnetisation, and can give an indication of the dominant ferromagnetic mineral carrying its remanence. Generally, magnetite-rich specimens have an MDF of between 10-20mT, whereas hematite-rich specimens often do not demagnetise to the 50% level. The MDF values are listed in the Appendix, and are sometimes used in describing the magnetic properties of the sections.

2.10.2 Volume Susceptibility

The magnetic susceptibility (k) is the ratio of the induced magnetisation (J) to the applied field (H):

$$J = kH$$

This is measured in a weak field (about 0.1mT) and is reversible. The volume susceptibility is typically in the range 2 to $10*10^{-4}$ SI units, and measures the total susceptibility of the ferromagnetic and paramagnetic components. Measurements were carried out on a "Highmoor" susceptibility bridge, similar to that described by Stephenson and de Sa (1970) and recently described by Collinson (1983:p 25).

2.10.4 Isothermal Remanent Magnetisation

Magnetite and hematite are the ferromagnetic minerals commonly found in geological materials. The presence, or absence, of either may indicate the detrital source, conditions during diagenesis, or more recent weathering effects. Pure magnetite has a saturation magnetisation 100 times greater than that of hematite (Tarling, 1983). It also saturates in direct fields of around 0.1T, while hematite requires fields of 1-3T for saturation.

Dealing with natural materials it is unlikely that the remanence is carried by pure magnetite or hematite, but IRM acquisition behaviour is a good indicator of the principal ferromagnetic mineral carrying the specimen's remanence.

For this study specimens were magnetised using a "Newport" high-field magnet, with a maximum field of 0.94T. Specimens were subjected to 14 incremental magnetisation

steps (directed along the specimen's "X-axis"), and the IRM was measured using the "Molspin" spinner magnetometer. The resulting IRM acquisition curve and coercivity spectra data were plotted using a graphics package developed by P. Riddy for an HP86 microcomputer. On average a specimen could be processed every 35-40 mins; therefore only representative specimens were selected for treatment.

IRM acquisition curves typical of magnetite-rich and hematite-rich specimens are shown in Fig 2.11 together with the IRM curve of a specimen containing a mixture of the two minerals. Parameters which the author has found particularly useful are the "peak IRM" (about 0.1 to 1.0 Am^2 for hematite rich specimens, and 5 to 20 Am^2 for magnetite rich specimens), and the "IRM-ratio", which is formally defined here as

$$\text{IRM-ratio} = \text{IRM at } 0.3T/\text{peak IRM}.$$

Values range typically between 0.7 and 0.99; specimens with values below 0.9 are probably hematite-rich, whilst those above 0.9 are more likely to be magnetite-rich. A more informed choice can be made when the IRM-ratio is used together with the peak IRM value.

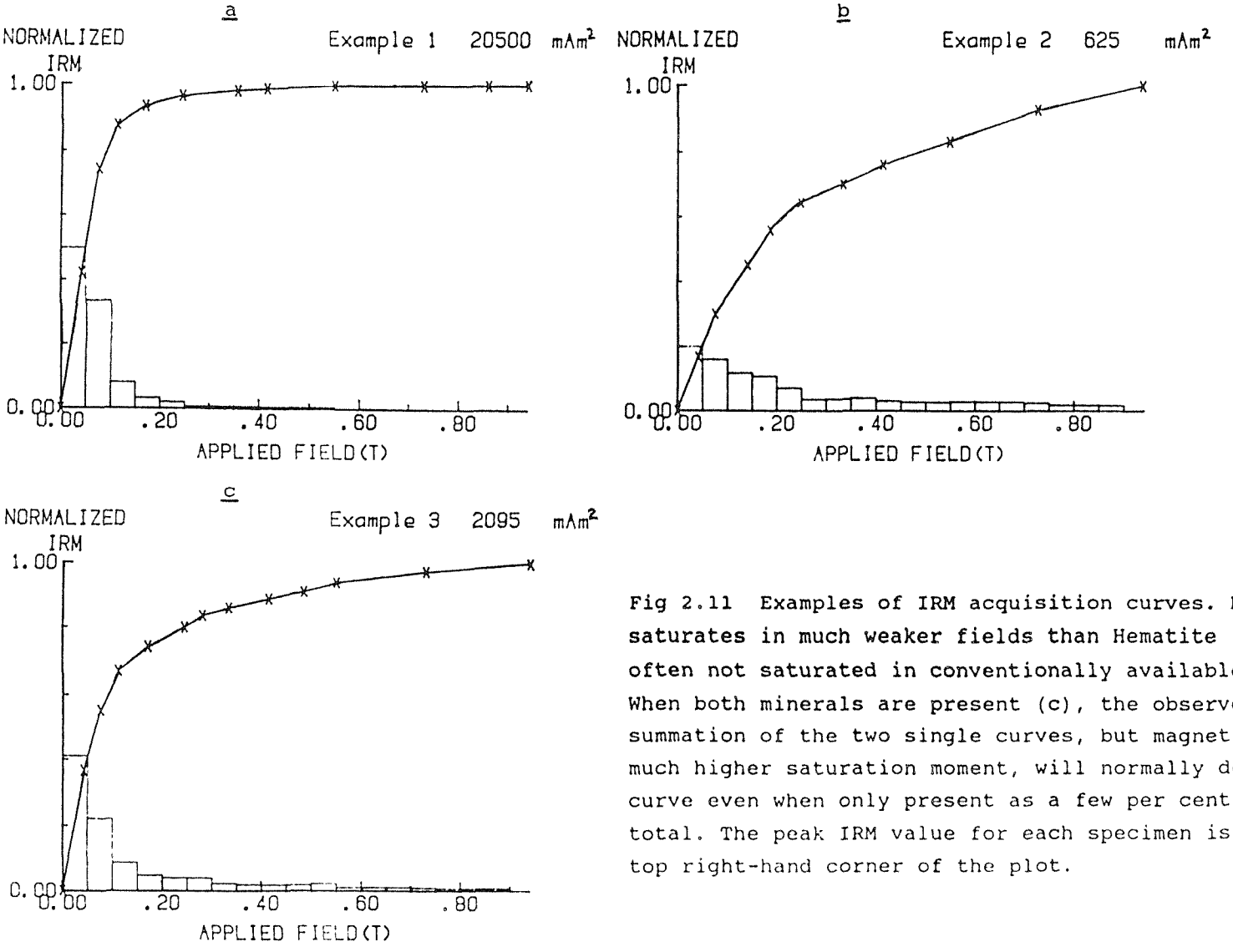

Fig 2.11 Examples of IRM acquisition curves. Magnetite (a) saturates in much weaker fields than Hematite (b), which is often not saturated in conventionally available fields. When both minerals are present (c), the observed curve is a summation of the two single curves, but magnetite, with a much higher saturation moment, will normally dominate the curve even when only present as a few per cent of the total. The peak IRM value for each specimen is shown in the top right-hand corner of the plot.

Chapter 3 Stratigraphic background

3.1 Stratigraphic subdivisions of the Tertiary

George et al (1968) defined the Tertiary sub-era to include the Palaeogene and Neogene Periods. They divided the Palaeogene into the Palaeocene, Eocene and Oligocene Epochs, and the Neogene into the Miocene and Pliocene Epochs.

The "Stage" concept was originally introduced by d'Orbigny (1852) as a chronostratigraphic unit for local and regional correlations. Curry's (1981) comments on the "Stage" are worth repeating: "A well-chosen stage should be based on beds with a varied flora and fauna, rich in forms of value for international correlation. If possible the base of the stage should be chosen within a continuously fossiliferous succession without non-sequences. It is preferable that a succession of faunal episodes should be recognizable within the stage in order to ensure it represents a reasonable duration of time. Whilst the quality of the base of the stage is of paramount importance, that of its upper parts is less important. This is because the upper limit will be defined by the lower limit of the stage which is chosen to succeed it."

By the end of the 19th Century the major stages of the Palaeogene had been defined using stratotype sections from NW Europe. Pomerol (1981) edited a volume which describes the stage stratotype and provides a historical review of the work carried out on the section for each of the important Palaeogene stages.

Hardenbol and Berggren (1978) defined eight commonly used stages for the Palaeogene and related the stratotypes of the stages to planktonic biostratigraphic zones. The positions of the eight Palaeogene stages are presented in Table 3.1. The Sparnacian (very latest Palaeocene) and Cuisian Stages (lower half of the Early Eocene) are also used in this study for work carried out in the Paris Basin.

Epoch		Stage	age (Ma)
			23.7
Oligocene	Late	Chattian	
			30.6
	Early	Rupelian	
			36.6
Eocene	Late	Priabonian	
			40.0
	Middle	Bartonian	
			43.6
		Lutetian	
			52.0
	Early	Ypresian	
			57.8
Palaeocene	Late	Thanetian	
			62.3
	Early	Danian	
			66.4

Table 3.1 The positions of the internationally recognised stages for the Palaeogene. The numerical ages are from Berggren et al (1985).

3.2 Biostratigraphic zonation schemes

Over the last 30 years biostratigraphic zonation schemes have been developed, based on a variety of different microfossil groups. Within each scheme a series of zones are defined using the first or last appearance datum (FAD or LAD) of a particular species. Each scheme provides an alternative method of subdividing and dating (relative) a geological succession. The different schemes play a particularly important role in petroleum exploration work and deep sea drilling investigations, where sediments have been deposited in environments markedly different from those of the stage stratotypes (which for the Palaeogene are based on epicontinental successions).

3.2.1 Planktonic foraminifera

A planktonic foraminifera zonation scheme was introduced by Bolli (1957a, b and c). Work by Bolli (1966), Berggren (1969), Stainforth *et al* (1975) and Blow (1979) established the standard zones P1 to P22 for the Palaeogene. King (1983) published a scheme for the Cenozoic deposits in the North Sea Basin (which at various times has been isolated from the open ocean waters) using parallel planktonic and benthonic zonal schemes.

3.2.2 Calcareous nannoplankton

A calcareous nannoplankton zonation scheme (NP1 to NP25 for the Palaeogene) was introduced by Martini (1971), and has proved extremely useful for the correlation of deposits in mid- to high-latitude sites. Bukry (1973) introduced a scheme (which was updated by Okada and Bukry, 1980) for deposits in low-latitude areas. Many of the zonal boundaries in the two schemes are in fact defined by the same biostratigraphic event. Martini and Muller (1986) recently updated Martini's earlier scheme. St rbaut (1988) introduced a refined zonation for sediments of Ypresian and Lutetian ages by dividing zones NP11 to NP14 into 15 subzones.

3.2.3 Dinoflagellates

A dinoflagellate zonation scheme for the Palaeogene was introduced by Costa and Downie (1976), and further refined by Costa *et al* (1978). It is based on the evolutionary trend of the genus *Wetzeliella.* Chateauneuf and Gruas-Cavagnetto (1978) assigned codes to the zones (W1 to W14), which extend from the upper part of the Late Palaeocene to the Oligocene. Other dinoflagellate species events can also be used to supplement the zonation scheme.

Dinoflagellates are particularly important for the correlation of the Late Palaeocene and Early Eocene deposits at the margins of the North Sea Basin because they appear to be less susceptible to local environmental conditions than do the nannoplankton and planktonic foraminifera.

Costa and Muller (1978) correlated the dinoflagellate and nannoplankton zones for the Palaeogene based on the biostratigraphic record at DSDP sites in the NE Atlantic. Morton et al (1983) criticised part of this correlation, in particular the position of the FAD of Wetzeliella astra and the lower boundary of the NP10 zone, and the proposed definition of the base of the Eocene. However, the bases of the two zones are believed to coincide, and W. astra has been used by most stratigraphers to define the base of the Eocene in the North Sea Basin, where NP10 is absent.

3.3 Geochronology

Absolute dating of the Palaeogene in NW Europe has proved less successful. Soper et al (1976) managed to obtain radiometric dates from basalts intercalated with sediments containing dinoflagellates from lavas in east Greenland. These are the only high-temperature radiometric dates directly relevant to defining absolute dates for the Palaeogene of the North Sea Basin.

The dating of glauconites from sediments from the North Sea Basin using the K/Ar and Rb/Sr methods has proved controversial. The approach adopted by Odin et al (1978) was criticised by Hardenbol and Berggren (1978), whose Palaeogene geochronology studies were based on an integrated magneto-biostratigraphic approach. A recent Palaeogene geochronology, based on glauconite age determinations, was published by Odin and Curry (1985).

The two most recent Cenozoic geochronologies based on magneto-biostratigraphic studies (the method favoured by the majority of stratigraphers) were published by Berggren et al (1985) and Haq et al (1987). The Palaeocene and Eocene portions of the Berggren et al time-scale are reproduced in Figs 3.1 and 3.2, and the Haq et al time-scale (their Fig 2) is reproduced in Fig 3.3. Although the two time-scales give similar dates for a number of boundaries (e.g. 66.4 and 66.5 Ma for the base of the Cenozoic) there are still major discrepancies between the two time-scales in dating other junctions (e.g. 57.8 and

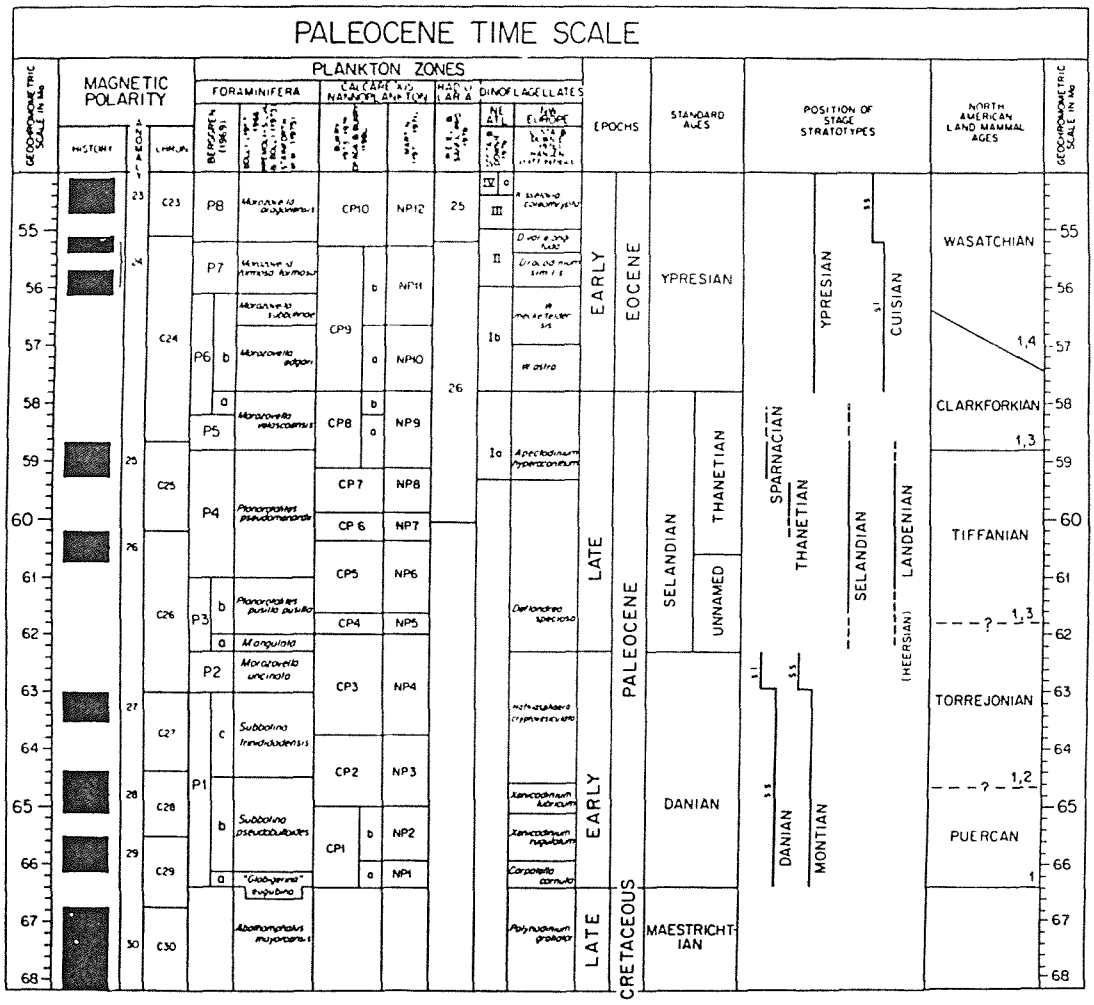

Fig 3.1 The Palaeocene portion of Berggren et al's (1985) magneto- biostratigraphic time-scale.

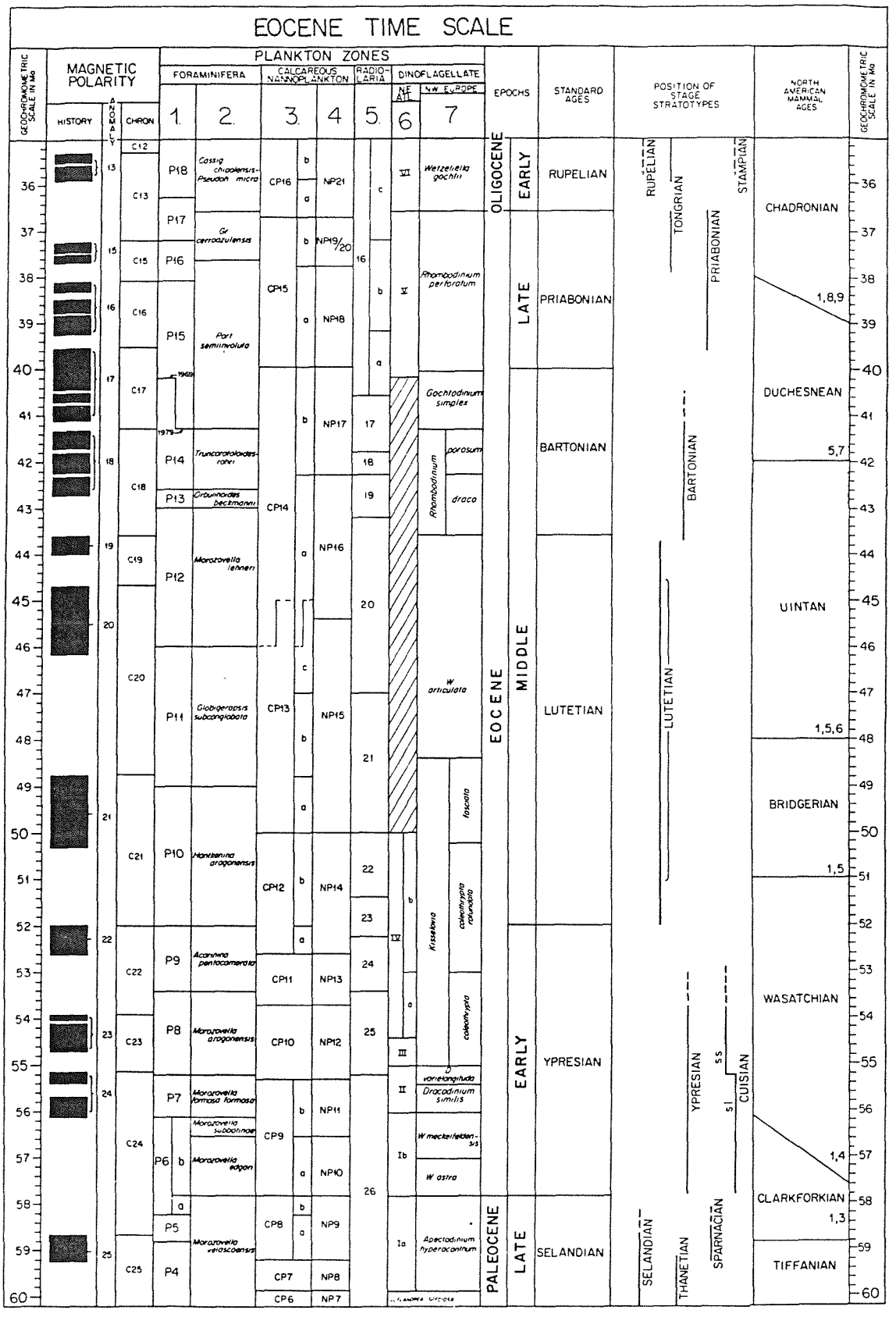

Fig 3.2 The Eocene portion of Berggren et al's (1985) magneto- biostratigraphic time-scale.

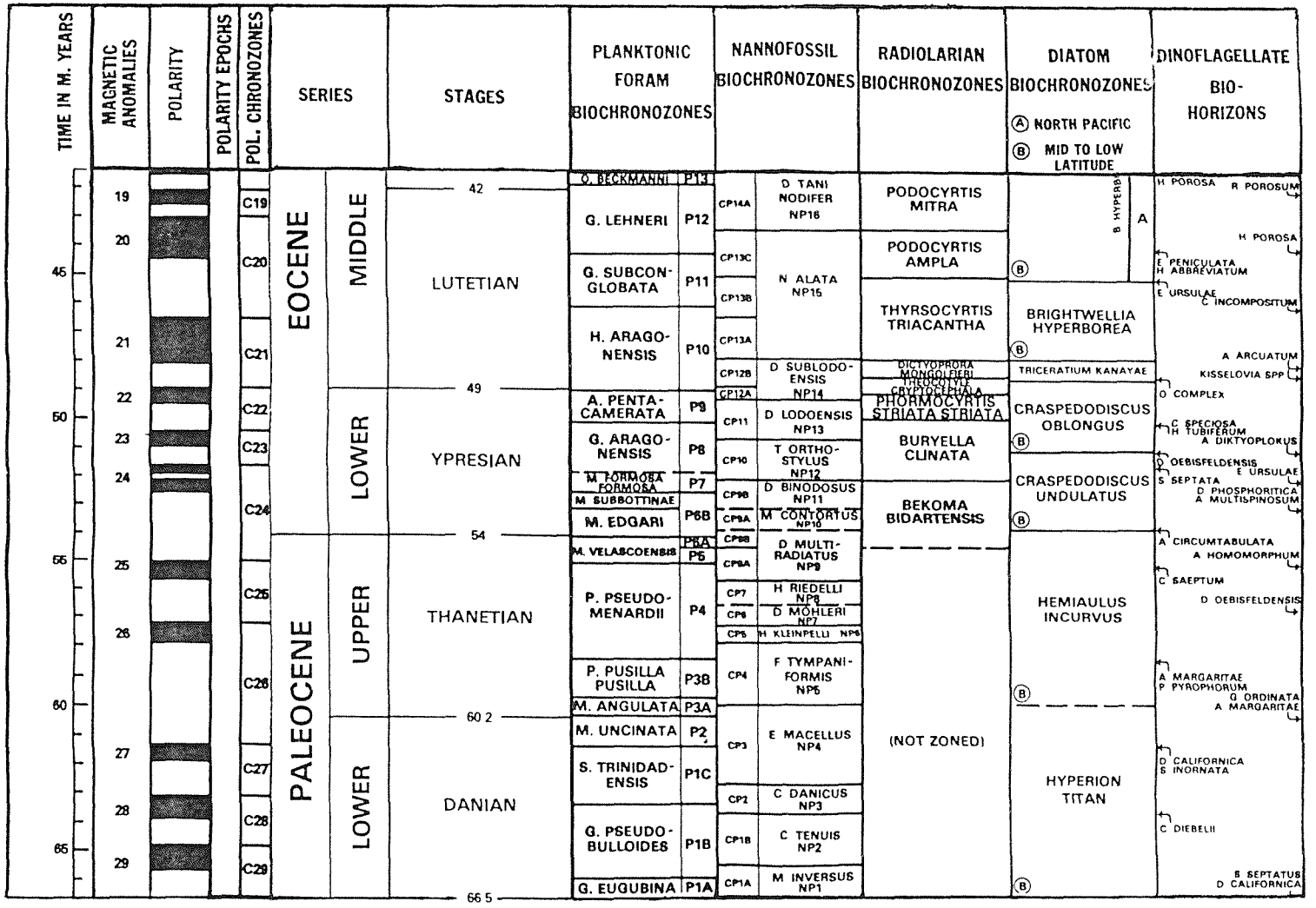

Fig 3.3 The Early Palaeogene portion of Haq et al's (1987) magneto- biostratigraphic time-scale.

54.0 Ma for the base of the Eocene). The time-scale of Berggren et al (1985) has been used throughout this study, partly because of the slightly higher resolution of the magnetic chron and biostratigraphic zone boundaries, but chiefly because of the detailed discussion provided by the authors, leading to the definition of each of the epoch and zone junctions.

3.4 Deposition during the Early Palaeogene in the North Sea Basin

Curry et al (1978), Ziegler (1981) and Pomerol (1982) provide detailed accounts of the deposition in the North Sea Basin during the Early Palaeogene. A palaeogeographic map for this period (modified from Ziegler, 1982) is presented in Fig 3.4.

The deposition of pelagic limestones typical of the Upper Cretaceous ceased at the end of the Danian. The Danian sea covered much of Denmark and northern Germany and most of the present-day North Sea area. The shift to a predominantly fine-grained clastic sedimentation was related to the eustatic sea-level fall associated with Laramide tectonism (Ziegler, 1981). The Shetland Platform was uplifted at this time and was a major source for material being deposited into the North Sea.

In Denmark the Kerteminde Marl and Holmehus Formations (Late Palaeogene) were deposited as a more or less uninterrupted sequence. Further to the south, in the Belgian Basin, the limestones that are used to define the Montian Stage (which are slightly younger than the Danian) are overlain by the shallow marine sediments of the Heersian (used in part to define the Landenian Stage).

In England and northern France the oldest Tertiary sediments are of Thanetian age, and they rest unconformably on Upper Cretaceous Chalk. In England these sediments were deposited in a shallow shelf environment, whereas those of the Paris Basin were deposited in a brackish/ fluviatile environment.

A major unconformity marks the upper limit of the

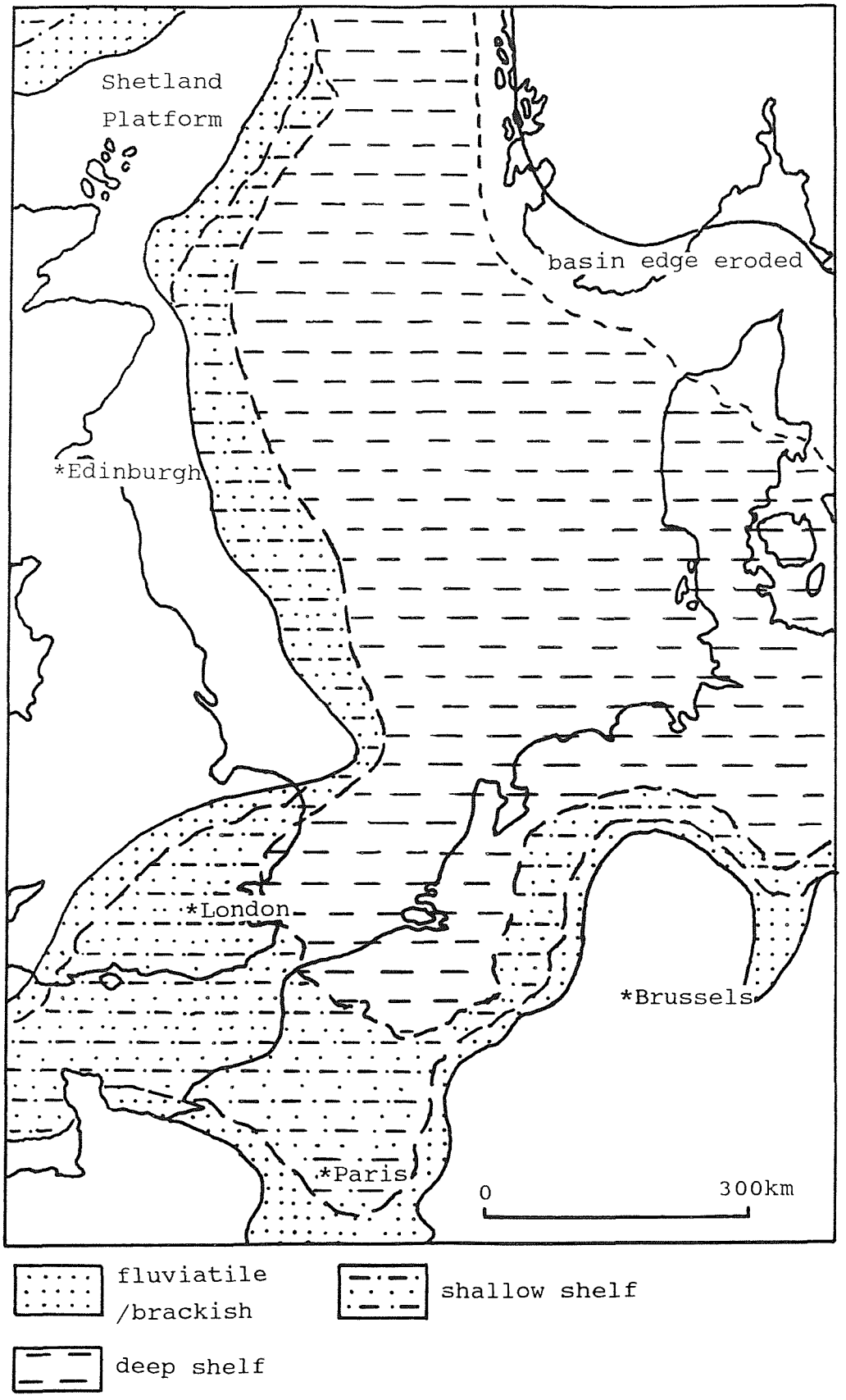

Fig 3.4 Simplified palaeogeographic map of the North Sea Basin during the Late Palaeocene/Early Eocene (modified from Ziegler, 1982)

Thanetian deposits. This hiatus is present in all of the sequences at the North Sea Basin margin, and is also present in the southern and central parts of the North Sea (separating the Lista and Sele Formations).

During the very latest Palaeocene (Sparnacian) fluviatile/lacustrine deposits covered much of the Anglo-Paris-Belgium Basin. In Denmark a much deeper-water facies persisted as the Olst/Fur Formations were being deposited.

Just prior to the end of the Palaeocene, sedimentation in all but the southern parts of the basin included a major volcaniclastic input. The source of this material was the Iceland-Faroe-Greenland igneous province (Knox and Morton, 1988).

The Ypresian Sea covered southern England, northern France, the low countries and continued up into Denmark. The sea extended eastwards from Germany into Poland and eastern Europe. Towards the end of the Early Eocene there must have been a steady sea-level fall, as the shelf-mud facies in the Hampshire, London and Belgium Basins was gradually replaced by a more sandy basin-margin facies. In the Paris Basin deposition ceased in the middle of the Ypresian.

A major hiatus marks the Early/Middle Eocene boundary before deposition recommenced at the start of the Lutetian Stage.

Chapter 4 The Palaeogene deposits of southern England

4.1 Introduction

This chapter outlines the work which has been carried out on the English Palaeogene, details the geographical distribution of sediments of this age in the UK, and briefly describes the formations which have been investigated in this study. Chapters 5, 6 and 7 deal with the magnetostratigraphic results from sections spanning the Late Palaeocene, the Palaeocene-Eocene boundary, and the Early Eocene respectively.

4.2 Historical background

Curry (1965) and King (1981) present detailed summaries of the work carried out on the English Palaeogene. The deposits have long attracted interest because of their rich and varied biota and their close proximity to London, which made them accessible to many early workers. Scientific work on these deposits began in the 18th Century, based mainly on the classification of macrofossils.

Perhaps the most important worker in this field, certainly of the 19th Century, was Joseph Prestwich, who in a series of papers published between 1846 and 1855 layed down the foundations of English Palaeogene stratigraphy. He introduced the term "Lower London Tertiaries" to include the deposits between the Chalk and the London Clay (units now assigned to the Thanet, Reading and Woolwich Formations). He redefined the term "London Clay" (previously used by Webster, 1814), described the Bagshot Beds and, adopted the terms "Bracklesham Beds" and "Barton Clays". He also attempted to correlate the English Palaeogene succession with similar deposits in northern France and Belgium.

Fisher (1862) published work on the distribution and subdivision of the, now-named, Bracklesham Group in the Hampshire Basin. Renevier (1873) adopted the term "Thanetian" as a stage name (the term is now used as the international stage name for the Late Palaeocene), based on

the, now-named, Thanet Formation of east Kent. Important Geological Survey memoirs were published by Whittaker (1872 and 1889).

Apart from the contributions of Stamp (1921a and b) and Wrigley and Davis (1937), stratigraphic work on the English Tertiaries remained rather neglected during the first half of this century. However, during the latter half there has been a resurgence of interest. The use of microfossils (chiefly dinoflagellates) to resolve stratigraphic problems has been of enormous help. Particularly useful papers include Costa and Downie (1976), Costa et al (1978), Bujak et al (1980) and Islam (1983 a and b), workers all associated with the Palynology Unit at Sheffield University.

The need to produce a formal lithostratigraphic classification, as defined by Hedberg (1976), for the deposits has led to further work. Important contributors include Ward (1977 and 1979) on the Palaeocene deposits of the London Basin, King (1981) on the London Clay Formation, and Edwards and Freshney (1987) on the Palaeogene of the Hampshire Basin. Knox, Morton, Harland and others (in various combinations) have published work on the "ash-series" and the Palaeocene-Eocene boundary in the southern North Sea Basin, since the mid 1970's.

Magnetostratigraphic work has been carried out chiefly by Townsend (1982) on the Late Palaeocene and Early/Middle Eocene Formations. The papers of Townsend and Hailwood (1985), Cox et al (1985), and Aubry et al (1986) summarise the developments in this field.

4.3 The distribution of Palaeogene sediments in southern England

The Palaeogene deposits of southern England are preserved in the London and Hampshire Basins (Fig 4.1). (The term "basin" is perhaps misleading here, as these centres of deposition originally formed part of the much larger Anglo-Paris-Belgium Basin, which occupied the southern part of the ancestral North Sea Basin. The London and Hampshire "basins" became separated during Miocene

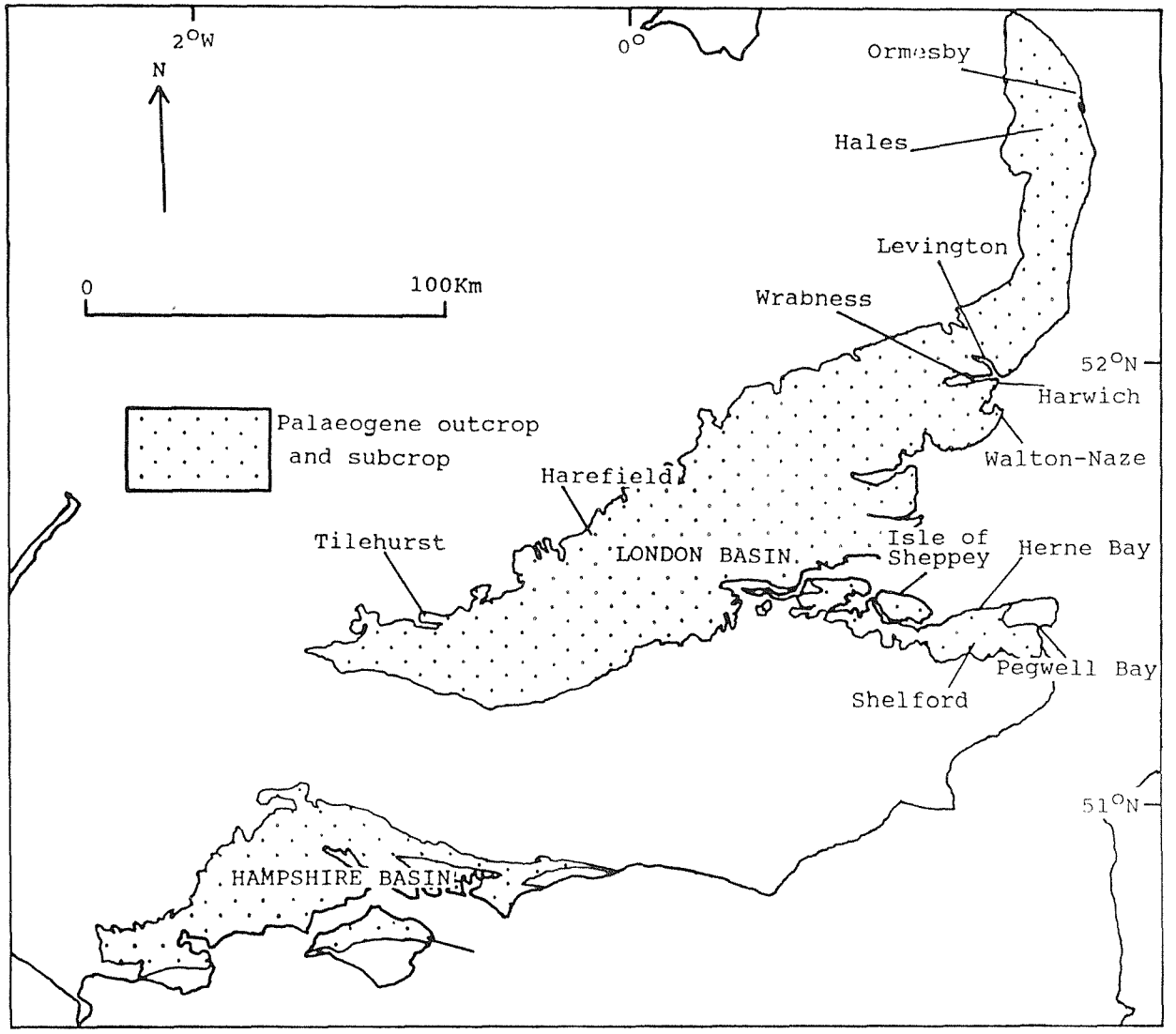

Fig 4.1 The Palaeogene deposits of SE England.

times due to folding and subsequent erosion, which removed the intervening material.) The oldest Palaeogene sediments (assigned to the Thanet Formation) are present only in the eastern part of the London Basin. The succession is most complete in the Hampshire Basin where there are beds ranging from Late Palaeocene to Early Oligocene age. The sequences can best be observed at the east and west ends of the Isle of Wight, where they are exposed as part of the vertical limb of a large monocline.

In East Anglia the Palaeocene is inaccessible, as it lies beneath a thick cover of Quaternary material. It is, however, well-known from a number of cored boreholes drilled by the British Geological Survey (BGS). Sediments in these boreholes show similarities to those in the London Basin, and to the offshore sequences in the southern North Sea.

4.4 The formations investigated in this study

The stratigraphic extents of the various formations investigated in this study are shown in Fig 4.2.

4.4.1 The Thanet Formation

The oldest Palaeocene sediments in southern England are assigned to the Thanet Formation. This formation is restricted to a triangular area outlined by Ramsgate, Epsom and Ipswich. In eastern Norfolk, buried deposits of an equivalent age, or slightly younger, are present. These sediments are lithologically intermediate between those of the onshore sequence and the offshore Lista Formation (Cox et al, 1985). The formation rests unconformably on the Upper Cretaceous chalk, marking a significant hiatus. It consists of sandy, clayey silts with levels of glauconite, especially at the base. The sections at Pegwell Bay and Herne Bay are used as formation co-stratotypes (Siesser et al, 1987) and are also used to define the Thanetian stage. Siesser et al (1987) assign the base of the formation to the NP6/NP7 nannoplankton zones and the top of the formation to the NP8 zone. The formation is about 25m thick

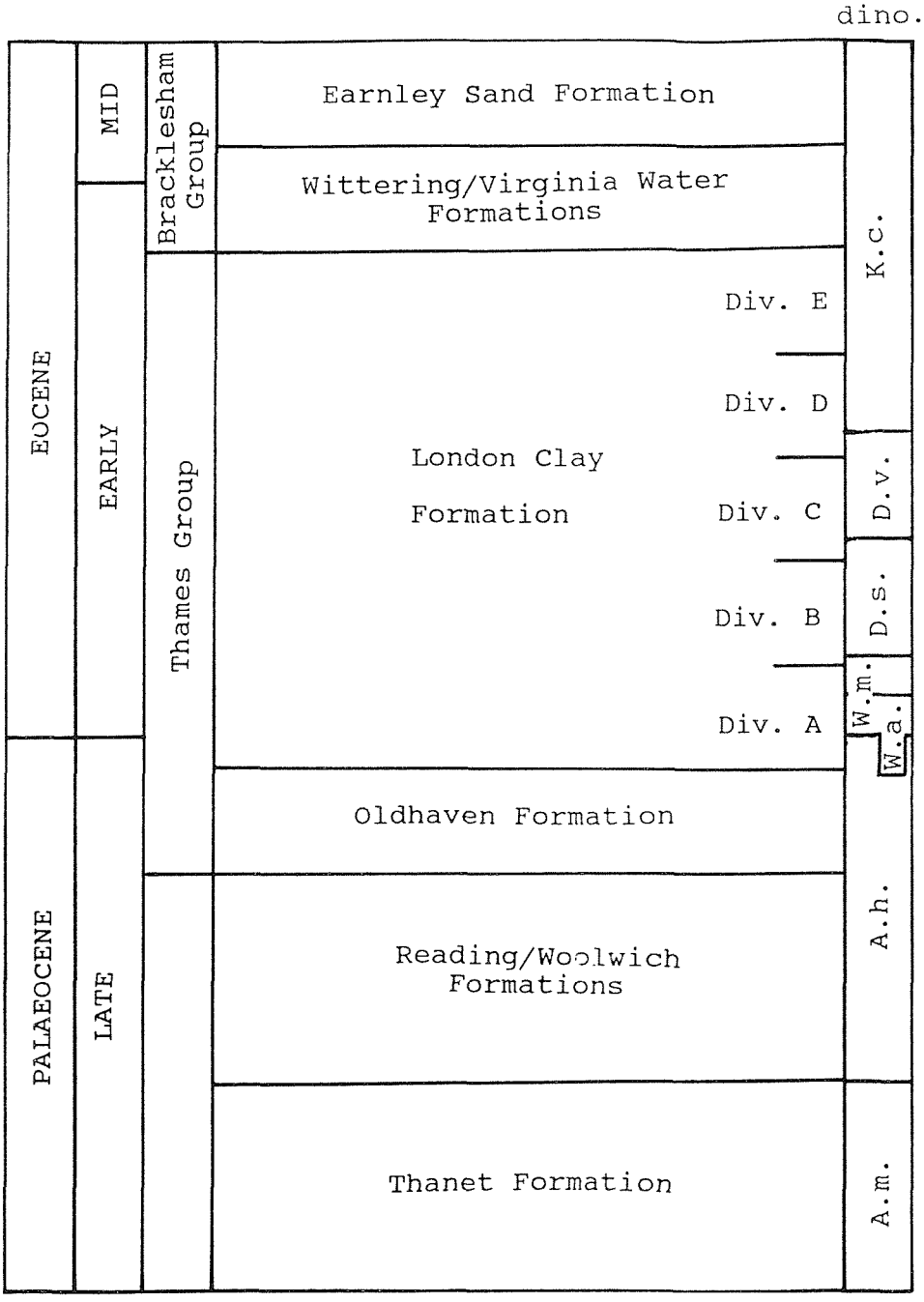

K.c.= Kisselovia coleothrypta
D.v.= Dracodinium varielongituda
D.s.= Dracodinium similis
W.m.= Wetzeliella meckelfeldensis
W.a.= Wetzeliella astra
A.h.= Apectodinium hyperacanthum
A.m.= Aliocysta margarita

Fig 4.2 The stratigraphy of the lower Palaeogene formations of SE England.

in the type area, thinning to just a few metres in the London area. Curry (1981) suggests that a significant part of it was eroded prior to deposition of the succeeding deposits.

4.4.2 The Woolwich and Reading Formations

The sediments assigned to the Woolwich and Reading Formations were deposited over a much larger part of southern England. The "Bottom Bed" was deposited in marine conditions. This 1-3m thick unit consists of sands and silts, rich in glauconite, and with occasional pebbles. In the western half of the London Basin and the Hampshire Basin this bed is overlain by the fluviatile/deltaic facies of the Reading Formation. This formation (which is typically about 30m thick) consists of red mottled clays with thin sandy units. In the eastern half of the London Basin, the "Bottom Bed" is overlain by the estuarine/ lagoonal sands and clays of the Woolwich Formation. The formation is typically about 5m thick, and contains an abundance of molluscs, often concentrated in shell beds (about 0.2m thick). Siesser et al (1987) assign the Woolwich and Reading Formations to the NP9 nannoplankton zone.

4.4.3 The Oldhaven Formation

The term "Oldhaven Formation" was introduced by King (1981) to include the glauconitic sands and sandy clays which lie above the Woolwich and Reading Formations, and beneath the London Clay Formation. Deposition was in an inner sub-littoral or marginal marine environment. The formation is between 8 and 10m thick east of London, thinning to about 2m in the Hampshire Basin. It has yielded no diagnostic microfaunas, but is underlain and overlain by beds of the Apectodinium hyperacanthum dinoflagellate zone and therefore it can be also assigned to this zone.

Recent studies by Knox et al (1983) have questioned King's (1981) model in which the Oldhaven Formation is taken to be older than the Harwich Member of the London

Clay Formation in East Anglia. However, King's basic model is retained for this study, as no replacement model has yet been published.

4.4.4 The London Clay Formation

The London Clay Formation (King, 1981) includes the London Clay, the Claygate Beds and (in the Hampshire Basin) several sand bodies previously referred to as the "Bagshot Sands" (Prestwich, 1847). The London Clay Formation is divided into five informal divisions (A to E), each corresponding to a major transgression/regression cycle. It forms part of a much larger deposit which originally extended across southern England, the English Channel and NW continental Europe. It is thickest east of London, reaching 150m in Kent, and thins progressively to the west.

Lithologically it consists of dark brown or bluish grey plastic clays, with no obvious macrostructure, and material no coarser than fine sand. Deposition was in a well -oxygenated marine shelf environment at depths of between 20 and 200m. Six Wetzeliella (dinocyst) zones have been identified in the formation. They extend from the Apectodinium hyperacanthum zone to the Kisselovia coleothrypta zone.

King (1981) includes the Oldhaven and London Clay Formations within the Thames Group.

4.4.5 The Wittering Formation

The stratotype of the Wittering Formation is at Whitecliff Bay on the Isle of Wight. Edwards and Freshney (1987) redefined the unit, so that the base and top of the formation coincides with the base and top of Plint's (1983) beds WB2 and WB9 respectively. The 11m of sediment assigned to the base of King's (1981) Wittering Division are now included in the upper part of the London Clay Formation.

The Wittering Formation can be broadly divided into three lithological units. The lower part consists of fine grained glauconitic sands and silty clays in thin bedded units, the middle part consists of greyish green glauco-

nitic shelly sandy silts, and the upper part consists of brown laminated clays (together with a 1m thick lignite bed, now called the Whitecliff Bay Bed). The Whitecliff Bay Bed marks a significant hiatus, as sediments below this level are assigned to the lower part of nannoplankton zone NP13 and the sediments above to the middle part of NP14. Aubry et al (1986) suggest that the hiatus is between 0.6 and 2.0 m.y in duration. The Wittering Formation is typically 40-50m thick in the Hampshire Basin although individual beds can only be traced over short distances.

The Wittering Formation is overlain by the green and greyish green silty sands of the Earnley Sand Formation (which was not sampled in this study). The Wittering Formation is the oldest unit of the Bracklesham Group.

4.4.6 The Virginia Water Formation

The Virginia Water Formation was introduced by King (1981), to replace the term "Lower Bagshot Sands" used originally by Prestwich (1847). The main outcrops are in Surrey and Berkshire with smaller outliers in Kent and Essex. A thickness of 20-30m is attained in the western part of the London Basin. The base of the Virginia Water Formation is conformable with the top of the London Clay Formation in the London Basin. Lithologically it consists of fine cross-stratified sands and laminated sands with thin clay seams. Depostion was probably in an inner sub-littoral/marginal marine environment. King (1981) equates this formation with the middle part of the Wittering Formation in the Hampshire Basin.

Chapter 5 Results from the Late Palaeocene of southern England

5.1 Introduction

Palaeocene sediments are present in the eastern parts of Norfolk and Suffolk under a cover of Quaternary deposits (varying in thickness from metres to many tens of metres). A magneto- litho- biostratigraphic study was carried out on the Palaeocene succession in the Ormesby borehole, Norfolk, by Cox et al (1985). They identified a 7.5m thick normal polarity zone in the Thanet Formation, which they correlated with the Thanet magnetozone in Kent (Townsend and Hailwood, 1985), and also the oldest known onshore Palaeocene sediments in southern England.

As part of the BGS's long term mapping program in East Anglia, a cored borehole was drilled in 1987 at Hales, 20km south-west of Ormesby (Fig 4.1). Magnetostratigraphic results from the Hales section are presented in this chapter, together with the results from a reinvestigation of the Ormesby borehole. It is now possible to very accurately correlate levels within the boreholes using short-term magnetic "events" (defined by 1 to 4 specimens). The Thanet Formation at Pegwell Bay, Kent has also been reinvestigated, including levels not sampled by Townsend (1982).

5.2 The Hales borehole

The Hales borehole (TM 36710 96874) revealed 12m of the Pleistocene Red Crag Formation and 45m of Palaeocene sediments on top of Upper Cretaceous chalk. The Palaeocene succession extends upwards from the Thanet Formation, through the Woolwich Formation to the lower part of the London Clay Formation (Harwich Member). Initially 92 evenly spaced specimens were taken from the core, and later a second group of 19 specimens was taken

NRM intensities were typically in the range 10-40mA/m, except for the interval 28m to 32m below datum (BD, which in this case is the top of the borehole) where values were

about 1mA/m. Specimens were demagnetised in peak fields varying between 20 and 50mT. Over 40% of the specimens produced SEP directions and only 3 specimens were of indeterminate polarity. Importantly, the SEP specimens are fairly well distributed through the section. Typical demagnetisation plots are shown in Fig 5.1 and 5.2. Fig 5.3 summarises the magnetostratigraphic results.

The borehole section is dominantly reverse polarity, except for a normal polarity magnetozone (HL-c) and seven shorter normal polarity intervals. HL-c is defined by 18 specimens and spans 8.1m. HL-e is the most important of the normal polarity "events" as it spans 3 to 4m (its base is loosely defined by two indeterminate polarity specimens). HL-h is defined by four specimens (spanning 1.24m), HL-f and HL-g by two specimens each, whilst HL-a,-b and -d are based on single specimens.

5.3 The Ormesby borehole

Johnston (1983) examined the palaeomagnetism of the Palaeocene sediments in the Ormesby borehole, and the results were published as part of the paper by Cox *et al* (1985). During the preparation of that paper a number of normal polarity specimens located in the section were omitted from the final draft, on the basis that the polarities could not be reliably defined from single specimens. These have been added to the Ormesby magneto-stratigraphic column (Fig 5.3), and the normal polarity levels within the succession redefined as OR-a to OR-i. Also included in the diagram are the results from the resampling phase, where critical levels in the borehole were reinvestigated. The NRM intensities of the Ormesby material are about 20mA/m and specimens were demagnetised in peak fields of 30 to 40 mT. The biostratigraphic data for the Ormesby borehole (presented by Cox *et al*, 1985) are are also included in Fig 5.3.

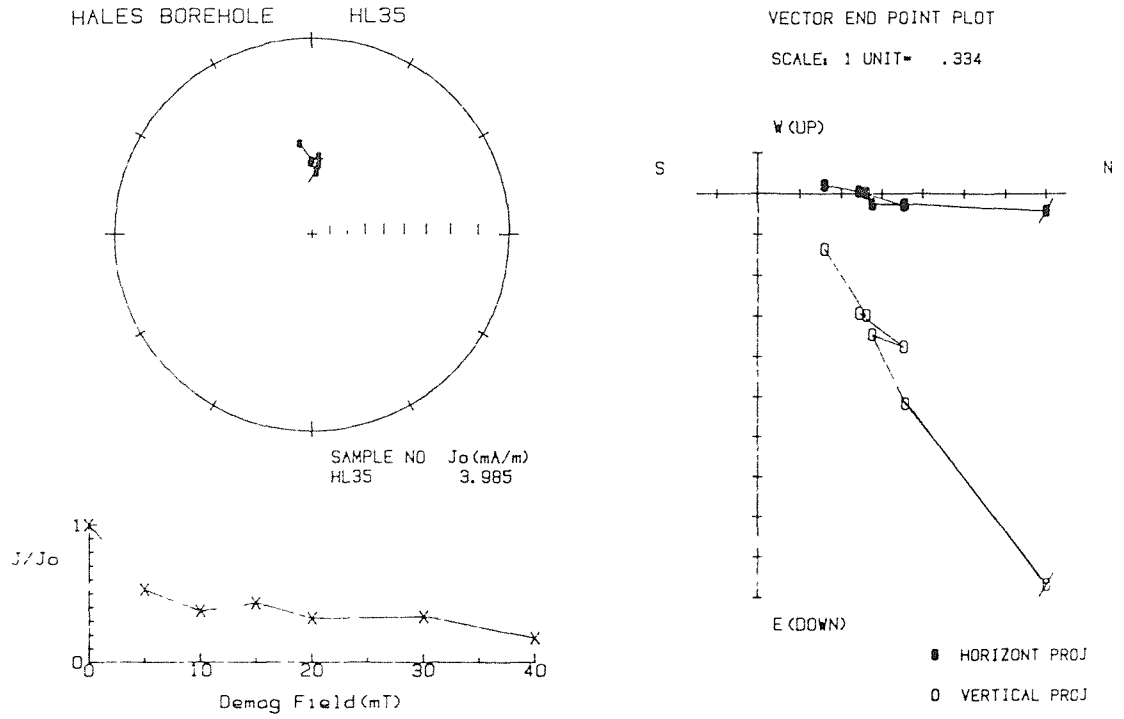

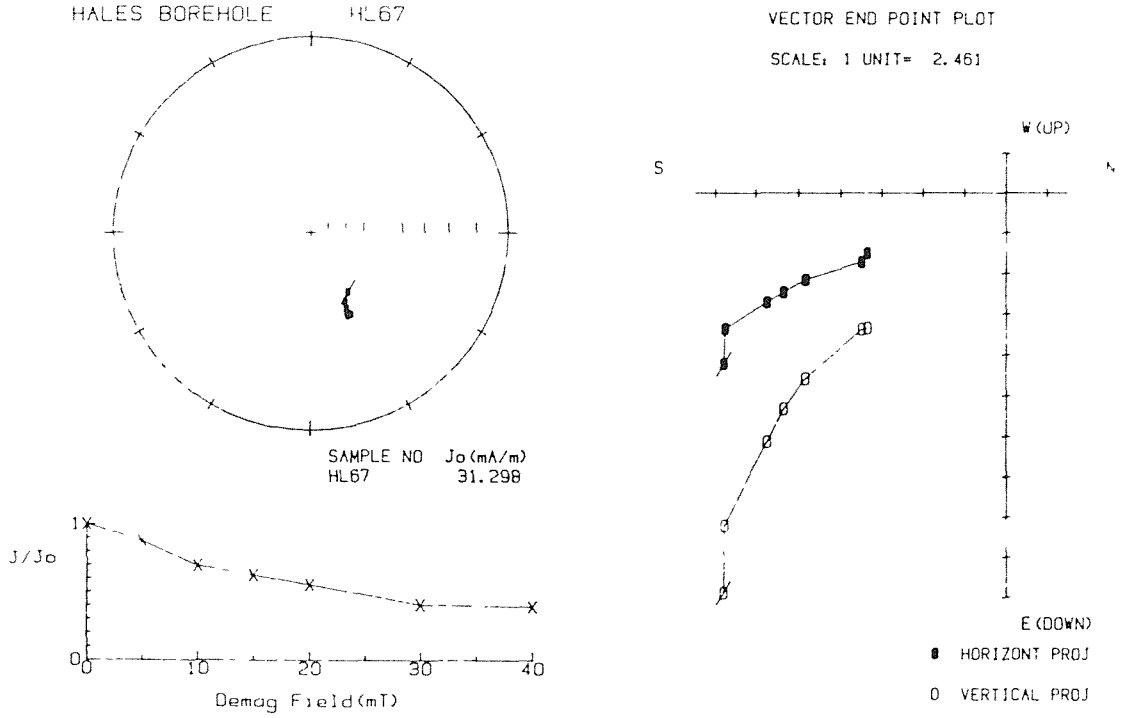

Fig 5.1 Typical normal polarity specimens from the Hales borehole. The lower plot is for a specimen from the Thanet Formation. The upper plot is for a specimen from the "unrecognised unit" at the base of the Woolwich Formation. For explanation of symbols see Fig 2.7. The declination is arbitrary with these borehole specimens.

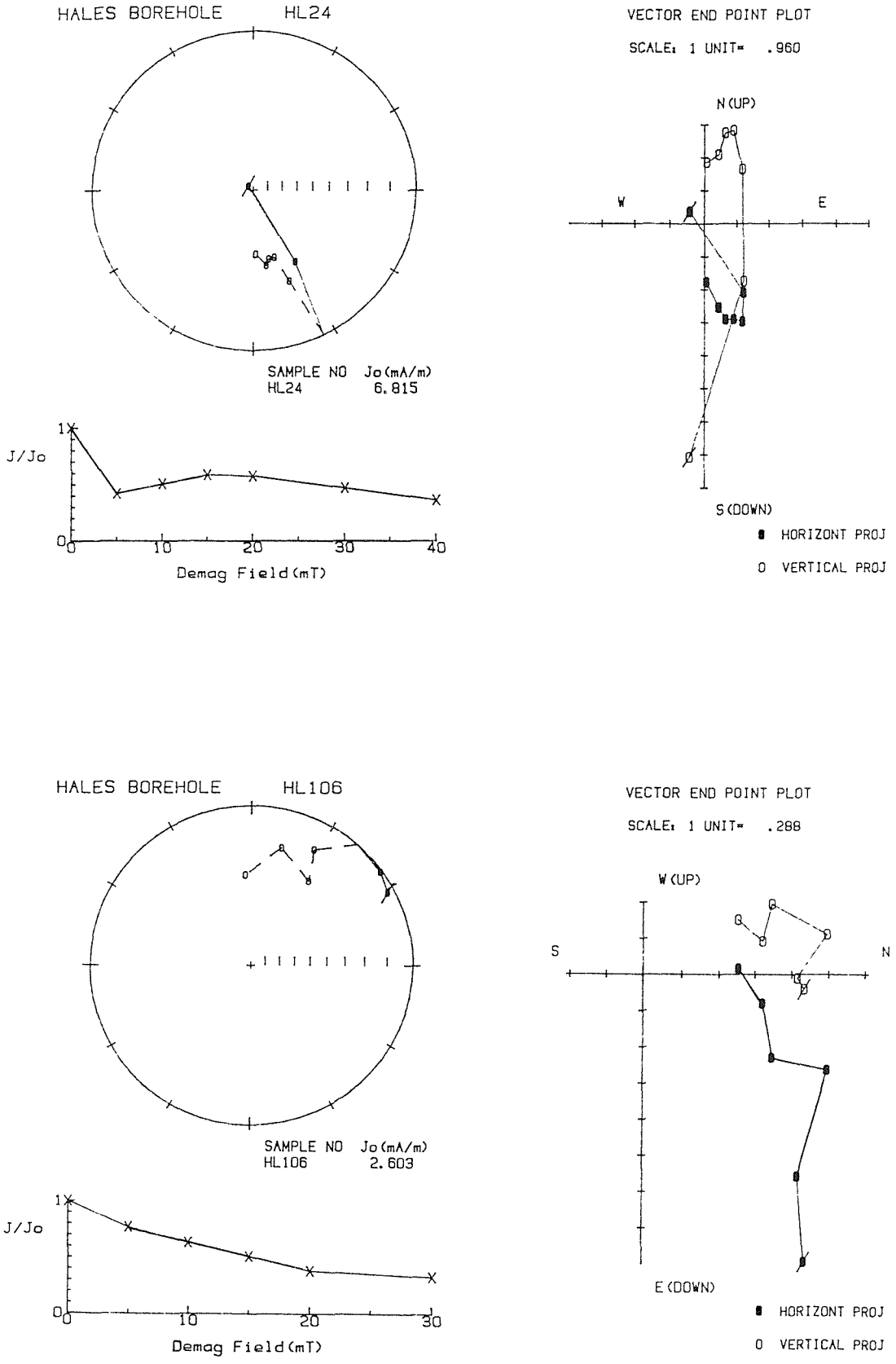

Fig 5.2 Typical reverse polarity specimens from the Woolwich Formation in the Hales borehole. For explanation of symbols see Fig 2.7. The declination is arbitrary with these borehole specimens.

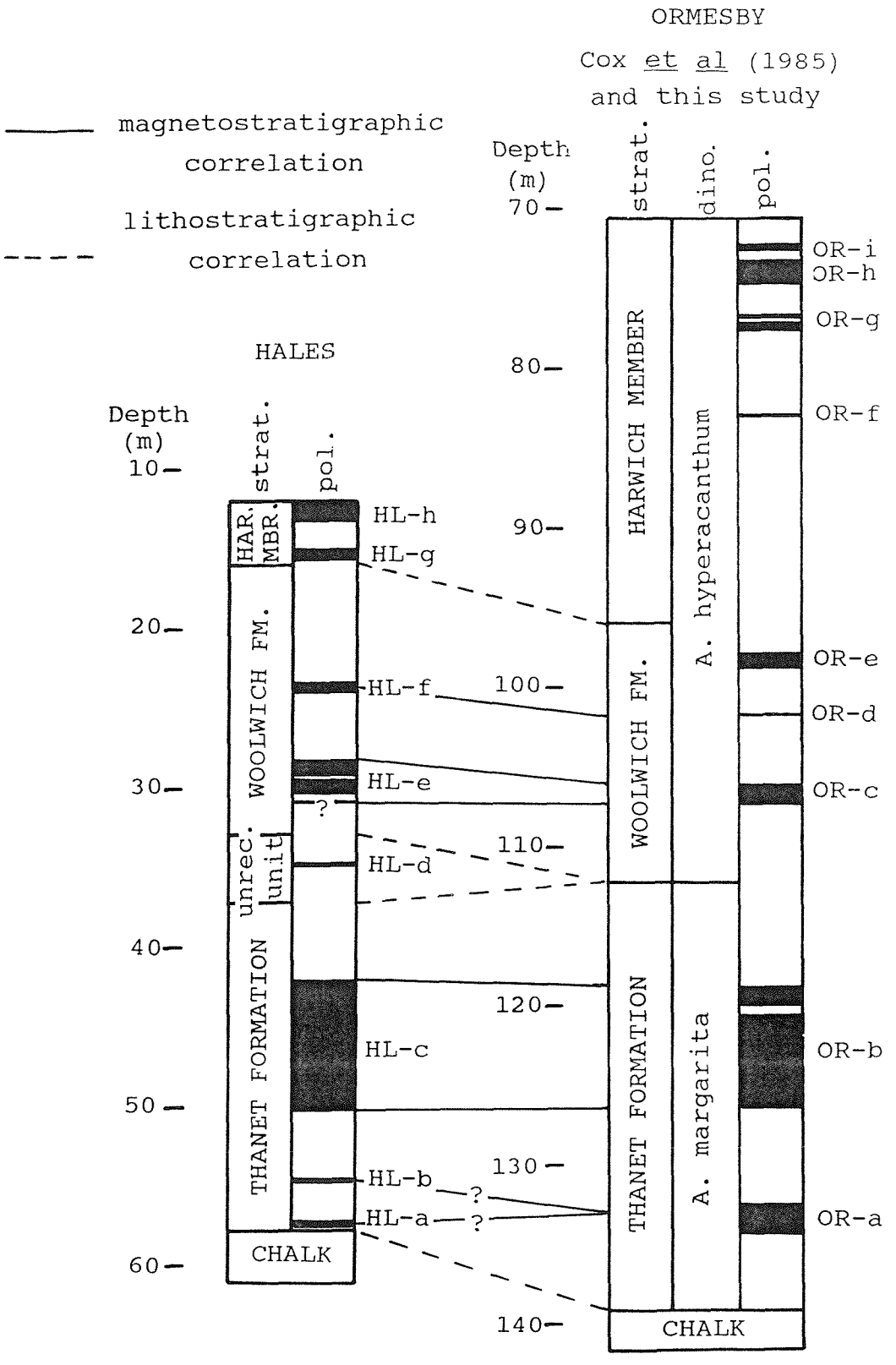

Fig 5.3 The magnetostratigraphy of the Hales and the Ormesby boreholes and their proposed correlation.

5.4 Correlation

The magnetozones HL-c (50.32 up to 42.23m) and OR-b (126.5 up to 119.0m) were identified in the middle part of the Thanet Formation in both boreholes, and a correlation of the two is proposed. The short reverse polarity interval within the upper part of OR-b (based on three specimens) could not be identified in HL-c. Its absence is probably due to core loss of about 1m at 43.5m BD in the Hales borehole.

Cox et al (1985) correlated OR-b with the Thanet magnetozone in Kent (which Aubry et al, 1986, correlated with Chron C26N). As yet, the biostratigraphic data are not available for the Hales borehole, and a direct correlation of HL-c to Chron C26N is not possible. However, the indirect correlation of HL-c (via OR-b and the Thanet magnetozone) to Chron C26N is assumed.

It must be noted that the Thanet Formation in the Ormesby borehole is assigned to the Alisocysta margarita dinoflagellate zone. Haq et al (1987: Fig 2) define the FAD and LAD of A. margarita within Chron C26R. The results from this study suggest that this dinoflagellate zone is at least as young as Chron C26N and extends into Chron C25R. A revision of the stratigraphic range of this species is recommended.

The base of the Woolwich Formation marks a significant hiatus. The reverse polarity sediments in the Thanet Formation below correlate with Chron C25R. Above this level in the Ormesby borehole, the reverse polarity sediments are assigned to the Apectodinium hyperacanthum dinoflagellate zone. The Woolwich Formation and basal part of the London Clay Formation therefore correlate with Chron C24BR. The hiatus must be at least 0.6 m.y, which is the duration of Chron C25N (Berggren et al, 1985).

The following "event" correlations are proposed:

1. HL-a (57.55 up to 57.41m) or HL-b (54.79 up to 54.47m) with OR-a (134.5 up to 132.75m). Requires tephra stratigraphy data to resolve this correlation.

2. HL-e (30.79 up to 28.36m) with OR-c (107.51 up to 106.25m).
3. HL-f (24.04 up to 23.30m) is tentatively correlated with OR-d (101.8m), which has a rather shallow positive inclination.
HL-d (34.97 up to 34.74m), HL-g (15.7 up to 15.18m) and Hl-h (13.28 up to 12.04m) cannot be correlated with any levels in the Ormesby borehole. OR-e (98.95 up to 98.0m), OR-f (83.53-83.41m), OR-g (79.81 up to 78.77m), OR-h (74.75 up to 73.44m) and OR-i (72.62 up to 72.48m) cannot be correlated with the Hales sequence of magnetic "events".

It is thought that the normal polarity levels defining HL-h, in the Hales borehole, may be the result of a weathering CRM. IRM measurements were carried out on four specimens taken from the top of the Hales borehole. IRM and NRM data are shown in table 5.1 (along with similar data from the top of the Ormesby borehole).

borehole	specimen	depth (m)	pol	NRM (mA/m)	IRM ratio	peak IRM (mAm^2)
Hales	HL1	12.04	N	3.00	.91	1967
	HL2	12.50	N	1.35	.87	1076
	HL3	13.02	N	14.06	.96	5324
	HL4	13.23	N	20.40	.98	10685
	HL101	13.33	R	8.81	.98	11524
	HL6	14.15	R	17.84	.96	8882
Ormesby	OR110	70.67	?	0.08	.93	164
	OR114	71.84	R	0.27	.78	491
	OR101	71.98	R	0.55	.78	671
	OR116	72.59	N	0.51	.76	872
	OR102	72.35	R	0.64	.83	464
	OR103	78.95	N	17.79	.97	9594
	OR104	79.62	N	32.52	.98	11595

Table 5.1. The IRM and NRM data from the top of the Hales and Ormesby boreholes.

The primary magnetisation of specimens HL1 and HL2 may have been altered as both the NRM and IRM data are notably different to those of HL3 to HL6. The magnetic "event" HL-h is based on normal polarity magnetisations in specimens HL1 to HL4. If HL-h were entirely a result of a CRM, then specimens HL3 and HL4 should have magnetic properties similar to HL1 and HL2. However, the following explanation is thought possible. HL1 and HL2, at the top of the borehole, have been altered to hematite whereas HL3 and HL4 have been altered to maghemite; and there is a transition to magnetite at 13.28m BD (between sites HL4 and HL101).

A similar change in magnetic properties occurs in the top few metres of the Ormesby borehole (Table 5.1). Cox et al (1985: p174) comment on an oxidised level extending about 3m down from the top of the Palaeocene succession. Specimens OR103 and OR104, some distance below the top of the Palaeocene, are more typical of the Harwich Member, with high NRM intensities. The IRM data suggest that the remanance for the bulk of the member is probably carried by magnetite. The specimens from the oxidised zone are magnetically different, with lower NRM intensities, which is probably carried by hematite. The likelihood that the change is a result of weathering prior to the deposition of the Red Crag Formation, as Cox et al (1985) suggested, can probably be discarded since sites at the very top of the section are reverse polarity (one would expect them to have a normal polarity CRM). The only other possible explanation is that the borehole also recovered the basal part of the Walton Member (which is known from a number of sections to be reverse polarity, and to possess magnetic properties similar to those at the top of the borehole). The latter explanation is considered the more likely, and a litho-logical reexamination of the top of the borehole is recommended to clarify the situation.

5.5 Summary

An accurate correlation of levels within the Palaeocene succession at Hales and Ormesby, in Norfolk, has been achieved. The single specimen normal polarity levels originally identified by Johnston (1983) in the Ormesby borehole appear to be positive records of short term inversions of the geomagnetic field, as evidenced from their recognition in the Hales borehole. In future it should be possible to correlate Palaeocene successions in southern England against this polarity scale, provided that a similar sampling interval is used.

Brief observations on rates of sedimentation in the two boreholes are summarised below.

1. The deposition rate during HL-c/OR-b, which are correlated with Chron C26N, was about 14m/m.y (the duration of Chron C26N (0.54m.y) is taken from Berggren et al, 1985).
2. The reverse polarity sediments below Chron C26N are much thicker in the Ormesby borehole. Either the sedimentation rate was much greater during this period at Ormesby, or the sediments are infact slightly older and the sequence is more complete at Ormesby. R. Knox (pers. comm.) is currently addressing this problem by investigating the composition of ash-layers found at the base of the two boreholes.
3. The deposition rate of the Woolwich Formation (based purely on formation thicknesses) was almost 30% greater at Hales, and includes a 5m thick unit not present at Ormesby.

The above points assume non-erosion at the formation boundaries and similar rates of compaction during diagenesis. R. Knox (BGS) is currently working on the tephra chonology of the two boreholes, which should provide an even better understanding of the history of sedimentation in the two boreholes.

5.6 Pegwell Bay

Townsend (1982) examined the base of the Thanet Formation in the Cliff-End section (TR 353643) at Pegwell Bay, Kent. The Thanet magnetozone was identified in this section and correlated with Chron C26N, on the basis that the Thanet Formation was no younger than NP8 (Aubry et al, 1986). Townsend (1982) found the upper part of the formation (at Herne Bay, Kent) to be reverse polarity. As the sampled sections did not have a stratigraphic overlap, the top of the Thanet magnetozone was never identified. A further 8 to 10m of the Thanet Formation, not sampled by Townsend (1982) is exposed in the cliff at the back of the hoverport terminal, 600m SE of the Cliff-End section. Curry (1981) states that the top of this section has a 6m overlap with the base of the Herne Bay section.

The basal part of the Thanet Formation was resampled (5 sites) together with 9 sites from the hoverport section. Specimens had NRM intensities typically in the range 2-6 mA/m, and were processed using the cryogenic magnetometer (to maximum fields of 35mT). Typical demagnetisation plots are shown in Fig 5.4 and 5.5. The magnetic polarity results are summarised in Fig 5.6. The Cliff-End section was found to be dominantly normal polarity, in support of the polarity results of Townsend (1982), based on specimens taken from eleven sites. Results from the hoverport section are rather confused with normal, indeterminate and reverse polarity sites.

Siesser et al (1987) estimate a stratigraphic gap of 7m between the top of the Cliff-End section and the base of the hoverport section. The top of the Thanet magnetozone must occur somewhere between the two sections. The two normal polarity sites in the hoverport section possibly represent short-term magnetic "events", and are considered not to be part of the Thanet magnetozone.

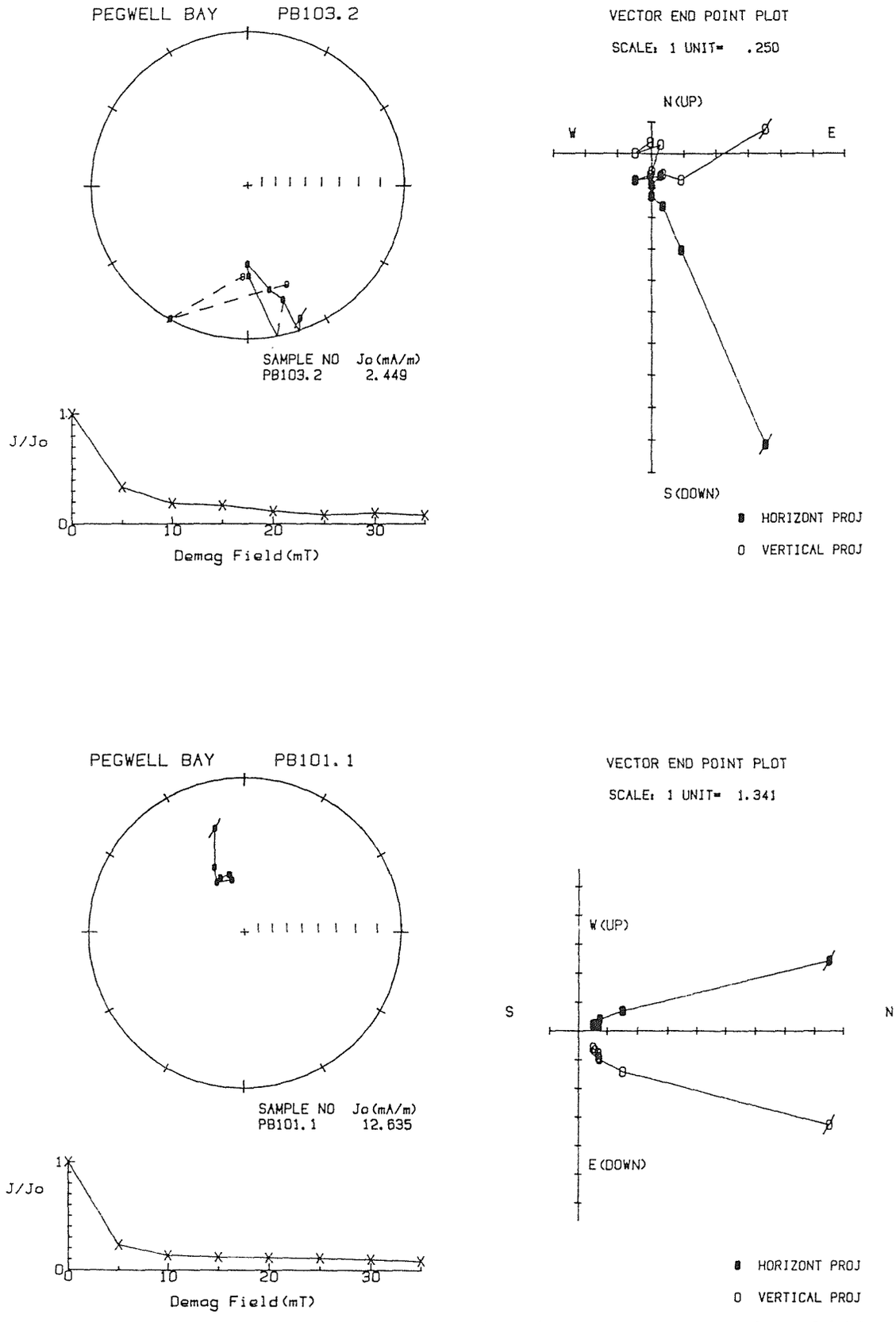

Fig 5.4 Examples of demagnetisation plots from the Cliff End section, Pegwell Bay. The upper plot shows a specimen with a reverse polarity and the lower plot a specimen with a normal polarity. For explanation of symbols see Fig 2.7.

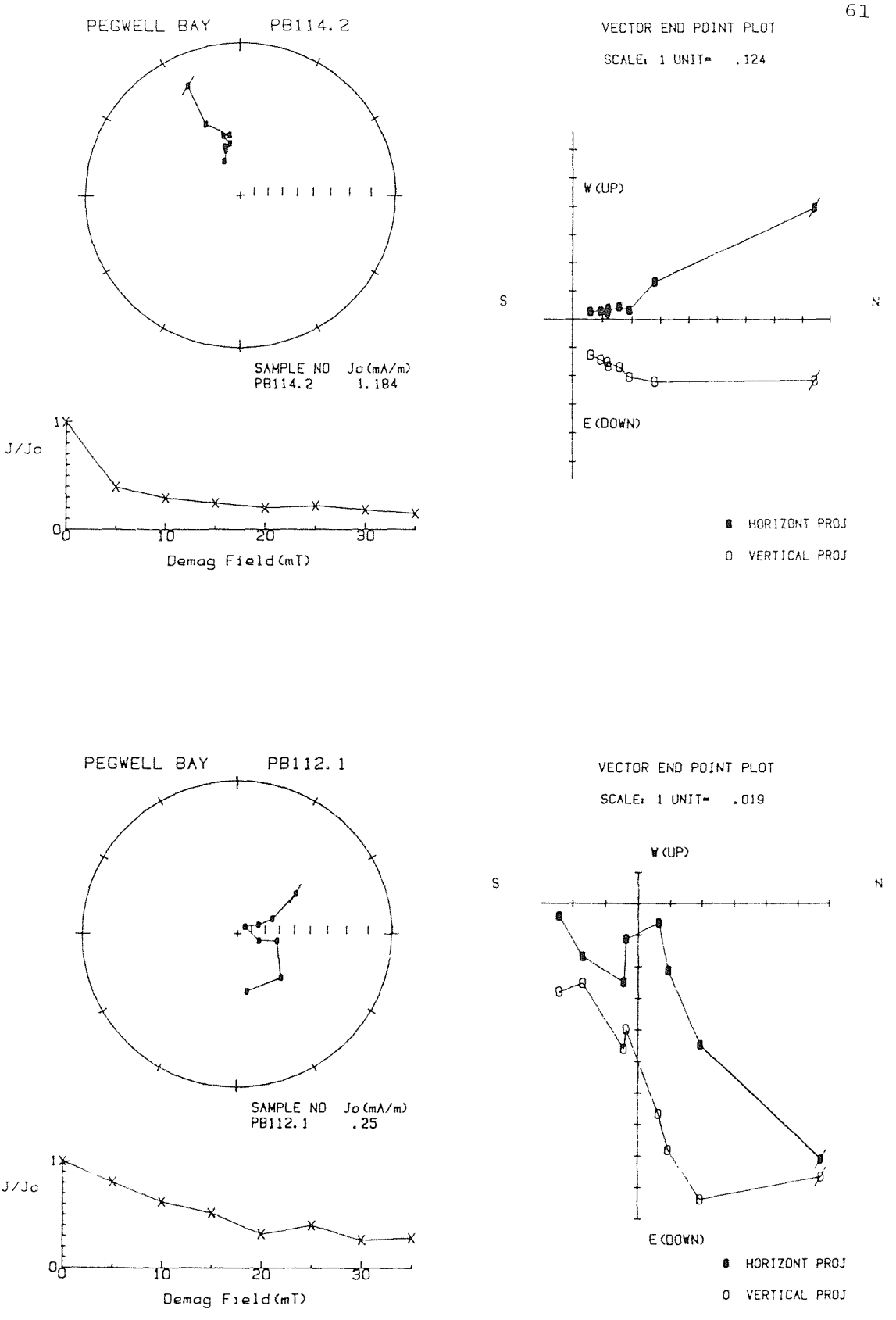

Fig 5.5 Examples of demagnetisation plots from the Hoverport section, Pegwell Bay. The upper plot shows a specimen with a normal polarity and the lower plot a specimen with a reverse polarity. For explanation of symbols see Fig 2.7.

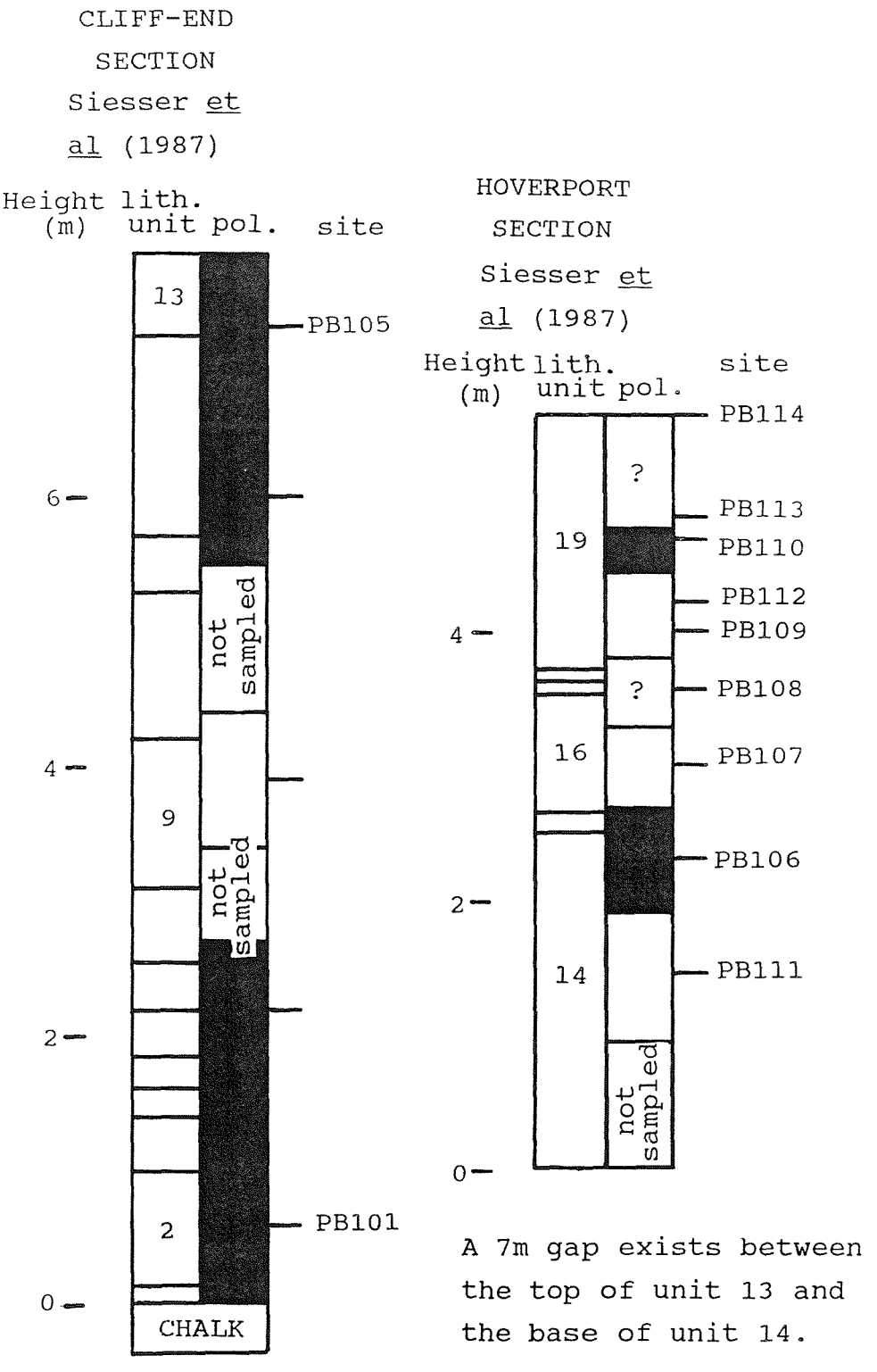

Fig 5.6 The magnetostratigraphy of the Thanet Formation at Pegwell Bay.

5.7 Overall summary

The magnetostratigraphic history of the Palaeocene succession in southern England is now quite well-known from the work carried out by Townsend (1982), Johnston (1983) and the present study. The base of the Thanet Formation in the Norfolk boreholes represents the oldest known Palaeocene sediments in southern England (Chron C26R). The base of the formation is younger in Kent (where the Thanetian stage stratotype is defined) because its base correlates with Chron C26N. This suggests that the first Palaeocene transgression progressed rather slowly from Norfolk to Kent. Assuming that the sedimentation rate in the Hales borehole during Chron C26R was similar to that during Chron C26N, a figure of 0.5 m.y. is a realistic estimate for this interval of time.

The Thanet/Woolwich Formation junction marks a significant hiatus. The upper part of the Thanet Formation was deposited during Chron C25R, whereas the Woolwich Formation and lower part of the London Clay Formation were deposited during C24BR. Chron C25N is absent from the English Palaeocene succession.

A series of short period "events" has also been identified in the Norfolk borehole Palaeocene sequences. These should allow a detailed correlation of the English Palaeocene succession if a sampling interval of 0.3 to 0.5m is used. They may prove very useful in assessing variations in sedimentation rates between localities, especially if used alongside the tephra chronology.

Chapter 6 Results from the Palaeocene-Eocene boundary beds in southern England

6.1 Introduction

The base of the Eocene (defined in the North Sea Basin as the FAD of the dinoflagellate *Wetzeliella astra*) practically coincides with the base of the London Clay Formation. This chapter presents results from work carried out on the Oldhaven Formation and the basal part of the London Clay Formation. The chapter is divided into three sections, dealing respectively with the following aspects:

1. The Harwich and Walton Members in East Anglia.
2. The Oldhaven and London Clay Formations in Kent.
3. The Tilehurst Member.

Local correlations are discussed at the end of each section. The magnetostratigraphic results are then used to resolve some of the longer distance correlation problems encountered by Townsend and Hailwood (1985).

6.2 East Anglia

The lower part of the London Clay Formation is exposed in a number of river-cliffs, coastal-cliffs and beaches in north Essex and south Suffolk. Townsend (1982) sampled the Harwich and Walton Members at Wrabness, and the Harwich Stone Band (HSB) at Harwich. A normal polarity zone was identified in the upper part of the Harwich Member at Wrabness. New results from nearby sections at Levington and Walton-on-the-Naze are presented below and compared with the existing data from Wrabness and Harwich. Results of an IRM study of material from three of the sections are also included.

6.2.1 Magnetostratigraphic analysis

6.2.1.1 Levington

The river-cliff section on the east bank of the Orwell at Levington (TM 225387) near Ipswich was sampled (Fig 6.1). This poorly documented exposure of the London Clay Formation was briefly described by George and Vincent

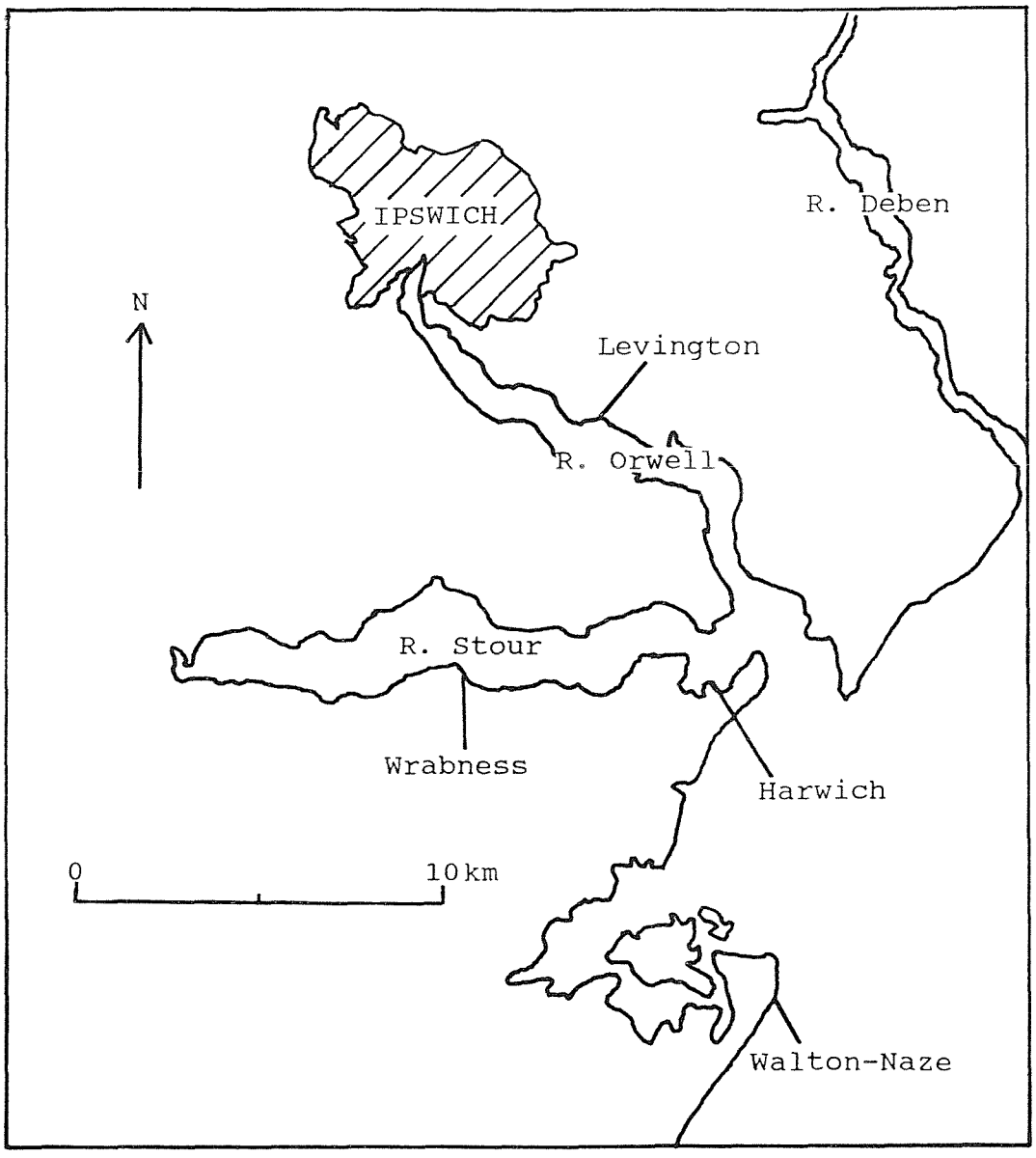

Fig 6.1 The location of the East Anglian sections.

(1976). The 10m section begins 1.2m below the HSB and extends almost to the top of the Harwich Member. An unquantified number of degraded ash beds outcrop in the section. The section was sampled at eleven sites, one of which was an oriented block from the HSB.

NRM intensities varied dramatically (1-250mA/m), certainly a result of sampling a mixture of ash and non-ash levels. Intensities progressively decrease with ascending stratigraphic height in the section. Demagnetisation (typically up to 25/30 mT) resulted in the definition of SEP directions for 8 of the 21 specimens. The remaining specimens exhibit well-defined demagnetisation "trends". Typical demagnetisation data are presented in Fig 6.2. The magnetostratigraphy is summarised in Fig 6.3. The sequence is normal polarity, except for the HSB, which is reverse polarity (defined by 3 specimens).

6.2.1.2 Walton-on-the-Naze

The beach and cliff section at Walton-on-the-Naze (TM 267238) exposes the upper part of the Harwich Member (A1), and the lower part of the Walton Member (A2) stratotype (King, 1981). An earlier stratigraphic study by George and Vincent (1977) described a 3.34m thick succession across what is now the A1/A2 junction.

The top 4m of the Harwich Member was sampled at six levels and the lower 8.3m of the Walton Member at eleven. Sediments from the ash-bearing Harwich Member had NRM intensities of about 10mA/m, whereas the ash-free Walton Member had typical values of about 1mA/m. Most of the specimens were demagnetised to 30 mT, and example plots are shown in Fig 6.4. The magnetostratigraphic results are presented in Fig 6.3. The section is dominantly reverse polarity, but specimens from sites WN6,8,9 and 10 (spanning 2.5m) produced ambiguous directions. Site WN7 is reverse polarity, whereas site WN11, just above the ambiguous level, is normal polarity.

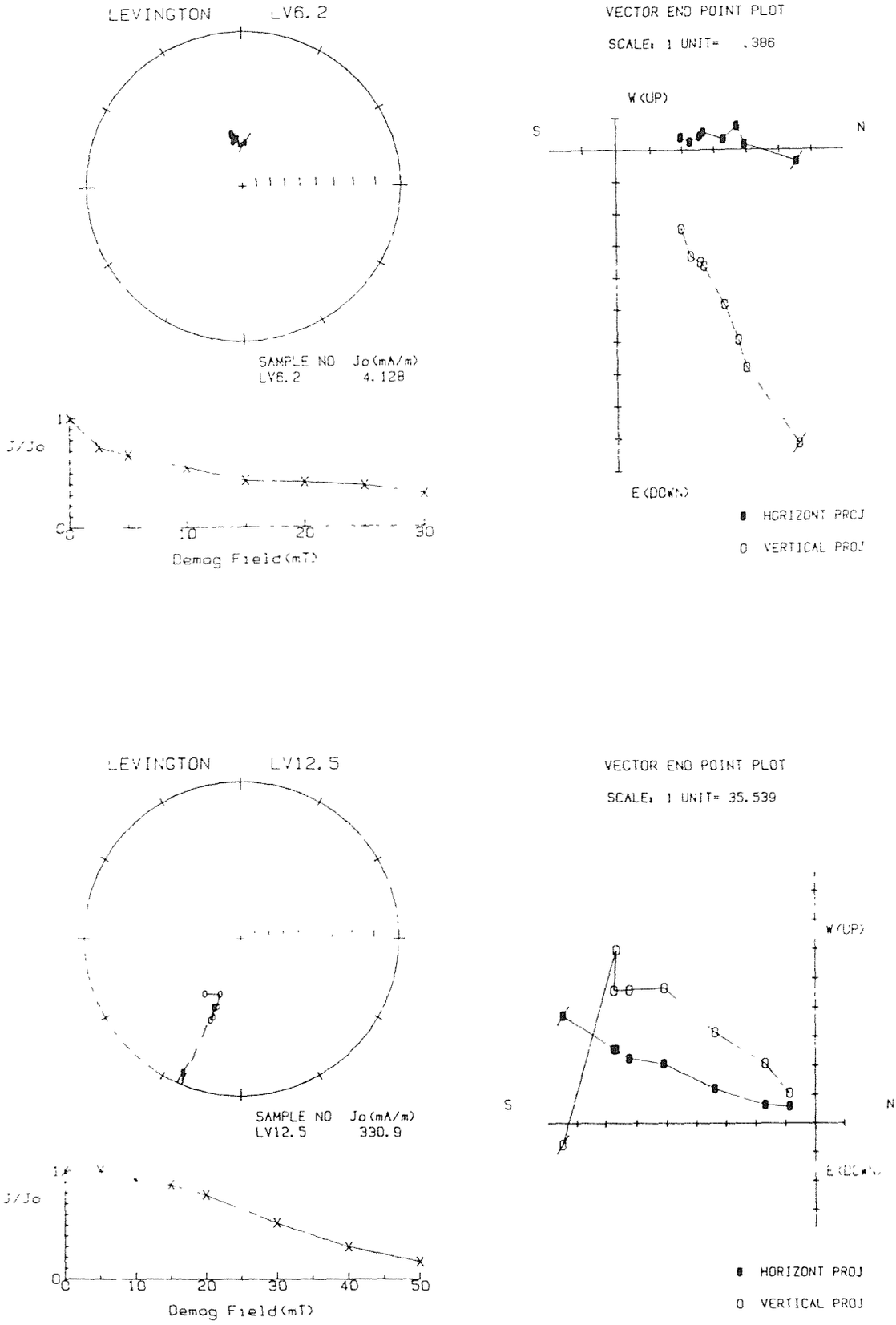

Fig 6.2 Examples of demagnetisation plots from the Harwich Member at Levington. The upper plot shows a specimen with a normal polarity. The lower plot shows a specimen from the Harwich Stone Band with a reverse polarity. For explanation of symbols see Fig 2.7.

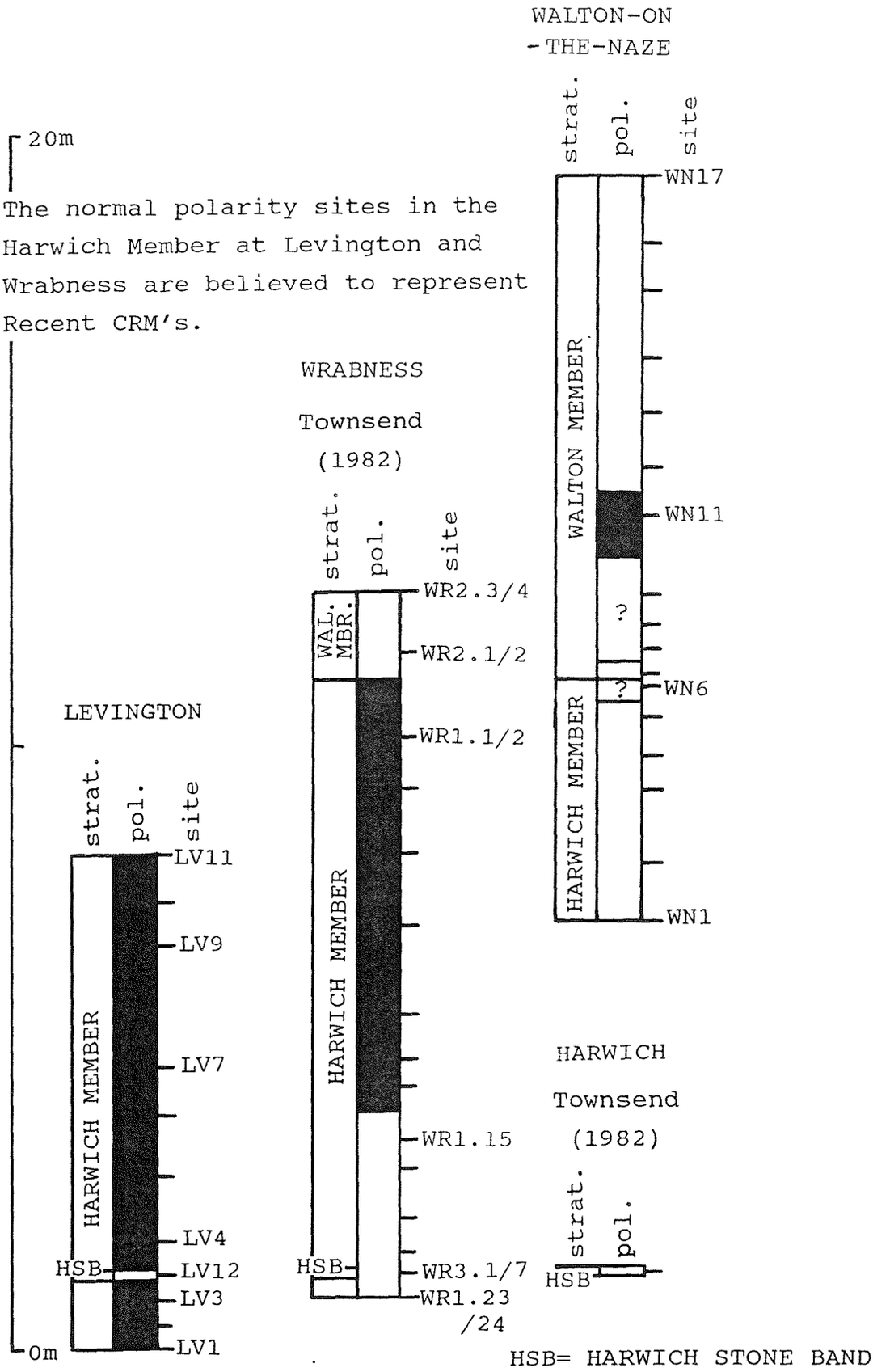

Fig 6.3 The magnetostratigraphy of the Harwich and Walton Members in East Anglia.

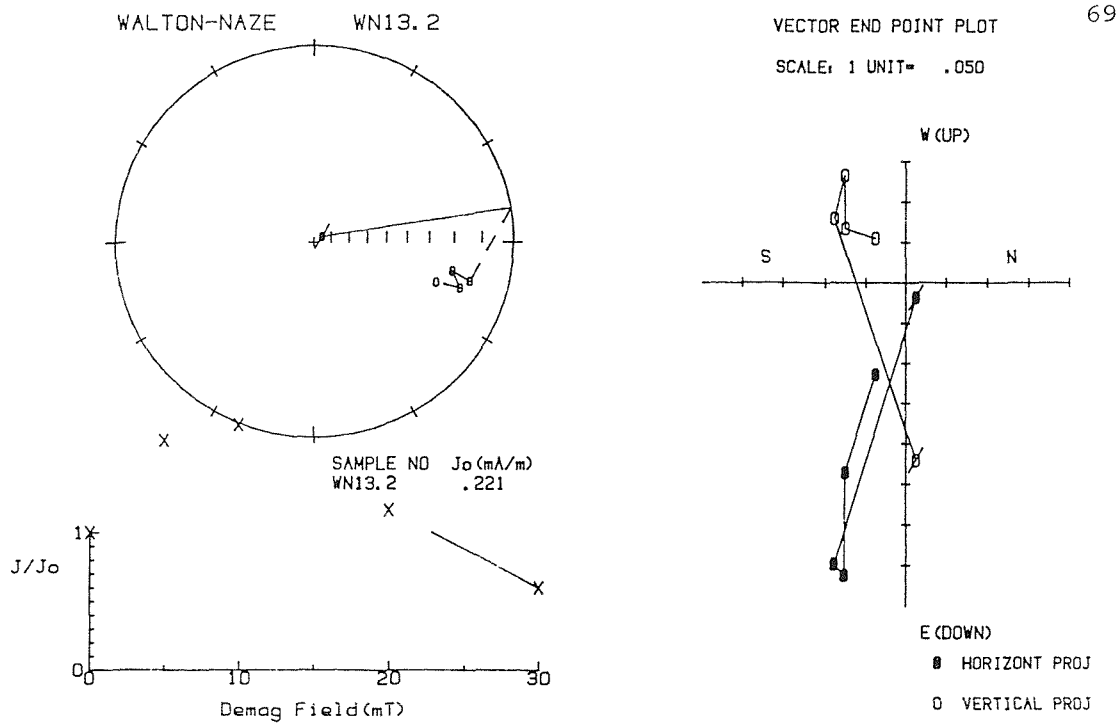

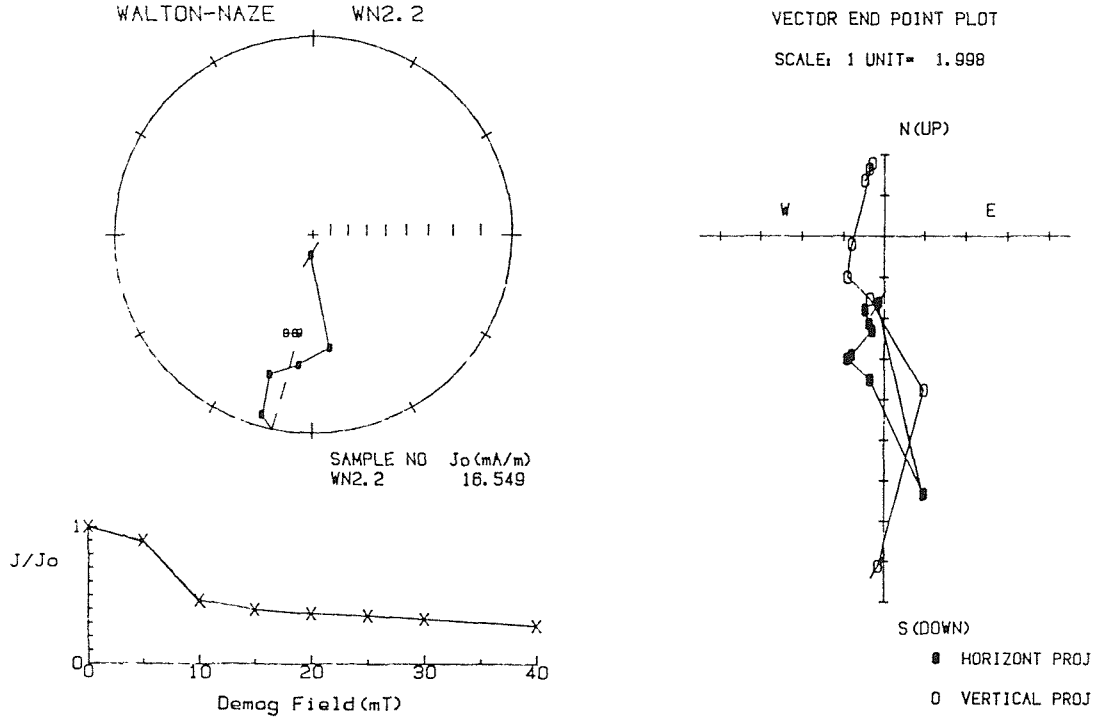

Fig 6.4 Typical reverse polarity specimens from the Walton-on-the-Naze section. The lower plot is for a specimen from the Harwich Member, and the upper plot is for a specimen from the Walton Member. For explanation of symbols see Fig 2.7.

6.2.2 IRM analysis

Representative specimens from three of the East Anglian sections were subjected to IRM analysis. Results for individual specimens are presented in Table 6.1, including the IRM-ratio and peak IRM values, as well as the NRM intensities.

6.2.2.1 Levington

Three specimens from the section were processed (Table 6.1). The HSB is positioned at 1.2m above the base of the section. The lower part of the section is magnetically different to the upper part, with much greater IRM-ratios and peak IRM values. NRM intensities generally show a decrease with ascending stratigraphic height. This behaviour is probably related to a change of the magnetic mineralogy in the section. The lower part is characterised by magnetite (or maghemite) -rich sediments and the upper part by hematite-rich sediments.

6.2.2.2 Walton-on-the-Naze

Three specimens from each of the Harwich and the Walton Members were processed (see Table 6.1). The base of the Walton Member is at 4.0m in the section (between specimens WN6.1 and 7.1). The specimens from the Harwich Member generally have greater IRM-ratios and slightly higher peak IRM values. The two specimens adjacent to the Harwich/ Walton member junction exhibit intermediate IRM behaviour. NRM intensities decrease upsection in a similar fashion (typical values for the Harwich Member being about 10mA/m, and for the Walton Member 0.5mA/m).

6.2.2.3 Wrabness

Six specimens from the Harwich Member and two specimens from the Walton Member were processed (Table 6.1). The HSB is positioned at 0.41m in the section and the base of the Walton Member is at 10.0m. An abrupt change in the magnetic properties of the sediment occurs between specimens WR1.19 and WR1.14. Below this level the IRM-ratio and peak IRM

values are typically about 0.95 and >10000 mAm^2 respectively. Above this level, the values are much lower (0.75 and 1000 mAm^2). The NRM intensity data (listed in Townsend, 1982) suggest that the transition takes place at 3.0m above the base of the section (between sites WR1.18 and WR1.15). This behaviour is again probably related to changes in the magnetic mineralogy, with the magnetic properties of lower parts of the section being dominated by magnetite, and those of the upper parts by hematite.

locality	Mbr	specimen	pol	height (m)	NRM (mA/m)	IRM ratio	peak IRM (mAm^2)
Levington	H	LV11.2	N	8.15	2.11	.74	1427
	H	LV5.2	N	2.85	12.39	.87	3512
	H	LV2.2	N	0.40	30.16	.97	12502
Walton-on	W	WN16.2	R	11.20	0.31	.73	1311
the-Naze	W	WN10.1	R	5.40	0.38	.77	1132
	W	WN7.1	R	4.05	2.14	.90	4658
	H	WN6.1	R	3.90	5.25	.85	3437
	H	WN4.1	R	2.75	7.92	.94	8446
	H	WN1.1	R	0.00	15.13	.96	1320
Wrabness	W	WR2.4	R	11.68	1.14	.83	682
	W	WR2.2	R	10.63	1.45	.74	1201
	H	WR1.2	N	9.18	1.82	.70	1167
	H	WR1.3	N	8.33	8.57	.81	4264
	H	WR1.8	N	5.59	1.10	.71	1214
	H	WR1.14	N	3.46	2.41	.76	1951
	H	WR1.19	R	1.29	26.43	.95	14749
	H	WR1.23	R	0.00	30.96	.95	20920

Table 6.1 The IRM acquisition and NRM intensity data for the East Anglia London Clay Formation sections.

6.2.3 East Anglia sections: summary and conclusions

The magnetostratigraphic results from the sections at Levington, Walton-on-the-Naze, Wrabness and Harwich are presented in Fig 6.3. The two most distant localities are only 25km apart (Levington and Walton-on-the-Naze), and there are only minor variations in the lithology between the sections. The HSB in the Harwich Member and the glauconitic base of the overlying Walton Member are the most important stratigraphic markers.

The core-drilled specimens taken from the HSB at Levington, Wrabness and Harwich are all reverse polarity. At Levington, the sediments above and below the HSB are normal polarity. At Wrabness, a normal polarity zone commences at 2.6m above the HSB and continues to the top of the Harwich Member. Two reverse polarity sites are present in the lower part of the Walton Member. At Walton-on-the-Naze, the Harwich Member is reverse polarity, as is the bulk of the Walton Member. At Harwich, only the reversely magnetised HSB was sampled.

The normal polarity zones at Levington and Wrabness appear to be correlative; however, they are probably the result of a recent weathering overprint. If the normal polarity zone in the two sections was the result of a simple DRM, then its base and top are clearly diachronous. Both sections are in degraded river-cliffs, where the rates of erosion are likely to be much lower than in the sea-cliff at Walton-on-the-Naze (where the cliffs are receding at about 1m per year). However, the magnetostratigraphic data alone cannot explain the reverse polarity Walton Member which overlies the altered sediments in the Wrabness section. Assuming Townsend (1982) correctly interpreted the demagnetisation data from the Walton Member, an explanation is required.

The results from the "fresher" section at Walton-on-the-Naze are critical to the argument. The Harwich and Walton Members in this section are dominantly reverse polarity. The NRM intensity and IRM data indicate that the magnetic properties of the two members are quite different

(the Harwich Member being dominated by magnetite and the Walton Member by hematite). Assuming a similarly hematite-rich Walton Member at Wrabness, it may have been unaffected by the normal polarity overprint, and thus retained its reverse polarity DRM. The upper part of the Harwich Member (originally magnetite rich) was, however, altered and acquired a normal polarity magnetisation. The argument is strengthened further by the fact that the base of the (now) hematite rich normal zone terminates 0.6m above reverse polarity, magnetite-rich sediments.

The normal polarity sites at Levington are also believed to be the result of weathering. The top of the section is more altered (the magnetic mineralogy being dominated by hematite) with the base only partially oxidised to maghemite. Fortunately, the calcite-cemented HSB appears to have retained its original reverse polarity magnetisation.

It is concluded that both the Harwich and Walton Members of the London Clay Formation in East Anglia are characterised by reverse polarity. The previously held view, that the Harwich Member was in part normal polarity can now be discarded. As the members span the Apectodinium hyperacanthum to Wetzeliella meckelfeldensis dinoflagellate zones they are correlative with Chron C24BR. The sampling of the other, smaller calcite concretions in the Harwich Member may prove useful to further studies.

6.3 KENT

6.3.1 Shelford

Townsend (1982) examined the section at Herne Bay, where the beach and cliffs expose a succession from the top of the Thanet Formation up to the lower part of the London Clay Formation. The section was found to be reverse polarity, except for a thin normal polarity zone identified in the upper part of the Oldhaven Formation.

A section at the nearby Shelford sand pit (TR 160600), 3km to the north-east of Canterbury, has a well exposed Palaeogene sequence extending from the base of the Woolwich Formation to division A3 of the London Clay Formation. A detailed description of the section was given by Ward (1972). The unconsolidated lithologies of the Woolwich Formation were not sampled. A black flint pebble bed (0.3m thick) rests on top of the Woolwich Formation, marking a significant hiatus. The bulk of the Oldhaven Formation above comprises a series of well-sorted, fine grained, glauconitic sands, 5.2m thick. Sampling of this formation was restricted to five sites where thin clay seams outcrop. The lowest 7m of the overlying Walton Member (A2) of the London Clay Formation was sampled at 0.5m intervals.

All the specimens were weakly magnetic (about 0.5mA/m). Demagnetisation was carried out with maximum fields varying between 10 and 40 mT. Polarity determinations are based on demagnetisation "trends" (example plots are shown in Fig 6.5). The magnetostratigraphic results are presented in Fig 6.6. The Oldhaven Formation was found to be dominantly reverse polarity. The London Clay Formation is also reversely magnetised, except for two normal polarity sites in the London Clay Basement Bed.

The magnetostratigraphic results from Herne Bay and the lowest 5m of the Harty borehole are drawn alongside the Shelford section results in Fig 6.6.

6.3.2 The Oldhaven Formation

Results from exposures of this formation at Shelford are somewhat different to those from the other two

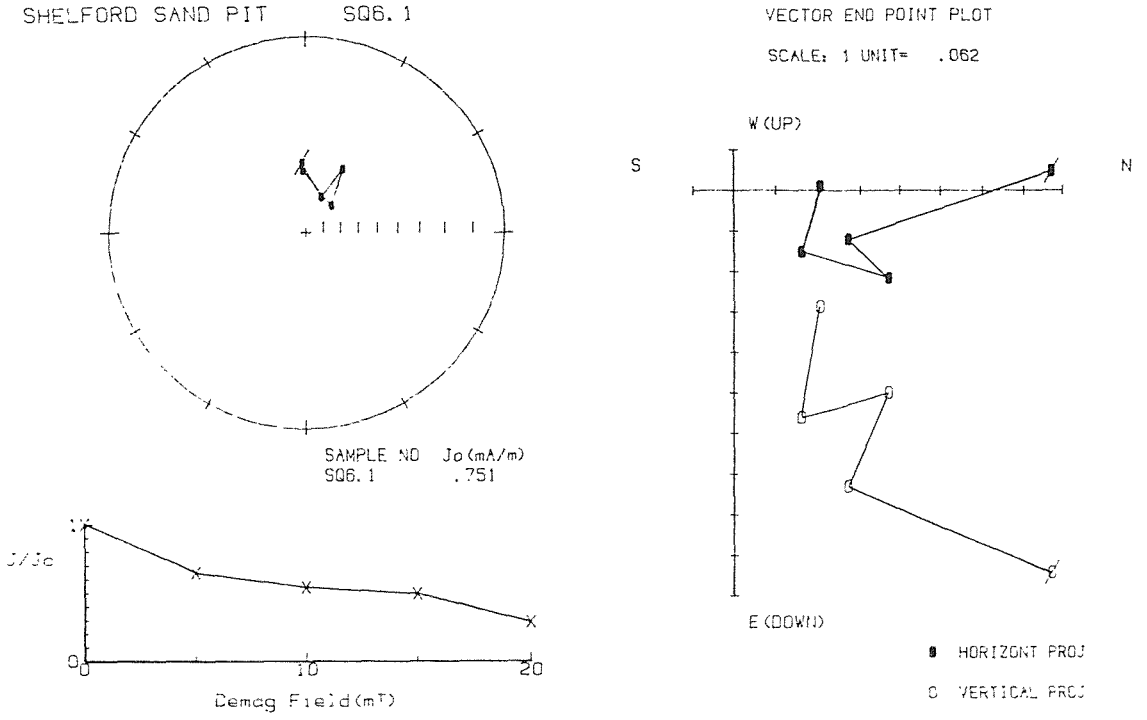

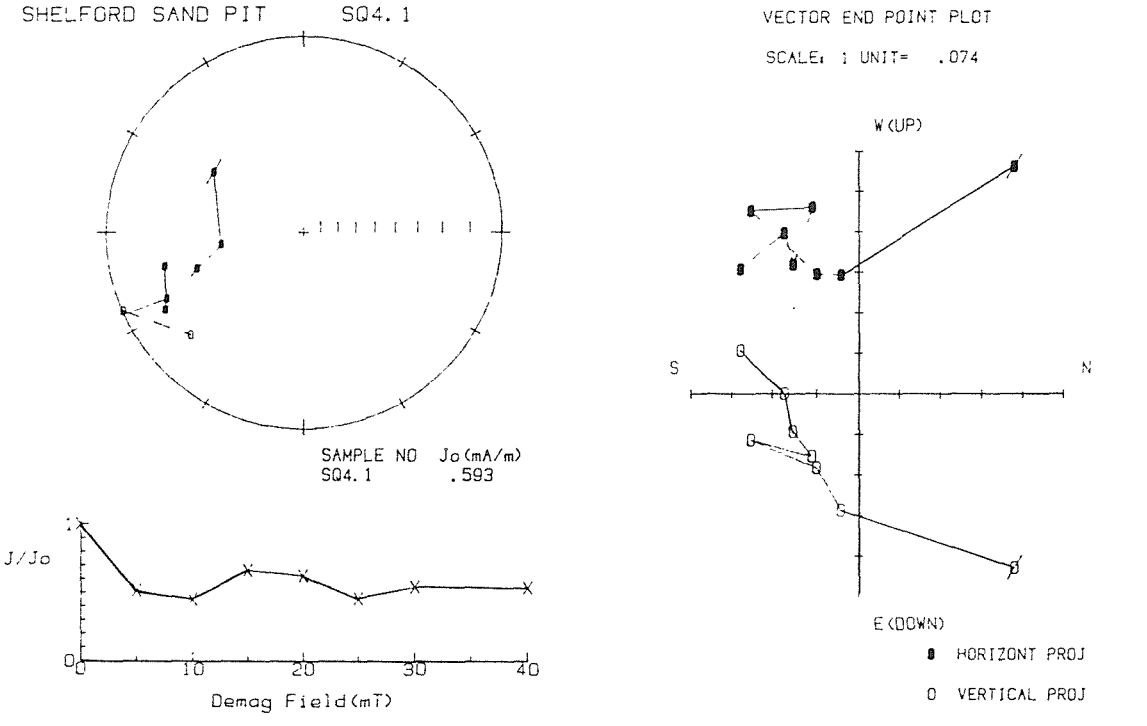

Fig 6.5 Examples of demagnetisation plots from the section at Shelford. The upper plot shows a specimen from Division A1 with a normal polarity. The lower plot shows a specimen from the Oldhaven Formation with a reverse polarity. For explanation of symbols see Fig 2.7.

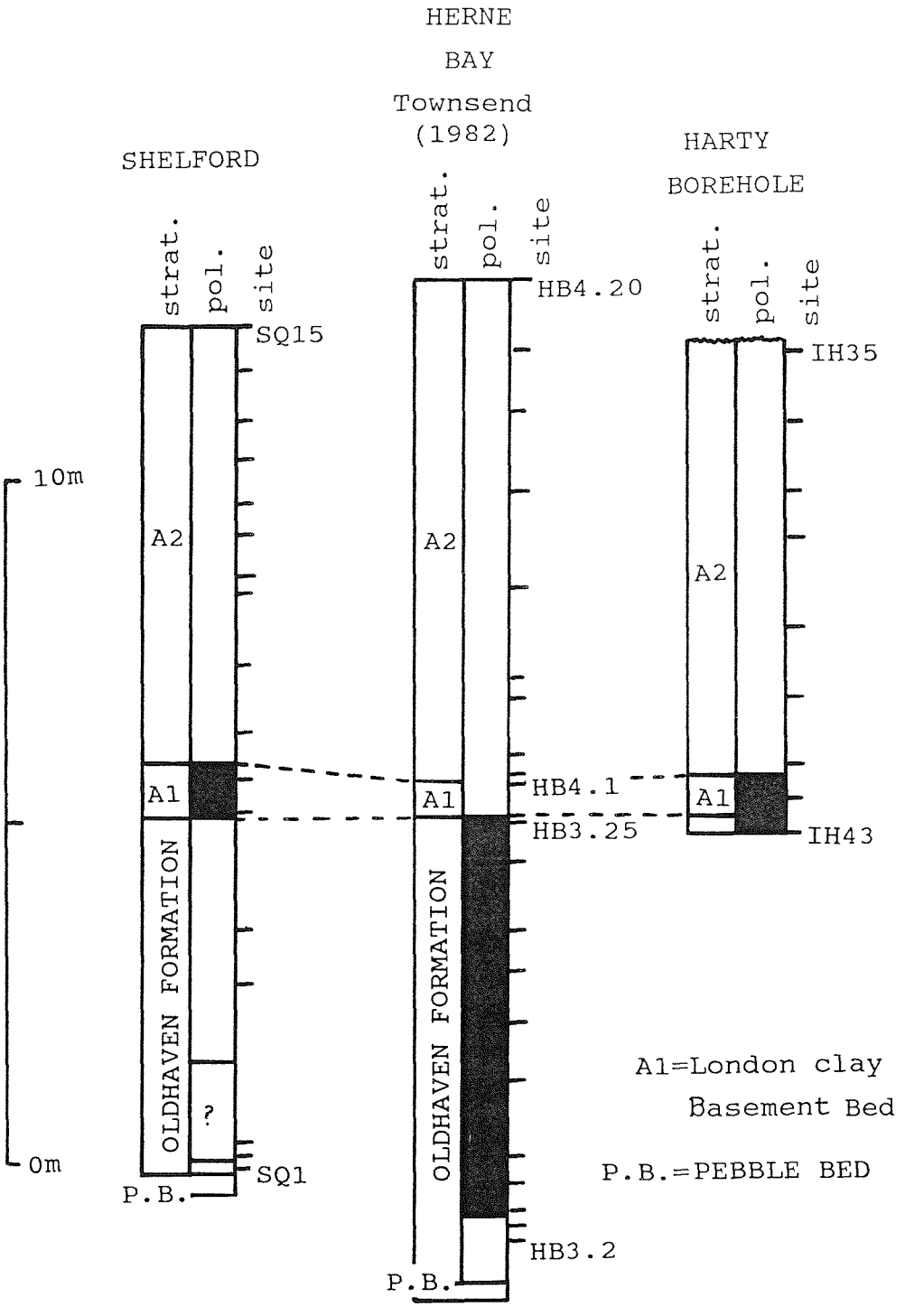

Fig 6.6 The magnetostratigraphy of the Oldhaven Formation and lower part of the London Clay Formation in Kent.

localities (the single specimen from the top of the formation at Harty carries a normal polarity magnetisation, as does most of the formation at Herne Bay). IRM measurements were carried out on representative specimens from the three localities. At Shelford the NRM intensites are typically about 0.5mA/m, and the remanence is probably carried by hematite (a typical IRM plot is shown in Fig 6.7). At Herne Bay and Harty, the NRM intensities are typically about 10mA/m and the remanence is probably carried by magnetite (a representative IRM plot is also shown in Fig 6.7)

It is unlikely that the formation at Shelford has suffered a recent weathering overprint (which in any case would have produced a normal polarity CRM). Two explanations are possible. The first is that the sampling interval at Shelford was too coarse, and the strongly magnetic normal polarity material was not sampled. A second explanation is that the specimens from Herne Bay and Harty (which were demagnetised only to 20mT) did not have the present-day normal polarity viscous components fully removed. (The source of the strongly magnetic material is thought to be disseminated volcanic ash, described by Knox (1983), which is perhaps locally concentrated at Herne Bay and Harty.) The second explanation is considered the more likely.

6.3.3 The London Clay Formation

The base of the London Clay Formation is characterised by an oxidised, glauconitic, clayey silt, 0.8 to 1.0m thick, previously referred to as the London Clay Basement Bed. This bed may in fact represent part of division A1 (C. King, pers. comm.). At Shelford and Harty this unit carries a normal polarity. The single site in the unit at Herne Bay was reverse polarity; however this site was in the upper 5cm of the bed. This normal polarity level is thought to represent a short term magnetic "event", an assumption which is strengthened by the presence of two normal polarity sites in a similar unit in the Formation de

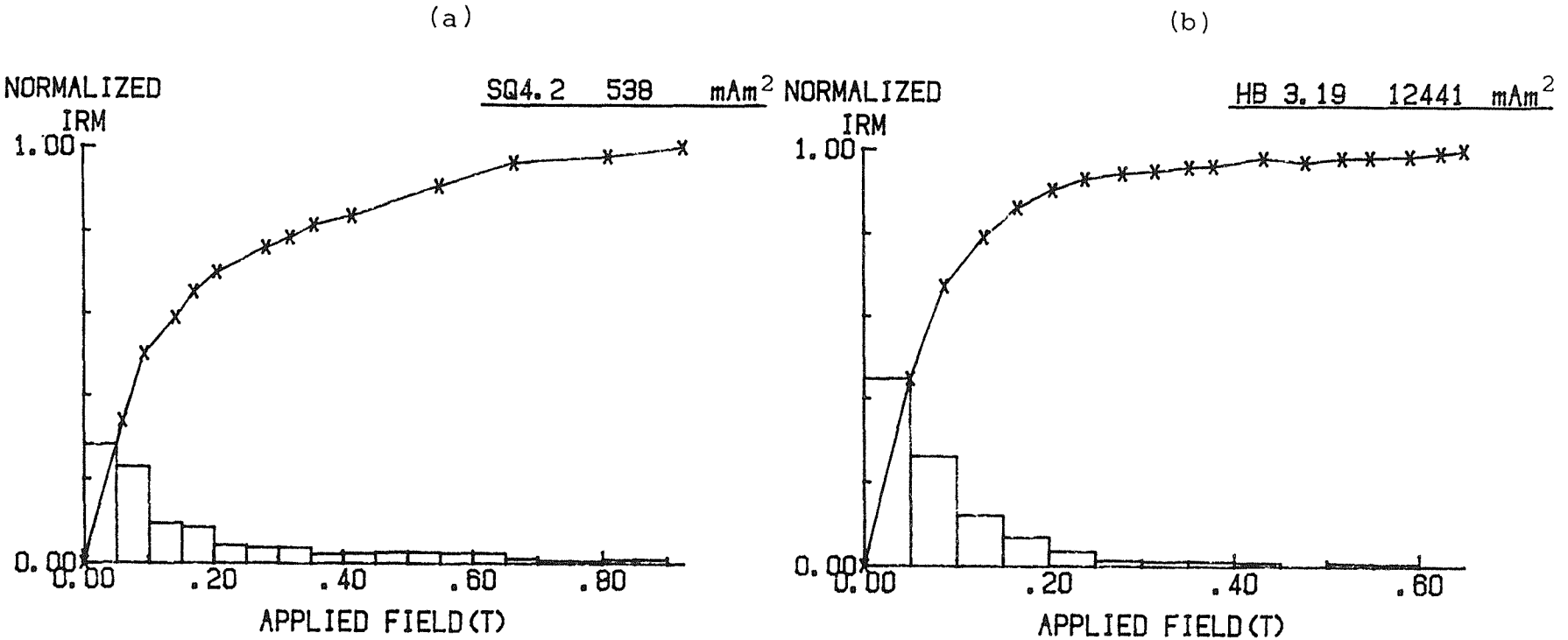

Fig 6.7 Typical IRM plots for specimens from the Oldhaven Formation of north Kent. The specimen from Shelford (a) has a remanence carried by hematite, whereas the specimen from Herne Bay (b) has a remanence carried by magnetite.

Varengeville, near Dieppe (see Chapter 9). The remainder of the London Clay Formation (A2) is reverse polarity.

6.3.4 Kent sections: summary and conclusions

Contrary to the conclusions of Townsend and Hailwood (1985), based on preliminary investigations, the Oldhaven Formation of SE England is now thought to be characterised by reverse polarity. The London Clay Basement Bed (?A1) is in part normal polarity; however a reexamination of this interval is recommended to accurately define the nature of the magnetisation. The sections at Herne Bay, Shelford and Swanscombe require to be sampled in detail.

The Walton Member of the London Clay Formation in Kent is reverse polarity. This is in keeping with similar results from the member at Harty, Walton-on-the-Naze, Whitecliff Bay and other localities.

6.4 The Tilehurst Member

King (1981) divided the Oldhaven Formation in the west and north of the London Basin and in the Hampshire Basin, into the Twyford (lower) and Tilehurst (upper) Members. In the London Basin, the Tilehurst Member is overlain by the Swanscombe Member (A1). In the Hampshire Basin, the Swanscombe Member is absent and the Tilehurst Member is overlain by the Walton Member (A2). Knox et al (1983) examined material from the Tilehurst, Swanscombe and Walton Members at five sections across the London and Hampshire Basins. Using dinoflagellates, they demonstrated that the Tilehurst Member is younger in the Hampshire Basin than in the eastern part of the London Basin. Townsend (1982) examined the magnetostratigraphy of the Tilehurst and Swanscombe Members at Harefield, in Middlesex. In the present study, sections through the Tilehurst and Walton Members at Whitecliff Bay and Tilehurst were investigated and the results are compared with those obtained from the section at Harefield.

6.4.1 Whitecliff Bay

Costa and Downie (1976) identified the Wetzeliella meckelfeldensis dinoflagellate zone at about 5m above the base of the London Clay Formation at Whitecliff Bay. Knox et al (1983) did not examine material from the Whitecliff Bay section, but they identified the W. meckelfeldensis zone at the base of the Tilehurst Member in the Bunker's Hill borehole, 35km to the northwest. For the present study, three sites in the Tilehurst Member and two sites in the Walton Member were sampled at Whitecliff Bay (SZ 640860). NRM intensities for this 4.35m section were typically in the range 1-2mA/m. All five sites carry a clear reverse polarity magnetisation, although only one specimen had a well-defined SEP (typical demagnetisation plots are shown in Fig 6.8).

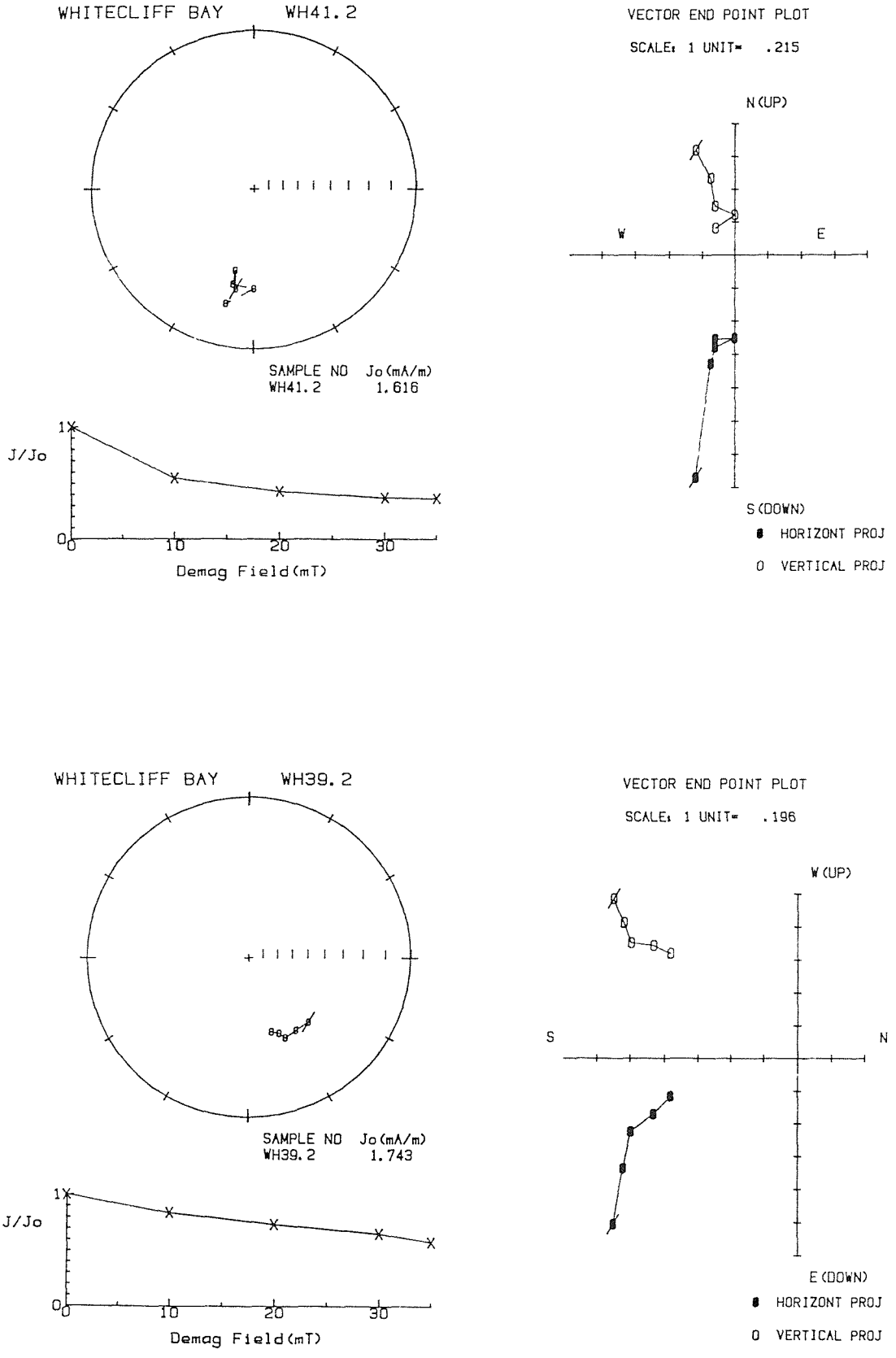

Fig 6.8 Typical reverse polarity specimens from the Tilehurst Member at Whitecliff Bay. For explanation of symbols see Fig 2.7.

6.4.2 Tilehurst

The Tilehurst Member stratotype (King, 1981) is exposed in the disused pit at Tilehurst (SU 683734), near Reading. Four metres of clayey silts and fine grained sands lie on top of the Reading Formation, and are topped by the Walton Member. Knox et al (1983) assigned the Tilehurst Member at this locality to the Wetzeliella astra dinoflagellate zone. The exposure is not ideal, being rather overgrown and degraded. A total of twelve stratigraphic levels were sampled, one in the Reading Formation, nine in the Tilehurst Member and two in the Walton Member.

NRM intensities are typically in the range 5-10mA/m throughout the section. Specimens were demagnetised in peak alternating fields up to between 20mT and 50mT. All specimens had an MDF of 6mT or less. Typical demagnetisation data are presented in Fig 6.9. The magnetostratigraphic results are presented in Fig 6.10. The single site at the top of the Reading Formation is reverse polarity. Sites TH5, TH6 and TH8 in the Tilehurst Member are normal polarity, as are the two sites in the Walton Member.

Four specimens from the Tilehurst Member and two specimens from the Walton Member were chosen for IRM analysis. Typical IRM acquisition data are shown in Figs 6.11 and 6.12. There is a general decrease in both the peak IRM (2400 to 600 mAm^2) and the IRM-ratio (0.9 to 0.75) with ascending stratigraphic position. The IRM behaviour becomes increasingly "hematite-like" upsection, which is rather curious as the MDF of all the specimens is very low. The magnetic properties show no systematic change across the base of the Walton Member as is the case at Walton-on-the-Naze and Harty.

Knox et al (1983) assigned the lower half of the Tilehurst Member at Harefield to the Apectodinium hyperacanthum zone and the upper half of the member to the W. astra zone. Townsend (1982) identified two normal polarity sites near the base of the Tilehurst Member at this locality (Fig 6.10). These two normal sites are tentatively correlated with the interval +1m to +2.5m in

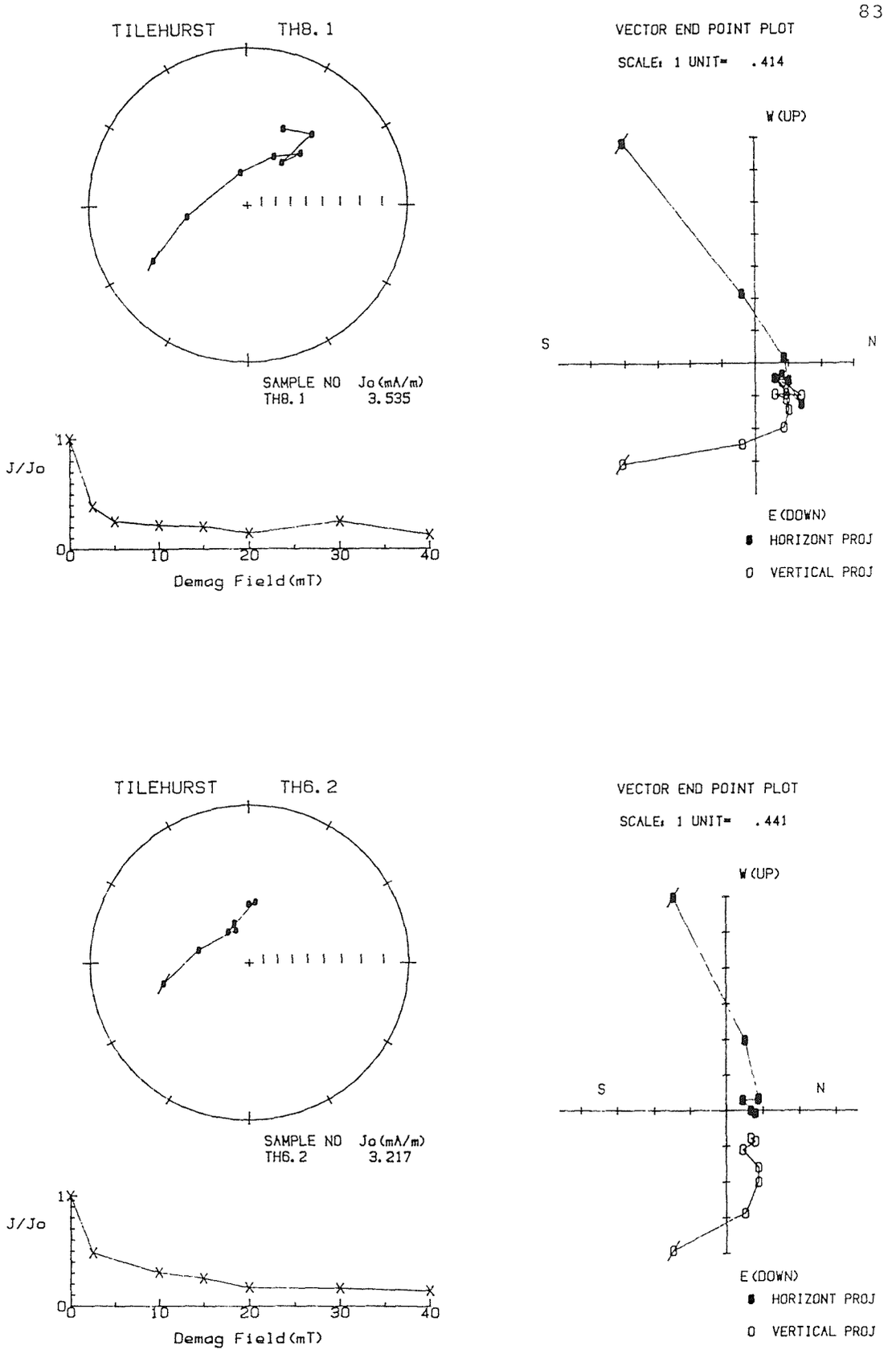

Fig 6.9 Typical normal polarity specimens from the Tilehurst Member at Tilehurst. For explanation of symbols see Fig 2.7.

——— magstrat. corr.

— — biostrat. corr.

W.m.= Wetzeliella meckelfeldensis

W.a.= Wetzeliella astra

A.h.= Apectodinium hyperacanthum

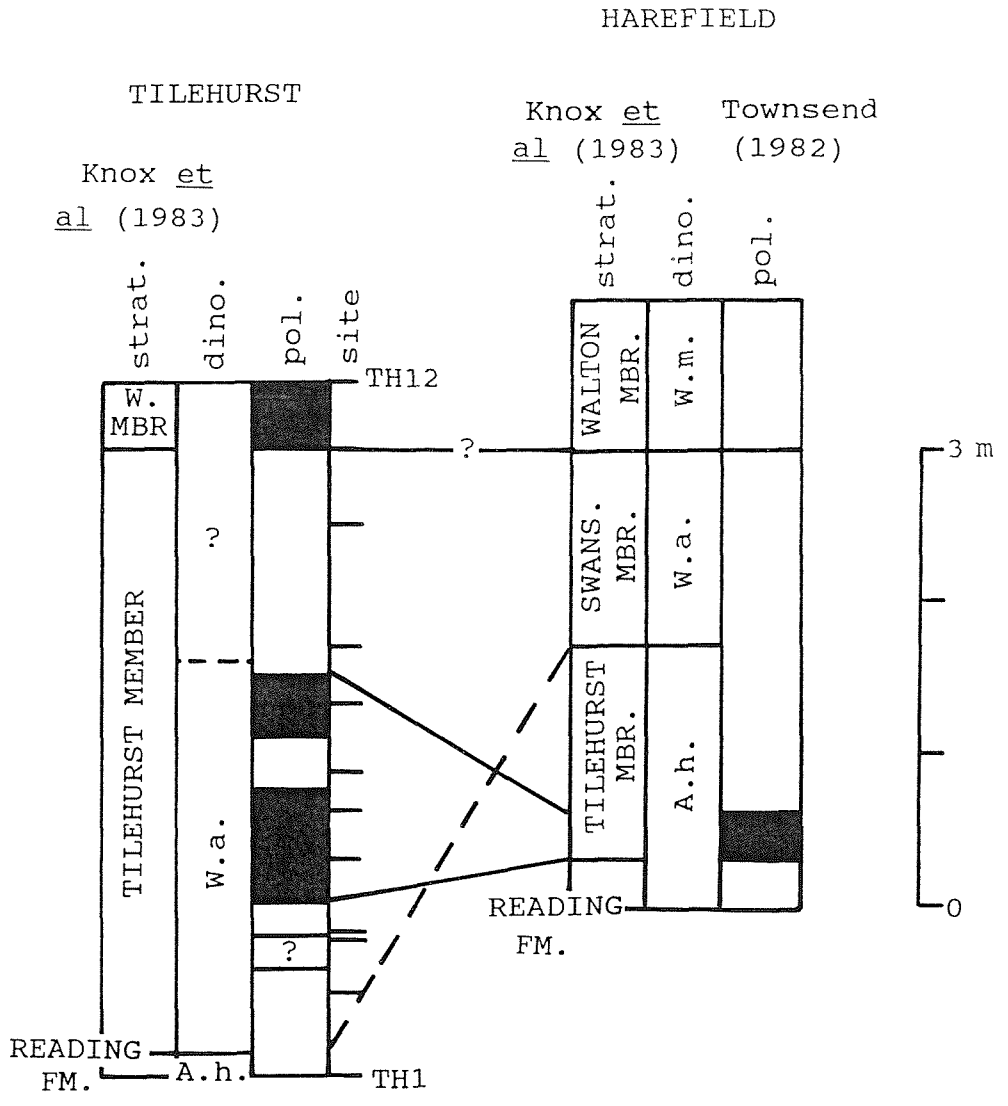

Fig 6.10 The magnetostratigraphy of the Tilehurst Member at Tilehurst and Harefield.

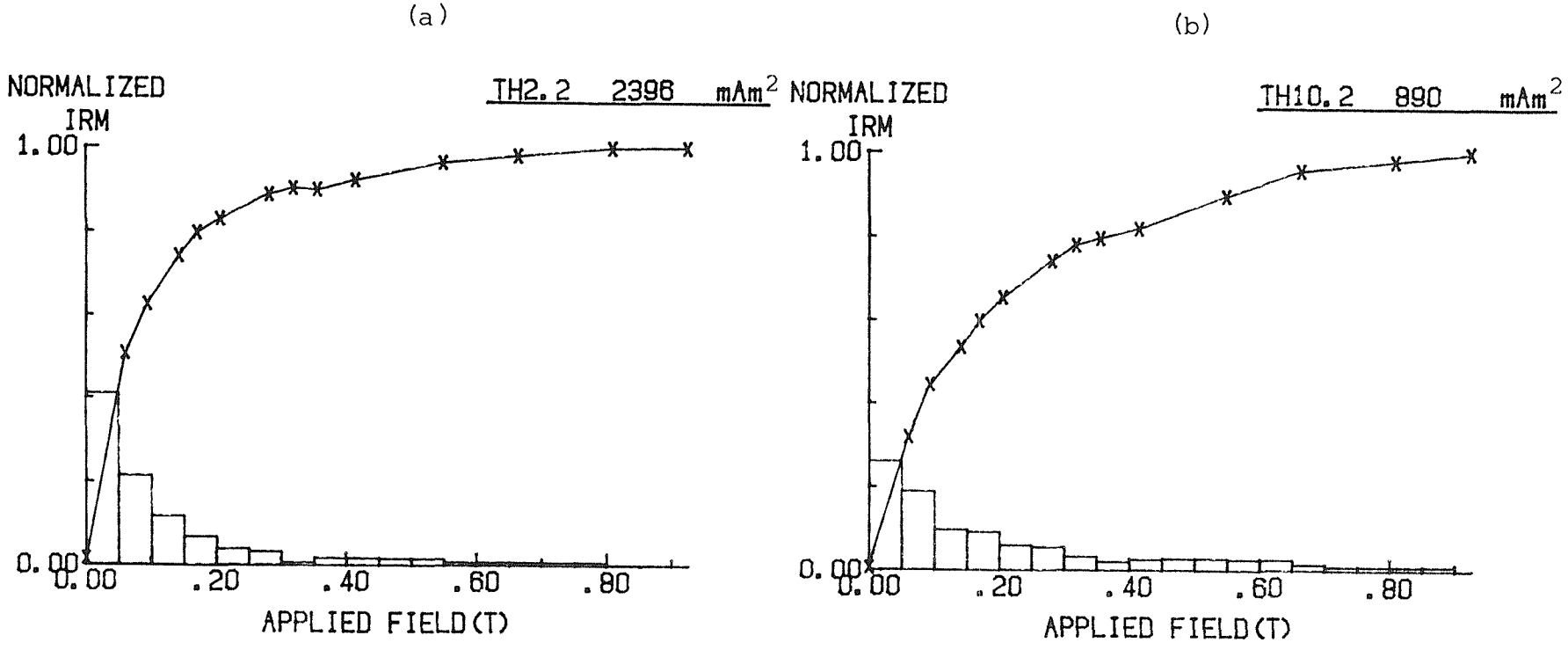

Fig 6.11 Typical IRM plots for specimens from the Tilehurst Member at Tilehurst. The curves both show that the remanence for this unit is carried by hematite, although TH2.2 (a) may contain a small proportion of magnetite.

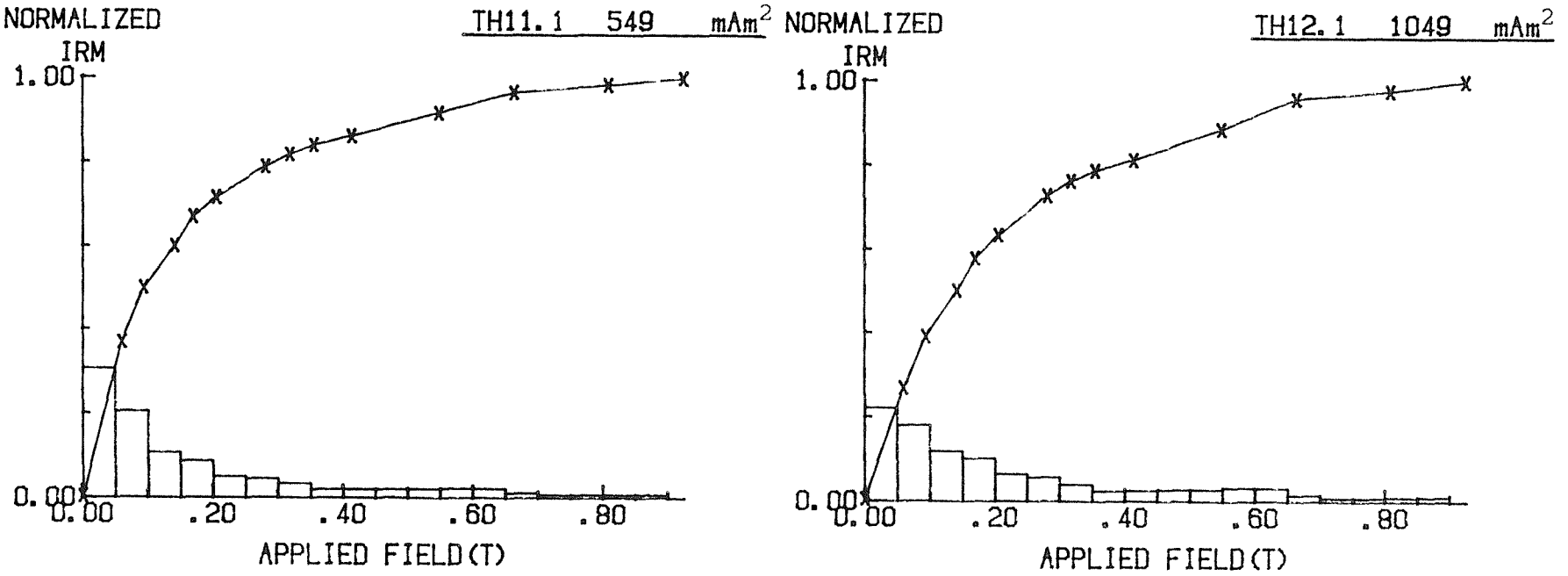

Fig 6.12 Typical IRM plots for specimens from the Walton Member at Tilehurst. The plots show that the remanence of this unit is also dominated by hematite.

the Tilehurst section. The implication of such a correlation is that the W. astra zone is diachronous between the two localities. The normal polarity sites in the Walton Member are rather unusual as the unit is dominantly reverse polarity at more than half a dozen localities in SE England; however the sites at Tilehurst only span 0.45m.

6.4.3 Tilehurst Member: summary and conclusions

Knox et al (1983) demonstrated that both the base and top of King's (1981) Tilehurst Member are diachronous across southern England. The palaeomagnetic data from Whitecliff Bay and Tilehurst support this theory, as normal polarity sites in the member at Tilehurst were not identified at Whitecliff Bay. The normal polarity sites do correlate with levels in a similar section at Harefield (45km to the east); however this correlation implies diachroneity of the base of the W. astra zone.

This palaeomagnetic study has demonstrated that both the Tilehurst Member and the base of the W. astra dinoflagellate zone are probably diachronous in central southern England. Many workers are expressing doubts about the validity of the W. astra zone in particular. Suggested future work to resolve whether the Tilehurst Member and/or the W. astra zone are diachronous are outlined in Section 6.6.

6.5 Correlation of the basal part of the London Clay Formation in southern England

The basal part of the London Clay Formation has been investigated in five areas (East Anglia, Kent, Harefield, Tilehurst and Whitecliff Bay). Between one and four sections from each of the areas has been used to define a local magnetostratigraphic section. In doing this, problems associated with weathering CRM's, incomplete demagnetisation and interpretation of some of the sections, and the validity of short-term magnetic "events" within the areas have been resolved.

Most of the sections investigated by Townsend (1982) and the present study have also been studied for dinoflagellates. A correlation of the magnetostratigraphic sections for each area is attempted using the palaeomagnetic and biolithostratigraphical data in Fig 6.13.

At Whitecliff Bay, the dinoflagellate and palaeomagnetic data suggest that the Tilehurst Member at this locality is significantly younger than the Palaeocene/Eocene boundary. The levels assigned to the Tilehurst Member (used by King, 1981, as a chronostratigraphic unit) may represent a near shore facies, equivalent in age to the base of the Walton Member in the eastern part of the London Basin.

The sections in Kent, Harefield and Tilehurst span the Palaeocene/Eocene boundary. It is proposed to correlate the normal polarity sites in the London Clay Basement Bed at Kent (and Varengeville) with those in the lower half of the Tilehurst Member at Harefield and Tilehurst. The two units are assigned to the W. astra zone (although as pointed out in the preceeding section, this zone is diachronous between Harefield and Tilehurst).

Townsend and Hailwood (1985) used the normal polarity magnetozones identified in the upper part of the Oldhaven Formation and the upper part of the Harwich Member to correlate the two units. This correlation was quite logical because the two units are assigned to the upper part of the Apectodinium hyperacanthum zone, but it cast doubts on King's (1981) model, in which the Oldhaven Formation is older than the Harwich Member. The present study has shown that the two units are in fact reverse polarity. From the palaeomagnetic data alone, it is not possible to resolve the exact stratigraphic relationship of the Oldhaven Formation and the Harwich Member.

King (1981: p 113) discusses the literature dealing with the dinoflagellate zones at the Harwich/Walton Member junction in East Anglia. He suggests that the base of the W. astra zone occurs just above the base of the Walton Member, with the FAD of W. meckelfeldensis at about 5m

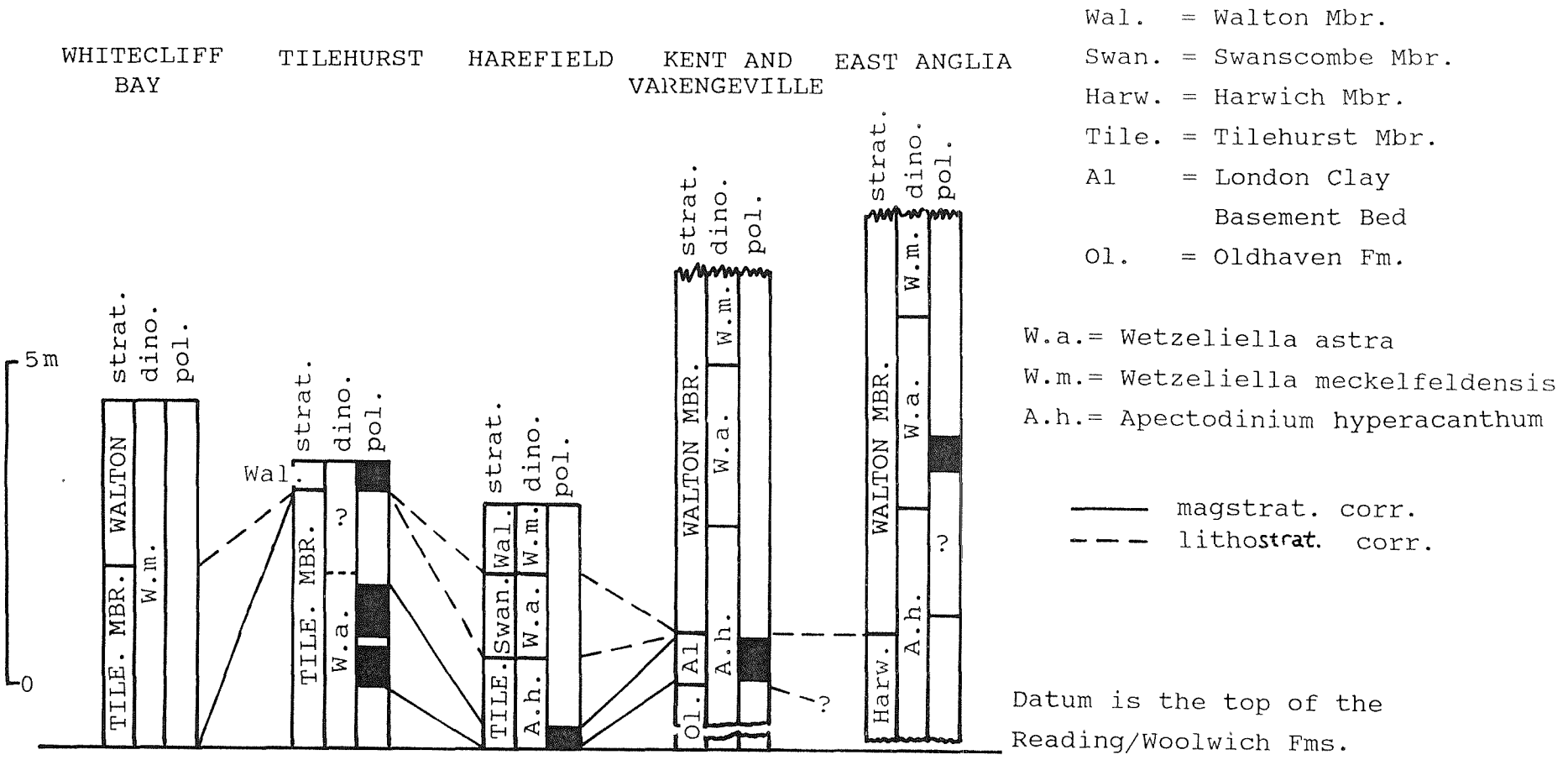

Fig 6.13 The proposed magnetostratigraphic correlation of the Oldhaven Formation and the basal part of the London Clay Formation across southern England.

above the base of the same member. It is therefore possible that the normal polarity sites in the London Clay Basement Bed and the Tilehurst Member may correlate with the sites in the lower part of the Walton Member in East Anglia (in the Walton-on-the-Naze section, Sites WN8,9 and 10 have indeterminate polarities and site WN11 is normal polarity). Such a correlation is possible since all the sites are within the W. astra zone. However, this would then imply diachroneity of the base of the Walton Member across southern England (something other workers may strongly disagree with). It could be argued that it is possible to correlate the two normal polarity sites at the base of the Walton Member at Tilehurst with the normal polarity site in this member at Walton-on-the-Naze. This correlation necessitates a small hiatus within the lower part of the Walton Member in East Anglia to accommodate the period of time during which the London Clay Basement Bed in Kent was being deposited. Such a hiatus is not known in the stratotype section at Walton-on-the-Naze. The author would prefer to see an updated study of the dinoflagellate stratigraphy of key areas before commenting further.

6.6 Summary and conclusions

Normal polarity sites identified in the London Clay Basement Bed and the Tilehurst Member may be of use in defining the Palaeocene/Eocene boudary in southern England. In most of the sections the normal polarity sites are within the W. astra dinoflagellate zone. However, the palaeomagnetic and lithostratigraphic evidence from the Harefield and Tilehurst sections suggest that the W. astra zone may be slightly diachronous. Workers using this zone for detailed correlations between sections in southern England must proceed cautiously and make use of all available data.

The palaeomagnetic specimens used in Townsend's (1982) study, and in the present study, would be ideal for investigating the association of the W. astra zone with the Palaeocene/Eocene boundary in southern England. The sites

are positioned with an accuracy of to within a few centimetres and the polarity for each specimen is also available. Such a study would allow the dinoflagellate zonation scheme to have a potential resolution similar to that of the palaeomagnetic study. If suitable borehole material from Middlesex and Essex (or indeed anywhere in the London Basin) were to become available, this would provide an excellent opportunity for an integrated magneto-litho-biostratigraphic study. This is the best way to resolve the Oldhaven Formation/Harwich Member correlation problem.

Chapter 7 Results from the Early Eocene of southern England

7.1 Introduction

This chapter deals with work carried out on the London Clay and Virginia Water Formations at Sheppey, and the London Clay and Wittering Formations at Whitecliff Bay. The sections at the two localities provide the best opportunity to investigate the Early Eocene magnetostratigraphic history of southern England (and indeed NW Europe). The Sheppey sections include material from two boreholes which, together, span the entire unexposed part of the London Clay Formation (80m).

The palaeomagnetism of the section at Whitecliff Bay was first studied by Townsend (1982). A reexamination of parts of the London Clay and Wittering Formations at this locality has been carried out. The magnetostratigraphic results from the two localities are then compared, and a number of normal polarity magnetozones, which have been identified in both sections, are correlated with the magnetic polarity time-scale of Berggren et al (1985).

7.2 The Isle of Sheppey

The Isle of Sheppey is situated 70km east of London, on the north Kent coast (Fig 4.1). The world famous London Clay Formation exposures have yielded a rich and varied biota, and have been studied scientifically since the 18th century. Important contributions include Prestwich (1847 and 1854), Whittaker (1872), Davis (1936), King (1981 and 1984) and Islam (1983 b).

The London Clay Formation at Sheppey is 140m thick, although only the upper 53.5m is exposed. King (1984) published the first detailed stratigraphic account of the exposed portion. The unexposed part of the formation is known from a number of boreholes, notably the Sheerness New Town Well (Shrubsole, 1878). The London Clay Formation rests unconformably on the Oldhaven Formation and is topped conformably by the Virginia Water Formation. A detailed

correlation of the London Clay Formation in this area with exposures in Essex and the London area has been achieved by King (1981 and 1984).

For this study, the unexposed Oldhaven and London Clay Formations were sampled using material from two recently cored boreholes. The exposed London Clay and Virginia Water Formations were sampled at three localities along the northern coast of the isle. The positions of the two boreholes and the three coastal exposures are shown in Fig 7.1.

7.3 Demagnetisation characteristics

Specimens from the Oldhaven and London Clay Formations have NRM intensities in the range 10-30mA/m, whilst those from the Virginia Water Formation have values of 2-5mA/m. Most of the specimens were processed in maximum fields varying between 25 and 40 mT, which reduced the intensity to around 25% of the initial value. The majority of specimens carry a low stability component (?VRM) which is removed by the 10 mT step. Some specimens also carry a stronger component (presumed to be secondary) which may or may not be removed at the highest applied fields. Approximately 35% of the specimens produced SEP directions, over 60% showed well-defined directional "trends", and 3% had indeterminate polarities. A selection of representative demagnetisation plots is shown in Figs 7.2 to 7.6.

7.4 The unexposed Oldhaven and London Clay Formations

The unexposed part of the London Clay Formation at Sheppey totals over 80m. In 1984, the Harty and Warden Bay boreholes (with a 12m stratigraphic overlap) were drilled at Sheppey, providing a complete section through the London Clay Formation down to the Oldhaven Formation. The two cores were sampled at 1m intervals providing ninety-two palaeomagnetic specimens.

7.4.1 The Harty borehole

The Harty borehole (TR 015665) was drilled at the south-eastern corner of Sheppey. The borehole section

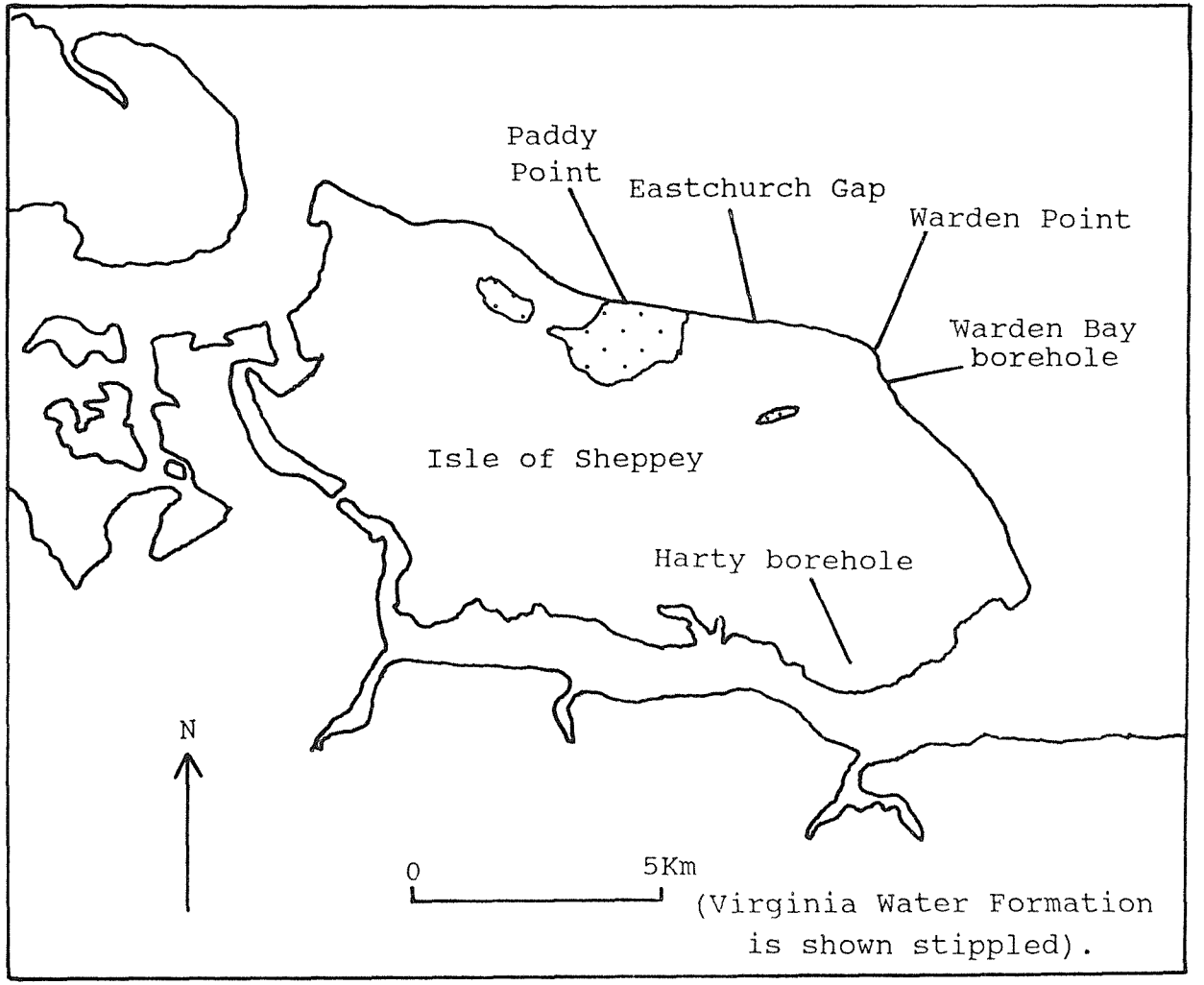

Fig 7.1 The location map of the Isle of Sheppey.

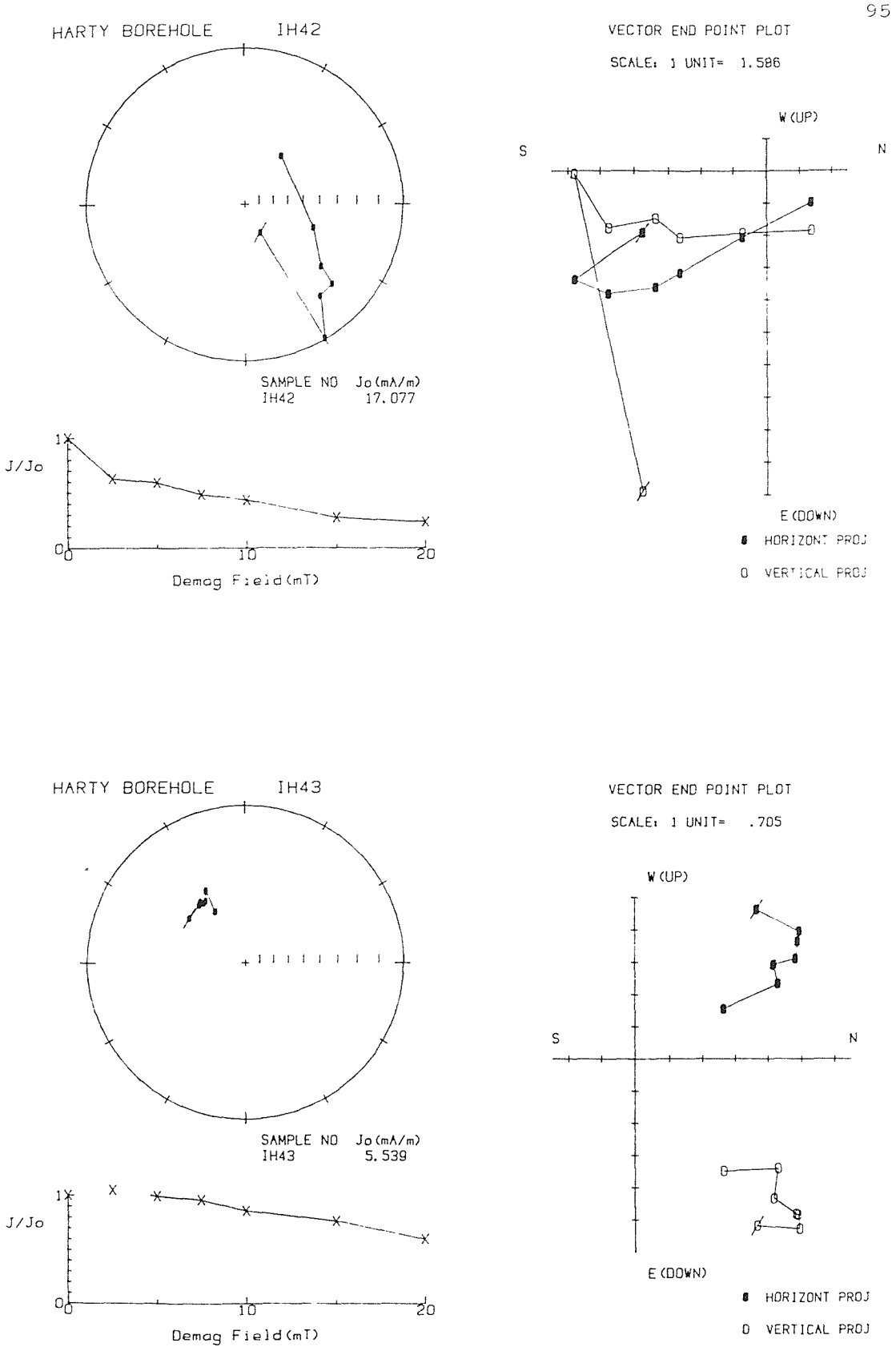

Fig 7.2 Normal polarity specimens from the lower part of the Harty borehole. The upper plot shows the single specimen form Division A1 of the London Clay Formation. The lower plot shows the single specimen from the Oldhaven Formation. For explanation of symbols see Fig 2.7. The declination is arbitrary with these borehole specimens.

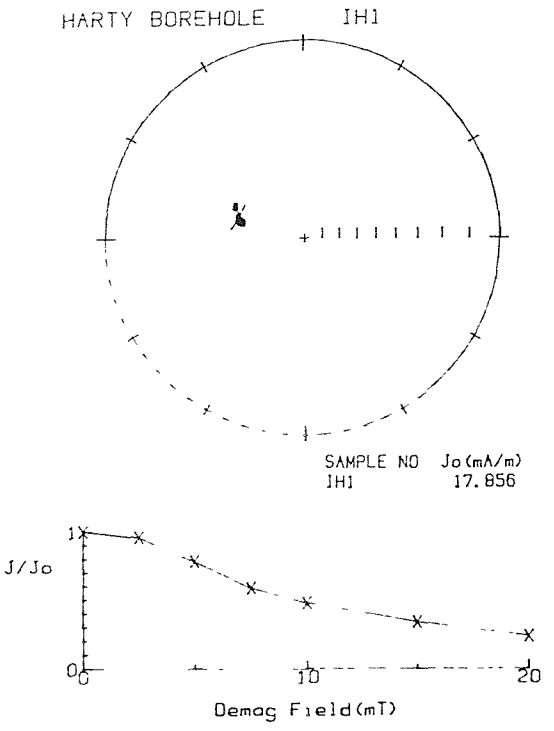

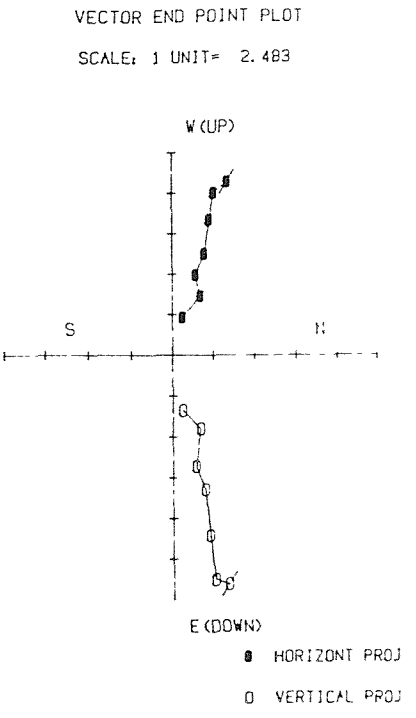

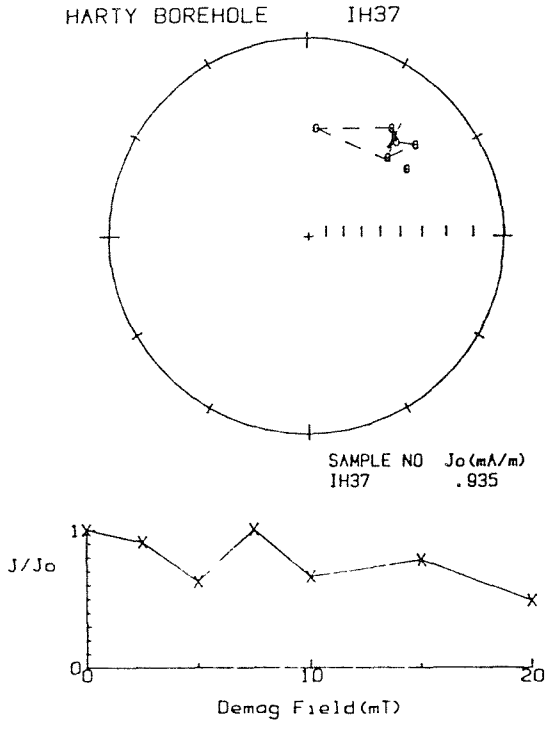

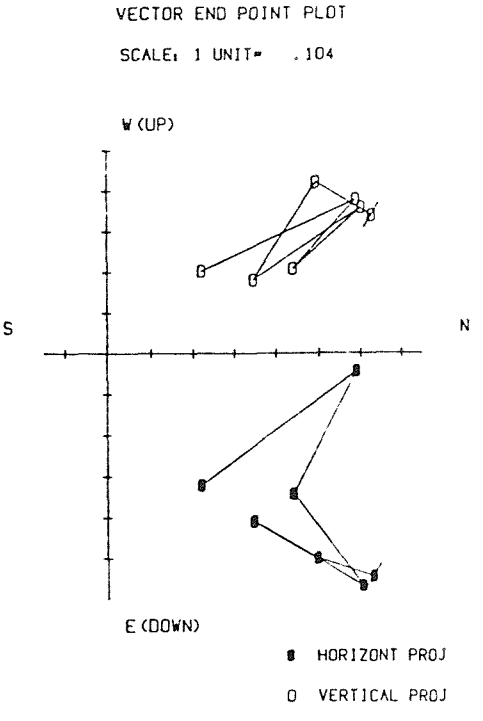

Fig 7.3 Examples of demagnetisation plots from the upper part of the Harty borehole. The upper plot shows a specimen from Division B with a normal polarity. The lower plot shows a specimen from Division A2 with a reverse polarity. For explanation of symbols see Fig 2.7. The declination is arbitrary with these borehole specimens.

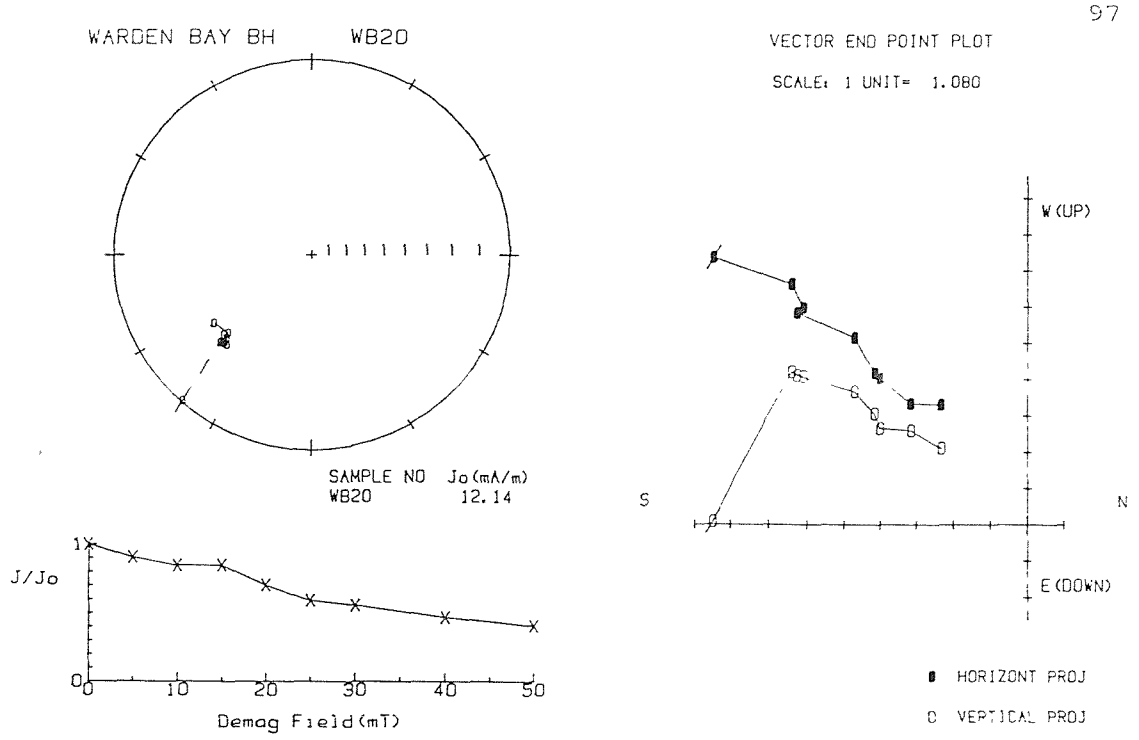

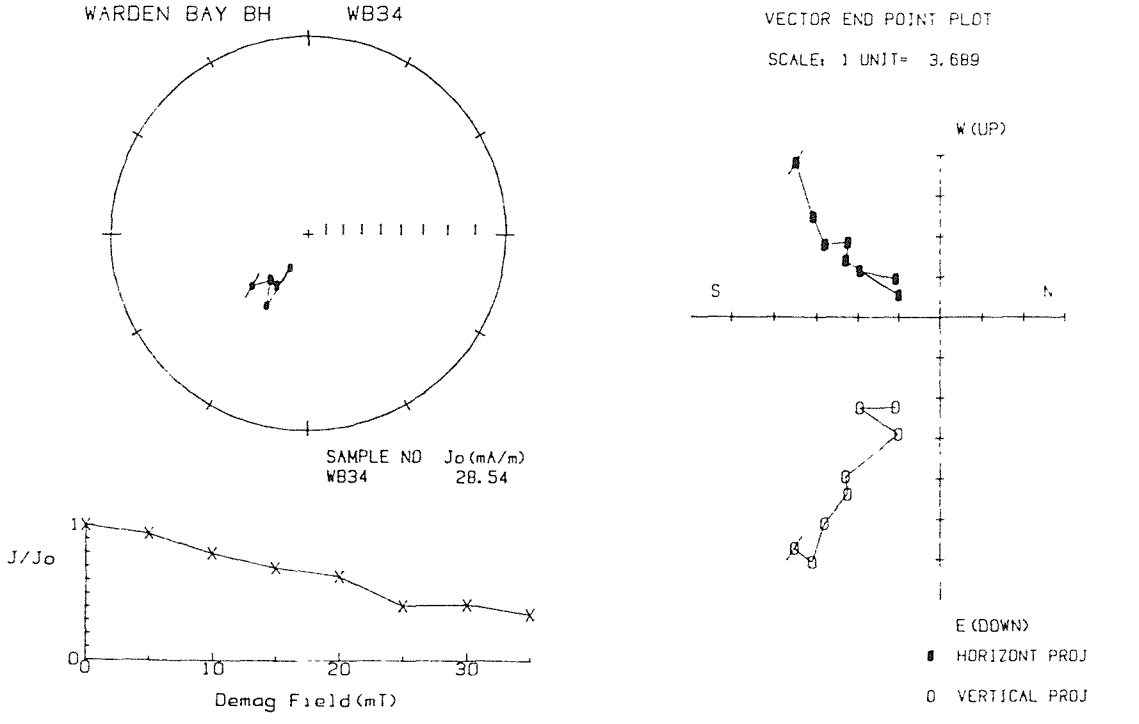

Fig 7.4 Examples of demagnetisation plots from the Warden Bay borehole. The upper plot shows a specimen from the lower part of Division C with a reverse polarity. The lower plot shows a specimen from Division B with a normal polarity. For explanation of symbols see Fig 2.7. The declination is arbitrary with these borehole specimens.

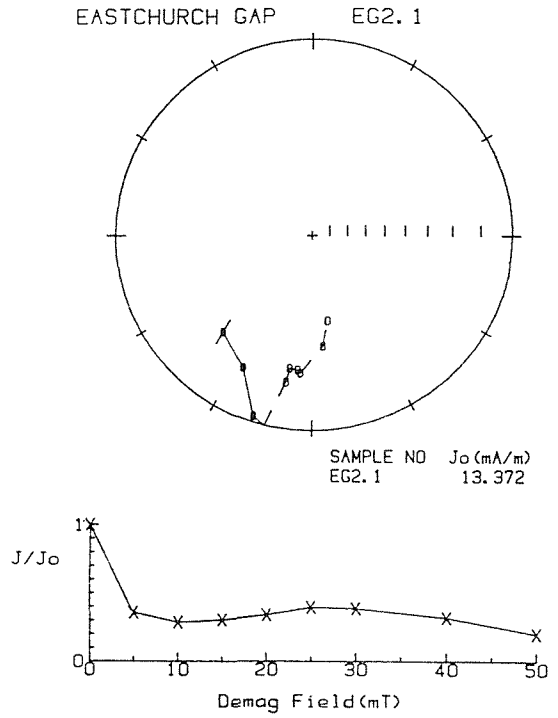

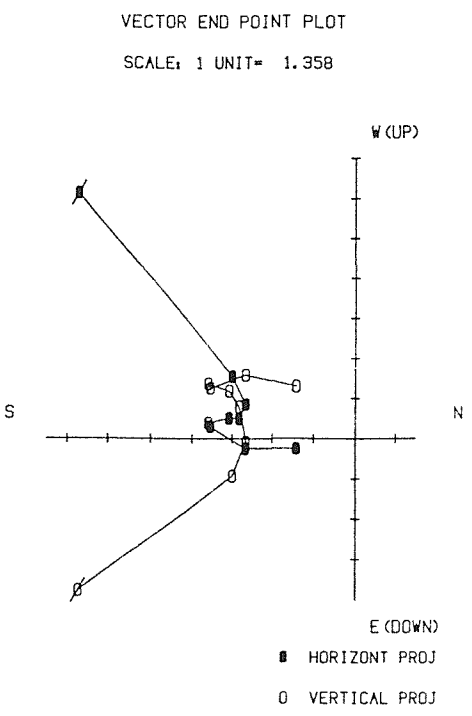

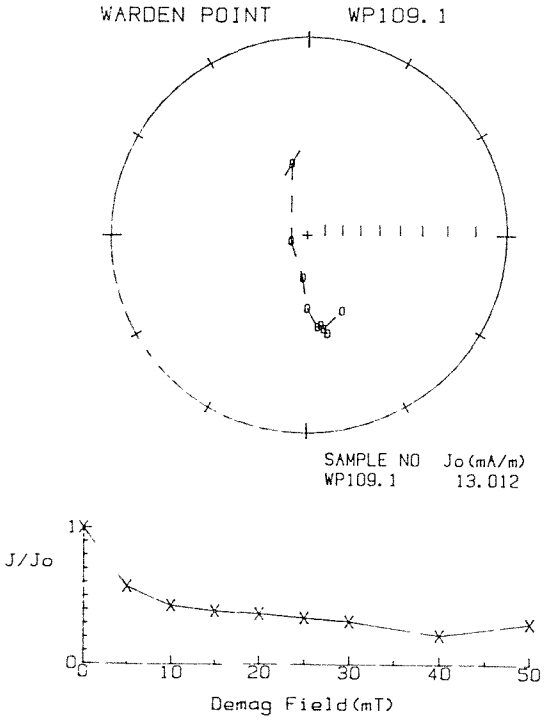

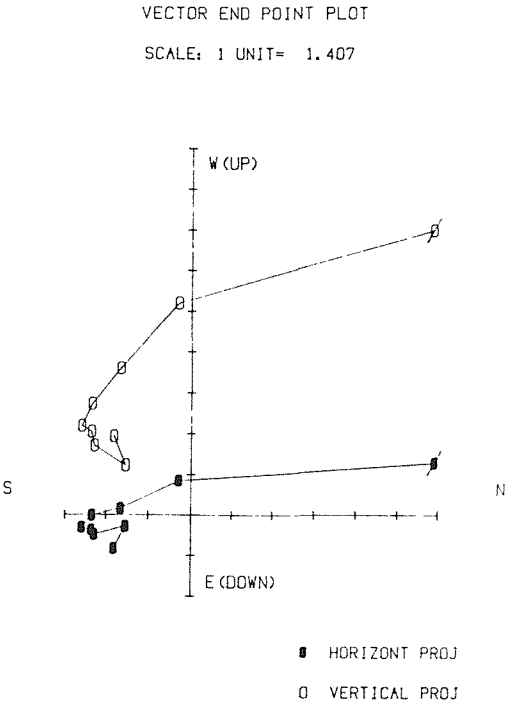

Fig 7.5 Typical reverse polarity specimens from the Warden Point and Eastchurch Gap sections. For explanation of symbols see Fig 2.7.

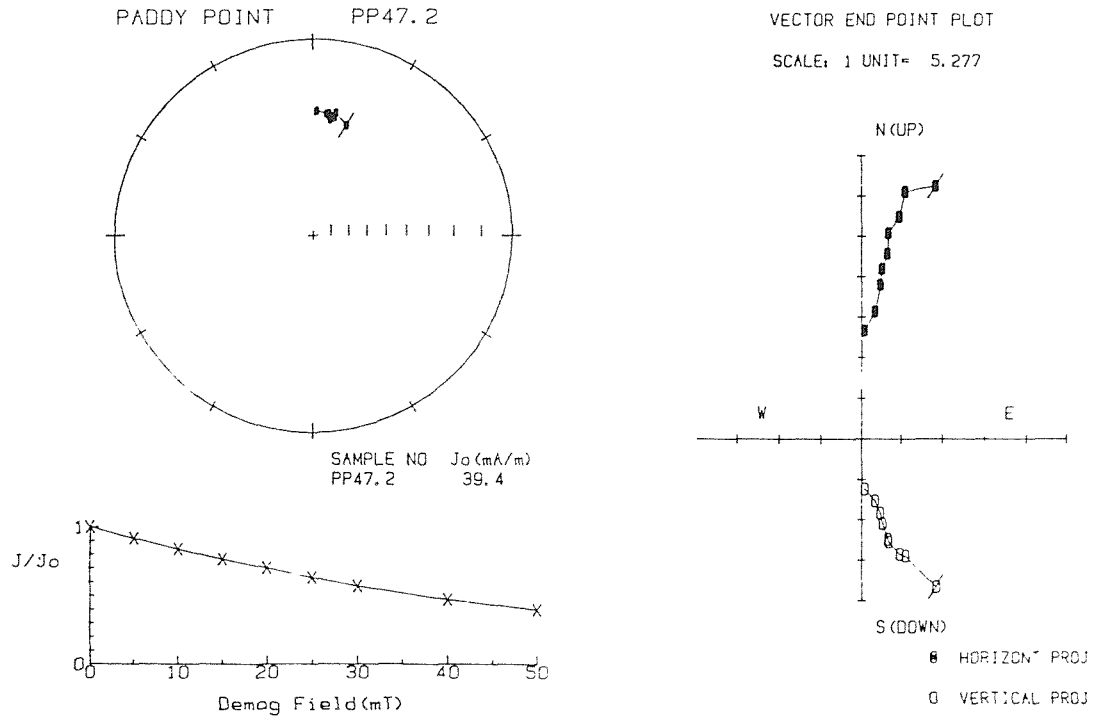

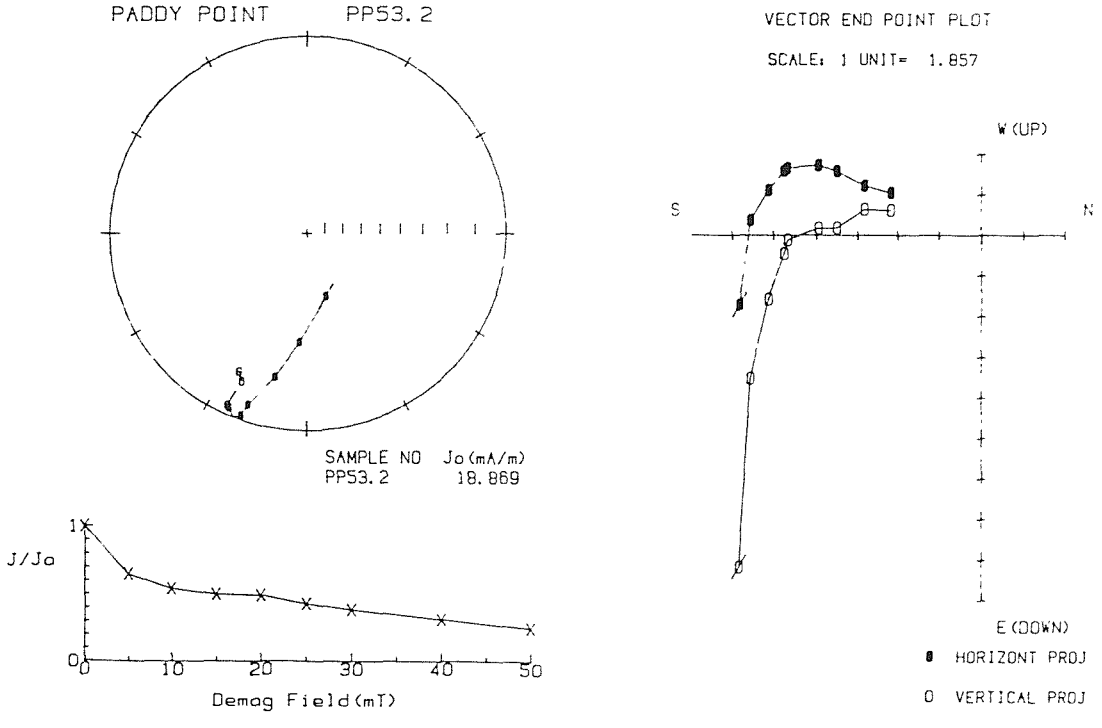

Fig 7.6 Examples of demagnetisation plots from the Paddy Point section. The upper plot shows a specimen with a normal polarity and the lower plot a specimen with a reverse polarity. For explanation of symbols see Fig 2.7.

extends from the upper part of the Oldhaven Formation to the middle of Division B of the London Clay Formation, a total stratigraphic thickness of 42m. NRM intensities exhibit significant variation. Specimens from the Oldhaven Formation, London Clay Basement Bed (?A1), Division A3 and Division B had typical NRM intensities of 10-30mA/m. Division A2 is characterised by much lower intensities (about 0.5mA/m).(Section 7.9 examines in detail the magnetic properties of sediments from the lower part of the London Clay Formation.) The magnetostratigraphy is summarised in Fig 7.7.

A normal polarity magnetozone IH-a extends from the base of Division B to the top of the borehole. Normal polarity specimens were identified in the top of the Oldhaven Formation/London Clay Basement Bed and at a number of other levels within Division A (which is dominantly reverse polarity).

7.4.2 The Warden Bay borehole

The Warden Bay borehole (TR 024717) extends from the lower part of Division B to just below the top of Division C, a total thickness of 50.3m. Two normal polarity magnetozones, WB-a and WB-b were identified (Fig 7.8). WB-a, in the lower part of the section is 17.7m thick. It is overlain by a reverse zone, 15m thick, which includes two normal polarity sites at about 30m BD. WB-b commences 8m above the base of Division C and continues to the top of the borehole.

7.5 The exposed London Clay and Virginia Water Formations

The most extensive outcrop of the London Clay Formation is on the Isle of Sheppey. The 6km long exposure along the northern coast of the Isle dips gently to the northwest, so that progressively younger beds outcrop at beach level between Warden Point and Paddy Point (Fig 7.1). The upper 53.5m of the London Clay Formation is exposed together with the lower 8m of the Virginia Water Formation.

Results of a detailed stratigraphic study were

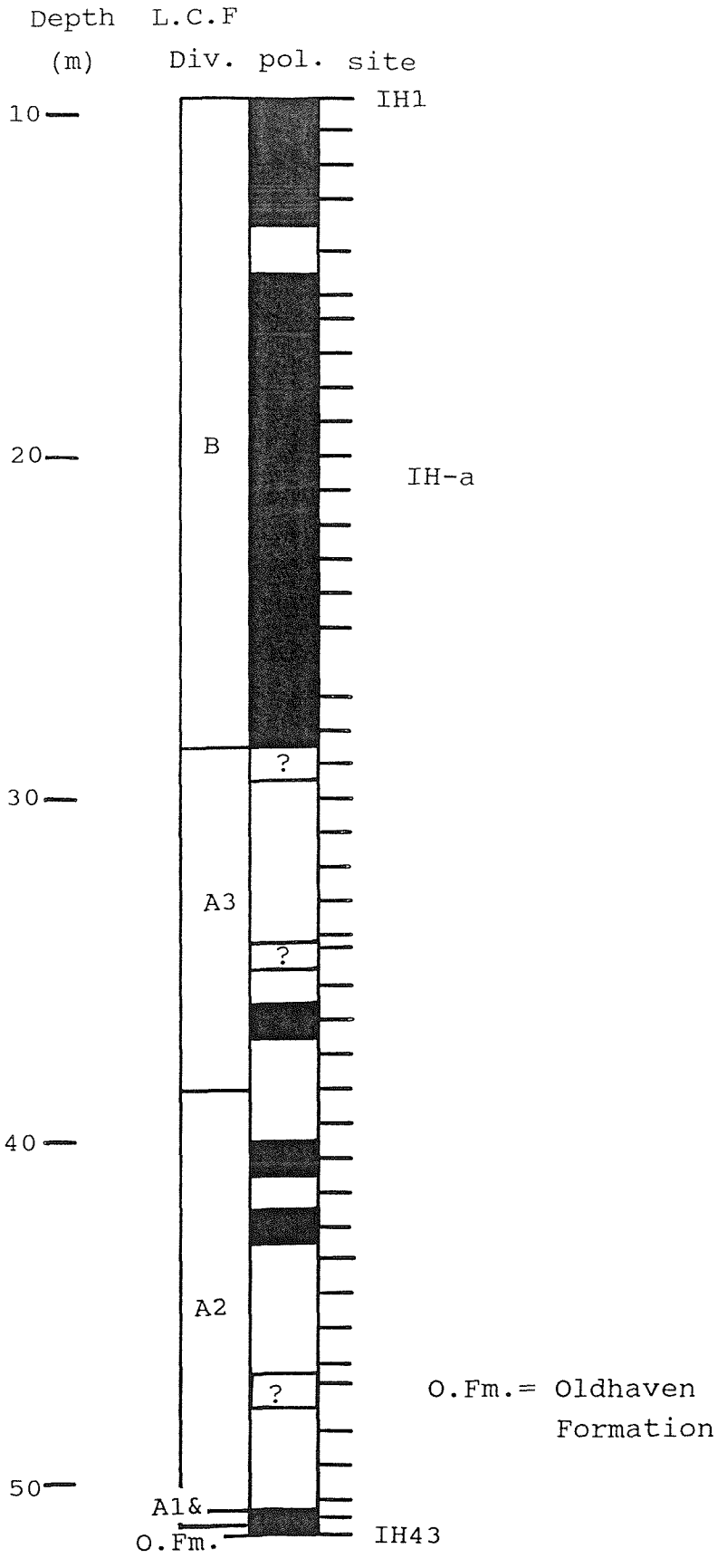

Fig 7.7 The magnetostratigraphy of the Harty borehole.

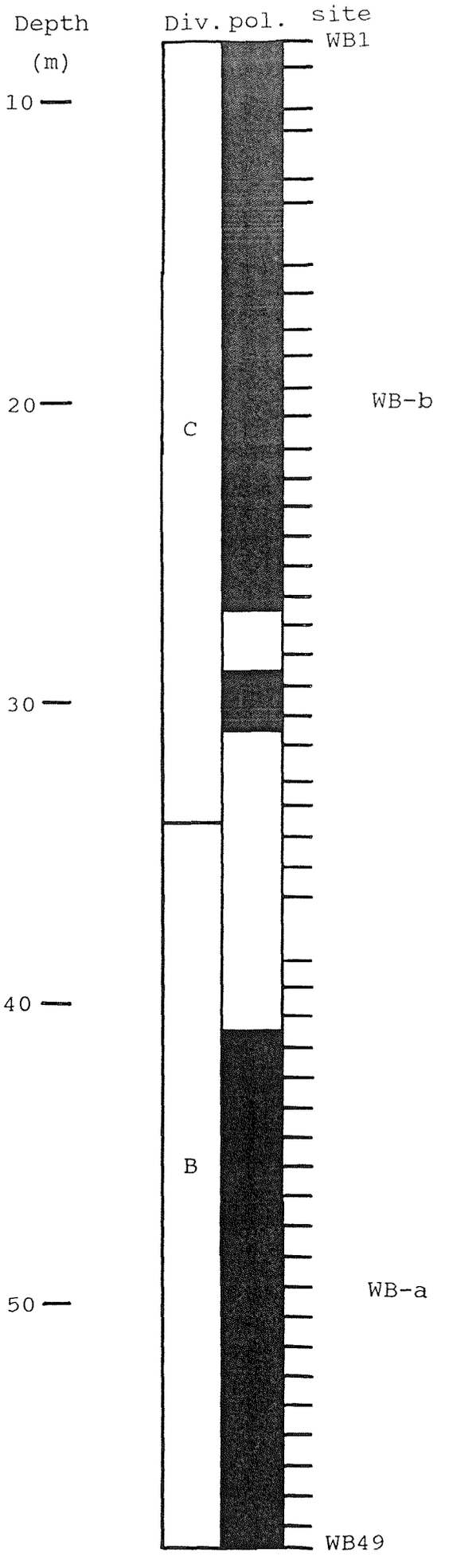

Fig 7.8 The magnetostratigraphy of the Warden Bay borehole.

presented by King (1984). Fourteen lithostratigraphic units were identified (Sh-1 to Sh-14). Correlation was aided by tracing a number of persistent septarian nodule horizons (coded A to P) along the exposures. The boundaries separating Divisions C and D were identified, and redefined from King (1981). Johnston (1983) carried out a magnetostratigraphic study on a 35m cliff section close to Warden Point.

For the present study the succession was sampled (as a composite section) at three localities: Warden Point, Eastchurch Gap and Paddy Point. Sections were sampled at 1m intervals, two samples being taken from each stratigraphic level. King's (1984) nodule band "A" was used as the height datum for site positions. The base of the exposed section has a 3-4m overlap with the top of the Warden Bay borehole.

7.5.1 Warden Point

The lowest 7.8m of the exposed London Clay was sampled along a 500 m stretch of beach and cliff exposures close to Warden Point (TR 021724). The specimens had NRM intensities typically in the range 15-35mA/m. The magnetostratigraphic results are presented in Fig 7.9. A normal polarity magnetozone, WP-a, 3.55m thick is defined by five sites at the base of the section.

7.5.2 Eastchurch Gap

Approximately 15m of the London Clay Formation is exposed in the cliff section west of Hens Brook as it enters the sea (TR 997730). Ten sites ranging from 8.6m to 19.45m OD were sampled. Apart from an indeterminate polarity site at the base of the section, the succession is reverse polarity throughout (Fig 7.9).

7.5.3 Paddy Point

The beach, cliff and back-cliff at Paddy Point (TR 971735) expose a 45m sequence from the upper part of the London Clay Formation to the Virginia Water Formation. Sampling commenced at nodule band "J", 18.45m OD, and

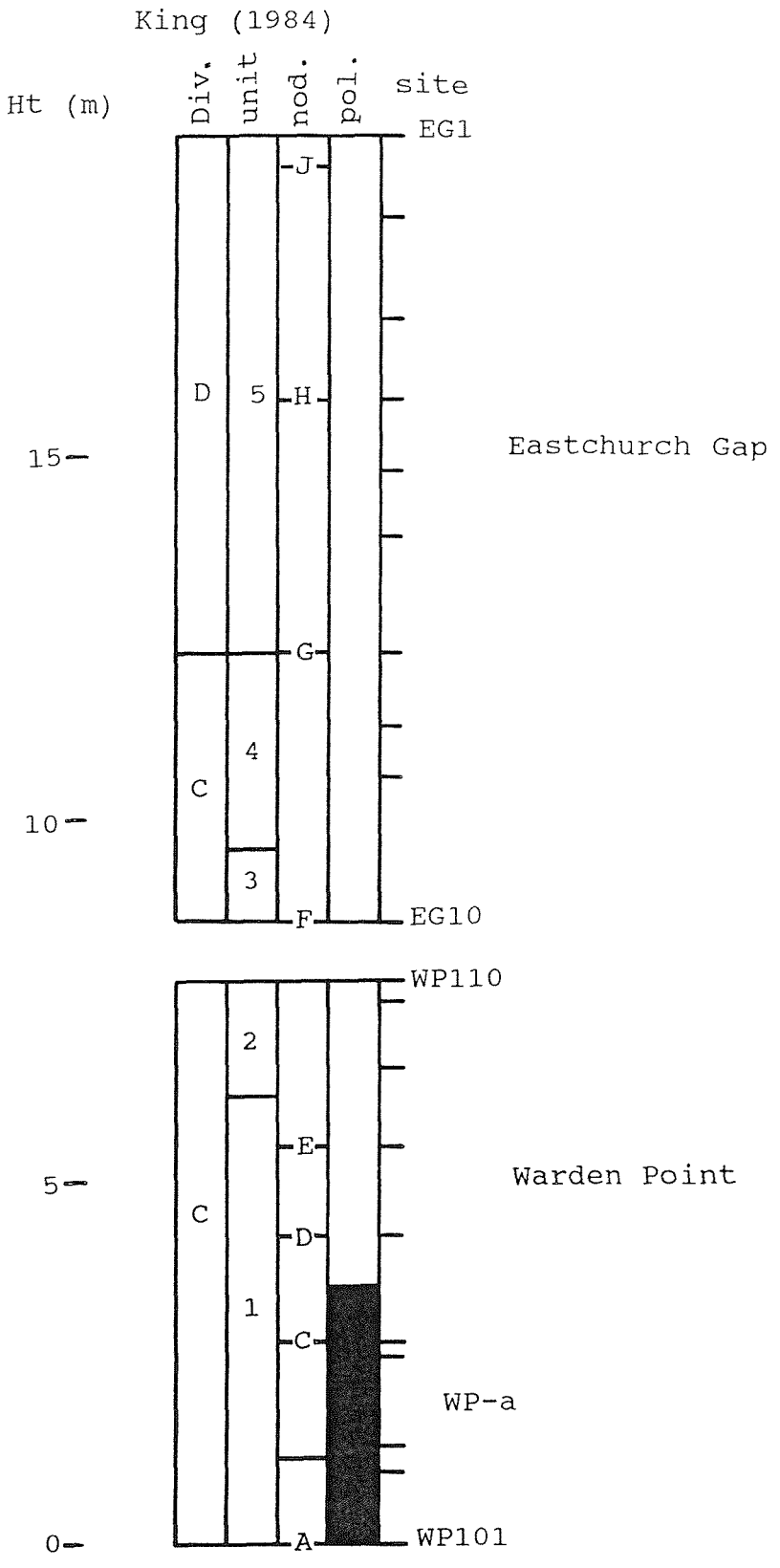

Fig 7.9 The magnetostratigraphy of the Warden Point and Eastchurch Gap sections.

extended to the lower part of the Virginia Water Formation, 61.25m OD.

The typical NRM intensity values for the London Clay and Virginia Water Formations are 10-30 and 2-5mA/m respectively. The difference probably reflects the change of depositional environment (and its influence on the dominant remanence carrier) as the shelf-mud facies, characteristic of the London Clay Formation, rapidly shallowed to the marginal marine facies of the Virginia Water Formation. The magnetostratigraphy is summarised in Fig 7.10. A normal polarity magnetozone, PP-a, commences at 25.1m OD and continues to the top of the section.

7.6 Synthesis of the Sheppey magnetozones

The two boreholes and three coastal exposures at Sheppey form a composite sequence extending upwards from the top of the Oldhaven Formation to the lower part of the Virginia Water Formation. The magnetostratigraphic results from the five sections are combined in Fig 7.11, with each section drawn in its relative stratigraphic position. Three discrete normal polarity magnetozones have been identified, and for discussion purposes are referred to as Shep-1 to -3 in ascending stratigraphic order.

7.6.1 Shep-1

Located at the top of the Harty borehole (IH-a) and the lower part of the Warden Bay borehole (WB-a). This magnetozone commences at the base of Division B and terminates 7m below the top of this division.

7.6.2 Shep-2

This appears in the upper third of the Warden Bay borehole (WB-b) and the lower half of the Warden Point section (WP-a). This magnetozone begins 8m above the base of Division C and terminates 8.75m below the top of this division.

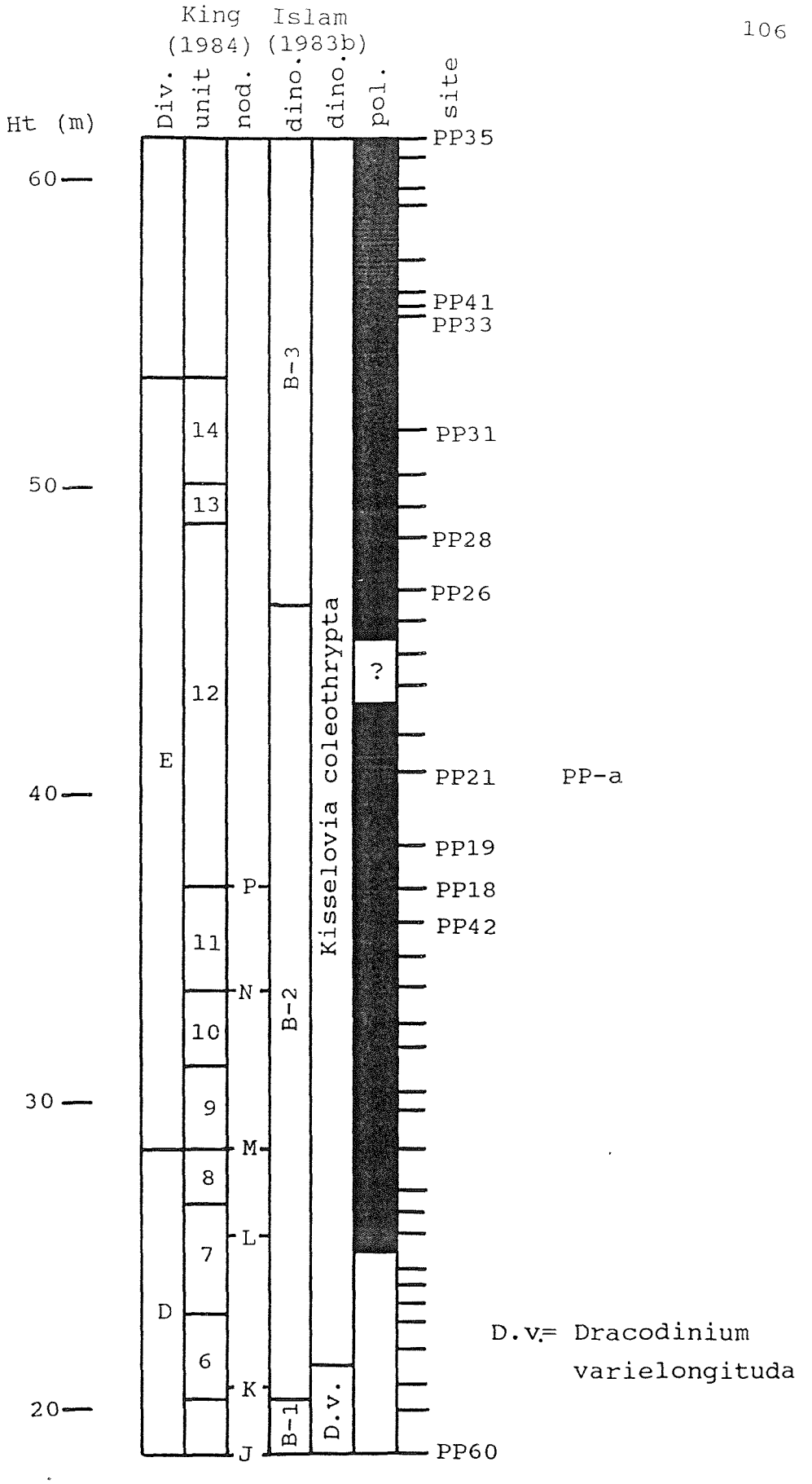

Fig 7.10 The magnetostratigraphy of the Paddy Point section.

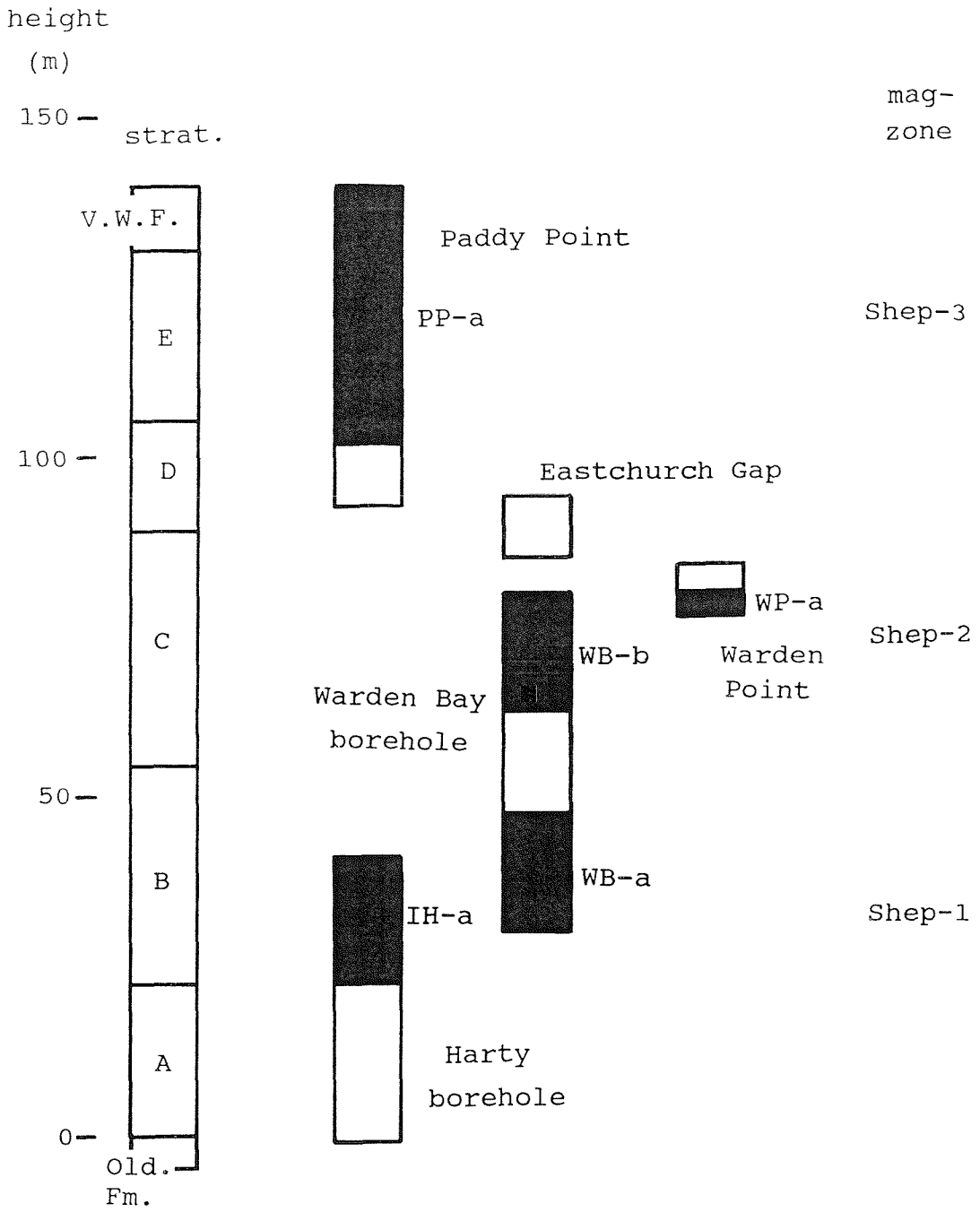

Fig 7.11 Synthesis of the Sheppey magnetozones.

7.6.3 Shep-3

This is identified in the Paddy point section as PP-a. Its base is positioned 3.35m below the top of Division D and it extends to the top of the sampled section (lower part of the Virginia Water Formation).

7.7 Whitecliff Bay

Following work by Townsend (1982), Whitecliff Bay (SZ 640860) was proposed by Townsend and Hailwood (1985) as the southern U.K. Eocene magnetostratigraphic type-section. Initial attempts at a magnetostratigraphic correlation of the upper part of the London Clay Formation between Sheppey and Whitecliff Bay proved difficult. After an examination of Townsend's data (1982, p225-9), it was decided to reinvestigate critical levels in the upper half of the London Clay Formation and the Wittering Formation at Whitecliff Bay. Townsend (1982) identified three magnetozones (coded WB-b, WB-c and WB-d) in this part of the succession. Aubry et al (1986) used calcareous nannoplankton biostratigraphy to correlate the polarity sequence with the marine magnetic anomaly sequence. These authors combined WB-b and WB-c and correlated the combined magnetozone with Chron C24AN. WB-d was correlated with Chron C23N.

The polarity results from the present study are presented in Fig 7.12. A noticeable feature of the diagram is the erratic site interval; the study was designed to clarify Townsend's (1982) data. The lithostratigraphic thicknesses of the various units are based on King (1981) and Plint (1983). The top of the London Clay Formation was redefined by Edwards and Freshney (1987) to include 11m of sediment (Plint's WB1 unit) previously included in the base of the Wittering Formation. A modified version of Townsend and Hailwood's (1985, Fig 7) polarity sequence is shown in Fig 7.12.

The NRM intensity values exhibit significant variation in the section. The top of Division B and Division C1 have values of 2-5mA/m. The interval including Division C2 up to the top of Plint's WB4 has values of 0.4-0.8 mA/m whilst

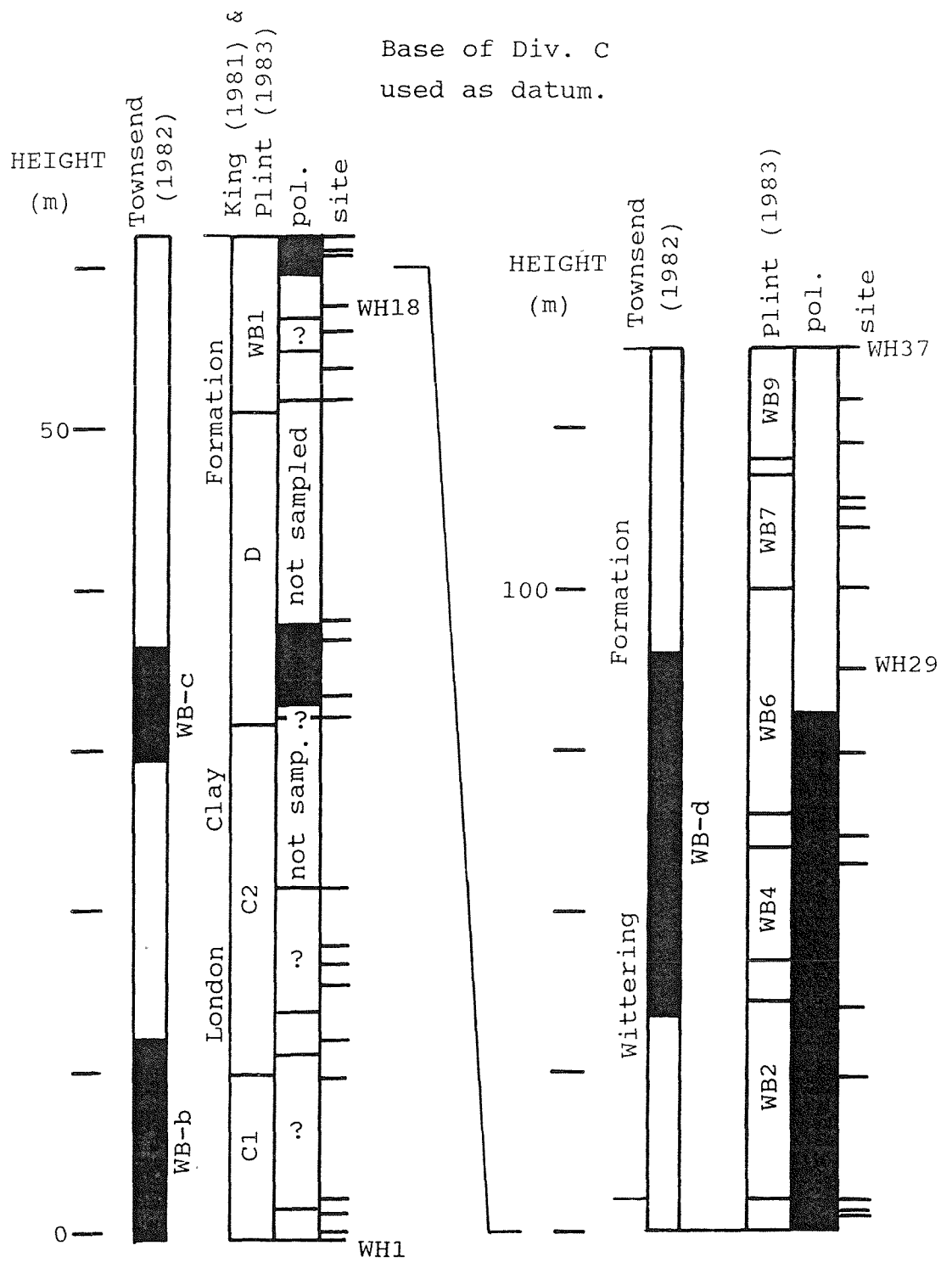

Fig 7.12 The magnetostratigraphy of the upper part of the London Clay Formation and Wittering Formation at Whitecliff Bay.

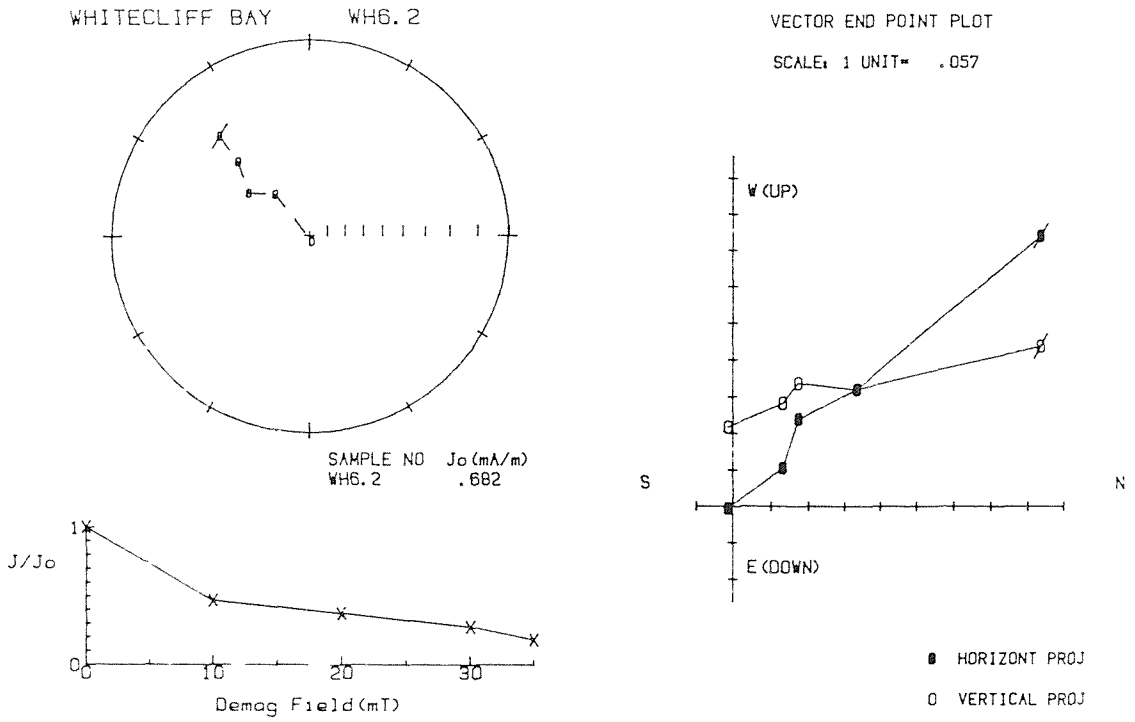

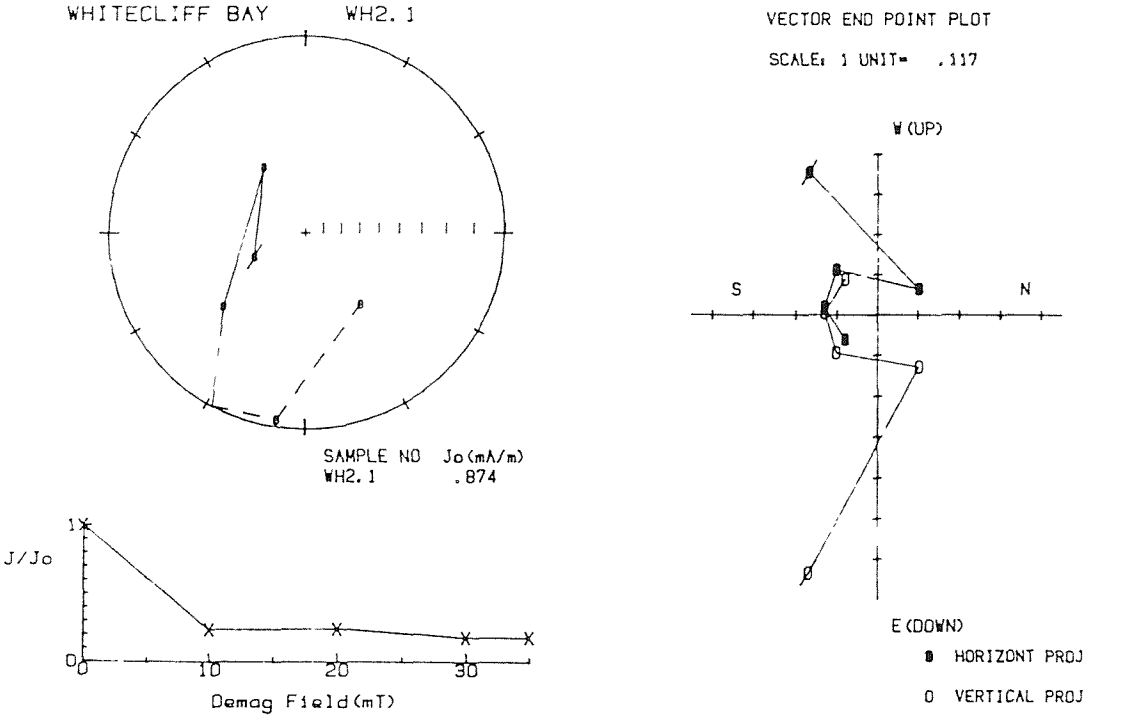

Fig 7.13 Typical reverse polarity specimens from the lower part of Division C of the London Clay Formation at Whitecliff Bay. For explanation of symbols see Fig 2.7.

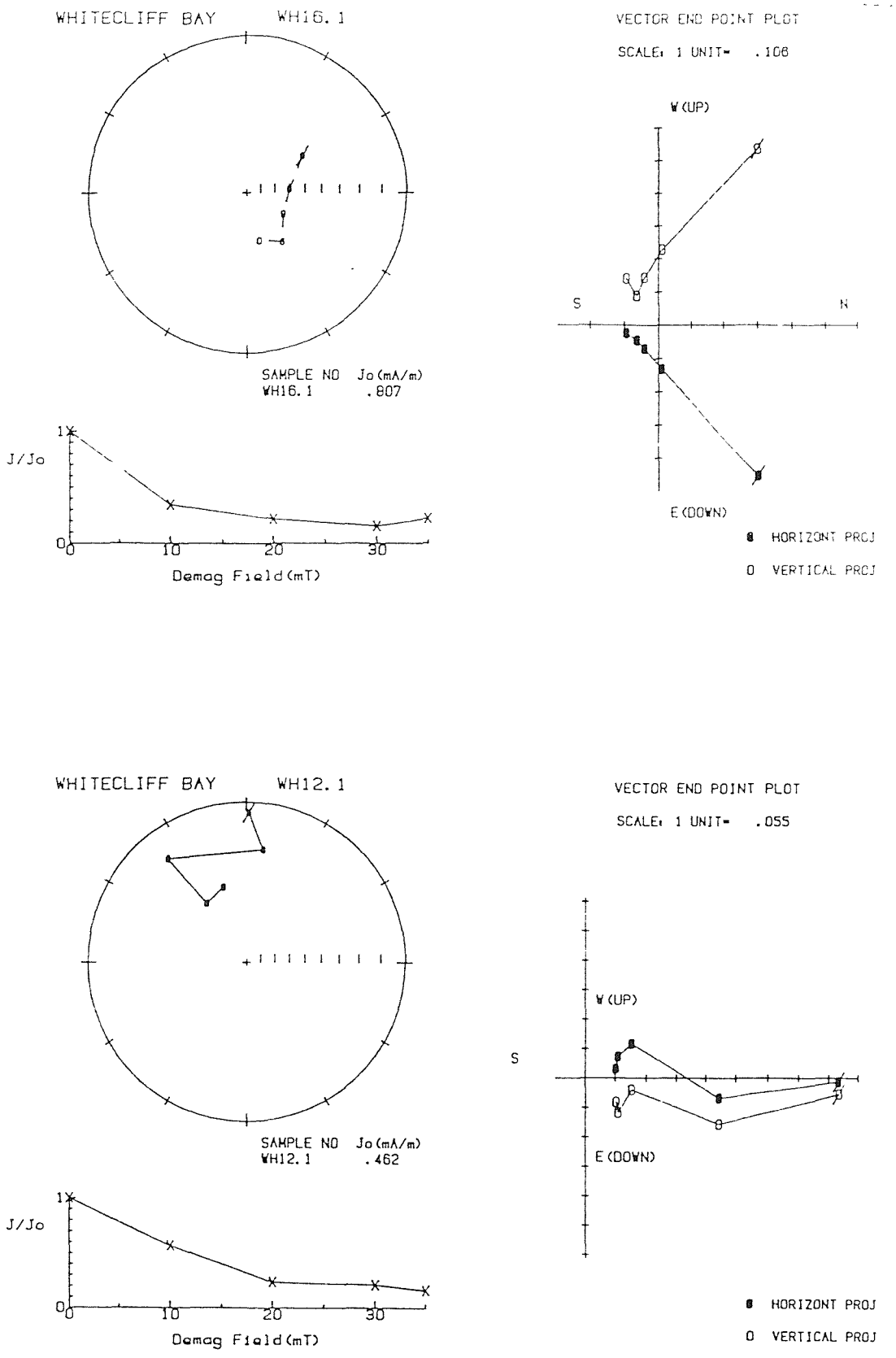

Fig 7.14 Examples of demagnetisation plots from the upper part of the London Clay Formation at Whitecliff Bay. The upper plot shows a specimen with a reverse polarity and the lower plot a specimen with a normal polarity. For explanation of symbols see Fig 2.7.

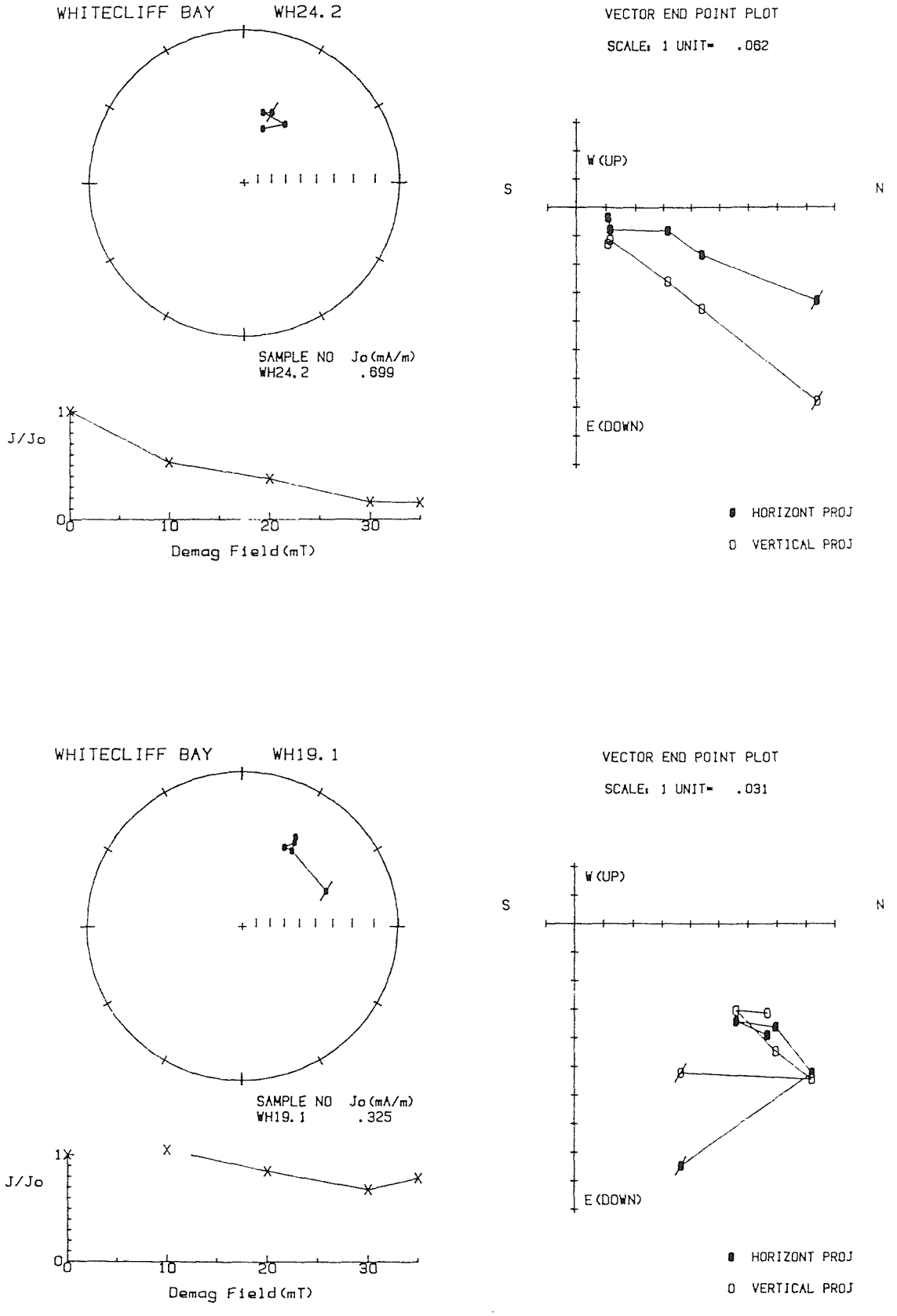

Fig 7.15 Typical normal polarity specimens used to define the magnetozone WB-d at Whitecliff Bay. For explanation of symbols see Fig 2.7.

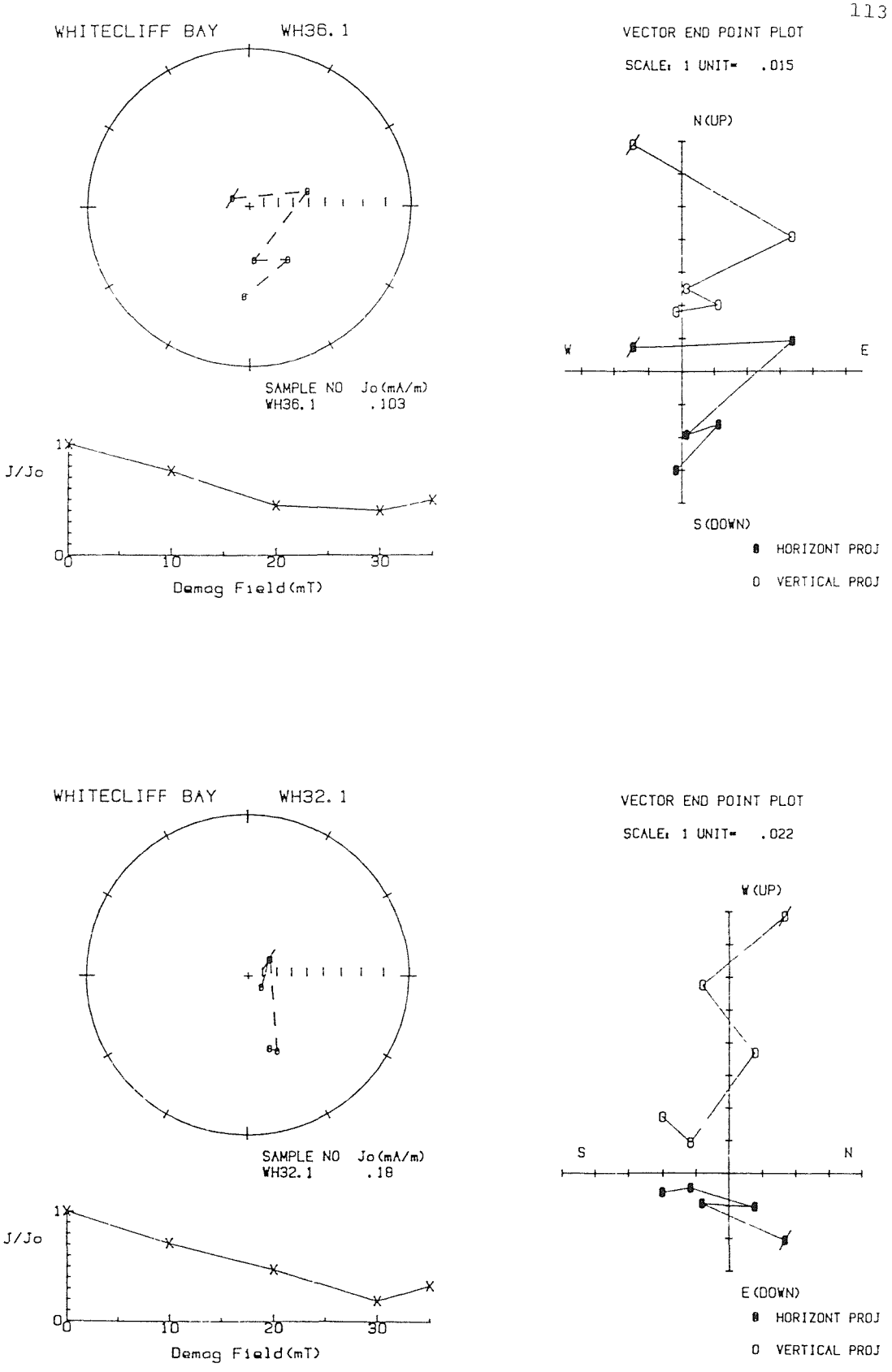

Fig 7.16 Typical reverse polarity specimens from the upper part of the Wittering Formation at Whitecliff Bay. For explanation of symbols see Fig 2.7.

Plint's WB5 up to the top of WB9 has values of about 0.2mA/m. The majority of the specimens were processed on the cryogenic magnetometer (maximum field 35mT). A number of representative demagnetisation plots are shown in Figs 7.13 to 7.16.

The magnetozone WB-b could not be identified in the basal part of Division C1. Specimens from this level had either reverse or indeterminate polarities (see Fig 7.13). Indeterminate polarity specimens also dominate Division C2. Two normal polarity sites just above the Division C/D junction may represent part of WB-c (see Fig 7.14).

The WB-d magnetozone is now also redefined. It commences within Plint's WB1 unit (at 59.3m OD) and terminates in WB6 (at 92.35m). (The Sites WH19-23, from levels that Townsend (1982) reported as having a reverse polarity, all have fairly good normal polarity "trends; see Fig 7.15.) The remainder of the Wittering Formation is reverse polarity.

7.8 Correlation

The sequence of normal polarity magnetozones identified in the Sheppey sections are correlated with the Whitecliff Bay sequences using the results from Townsend (1982) and the present study, together with Johnston's (1983) study of the section at Warden Point. The magnetostratigraphic sequences are shown in Fig 7.17.

7.8.1 Shep-1

The base of both the Shep-1 and WB-a magnetozones coincide with the base of Division B of the London Clay Formation. Aubry et al (1986) correlated WB-a with Chron C24BN, and a correlation of Shep-1 to Chron C24BN is therefore proposed. Shep-1 is notably thicker than WB-a. Variable sedimentation rates, or a significant hiatus at the A/B or B1/B2 discontinuities could account for this.

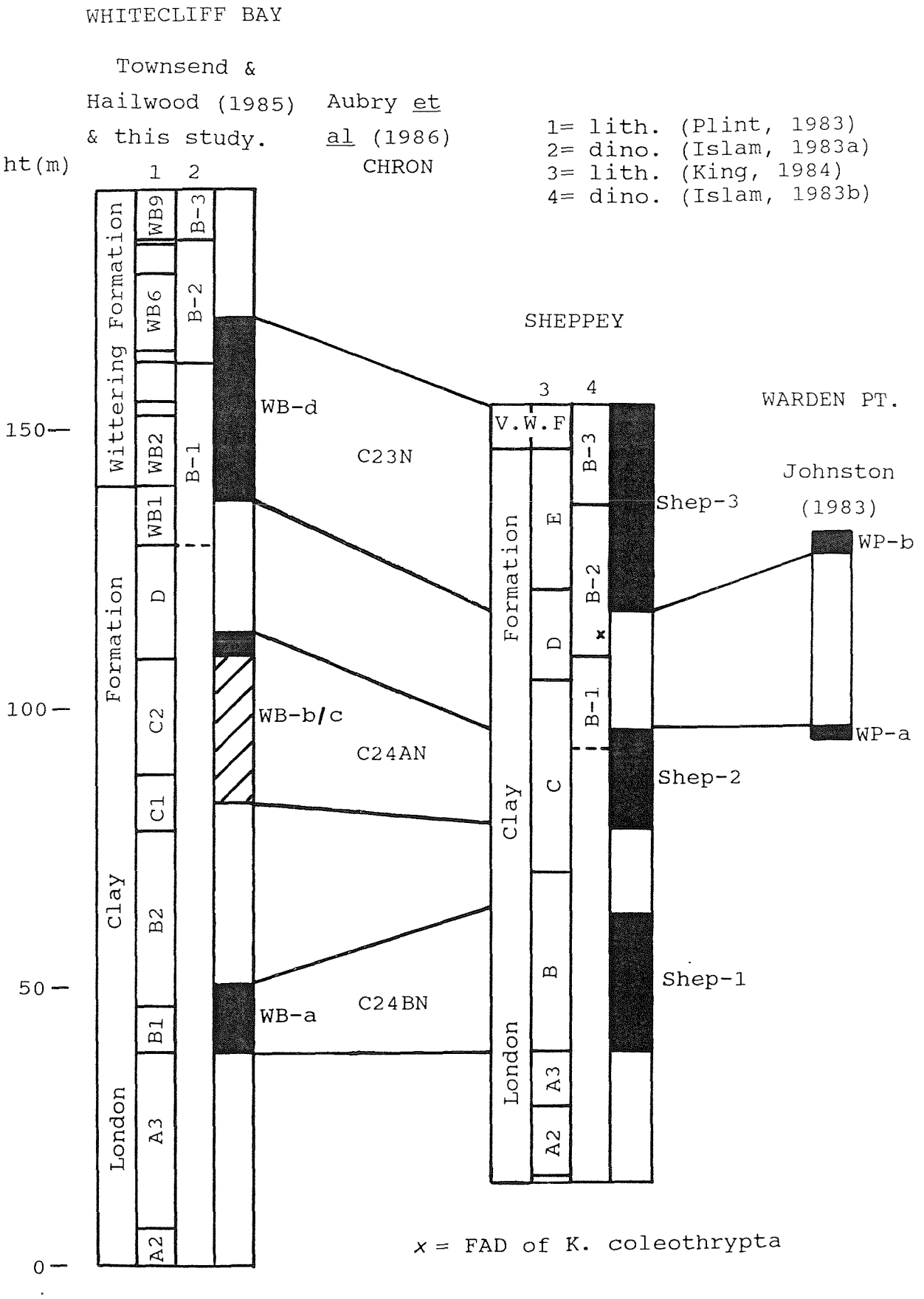

Fig 7.17 The magnetostratigraphic correlation of the Early Eocene between Sheppey and Whitecliff Bay.

7.8.2 Shep-2

The base of Shep-2 is positioned 8m above the base of Division C at Sheppey. At Whitecliff Bay, Townsend's (1982) WB-b magnetozone could not be identified. Possibly part of WB-c was located close to the Division C/D junction. Aubry et al (1985) combined WB-b and WB-c as portions of Chron C24AN. It is proposed to correlate Shep-2 with the very poorly defined normal polarity level in the middle and upper part of Division C and lower part of Division D at Whitecliff Bay. The material from this level is very weakly magnetic and is unlikely to yield a useful palaeomagnetic signal. It is proposed to correlate Shep-2 with Chron C24AN, in accordance with Aubry et al's (1986) correlation of the equivalent levels at Whitecliff Bay with this magnetic chron.

7.8.3 Shep-3

Magnetozone Shep-3 begins 3.35m below the base of Division E (above the Kisselovia coleothrypta FAD) and continues to the top of the exposed succession (in the Virginia Water Formation). It is proposed to correlate Shep-3 with WB-d (which begins 2.6m below the base of the Wittering Formation). Such a correlation does not necessarily imply that the base of Division E in the London Basin is equivalent to the base of the Wittering Formation in the Hampshire Basin. The correlation proves the diachroneity of Islam's B1/2 and B2/B3 biozone junctions (other workers have privately expressed doubts about using the biozones as chronostratigraphic markers). As Shep-3 begins above the FAD of K. coleothrypta, it can be correlated directly with Chron C23N.

Johnston (1983) identified two normal polarity magnetozones (WP-a and WP-b) in the cliff section at Warden Point. WP-a correlates with the top of Shep-2, since it occurs at the same level at the same locality. The reversed intervals separating Shep-2/3 and WP-a/b have different stratigraphic thicknesses (21.55m and 31m respectively). Johnston (1983) sampled the Warden Point section before

King (1984) had finalised his stratigraphic study. The present study uses the information in that paper, and the author was aided during sampling by C. King. It is very likely that the base of Shep-3 and WP-b record the same event; however as Shep-3 was identified in the Paddy Point section, it may indicate problems with King's (1984) correlation between Warden Point and Paddy Point.

Aubry (1983) identified the NP14 nannoplankton zone in the sediments from the lower part of the Earnley Sand Formation. Aubry et al (1986) correlated the reverse polarity sediments identified by Townsend and Hailwood (1985) above the Whitecliff Bay Bed (Plint's WB8) with Chron C21R. Reverse polarity sediments were identified at this level in the present study, and a similiar correlation with Chron C21R is proposed. There is no record of Chron C22N in the Whitecliff Bay section.

7.9 The magnetic properties of the Sheppey specimens

7.9.1 NRM intensity

The NRM intensity data for the Sheppey specimens (listed in the Appendix) indicate that throughout most of the section the material is quite strongly magnetic (10-30mA/m). Specimens from Division A2 of the London Clay Formation (Harty borehole) are particularly interesting because of their uniformly low values (about 0.5mA/m). The contrast in values is illustrated in Fig 7.18a, which is a plot of NRM intensity versus depth for the Harty borehole.

7.9.2 Volume Susceptibility

A downhole plot of Volume Susceptibility (VS) for the Harty borehole is shown in Fig 7.18b. The changes in VS values almost parallel those in the NRM intensities. For most of the section, the values are between 8 and $12*10^{-4}$ SI units, whereas Division A2 has an average value of $2*10^{-4}$ SI units.

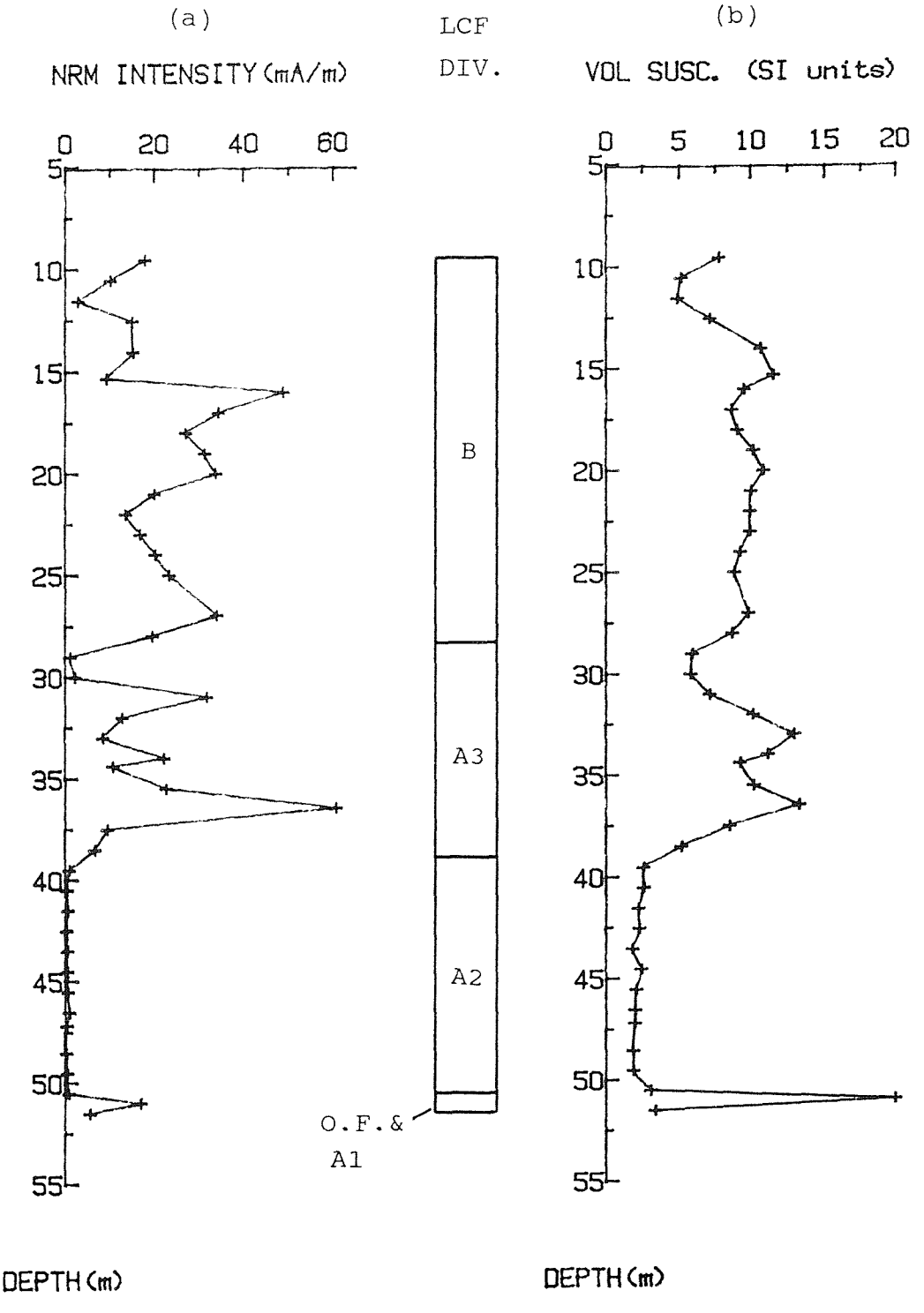

Fig 7.18 Downhole plots of (a) NRM intensity, and (b) Volume Susceptibility for the Harty borehole.

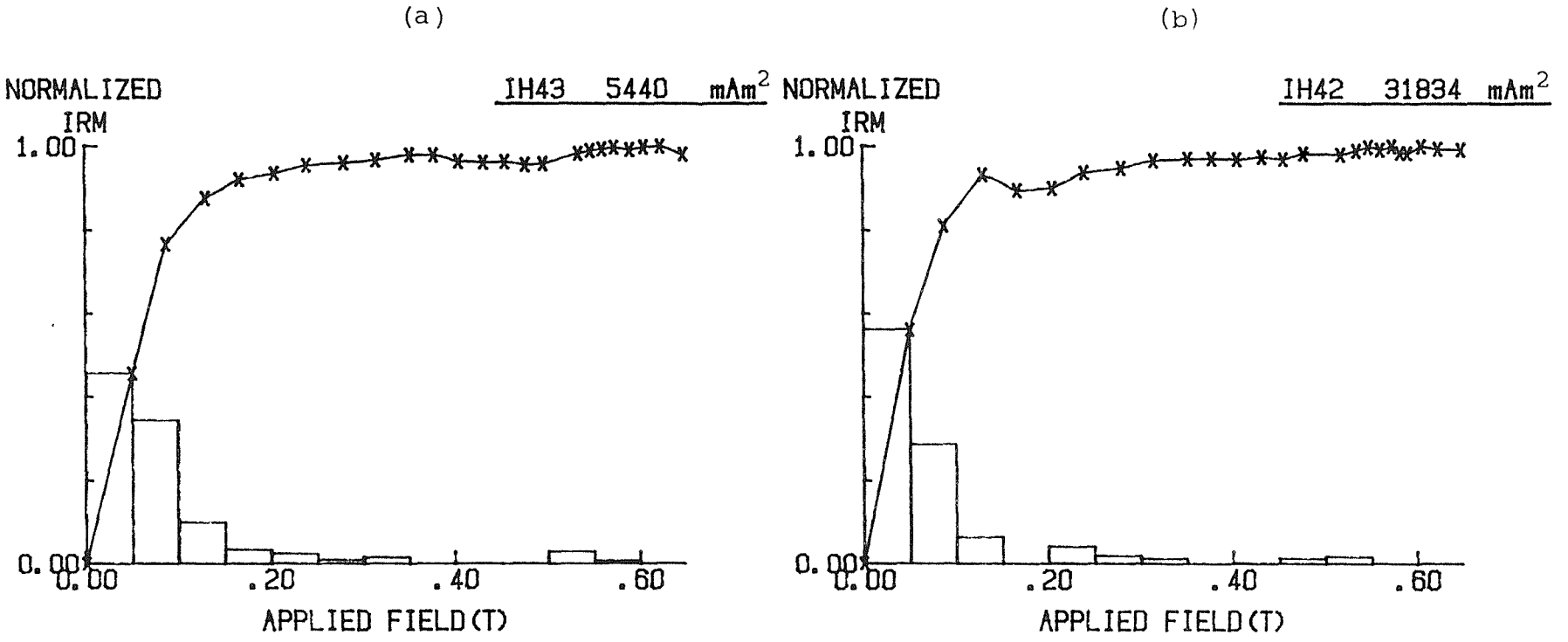

Fig 7.19 Typical IRM plots for specimens from the lower part of the Harty borehole. Both the Oldhaven Formation (a) and Division A1 of the London Clay Formation (b) have a remanence carried by magnetite (note the very high peak IRM of specimen IH42).

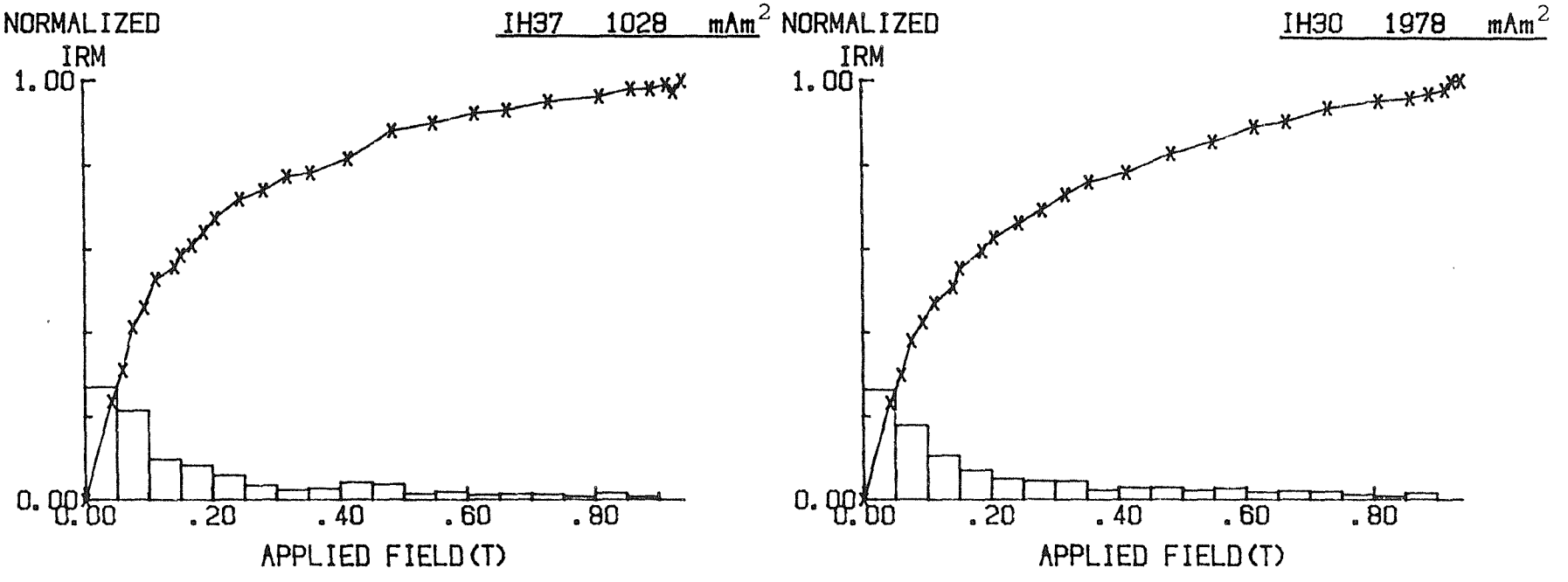

Fig 7.20 Typical IRM plots for specimens from Division A2 of the London Clay Formation in the Harty borehole.The remanence of this unit is carried by hematite (note the very much lower peak IRM values as compared with those for the specimens shown in Fig 7.19).

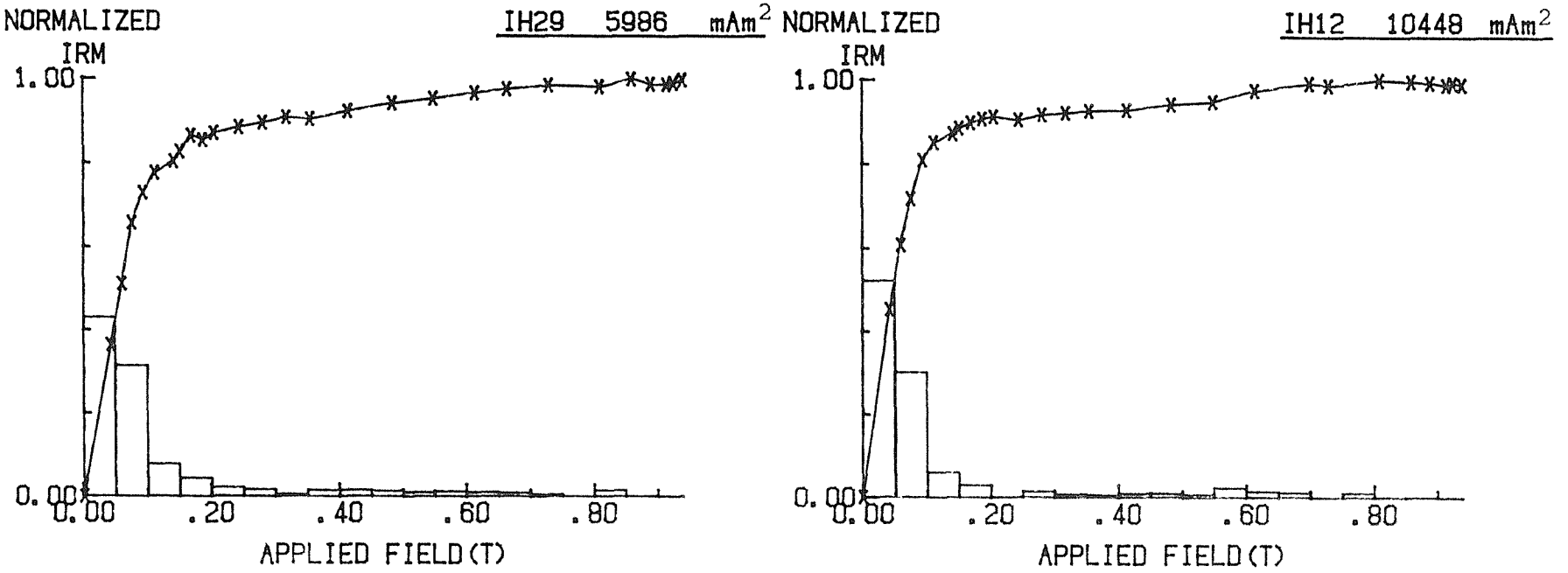

Fig 7.21 Typical IRM plots for specimens from Divisions A3 and B of the London Clay Formation in the Harty borehole. The remanence of these Divisions is carried by magnetite (note the almost total saturation at 0.3T, and the high peak IRM values).

7.9.3 IRM analysis

Thirty-seven specimens from the Sheppey sections were subjected to IRM analysis. Most of the specimens had IRM -ratios greater than 0.9, with peak values between 5 and 30 Am^2. The five specimens that were processed from Division A2 had an average IRM-ratio of 0.76 and a peak IRM of 1.26 Am^2. Representative IRM acquisition curves from the Harty borehole are presented in Fig 7.19 to 7.21.

7.9.4 Summary

Non-destructive palaeomagnetic techniques have been used to investigate the magnetic mineralogy of the sediments in the composite Sheppey section. Most of the section is characterised by quite strongly magnetic material whose remanence is probably carried by magnetite. However, the magnetic properties of Division A2 (in the Harty borehole) are very different, and the remanence at this level is probably carried by hematite. The Division A2/A3 junction marks a transitional phase, as there is a steady increase in NRM and VS (effectively linear) in the specimens adjacent to this boundary (Fig 7.18). The change in mineralogy does not appear to be related to a significant change in the lithology (Division A2 is a silty clay unit, not dissimilar to the lithology of the rest of the formation). As the A2/A3 junction represents an important transgression surface, the change in magnetic properties may be the result of a change in the sediment source, possibly reflecting the effects of changes in the palaeoceanographic circulation conditions.

The only other sampled section that has included the A2/A3 junction is at Whitecliff Bay (Townsend, 1982). Interestingly, the NRM intensities of sediments close to the boundary there (listed in Townsend, 1982) do not show a similar change. The sediment at Whitecliff Bay was deposited much closer to the edge of the basin, and so local conditions may have restricted ocean currents transporting material into the area. The sediments in this part of the section at Whitecliff Bay may have been derived from a more

local source.

It is believed that the A2/A3 transgression surface, away from the edge of the depositional basin, can be distinguished on the basis of the difference in the magnetic properties of Divisions A2 and A3. It may be possible to use this "marker" to supplement conventional magneto- and lithostratigraphic work.

7.10 Overall summary

The geomagnetic polarity sequence representing Chrons C24BR to C21R has been recorded in the Early Eocene sediments of southern England. The polarity sequences in sections at Sheppey and Whitecliff Bay are very similar (although the top of the Sheppey section terminates just below the top of the magnetozone representing Chron C23N). Using the magnetozone boundaries in the two sequences as absolute time-planes, it is possible to accurately correlate a number of levels between the two areas, and to correlate the sequences with the geomagnetic polarity time-scale.

The dinoflagellate zones that were used by Islam (1983a and b) to correlate the Whitecliff Bay and Sheppey sections are diachronous. The species used to define the biozones appear to be strongly facies controlled.

The Whitecliff Bay section contains no record of Chron C22N, supporting the studies of Aubry *et al* (1986). Its absence is attributed to a major regression, which is marked by the Whitecliff Bay Bed, in the upper part of the Wittering Formation.

King (1981) suggested that the transgression surfaces marking the major divisions in the London Clay Formation probably represented near-synchronous events. The magneto-stratigraphic evidence suggests that this is true for the bases of Divisions B and C; however the data from the base of Division D at Whitecliff Bay is not good enough to test this model. King (1981) correlated Division E in the London Basin with the lower part of the Wittering Formation. The magnetostratigraphic data support this correlation, as

the magnetozone representing Chron C23N begins 3.35m below Division E at Sheppey, and 2.6m below the base of the Wittering Formation (as defined by Edwards and Freshney, 1987) at Whitecliff Bay.

The magnetic properties of Division A2 at Sheppey are very different from those of the adjacent units. These properties may enable the unit to be recognised in areas which, during sedimentation, were away from the edge of the depositional basin, and thus to supplement the polarity and litho- stratigraphy.

Chapter 8 Results from the Early Eocene of Belgium

8.1 Introduction

The Ypresian (Early Eocene) Stage is defined in the world famous Ieper Clay Formation of Belgium and northern France. This chapter presents the results of the first palaeomagnetic study of the Ieper Clay Formation. Sections at ten localities were sampled, which together span about three quarters of the formation (the second quarter is known only from borehole material, which was not sampled in this study). Chrons C24AN and C23N have been identified in the formation and can be accurately correlated with the biolithostratigraphic scale developed by Steurbaut and Nolf (1986). Chron C24BN has been identified in a section not studied by Steurbaut and Nolf (1986). On the basis of these results the position of the NP11/NP12 nannoplankton junction in the time-scales of Berggren et al (1985) and Haq et al (1987) may have to be revised.

8.2 Historical Background

The term "Ypresian" was introduced by Dumont (1849) to describe the period of time during which sediments between the base of the Ieper Clay and the top of the Aalterbrugge Lignite Horizon were deposited. The terms "Ypres Beds" and "Argile Ypresien" were first used by Lyell (1852). Prestwich (1855 and 1888) correlated the Early Eocene strata of Belgium and northern France with the succession in England. The term "Ieper Clay" was introduced by d'Omalius d'Halloy (1862). Other important works of the 19th Century include those of Ortlieb and Chellonneix (1870) and Gosselt (1874), which were mainly used to compile the Belgium geological map of 1892. The stratigraphic divisions of the Early Eocene presented on the legend of this map have been widely accepted until recently. Willems et al (1981) provide a comprehensive review of the historical background to the Ypresian Stage.

A detailed stratigraphy of the Ieper Clay Formation was not available until the work of Steurbaut and Nolf (1986),

and King (in press). These authors demonstrate, independently, that the accepted correlations of units within the formation are incorrect, and they present revised schemes. These two works, in addition to the examination of numerous field exposures, used a large number of borehole sections to redefine the stratigraphy. The present study relies almost entirely on the information in these two papers to provide the basic lithostratigraphic and biostratigraphic framework to which the magnetostratigraphy is linked.

Steurbaut and Nolf (1986) list publications based on the various fossil groups. Dinoflagellates have been studied the most intensively (mainly by de Conninck from the mid 1960's to the present). Calcareous nannoplankton, foraminifera, diatoms, radiolarians and ostracods have all been studied to varying degrees.

8.3 The distribution of Late Palaeocene and Early Eocene sediments in the Belgium Basin

Late Palaeocene and Early Eocene sediments are present in northern France, virtually all of Belgium, and the southern part of the Netherlands (Willems et al, 1981 Fig 2). They are present beneath a thin Quaternary cover in the western half of this area (Fig 8.1 shows the field exposures that were sampled for this study). In the eastern half of the Belgium Basin they are present below younger Tertiary sediments, and are known mainly from boreholes (chiefly the Knokke, Kallo and Mol wells; Steurbaut and Nolf, 1986).

8.4 The formations investigated in this study

8.4.1 The Landen Formation

The upper 14m of the Erquelinne Member of the Landen Formation was sampled at Flines-les-Raches in northern France. This unit consists of well sorted sands, with very occasional, thin, impersistent clay seams. The sands vary between white, dark red and brown in colour, with irregular glauconite rich levels. The sands are probably of continental or fluviatile origin and are considered to be

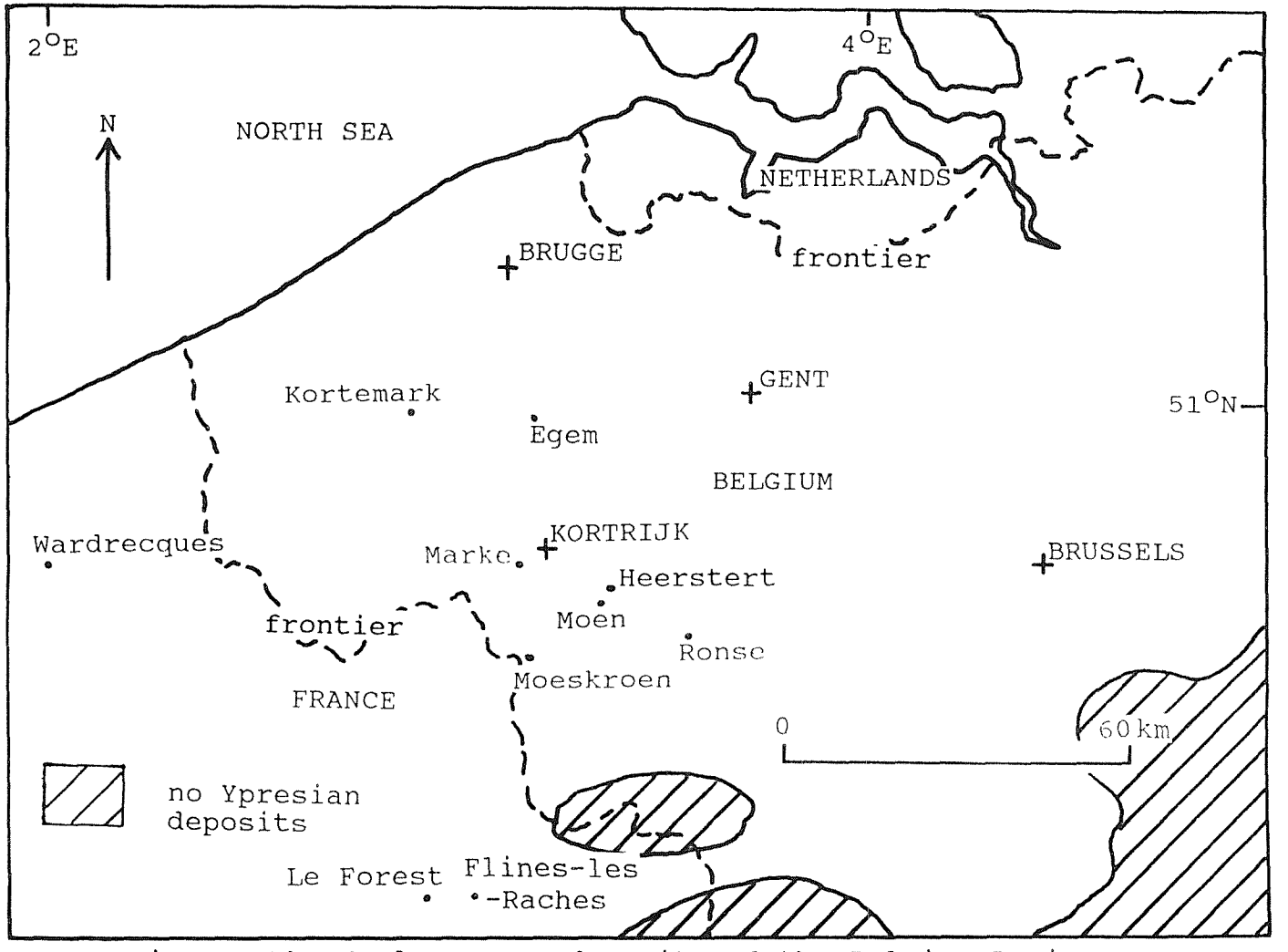

Fig 8.1 The Early Eocene deposits of the Belgium Basin.

Sparnacian (latest Palaeocene) in age.

8.4.2 The Ieper Clay Formation

The stratigraphy of the Ieper Clay Formation has been completely revised by Steurbaut and Nolf (1986), and King (in press) who have developed, independently, very similar lithostratigraphic correlation schemes. Steurbaut and Nolf's (1986) scheme relies very heavily on calcareous nannoplankton data, and subdivides the formation into eight members (Fig 8.2a). These authors assign the base and top of the formation to the NP11 and NP13 nannoplankton zones respectively, and they introduce nine subzones to cover the intervening interval. The formation reaches a maximum thickness of 165m in the north of Belgium (in the Knokke well), where virtually all of the succession belongs to a clay facies. To the south, nearer to the palaeocoast, the facies becomes more sandy (e.g. the Mons-en-Pevele Sand, and the Panisel Sand Members in the middle and upper part of the formation respectively).

King (in press) has extended his (1981) London Clay Formation division scheme to the Ieper Clay Formation. The scheme is based on the recognition of five major transgression-regression cycles within the formation. Glauconite horizons and pebble beds are used to identify transgression surfaces and these, together with a wide variety of palaeontological data, are used to define an "event" stratigraphy. King's Ieper Clay Formation scheme is summarised in Fig 8.2b.

8.4.3 The Vlierzelle Formation

Steurbaut and Nolf's (1986) Pittem Clay Member of the Vlierzelle Formation was sampled for the present study at Egem. This member is an oxidised sandy clay and clayey silt, with levels of glauconite. The lower 5m of the member is exposed at Egem, and although the section is barren of calcareous nannofossils, Steurbaut and Nolf assign the member elsewhere to the middle of the NP13 nannoplankton zone.

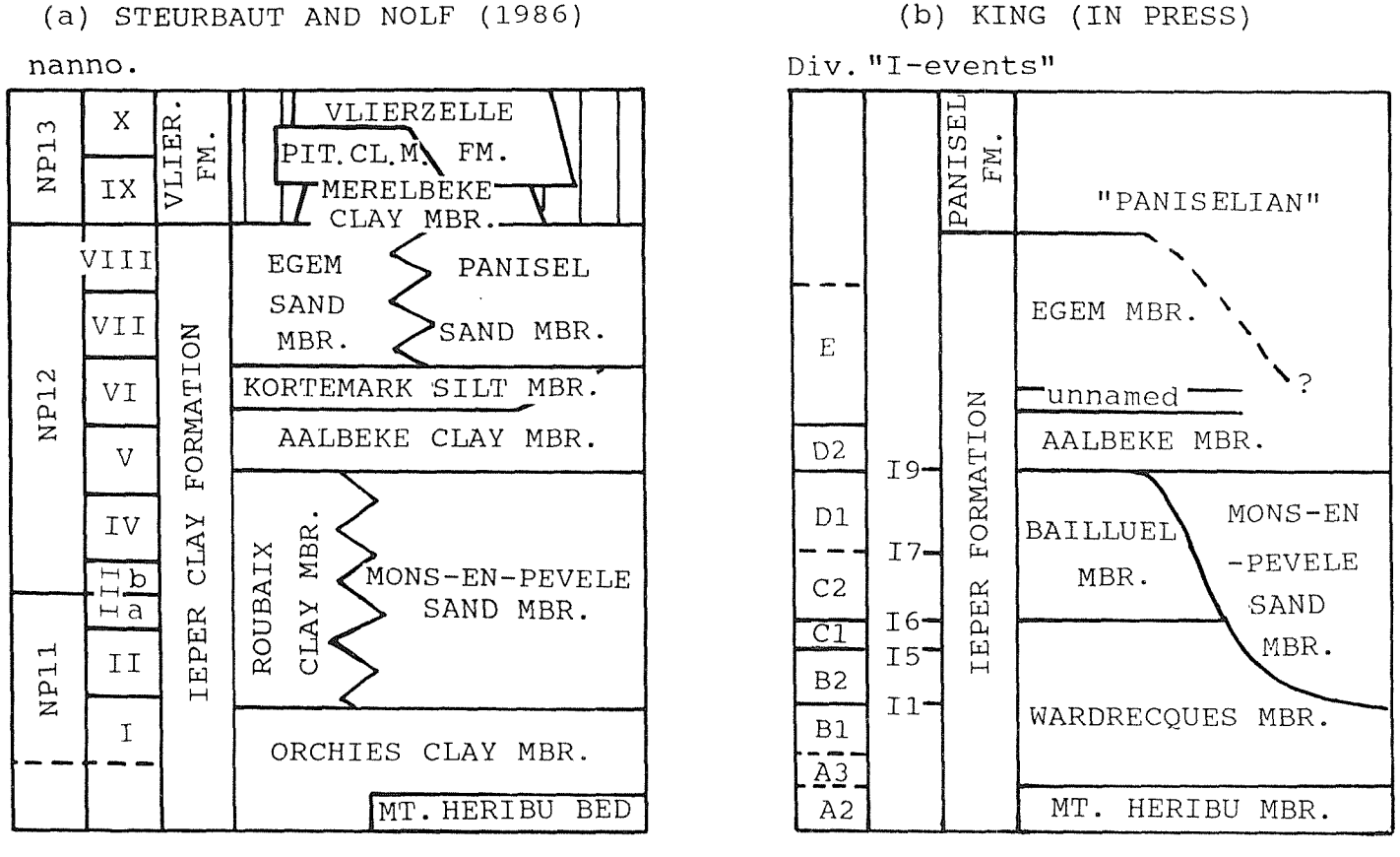

Fig 8.2 The stratigraphy of the Ieper Clay Formation. (a) Steurbaut and Nolf's (1986) scheme and (b) King's (in press) scheme.

8.5 Magnetostratigraphic results from France

8.5.1 Flines-les-Raches

The lectostratotype of the Orchies Clay Member is exposed in the "Briqueterie Bar Freres" clay-pit (map sheet Carvin (1:50,000), XXV-5; coords: X=659.6, Y=304.3). The upper 13.75m of the Landen Formation (eight sites) and the lower 1.75m of the Orchies Clay Member (four sites) were sampled at this locality. The top 3m of the exposure was too weathered to consider sampling. Specimens from the Landen Formation were very weakly magnetic (about 0.2 mA/m) and were processed using the cryogenic magnetometer (up to 35mT demagnetisation). Specimens from the Orchies Clay Member were slightly stronger (about 0.6 mA/m) and were processed on the "Molspin" equipment (in peak fields typically of 30-40mT).

The magnetostratigraphic results are presented in Fig 8.3. The magnetisation of the Landen Formation is very poorly defined and only three sites produced meaningful polarity results. The two sites in the lower part of the Orchies Clay Member are reverse polarity, whilst the two sites above are normal polarity.

8.5.2 Le Forest

The upper part of the Landen Formation and the lower 10m of the Orchies Clay Member are exposed at the clay pit at Le Forest (no grid reference is available). Unfortunately, due to lack of time, only the upper 4.5m of the exposed part of the Orchies Clay Member could be sampled (seven sites). It must be noted that beds from this level are somewhat disturbed, most probably the result of crioturbation during the Pleistocene. An 8cm thick cemented block at the top of the member was retrieved, and later core drilled, as a safeguard should the unlithified material have been overprinted.

NRM intensities showed wide variation, but for most of the specimens were about 0.4 to 0.6 mA/m. The majority of specimens were processed to 30-40 mT on the "Molspin" equipment. A rather unusual feature of the demagnetisation

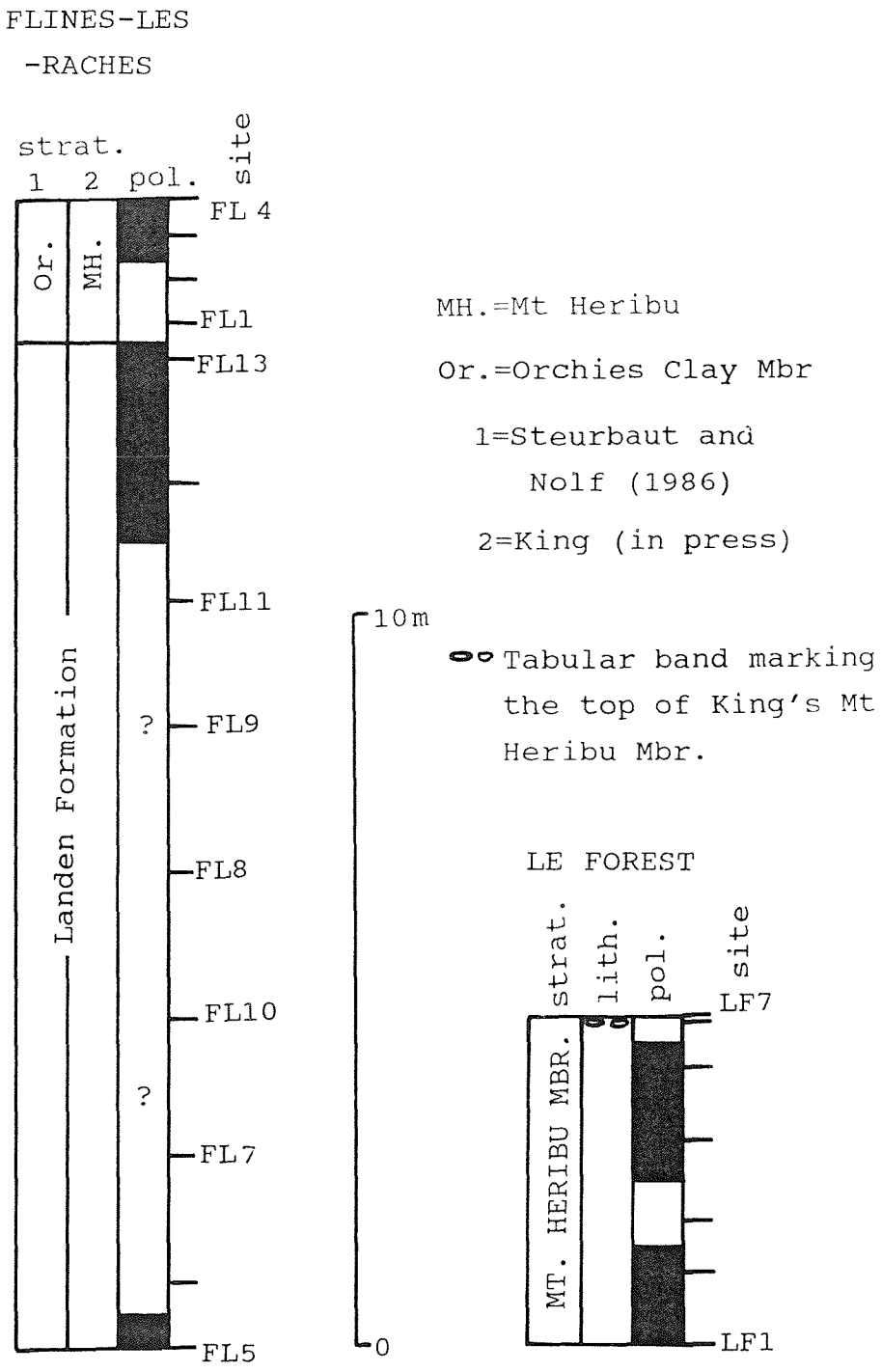

Fig 8.3 The magnetostratigraphy of the sections at Flines-les-Raches and Le Forest.

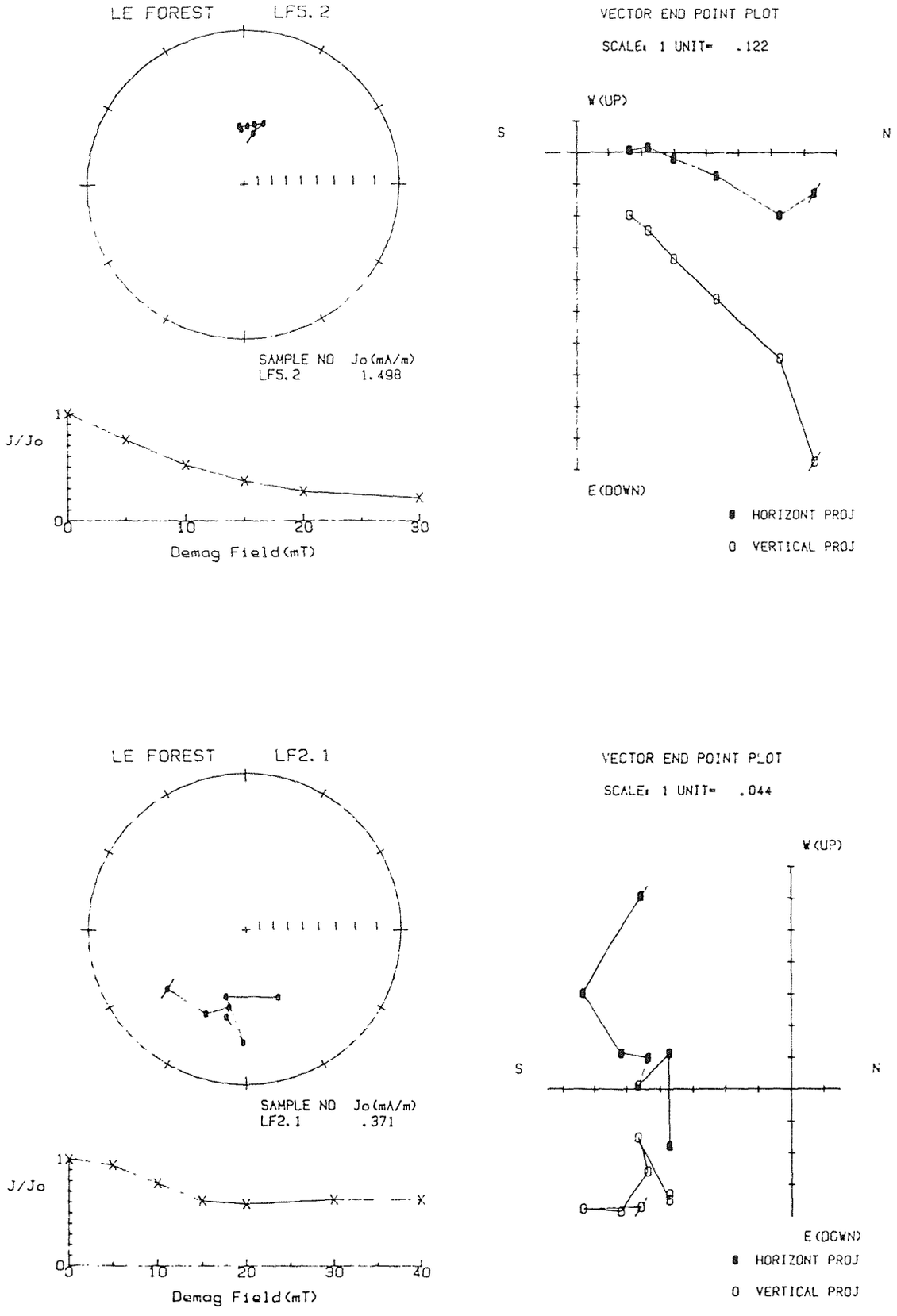

Fig 8.4 Examples of demagnetisation plots from the Mt Heribu Member at Le Forest. The upper plot shows a specimen with a normal polarity and the lower plot a specimen with an indeterminate polarity. For explanation of symbols see Fig 2.7.

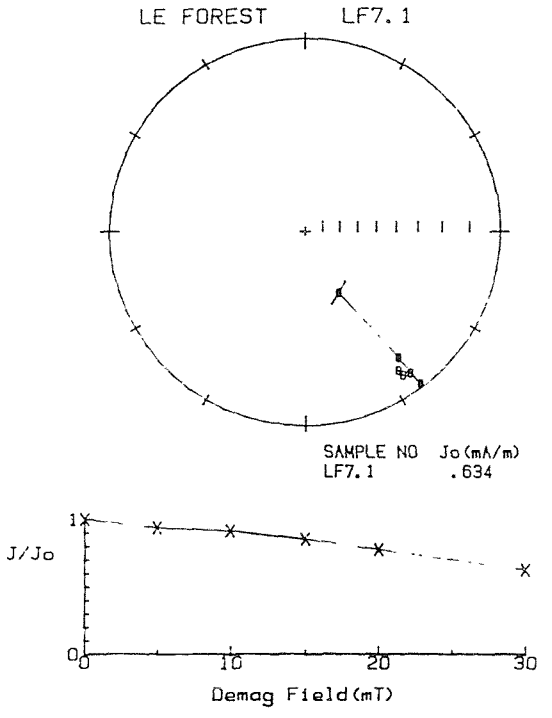

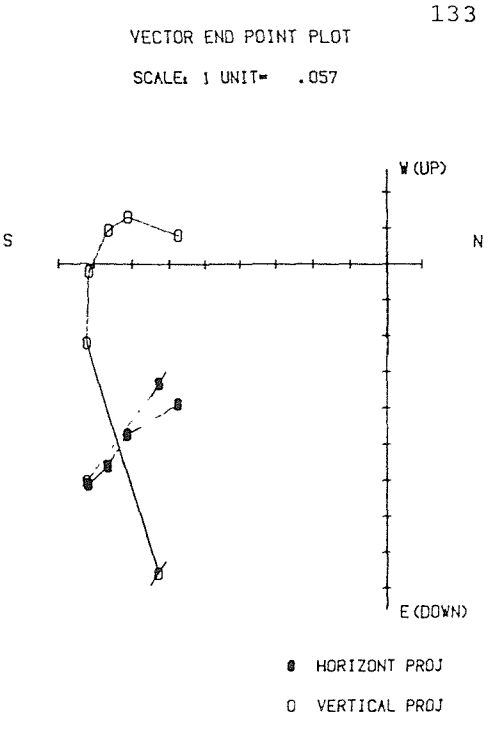

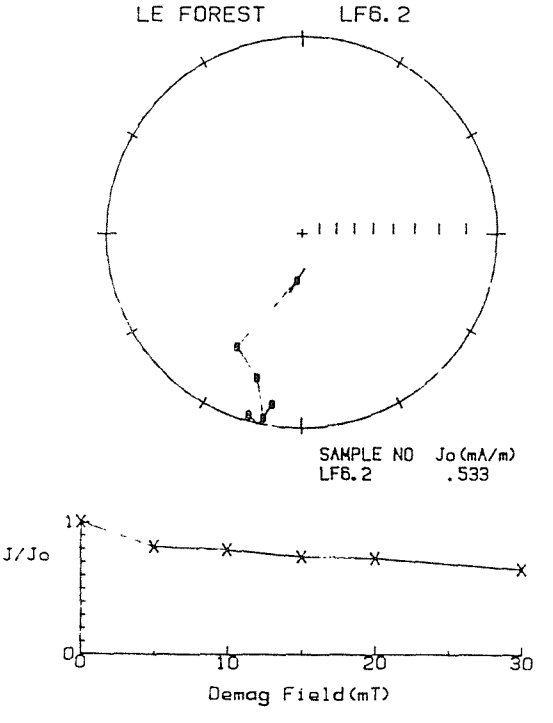

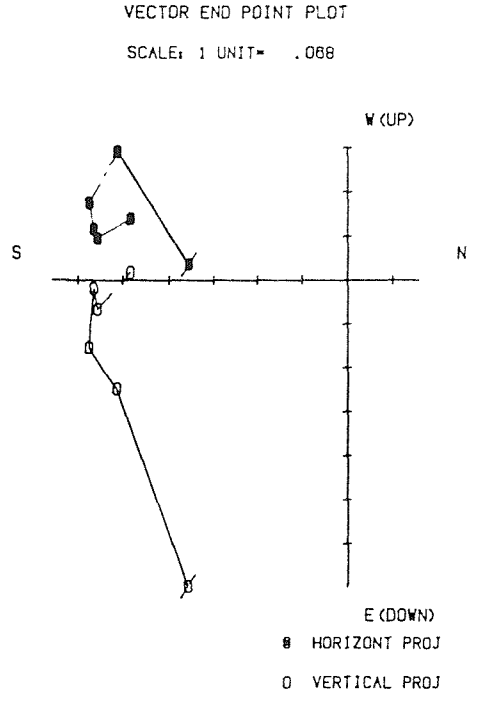

Fig 8.5 Typical reverse polarity specimens from the upper part of the Mt Heribu Member at Le Forest. For explanation of symbols see Fig 2.7.

data was that either specimens had very low MDF's (5-10 mT) or the MDF was not reached (this occurred with sister specimens from three sites). The material in the section was very hard and it is not inconceivable that some of the specimens suffered a Shock Induced Remanent Magnetisation (SIRM) during sampling. Typical demagnetisation data are presented in Fig 8.4 and 8.5.

The magnetostratigraphic results are presented in Fig 8.3. The results are rather confusing, with four normal polarity and three reverse polarity sites. It is worth noting that the specimens from the stone block produced a reverse polarity, and could represent the only reliable result.

The section at the nearby Wahagnies clay pit, which spans a similar stratigraphic interval, was too degraded to sample.

8.5.3 Wardrecques

King (1981) briefly described the clay-pit section at Wardrecques, 10km to the SE of St Omer in northern France (no grid reference is available). The section exposes the upper 26m of the Wardrecques Member and the lower 3m of the Bailluel Member (King, in press). However, during field-work in the spring of 1987 the Bailluel Member exposed at the top of the section appeared rather weathered, and only the Wardrecques Member was sampled (27 sites).

NRM intensities vary considerably with stratigraphic height. The four sites at the base of the section (spanning 3.4m) have values of about 1 mA/m, whilst those above (up to 18m OD) have values of about 10-30 mA/m. From 18m to the top of the section, the values are again about 1mA/m. IRM analysis was also carried out, after demagnetisation, on representative specimens from the section (the data are presented in Table 8.1). A major change in the magnetic properties of the sediments occurs between sites WQ17 and WQ20 (probably a change in mineralogy from magnetite to hematite).

Typical demagnetisation data are shown in Figs 8.6 and

8.7. The magnetic polarity results are shown in Fig 8.8. A normal polarity magnetozone, WQ-a, is present in the interval 0.55m to 18.05m. The top of WQ-a coincides with a significant change in the magnetic properties of the sediments in the section, and because of this, the results from the sites above this level should be ignored. The sediments in this interval (which has a dominantly reverse magnetisation) are believed to carry a CRM acquired sometime after deposition during a reverse polarity period. The three normal polarity sites at the very top of the section possibly represent a second CRM acquired in a later normal polarity interval.

specimen	pol	height (m)	NRM (mA/m)	IRM ratio	peak IRM (mAm^2)
WQ27.1	N	26.30	2.00	.73	1679
WQ20.1	R	19.40	1.38	.78	2965
WQ17.1	N	16.50	9.13	.93	6099
WQ13.1	N	12.00	27.59	.93	8639
WQ8.1	N	8.15	34.40	.94	9838
WQ4.2	N	3.40	1.91	.86	2631
WQ1.1	R	0.00	2.54	.88	2460

Table 8.1 The IRM acqusition data from the Wardrecques section.

8.6 The Kortrijk area

Four exposures near to the town of Kortrijk provide a composite section extending from the middle of Steurbaut and Nolf's (1986) Roubaix Clay Member, through the Aalbeke Clay Member to the base of the Panisel Sand Member.

8.6.1 Moen canal bank

The west bank of the Bossuit canal at Moen was chosen by Steurbaut and Nolf (1986) as the lectostratotype of the Roubaix Clay Member. A section similar to the one described in that paper was sampled along a transect on the west side of the canal bank, 50m south of the "3500" marker painted

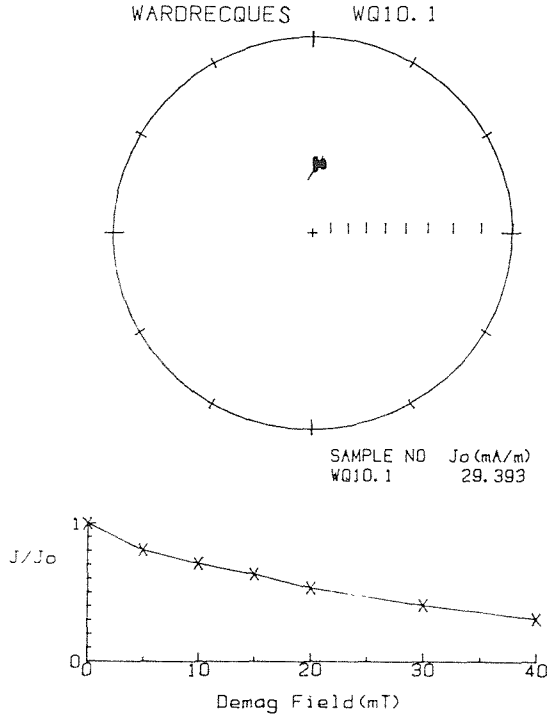

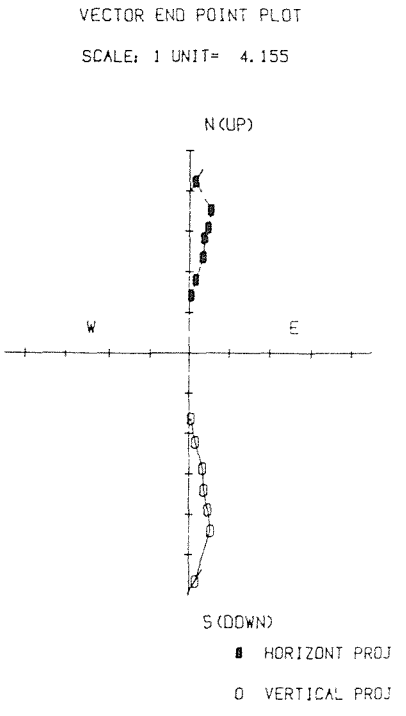

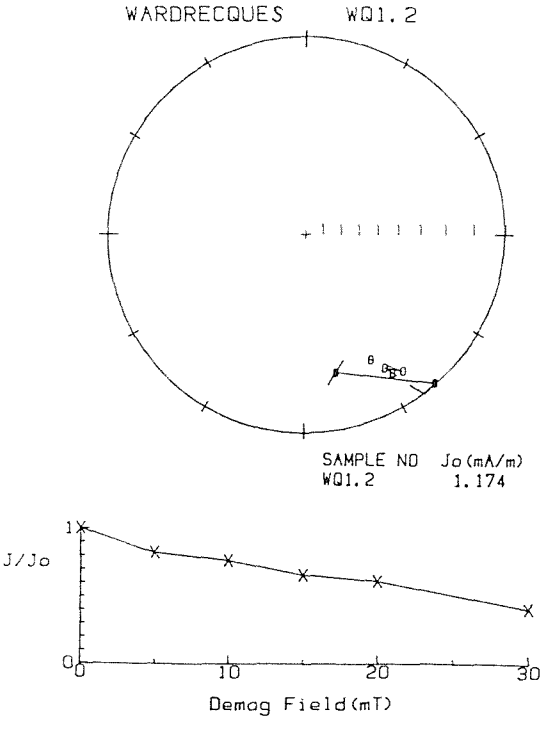

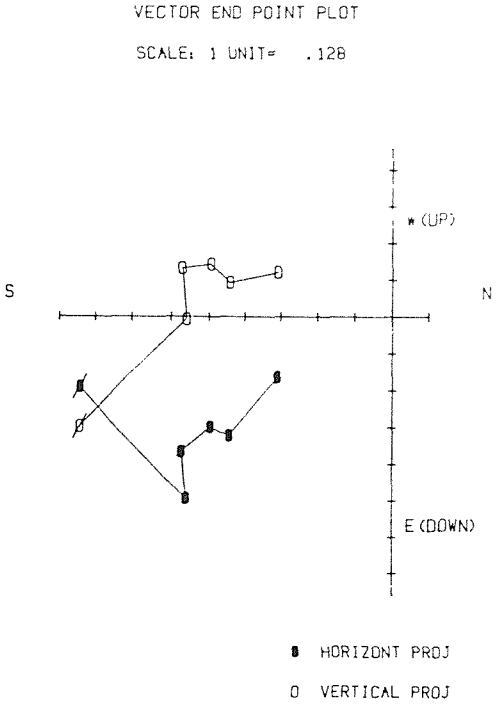

Fig 8.6 Examples of demagnetisation plots from the lower part of the Wardrecques Member at Wardrecques. The upper plot shows a specimen with a normal polarity and the lower plot a specimen with a reverse polarity. For explanation of symbols see Fig 2.7.

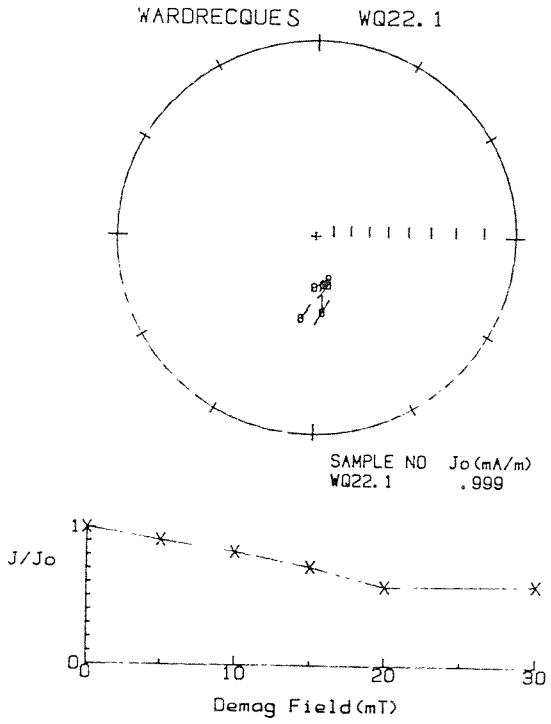

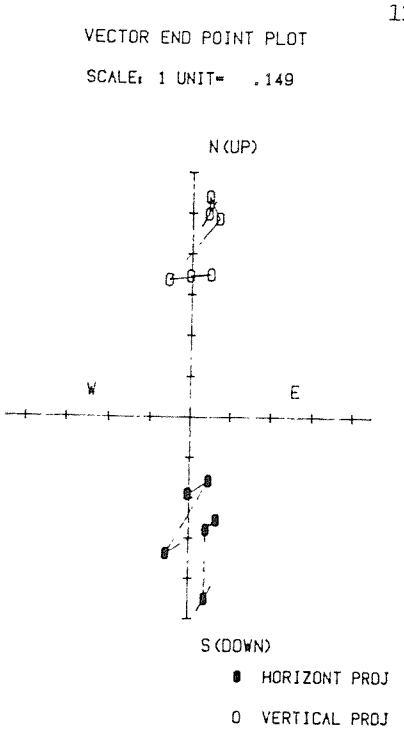

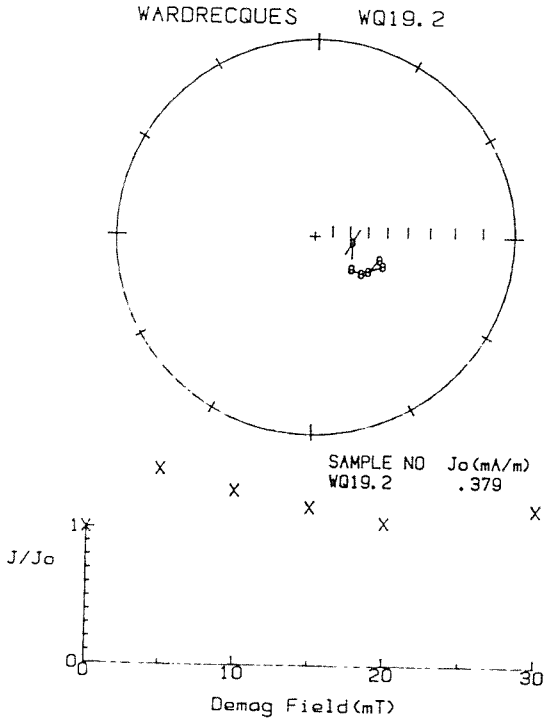

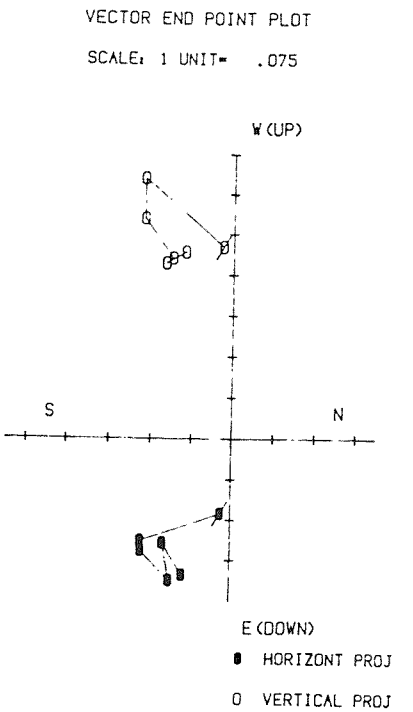

Fig 8.7 Typical reverse polarity specimens from the upper part of the Wardrecques Member at Wardrecques. For explanation of symbols see Fig 2.7.

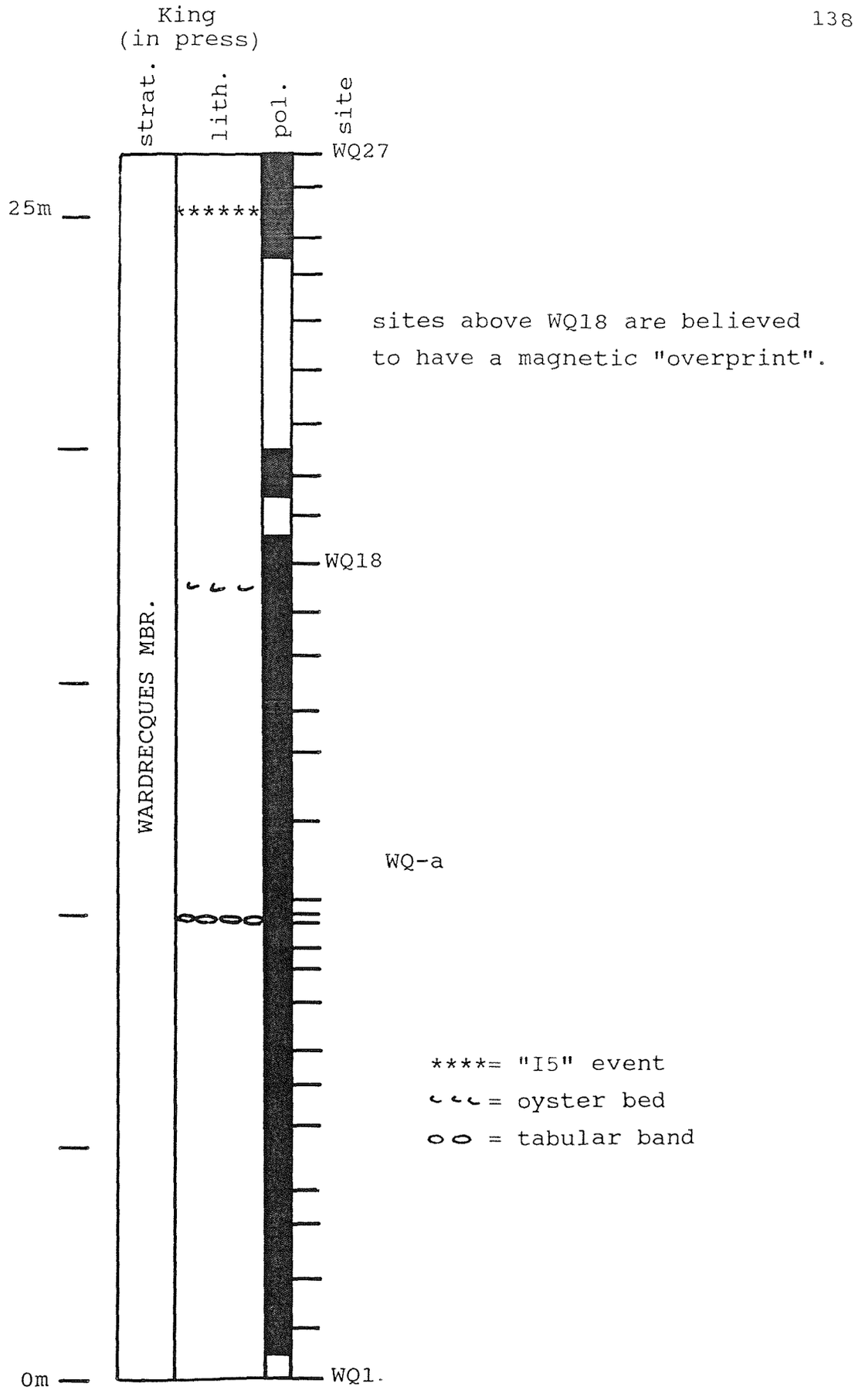

Fig 8.8 The magnetostratigraphy of the Wardrecques section.

on the towpath, at Moen. NRM intensities varied from 2-7 mA/m in the lower part of the section to about 1 mA/m in the upper part of the section. Representative demagnetisation data are presented in Fig 8.9. A simplified lithological log has been added to the magnetostratigraphic results (Fig 8.10). Important lithological units include the sandy interval at the base of the section, a 15cm thick glauconite level at +6m (taken as the junction between King's (in press) Wardrecques and Bailluel Members) and a Nummulite bed at +13.25m. Note that the sampled section begins at +1m.

A normal polarity magnetozone, MO-a, extends from the base of the section to 8.45m above datum (defined as site MO11 which has an indeterminate polarity). Steurbaut and Nolf (1986) identified the base of the Aalbeke Clay Member at the top of the Moen section. It was decided not to sample beyond site MO18, as the section appeared rather weathered above this.

8.6.2 Marke

The section at Marke is in the Koekelberg clay pit (map sheet 29/15; coords: X=69.0, Y=166.8). The top 13m of Steurbaut and Nolf's (1986) Roubaix Clay Member and the lowest 2m of the Aalbeke Clay Member are exposed. A number of minor faults are present in the section. In order to maximise the extent of the stratigraphic succession, the pit was sampled at both ends of the working face. NRM intensities varied between about 0.5 and 4 mA/m, with generally higher values in the upper part of the Roubaix Clay Member. Representative demagnetisation data are presented in Fig 8.11.

The magnetostratigraphic results are presented in Fig 8.10. The base of the Aalbeke Clay Member is taken as the site datum. Important lithostratigraphic markers occur at -12.7m (the glauconite horizon used to define the base of King's (in press) Bailluel Member) and at -10.8m and -8.3m (shell beds). According to Steurbaut and Nolf (1986, p 131), the NP11/NP12 nannoplankton zone junction occurs at

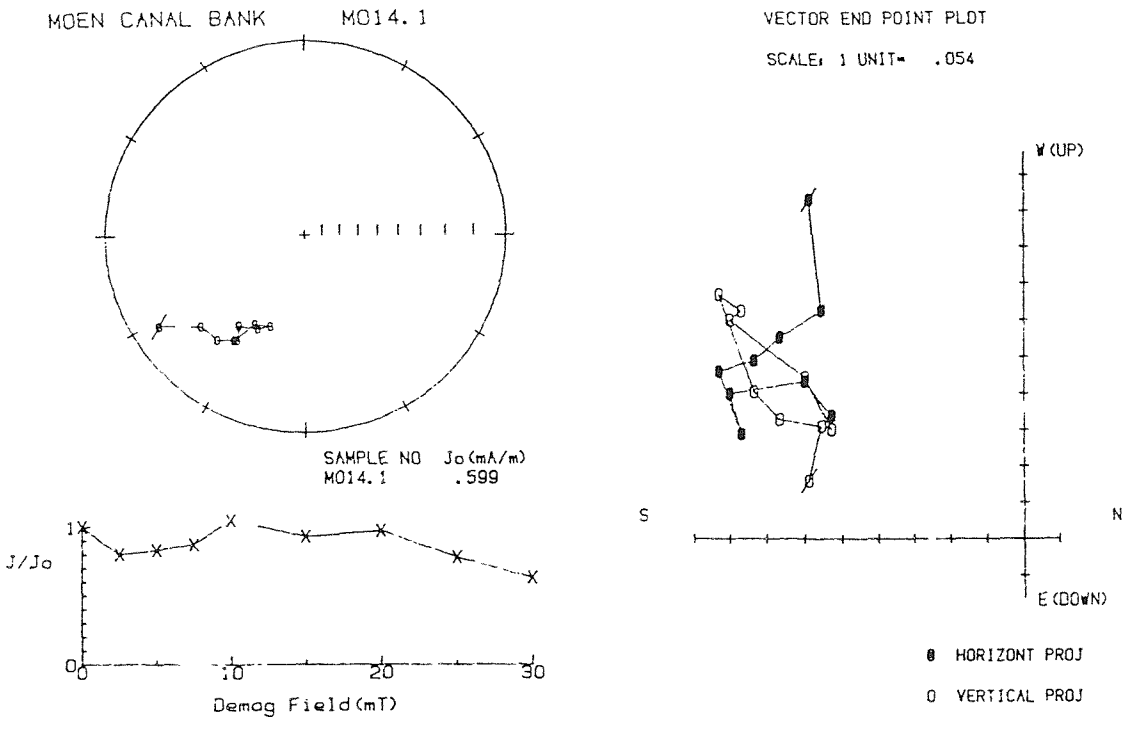

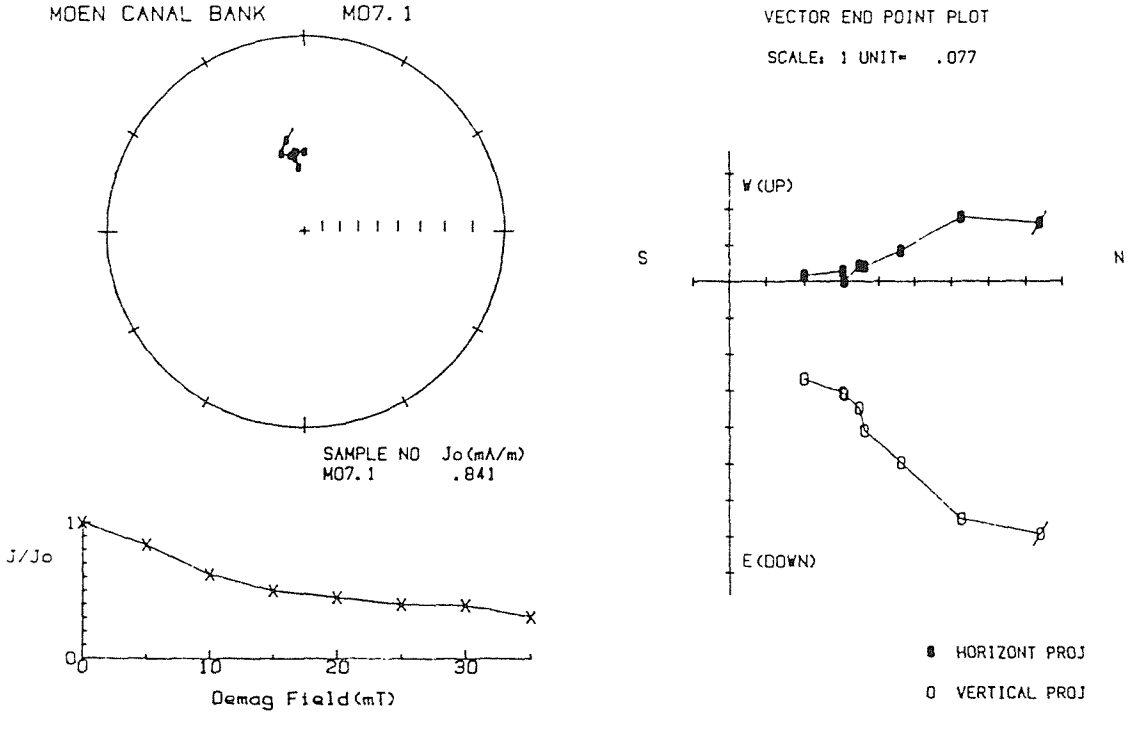

Fig 8.9 Examples of demagnetisation plots from the Moen canal bank section. The upper plot shows a specimen with a reverse polarity and the lower plot a specimen with a normal polarity. For explanation of symbols see Fig 2.7.

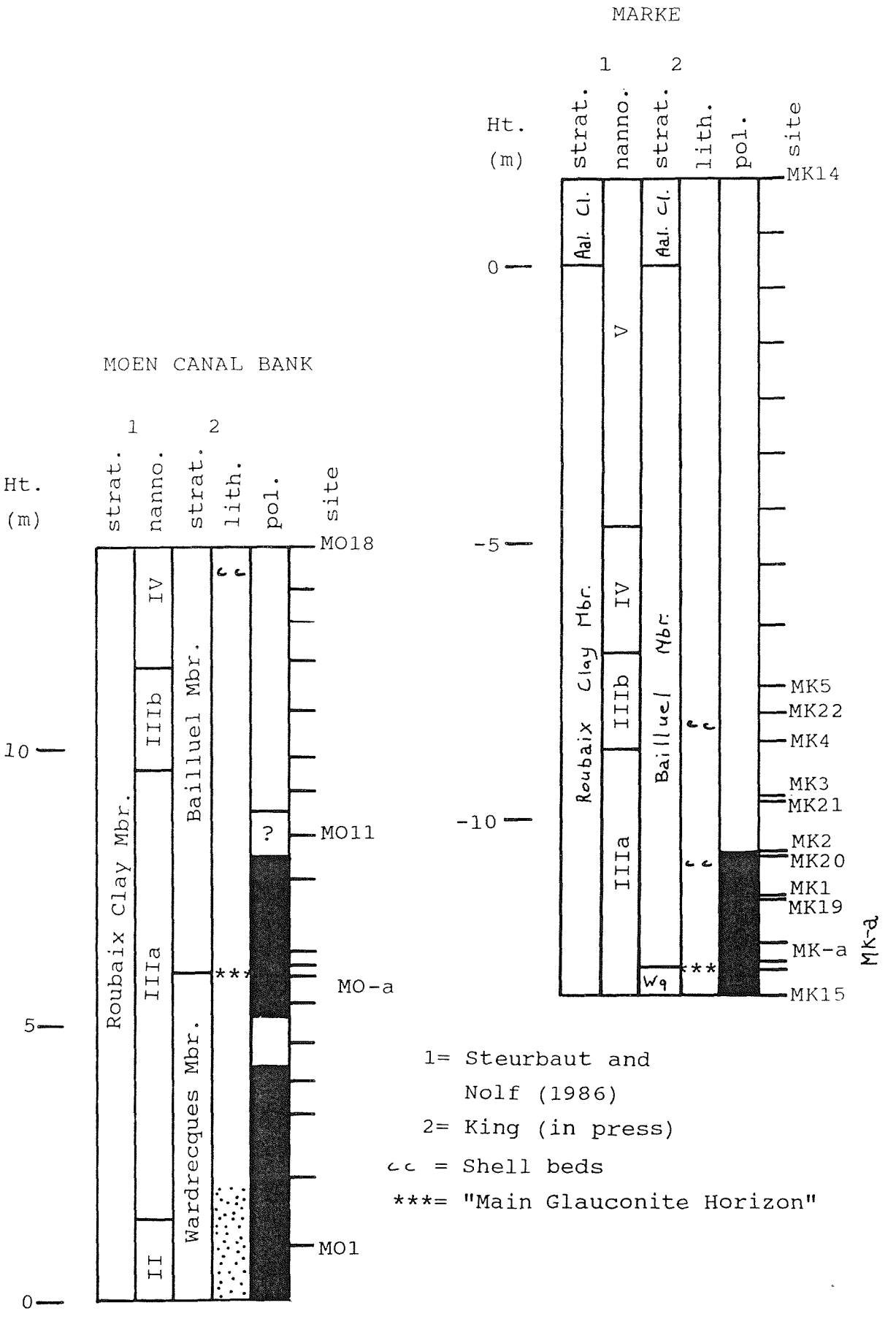

Fig 8.10 The magnetostratigraphy of the sections at Moen canal bank and Marke.

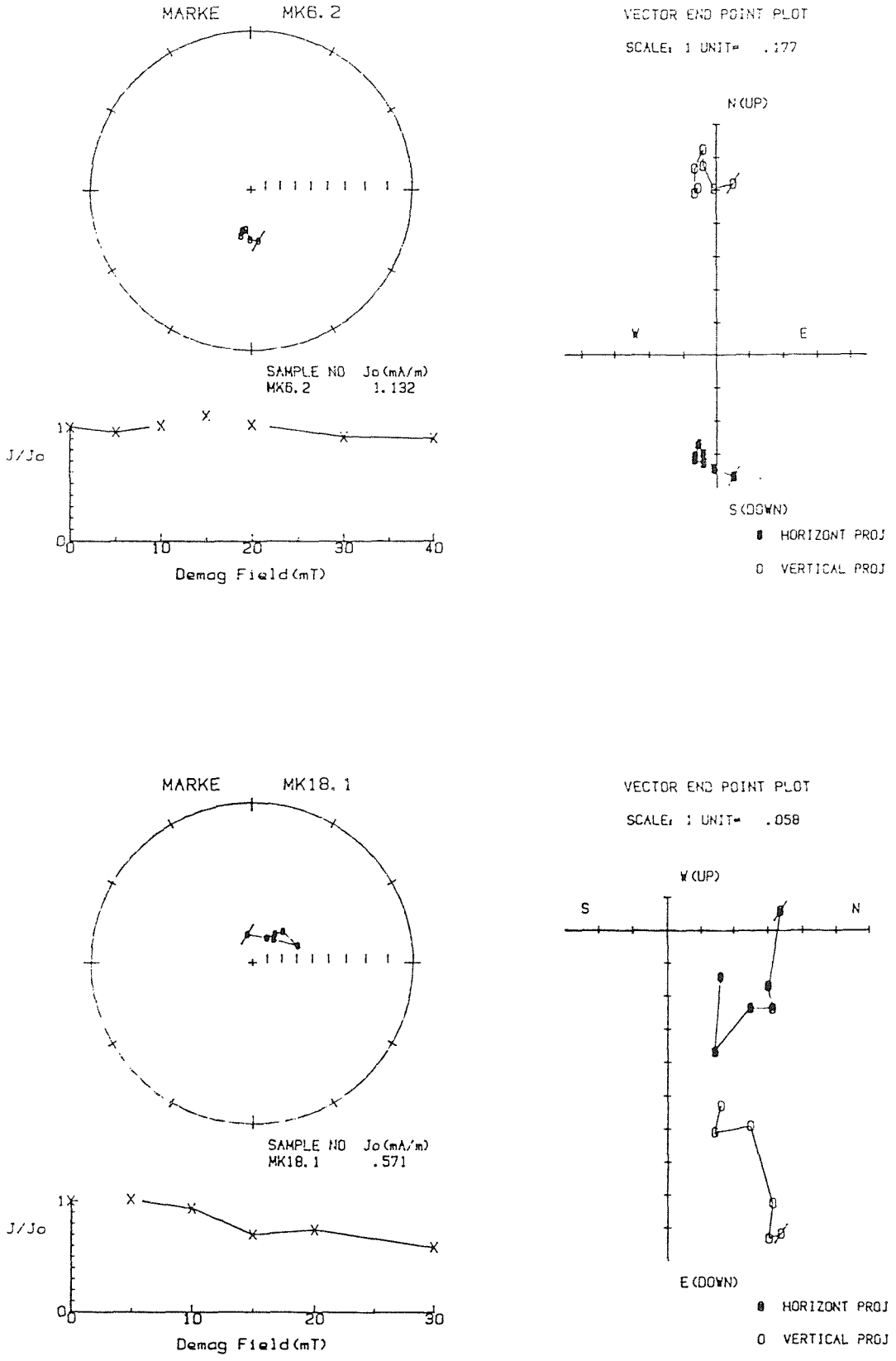

Fig 8.11 Examples of demagnetisation plots from the section at Marke. The upper plot shows a specimen with a reverse polarity and the lower plot a specimen with a normal polarity. For explanation of symbols see Fig 2.7.

about -9m in the sampled section. A normal polarity magnetozone, MK-a, was identified at the base of the section. The top of MK-a is very accurately located between sites MK20 and MK2 at -10.62m below datum.

8.6.3 Heerstert

The section at Heerstert is in the Kwadestraat pit (map sheet 29/6; coords: X=80.55, Y=165.55). Steurbaut and Nolf (1986) describe the succession as comprising 0.5m of the Roubaix Clay Member below 12m of the Aalbeke Clay Member, which in turn is topped by the basal 3m of the Panisel Member. Only the lower 4.2m of the Aalbeke Clay was sampled (six sites), as 1m above this level, the unit is intensively weathered to a soft yellowy clay.

NRM intensities for this section are very low (typically 0.2 to 0.3 mA/m). The magnetic polarity results are presented in Fig 8.12. A normal polarity magnetozone, HE-a, commences at 1.4m above the base of the Aalbeke Clay Member and continues to the top of the sampled section.

8.6.4 Moeskroen

The section at Moeskroen (the French spelling is Mouscron) is in the Bois Fichau pit (map sheet 29/6; coords: X=79.775, Y=164.725). The upper 7m of the Aalbeke Clay Member and the lower 3m of the Panisel Sand Member were sampled at a total of ten sites. NRM intensities varied from about 0.3 to 3 mA/m, with generally higher values in the upper part of the Aalbeke Clay Member. Typical demagnetisation plots are shown in Fig 8.13. The magnetostratigraphic results are presented in Fig 8.12. The locally developed oxidation band in the middle of the Aalbeke Clay Member extends from 3.68 to 4.92m in the sampled section. A normal polarity magnetozone MU-a is present from the base to the top of the section.

8.7 Ronse

(Map sheet 30/5; coords: X=98.525, Y=159.9). The disused railway cutting near Waaienberge exposes the upper part of

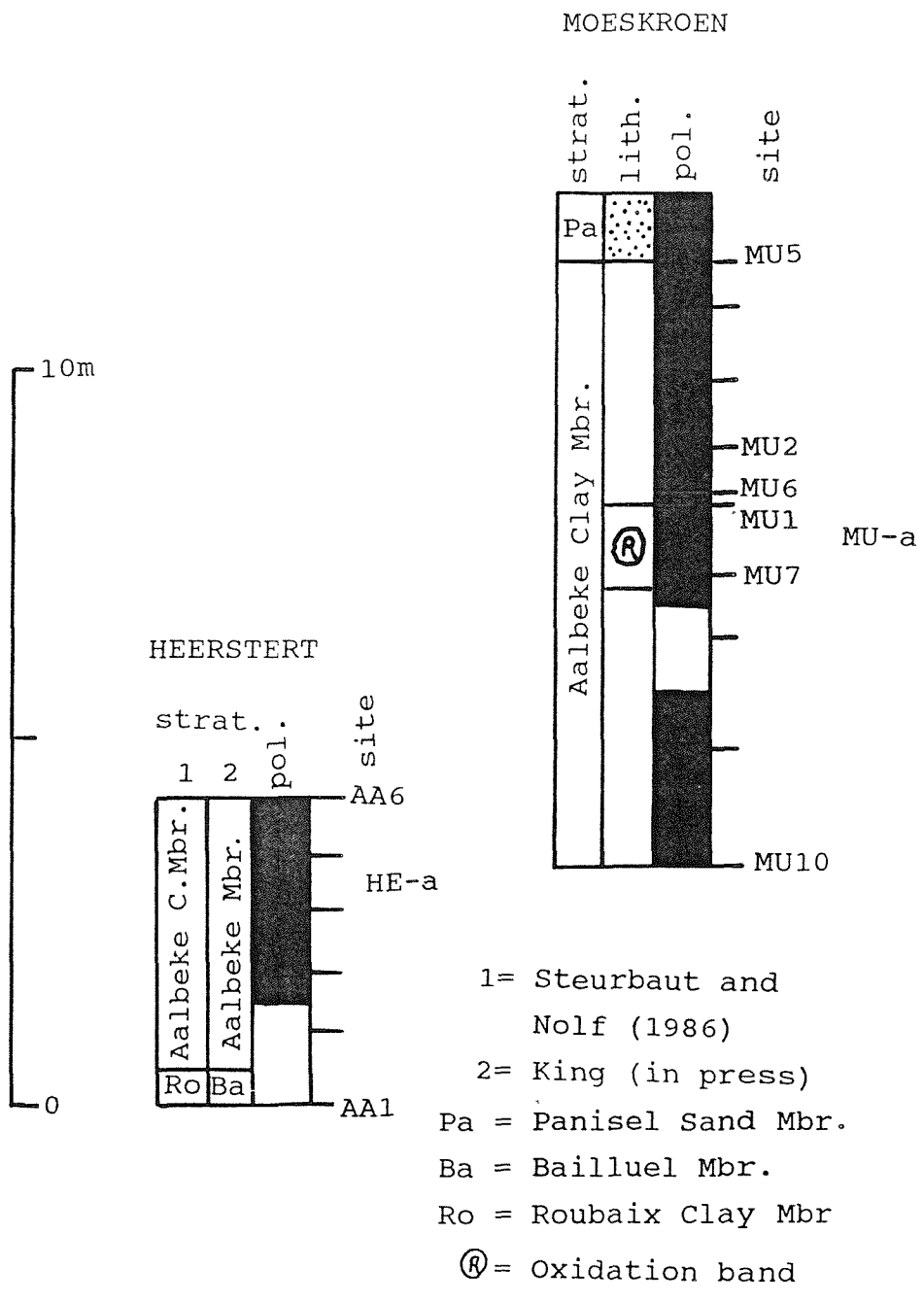

Fig 8.12 The magnetostratigraphy of the sections at Heerstert and Moeskroen.

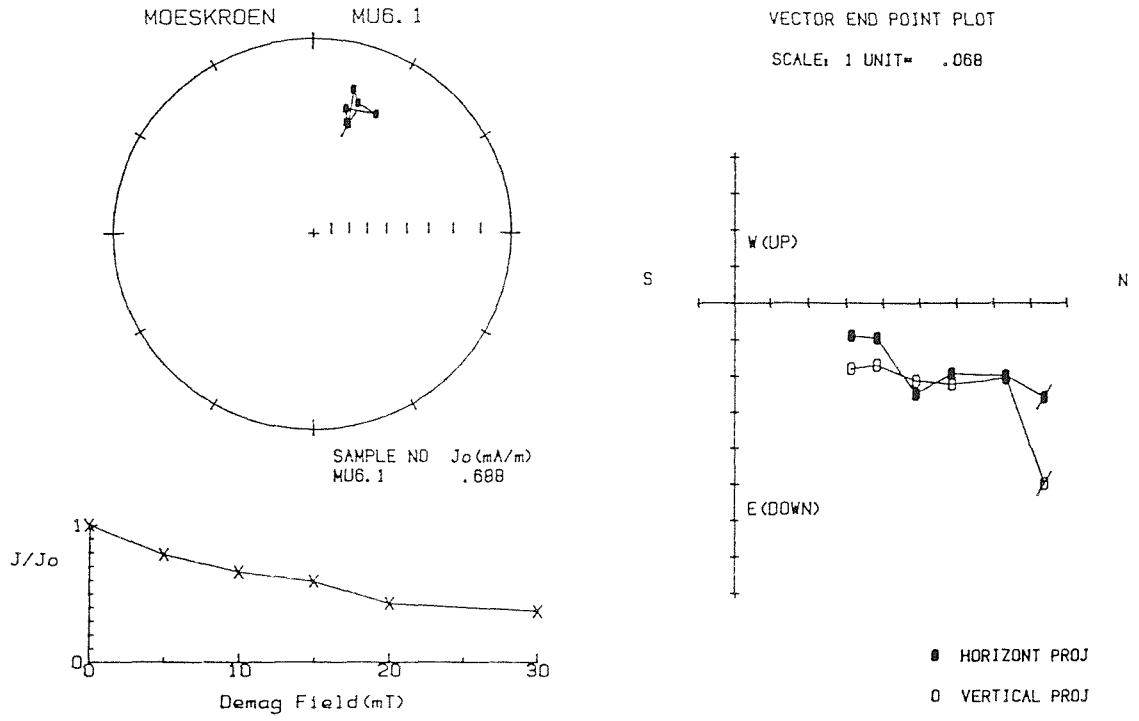

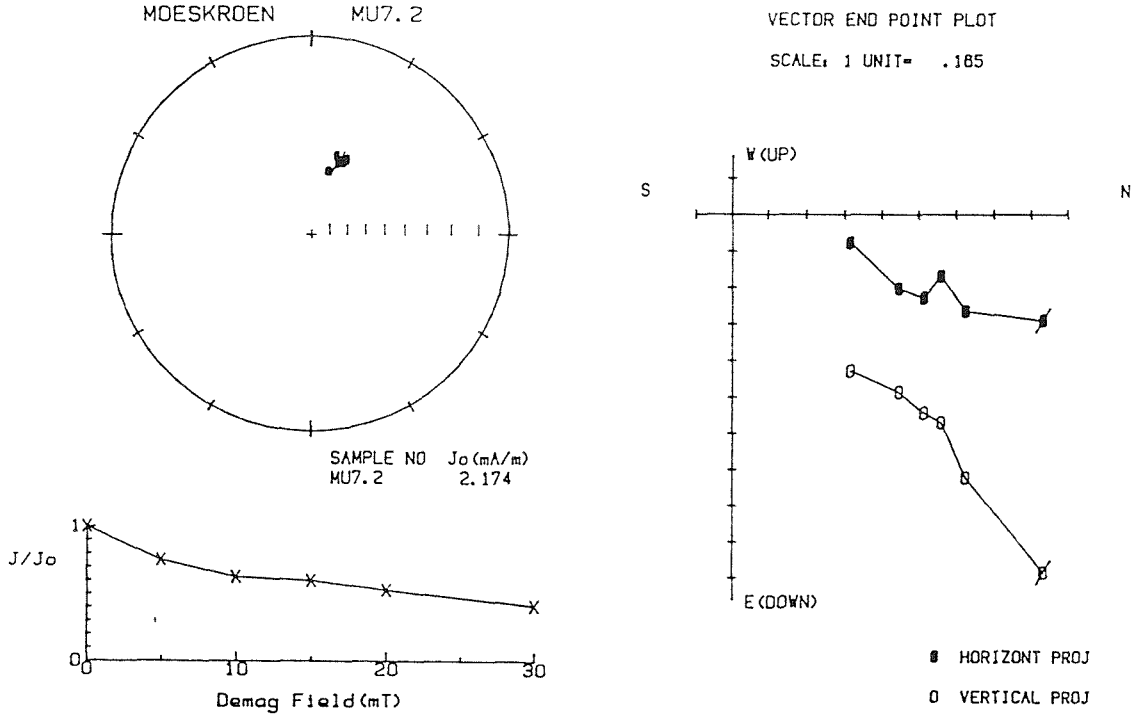

Fig 8.13 Typical normal polarity specimens from the Aalbeke Clay Member at Moeskroen. For explanation of symbols see Fig 2.7.

the Mons-en-Pevele Sand Member and the lower 3m of the Aalbeke Clay Member. The section is overgrown with vegetation and is very weathered, however, seven sites were sampled. NRM intensities varied between 0.1 and 6.9 mA/m. Demagnetisation results from this section are rather poor, with a couple of sister specimens producing contradictory polarities. The magnetic polarity results are summarised in Fig 8.14. These results should be treated with great caution.

8.8 Kortemark

This section is at the Desimpel clay pit (map sheet 20/3; coords: X=58.05, Y=190.4). The pit exposes the top of the Aalbeke Clay, the Kortemark Silt Member stratotype, and the lower half of the Egem Sand Member. The pit is worked from two levels; the lower one exposes 12m of the succession whilst the upper one exposes 20m. Sampling sites spanned a total thickness of 27.7m (Aalbeke Clay, 4 sites; Kortemark Silt, 25 sites; Egem sand, 2 sites).

NRM intensity measurements were originally carried out during July 1987 and the values were fairly uniform, varying between 0.5 and 1.5 mA/m. Demagnetisation commenced in January 1988 and so the NRM measurements were repeated. This time the intensities were in the range 2-30 mA/m. The "new" NRM was directed along the specimen Z-axis (parallel or antiparallel) presumably because they were stored "end-up". However, this component was easily removed at about 10mT (the MDF is typically 3-5mT). Typical demagnetisation plots are presented in Fig 8.15. The magnetostratigraphic results are presented in Fig 8.16. The section is normal polarity throughout (coded KM-a).

8.9 Egem

The section is in the Ampe clay and sand pit (map sheet 21/1; coords: X=70.15, Y=190.15). The upper third of the Kortemark Silt Member, the Egem Sand Member stratotype, and the lower part of the Pittem Clay Member were sampled (28 sites, including an oriented block from the shelly sand-

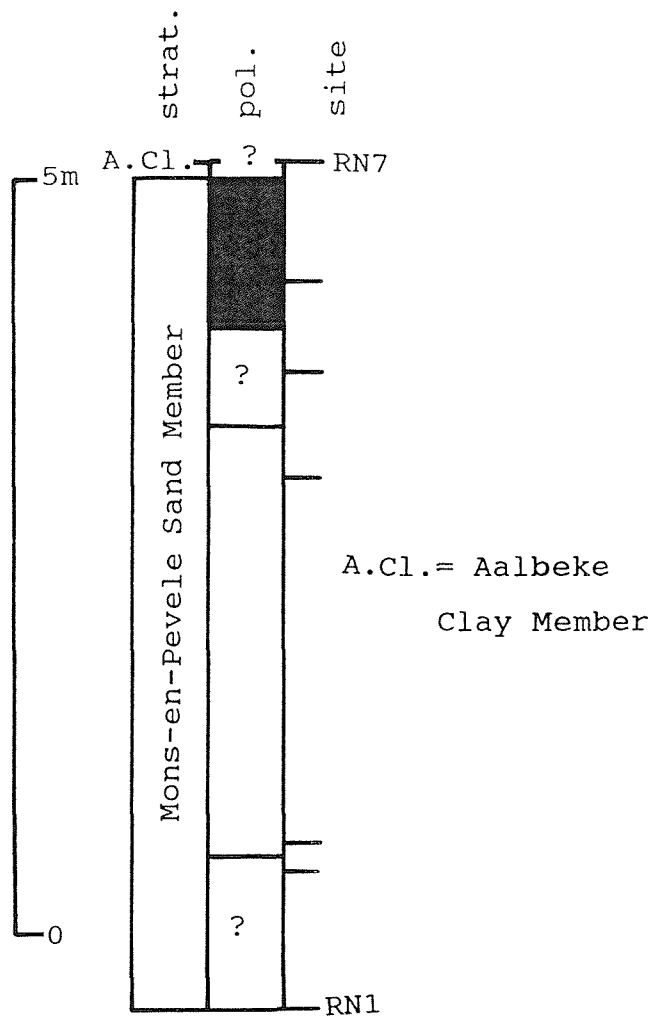

Fig 8.14 The magnetostratigraphy of the section at Ronse.

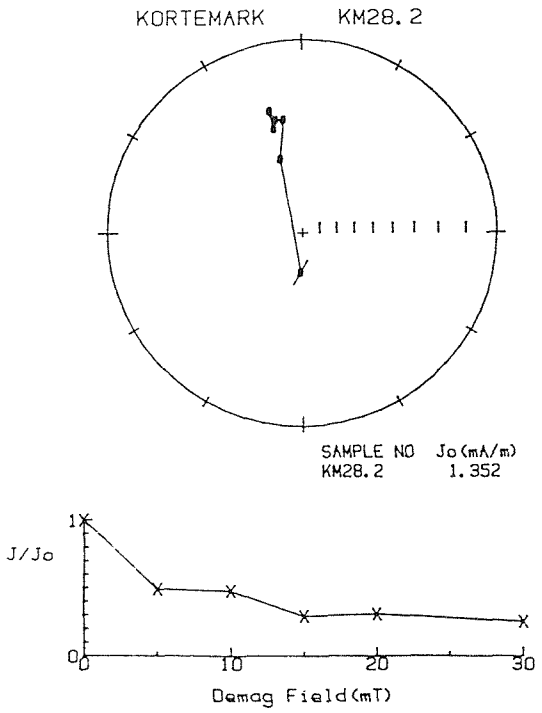

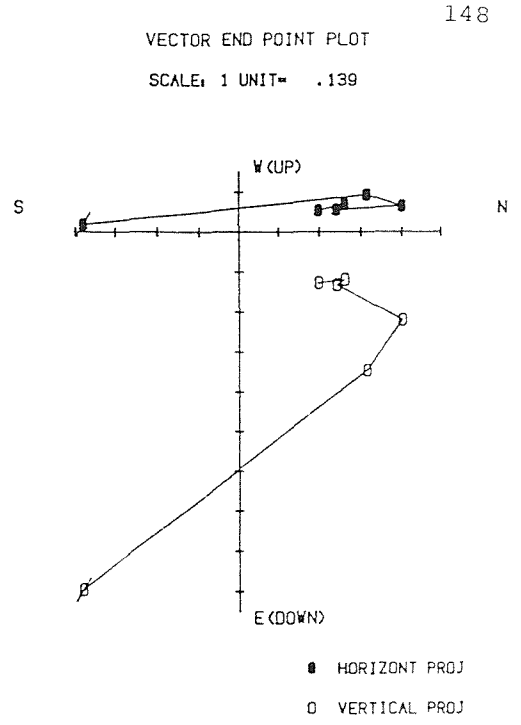

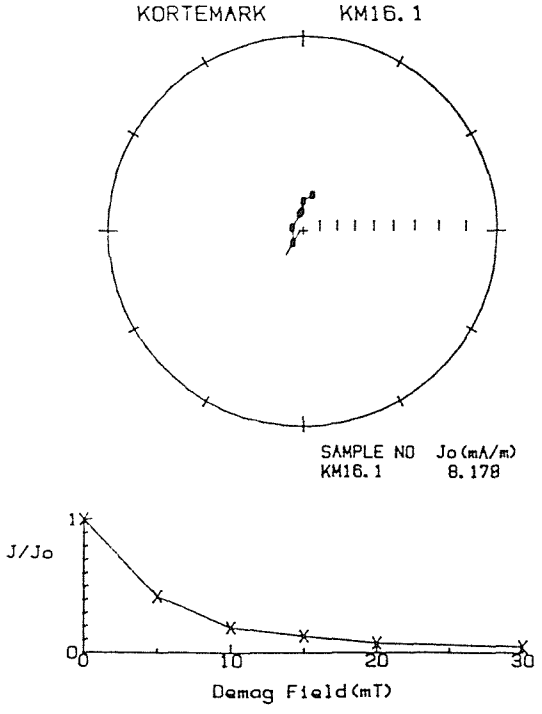

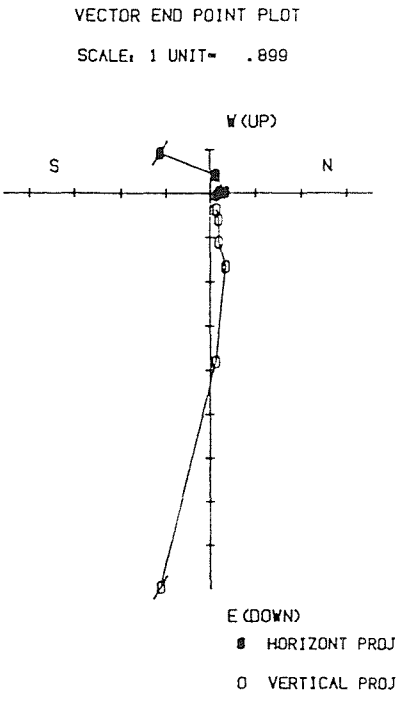

Fig 8.15 Typical normal polarity specimens from the Kortemark Silt Member at Kortemark. For explanation of symbols see Fig 2.7.

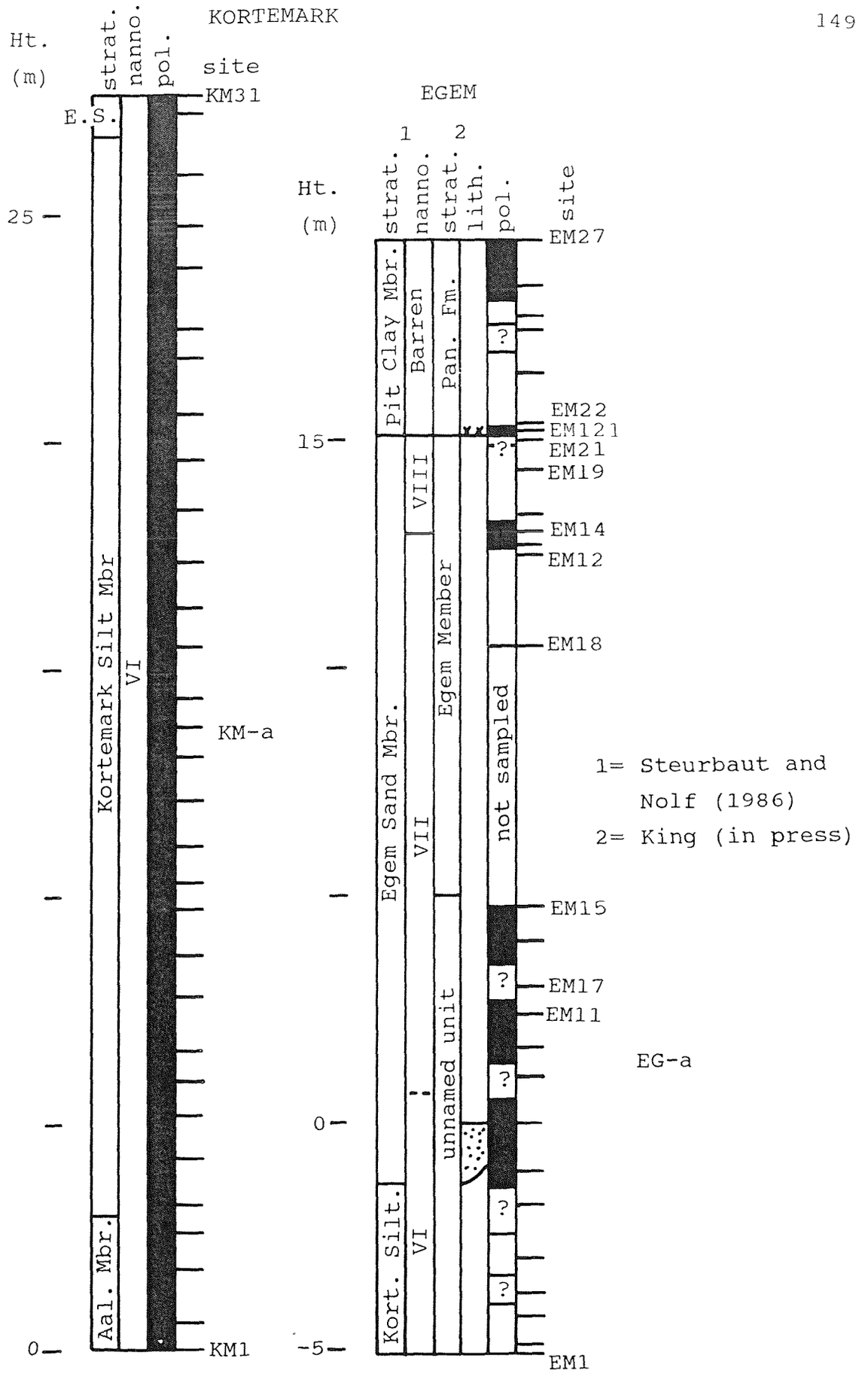

Fig 8.16 The magnetostratigraphy of the sections at Kortemark and Egem.

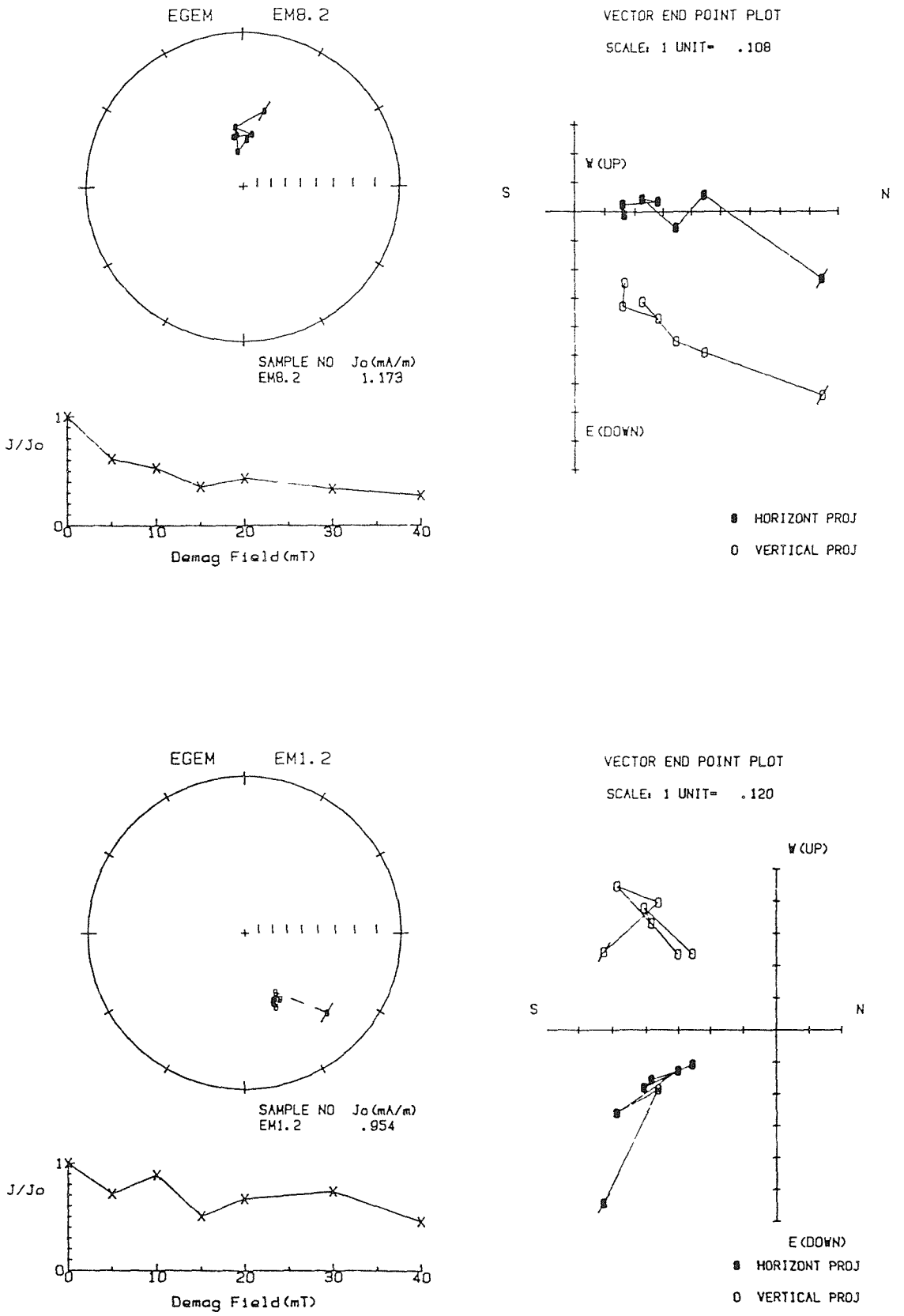

Fig 8.17 Examples of demagnetisation plots from the Kortemark Silt Member at Egem. The upper plot shows a specimen with a normal polarity and the lower plot a specimen with a reverse polarity. For explanation of symbols see Fig 2.7.

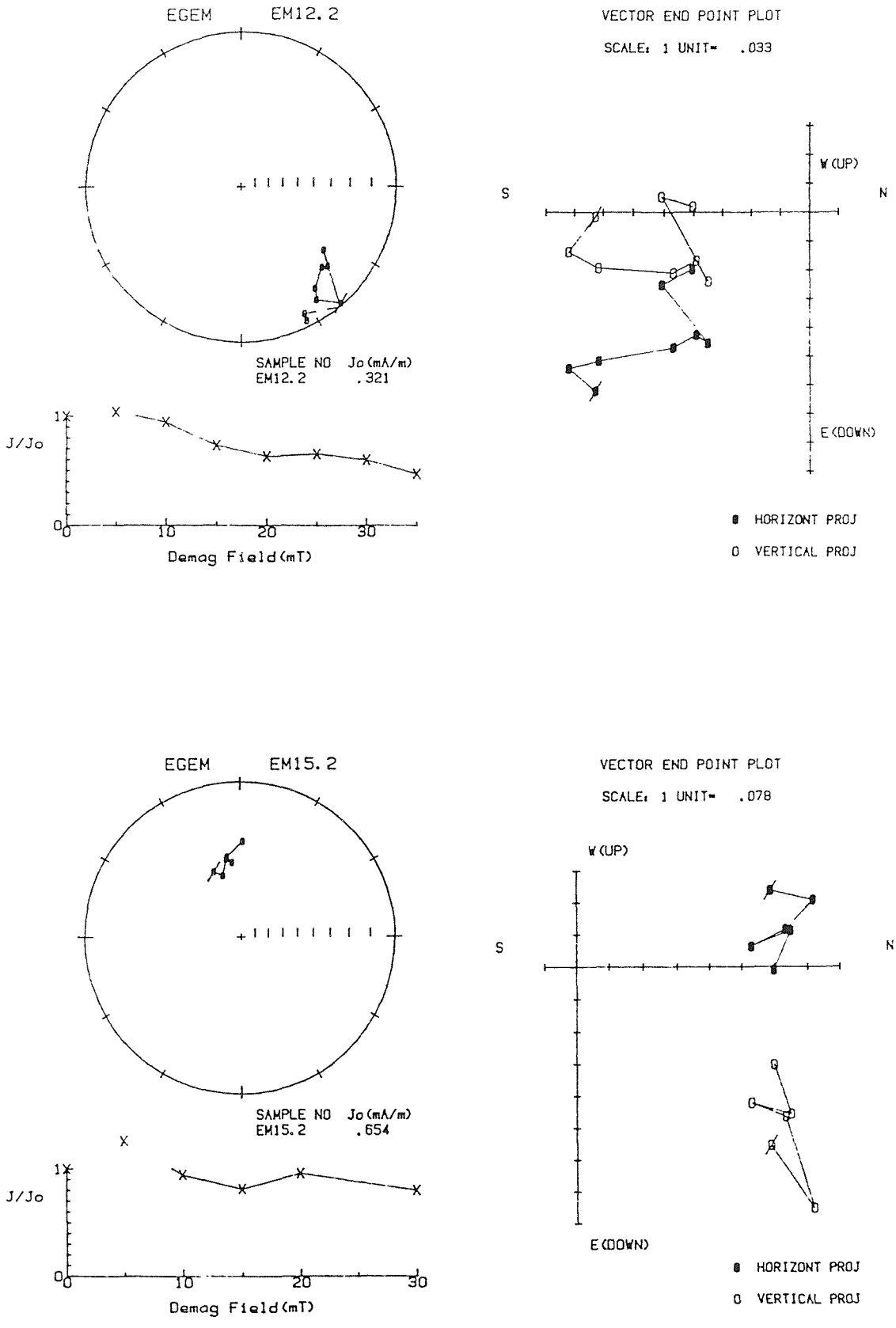

Fig 8.18 Examples of demagnetisation plots from the Egem Sand Member at Egem. The upper plot shows a specimen with a reverse polarity and the lower plot a specimen with a normal polarity. For explanation of symbols see Fig 2.7.

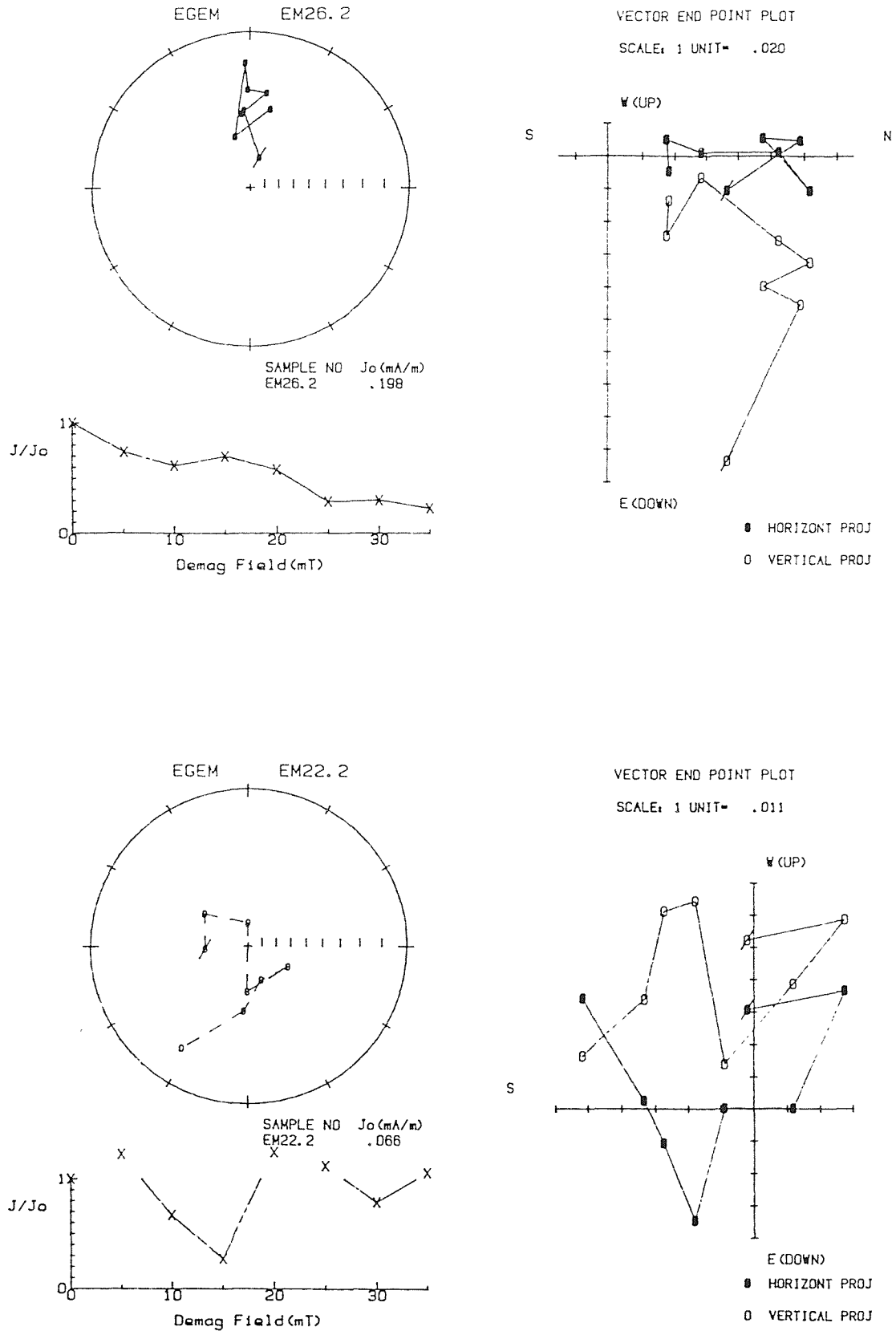

Fig 8.19 Examples of demagnetisation plots from the Pittem Clay Member at Egem. The upper plot shows a specimen with a normal polarity and the lower plot a specimen with a reverse polarity. For explanation of symbols see Fig 2.7.

stone at the base of the Pittem Member).

The specimens from the Kortemark Silt Member had NRM intensities of about 0.6 to 1.5 mA/m and could be processed using the "Molspin" equipment. Steurbaut and Nolf (1986) assign 20m of sediment at this locality to the Egem Sand Member. For the present study, the section was logged by C. King and the author, who estimate the Egem Sand Member to be much thinner (about 15m thick). The middle 5m of the Egem Sand Member, which is totally unlithified, was not sampled. The majority of sample sites above this level were located in thin clay seams, except for a few sites at the top of the member. The majority of the specimens were weakly magnetic (about 0.15 mA/m) and had to be processed on the cryogenic magnetometer. The specimens from the seven sites in the lower part of the Pittem Clay Member had NRM intensities typically in the range 0.1 to 0.4 mA/m, and most of these specimens were processed on the cryogenic magnetometer. Typical demagnetisation plots are shown in Figs 8.17 to 8.19.

The magnetic polarity results are presented in Fig 8.16. The Kortemark Silt Member is dominantly normal polarity, although three reverse and four indeterminate polarity sites were also identified in the member. This normal polarity level is coded EG-a and its top roughly coincides with the top of the Kortemark Silt Member. The remainder of the section above is dominantly reverse polarity, although the results are not particularly good. The two normal polarity sites at the top of the Pittem Clay Member should be treated with caution as this part of the section is very weathered.

8.10 Synthesis of the Ieper Clay Formation magnetozones

The ten exposures sampled in this study form a discontinuous sequence extending from the top of the Landen Formation, through the Ieper Clay Formation, to the base of the Vlierzelle Formation. The polarity results from eight of the ten localities are shown in Fig 8.20, with each of the sections drawn in its relative stratigraphic position.

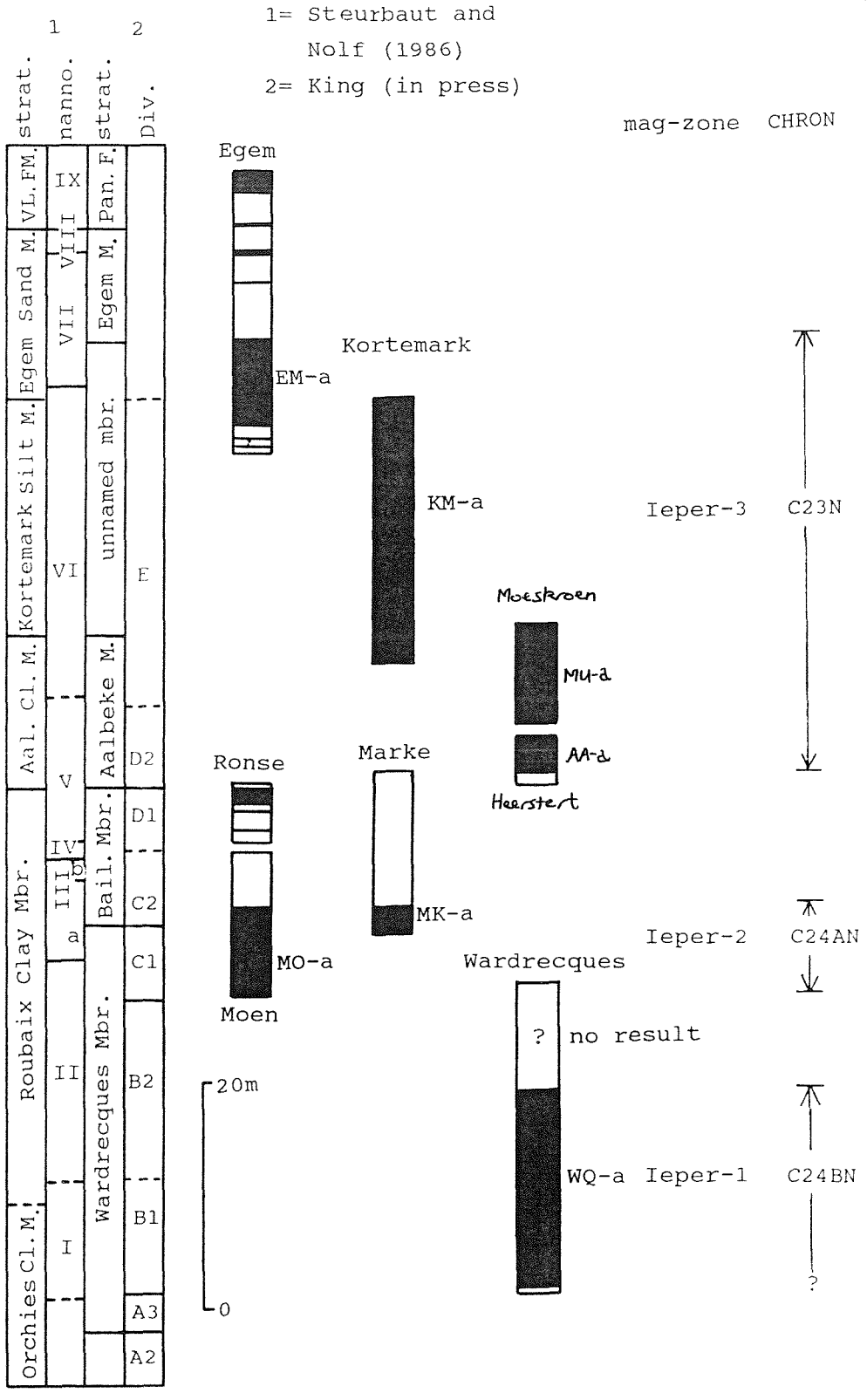

Fig 8.20 Synthesis of the Ieper Clay Formation magneto-zones and their proposed correlation with the geomagnetic polarity time-scale.

(The results from Flines-les-Raches and Le Forest are not included because the data from these sections are considered too poor.) Three discrete normal polarity magnetozones have been identified, and for discussion purposes are referred to as Ieper-1 to Ieper-3 in ascending stratigraphic order.

8.10.1 Ieper-1

The magnetozone WQ-a in the Wardrecque section is used to define Ieper-1. This magnetozone lies within levels of the Wardrecques Member which King (in press) correlates with Division B of the London Clay Formation. The top of Ieper-1 cannot be defined, as WQ-a is overlain by reverse polarity sediments which are thought to be the result of a secondary CRM.

8.10.2 Ieper-2

The normal polarity magnetozone Ieper-2 is present in the sections at Marke and Moen, where it is coded MK-a and MO-a respectively. The base of Ieper-2 has not been identified, but the lower part of this magnetozone is within the upper part of the Wardrecques Member. The top of Ieper-2 is positioned at 2.13m and 2.43m above the base of the Bailleul Member in the Marke and Moen sections respectively. This level is in the upper part of Steurbaut and Nolf's (1986) Roubaix Clay Member.

8.10.3 Ieper-3

The base of Ieper-3 is positioned 1.4m above the base of the Aalbeke Clay Member at Heerstert (HE-a). It occupies all of the Aalbeke Clay and Panisel Sand Members in the section at Moeskroen (MU-a). It continues up through to the top of the Kortemark Silt Member at Kortemark (KM-a), and terminates 5m above the base of the Egem Sand Member at Egem (where it is coded EM-a).

8.11 Correlation

The precise correlation of the magnetic polarity sequence with Steurbaut and Nolf's (1986) nannoplankton biozones is particularly important for two reasons. Firstly, the Ieper-1 to Ieper-3 series of magnetozones can then be correlated to the magnetic polarity sequence in the time-scales of Berggren et al (1985), and Haq et al (1987). Secondly, the Ieper Clay Formation is used to define the Ypresian, the international stage for the Early Eocene, and so it is extremely important to define the magnetostratigraphy of the formation. Fig 8.20 also illustrates the proposed correlation of the Ieper Clay Formation magnetozones with the geomagnetic polarity time-scale.

8.11.1 Ieper-1

The correlation of Ieper-1 is slightly problematic as Steurbaut and Nolf (1986) did not examine the section at Wardrecques where this magnetozone has been identified. However, King (in press) correlates the bulk of the Wardrecques section with Division B of the London Clay Formation. Ieper-1 can therefore be correlated indirectly with Chron C24BN via the Shep-1 and WB-a magnetozones in the English succession (see Chapter 7).

8.11.2 Ieper-2

The base of Ieper-2 is believed to coincide with the glauconite horizon marking King's (in press) I5 datum. King correlates the sediments below this level with Division B of the London Clay Formation, and those above with Division C. As the levels just above the I5 event are normal polarity, the base of Division C is thought to be younger in the Belgium Basin than in the London Basin, where it is reverse polarity. King's hypothesis that the base of Division C in the Belgium Basin marks a significant period of non-deposition is supported by the magnetostratigraphic data (Fig 8.20). Chron C24AN was identified in the middle part of Division C of the London clay Formation in the London Basin, and correlation of Ieper-2 with Chron C24AN

is proposed.

The top of Chron C24AN is conventionally placed just above the NP11/NP12 nannoplankton zone junction (e.g Berggren et al (1985)). The top of Ieper-2 is very accurately positioned at 2-3m below this level in Steurbaut and Nolf's (1986) Roubaix Clay Member at both Marke and Moen. The proposed correlation of Ieper-2 with C24AN raises two very important points:

1. The position of the NP11/NP12 junction in the magnetobiostratigraphic time-scales may have to be revised. The relative position of the zone junction and the top of Chron C24AN may not have been reliably defined in the pelagic successions (with their very much slower sedimentation rates) on which the time-scales are chiefly based.

2. Alternatively, the base of NP12 is younger in the more restricted North Sea Basin area than in the open oceans.

If the top of Chron C24AN is shown to be older than the base of NP12 in other North Sea Basin sections, then the reexamination of DSDP material from the NE Atlantic would help resolve this problem.

8.11.3 Ieper-3

Chron C23N is normally associated with the lower and middle part of the NP12 biozone, analogous to the position of Ieper-3 in the Belgium Basin sections. A direct correlation of Ieper-3 with Chron C23N is proposed.

8.12 Conclusions and suggestions for further work

Results from the first palaeomagnetic study of the Ieper Clay Formation have been presented. The base of the formation (Orchies Clay Member) is as old as Chron C24BR, whilst the very top of the formation (Egem Sand Member) can be correlated with Chron C22R. The normal polarity chrons, C24B, C24A and C23 have been identified, and this allows comparison of the calcareous nannoplankton zones of Steurbaut and Nolf (1986) with the most recent magneto-

biostratigraphic time-scales.

Future work should focus on the lower part of the Ieper Clay Formation (in borehole sections) in order to locate sediments below Chron C24BN. These sections would offer the chance to test the "A2/A3 transition" identified in the lower part of the London Clay Formation at Sheppey, as a magnetic marker.

The relative position of the top of Chron C24AN and the base of NP12 should be investigated at other sections. The results from Marke and Moen suggest that the top of Chron C24AN is older than the base of this biozone, which contradicts the currently accepted relative positions of these markers (Berggren et al, 1985).

Steurbaut (1988) suggests that the unconformity separating the Ypresian and Lutetian stages is shorter in duration in the Belgium Basin than in the Paris Basin. In the Belgium Basin there are a number of lithostratigraphic units which Steurbaut assigns to the middle part of nannoplankton zone NP13. Aubry et al (1986) demonstrate that Chron C22N is absent from the Hampshire Basin succession where there is a gap between the lower part of the NP13 and the middle of the NP14 nannoplankton zones. The formations just above the top of the Ieper Clay Formation should be investigated to see if Chron C22N may possibly be located within these levels.

Chapter 9 Results from the Late Palaeocene and Early Eocene of northern France and the Paris Basin

9.1 Introduction

This chapter presents the results from work carried out on the Late Palaeocene (Sparnacian) and Early Eocene (Cuisian) deposits in the Paris Basin and the Varengeville outlier. Although the French workers have expressed an interest in developing a magnetostratigraphy for these sequences (E. Hailwood, pers. comm.), the present study is believed to be the first of its type. The magnetic record within the Cuisian sediments is not particularly good, but it is possible to correlate the polarity sequence with the magnetic polarity time-scale of Berggren et al (1985).

9.2 Historical background

It was realised in the first half of the 19th Century that the Palaeogene deposits in and around the Paris area and the scattered outliers to the north, could be correlated with units in the Hampshire, London and Belgium Basins (e.g Dumont, 1849 and Prestwich, 1855). The Sparnacian (latest Palaeocene) and the Cuisian (Early Eocene) Stages were introduced by Dolfuss (1880). Although these terms are actually chronostratigraphic units, they are used by French stratigraphers as lithostratigraphic units (akin to the formation).

Feugeur (1963) in his monograph on the Ypresian of the Paris Basin provided an extremely detailed review of the work carried out on both the Sparnacian and the Cuisian (which were both included by him in the Ypresian). He also included details, or at least the location, of over 600 sections. Bignot (1980 and 1981) reviewed the work carried out on the Sparnacian and Cuisian stratotype sections. In Bignot's work the Sparnacian is used to cover the period of time between the top of the Thanetian and the base of the Ypresian, whilst the Cuisian represents the lower half of the Ypresian.

A general background to the stratigraphy of the French

Palaeogene is provided by Pomerol (1982).

In recent years important microplankton studies have been published. Chateauneuf and Gruass-Cavagnetto (1978) applied the dinoflagellate zonation scheme of Costa et al (1978) to the French Palaeogene. This enabled them to correlate the major lithostratigraphic units within the Cuisian with the successions in England and Belgium.

The most recent calcareous nannoplankton study has been by Aubry (1983). A condensed version of this thesis, which is written in English, was presented by Aubry (1986).Steurbaut and Nolf (1986) established a refined nannoplankton biozonation scheme for the Ypresian of the Belgium Basin. Steurbaut (1988) extended these zones to the Paris Basin by reinterpreting Aubry's (1983) data. In doing so he was able to very accurately correlate the upper part of the Cuisian with the middle part of the Ypresian in the Paris Basin.

9.3 The distribution of Palaeogene sediments in the Paris Basin and northern France.

The pattern of outcrop of the Late Palaeocene and Early Eocene deposits in the Paris Basin and northen France is presented in Fig 9.1. The exposure at Varengeville represents an outlier of the Dieppe Basin, which extends southeast from the Hampshire Basin under the east-central part of the English Channel. For Palaeogene stratigraphic purposes, the Varengeville outlier is one of the most valuable in NW Europe, as the sequence within it is intermediate between the English and Paris Basin successions. Sediments in the lower part of the section are assigned to the Sparnacian (= Woolwich Formation), whilst those in the upper part are equivalent to the lower and middle part of the London Clay Formation.

Further south into the Paris Basin the sediments are of basin margin facies. In Sparnacian times the environment was lagoonal, whilst in Cuisian times it was shallow marine to brackish (Feugeur, 1963). To the south and east of Paris, deposition was in a fluviatile/lacustrine environment. The location of the sections used to define the

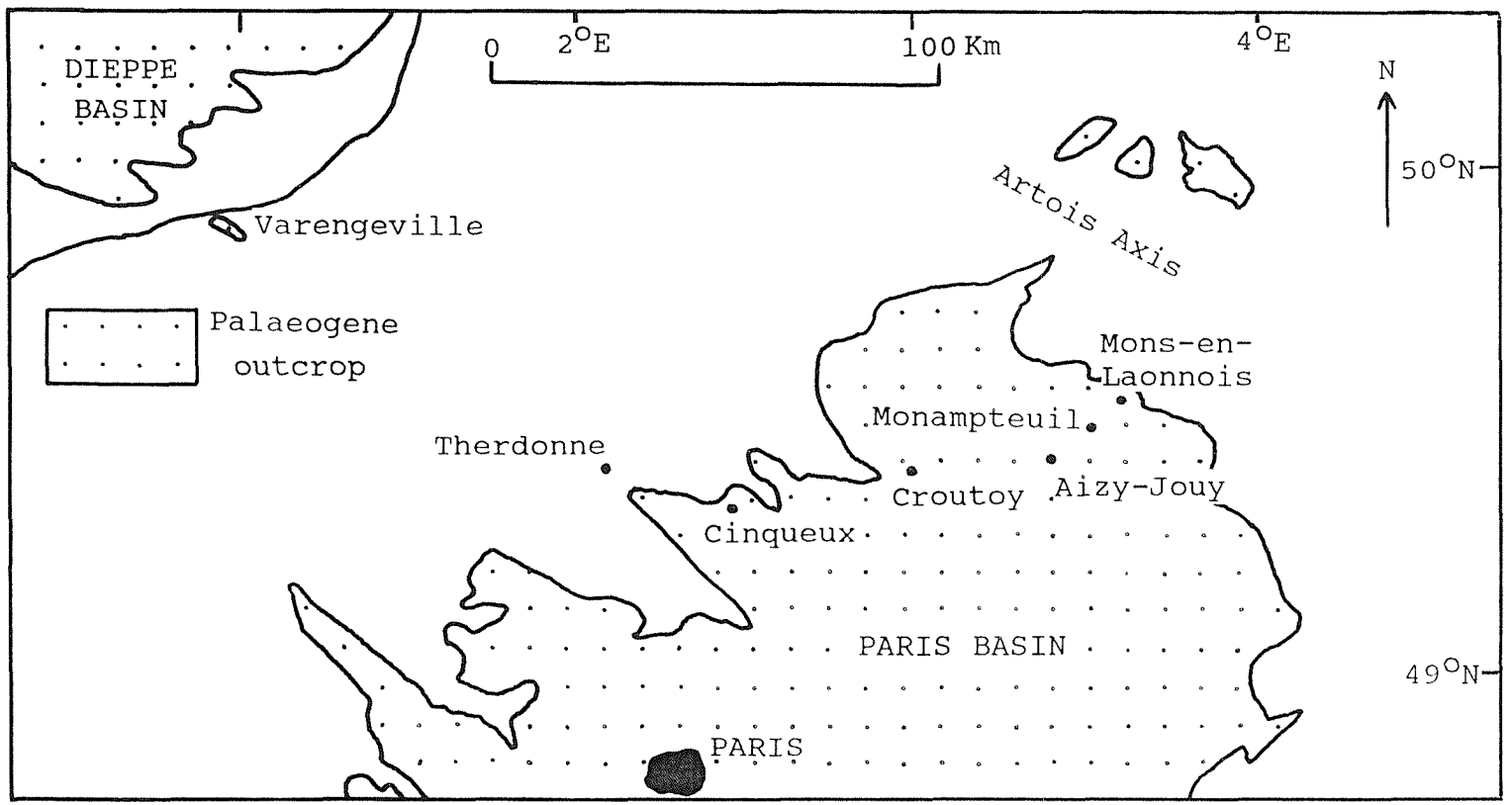

Fig 9.1 The distribution of Lower Palaeogene sediments in the Paris Basin and Northern France.

magnetostratigraphy of the Cuisian are in the northern part of the Paris basin, and are shown in Fig 9.1.

9.4 The formations investigated in this study

The Late Palaeocene and Early Eocene deposits of northern France and the Paris Basin have not yet been formally defined in the manner prescribed by Hedberg (1976). Instead people working on the French Palaeogene use the various stages (chronostratigraphic units) as lithostratigraphic divisions. The stratigraphy of the Late Palaeocene and the Early Eocene of nothern France and the Paris Basin is summarised in Fig 9.2.

9.4.1 "Thanetian" age deposits

The Sables de Bracheaux of the Paris Basin were thought to correlate with the Thanet Formation in England, because of the similarity of their mollusc assemblages, and thus to be Thanetian in age. However, Chateauneuf and Gruas-Cavagnetto (1978) assign this unit to the Apectodinium hyperacanthum dinoflagellate zone, making them much younger than the Thanet Formation. Eight metres of the upper part of the Sables de Bracheaux was sampled at Therdonne. There they consist of coarse grained sands varying in colour from white, grey and dark red to black. Occasional shell beds are present. Deposition was in a brackish/lacustrine environment.

9.4.2 Sparnacian age deposits

The Sparnacian (defined in the section at Epernay, 100Km to the east of Paris, by Dolfus, 1880) was reviewed by Bignot (1980). This unit consists of (ascending order) calcareous silts, lignites (each about 0.2m thick) interbedded with clays, blocky clays, and shell beds interbedded with laminated clays. The unit is about 10-15m thick in the northern part of the Paris Basin, and is assigned to the A. hyperacanthum dinoflagellate zone (Chateauneuf and Gruas-Cavagnetto, 1978), making it Late Palaeocene in age. The Sparnacian is correlated with the Woolwich and Reading

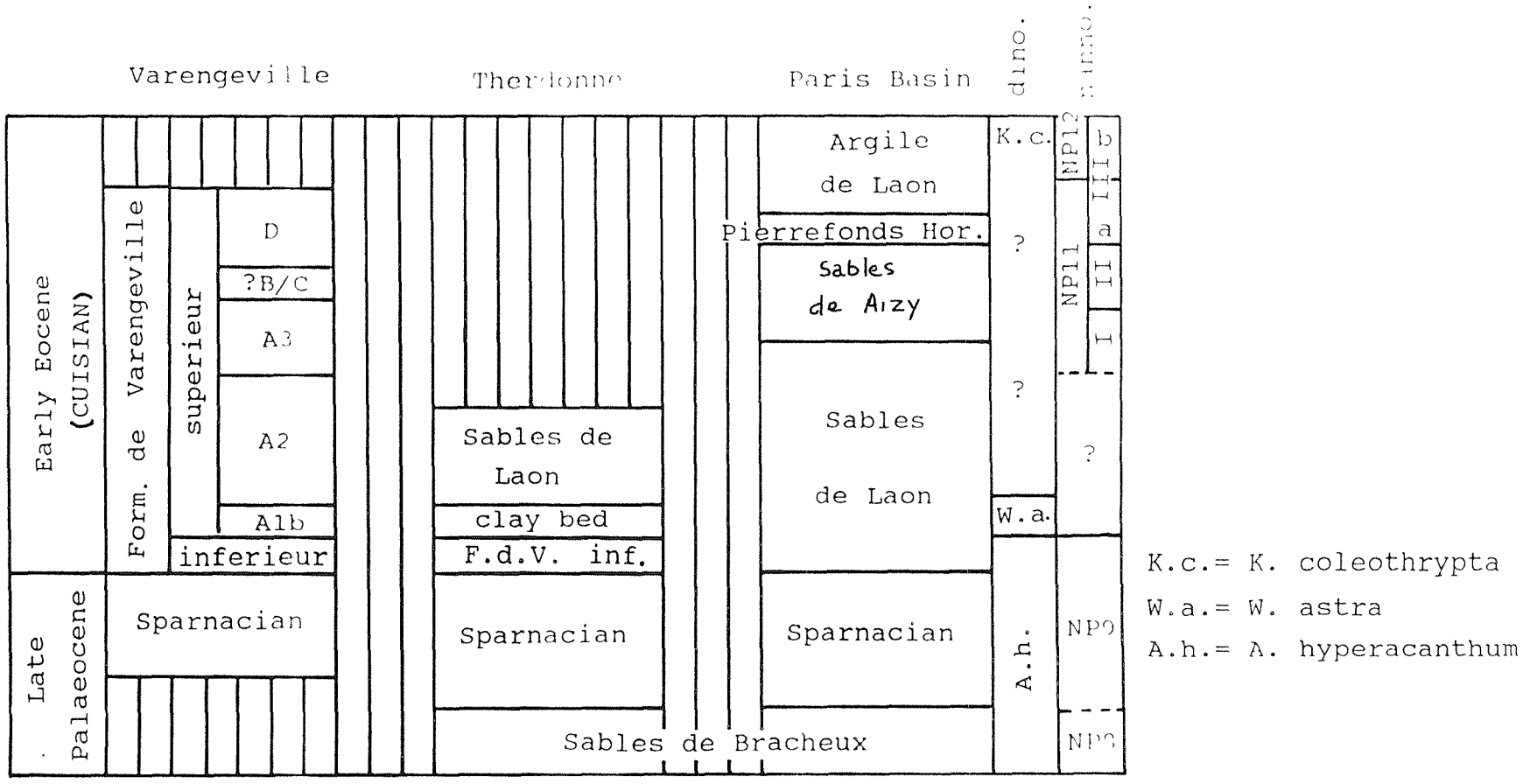

K.c.= K. coleothrypta
W.a.= W. astra
A.h.= A. hyperacanthum

Fig 9.2 The stratigraphy of the Lower Palaeogene of the Paris Basin and northern France.

Formations of England and the Landen Formation of the Belgium Basin.

9.4.3 The Formation de Varengeville

Gamble, in Destoumbes et al (1976), suggested that the Formation de Varengeville be informally divided into a lower (inferieur) and upper (superieur) unit to facilitate comparisons with the equivalent sequence in England. The Formation de Varengeville inferieur overlies the Sparnacian, and consists of well-sorted glauconitic sands identical in virtually every respect to the Oldhaven Formation of southern England. The unit at Varengeville is 5.1m thick and is assigned to the A. hyperacanthum dinoflagellate zone (Costa et al, 1978), making it very latest Palaeocene in age. C. King and the author identified a thin representative (0.75m thick) of this unit in the section at Therdonne, at the very edge of the Paris Basin.

The Formation de Varengeville superieur is equivalent to the lower half of the London Clay Formation (presumably younger Tertiary sediments existed above this level, but they have been removed and the unit is now topped with Quaternary gravels). The base of the formation is marked by a 1.4m thick oxidised glauconitic silty clay, very similar to the London Clay Basement Bed. C. King (pers. comm.) refers to this unit as A1b in correlations of the French and English successions. Above this bed, units equivalent to King's (1981) Divisions A2 and A3 can be recognised. An intensely glauconitic clay unit is above A3. Sediments from the levels above this unit contain Dracodinium varielongituda, and this suggests a correlation with Division D of the London Clay Formation. The glauconitic clay bed marks a period of condensed, or non, deposition. Steurbaut (1988) assigns the top of the formation to the upper part of NP11.

9.4.4 Cuisian age deposits

The terms "Sables de Cuise" (=Cuisian) was introduced by Dolfus (1880). Work on this unit has been reviewed by Bignot (1981). The Cuisian Stage is used to include all the

sandy formations between the top of the Sparnacian and the base of the Lutetian. The lithologies typical of the Cuisian are restricted to the Paris Basin, and represent the basin margin facies equivalent, for the most part, in age to the Formation de Varengeville. Major discontinuities almost certainly punctuate the Cuisian succession, but have not yet been documented. The stratotype at Cuise-la-Motte (14km to the east of Compiegne) exposes only the upper half (25m) of the unit. A borehole drilled in 1967, close to the stratotype, recovered a succession through the whole of the Cuisian, and has been exhaustively studied (Blondeau et al, 1976). Chateauneuf and Gruas-Cavagnetto (1978) assign the base and top of the Cuisian to the Wetzeliella astra and Kisselovia coleothrypta dinoflagellate zones respectively. Steurbaut (1988) suggests that the base and top of the Cuisian coincides with the base and middle part of the Ypresian respectively.

9.5 Palaeomagnetic results

9.5.1 Varengeville

The Palaeogene outlier at Varengeville was sampled in the cliff section near to the lighthouse at Phare d'Ailly. The sampled part of the Sparnacian totals 10.4m, the Formation de Varengeville inferieur totals 5.1m and the Formation de Varengeville superieur totals 17m. Specimens had NRM intensities typically between 0.2 and 0.5 mA/m, although one site just below the top of the Sparnacian had two specimens with intensities >8mA/m. Most of the specimens were processed on the "Molspin" equipment (maximum demagnetisation field of 30 to 40mT). Typical demagnetisation data are presented in Figs 9.3 to 9.5.

The magnetostratigraphic results are presented in Fig 9.6. Results from the Formation de Varengeville inferieur should be ignored as only four specimens from a total of ten remained consolidated during laboratory analysis, and the results from these specimens are very poor. The section is almost entirely reverse polarity, except for a normal polarity site at the base of the

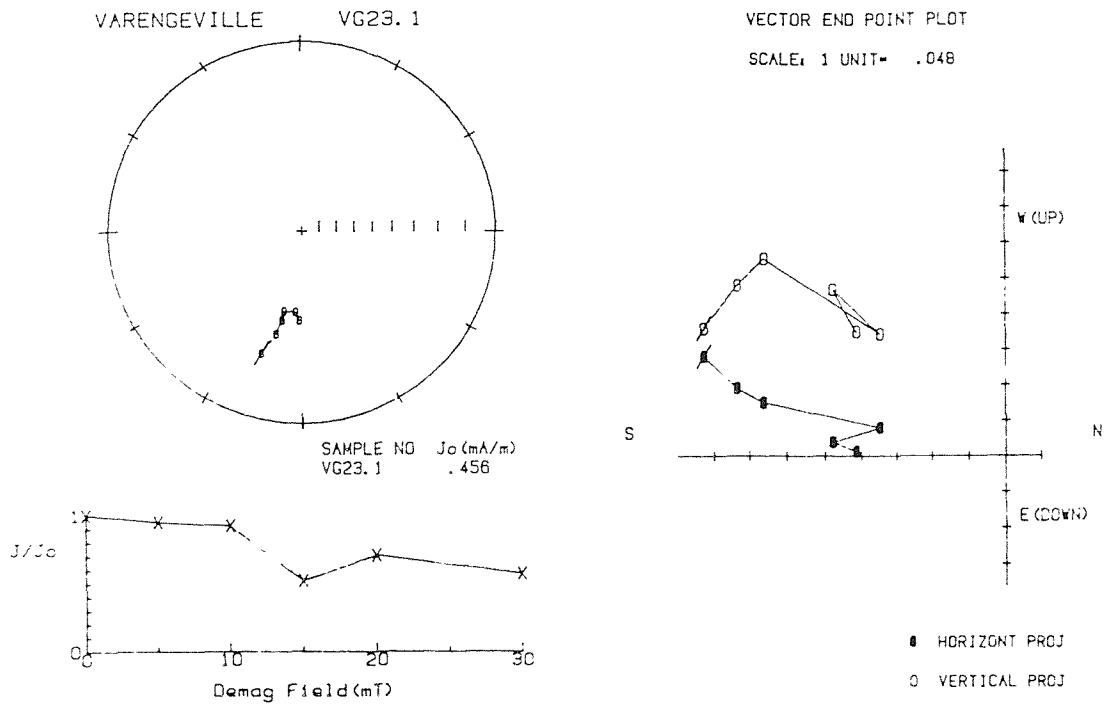

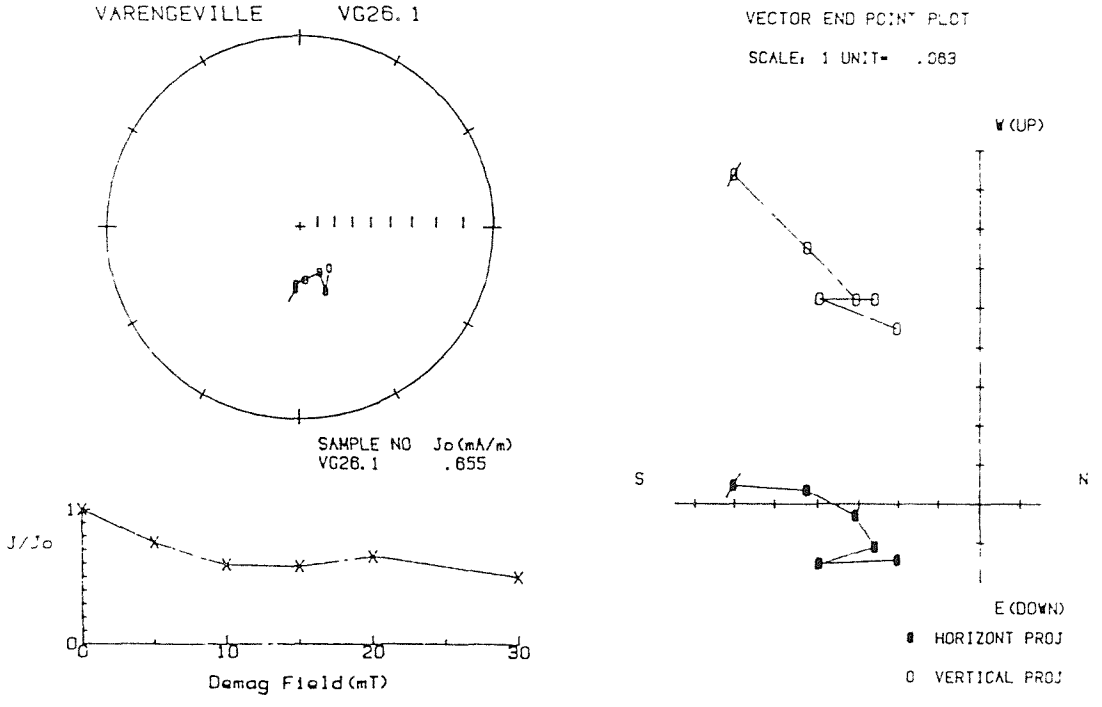

Fig 9.3 Typical reverse polarity specimens from the Sparnacian part of the section at Varengeville. For explanation of symbols see Fig 2.7.

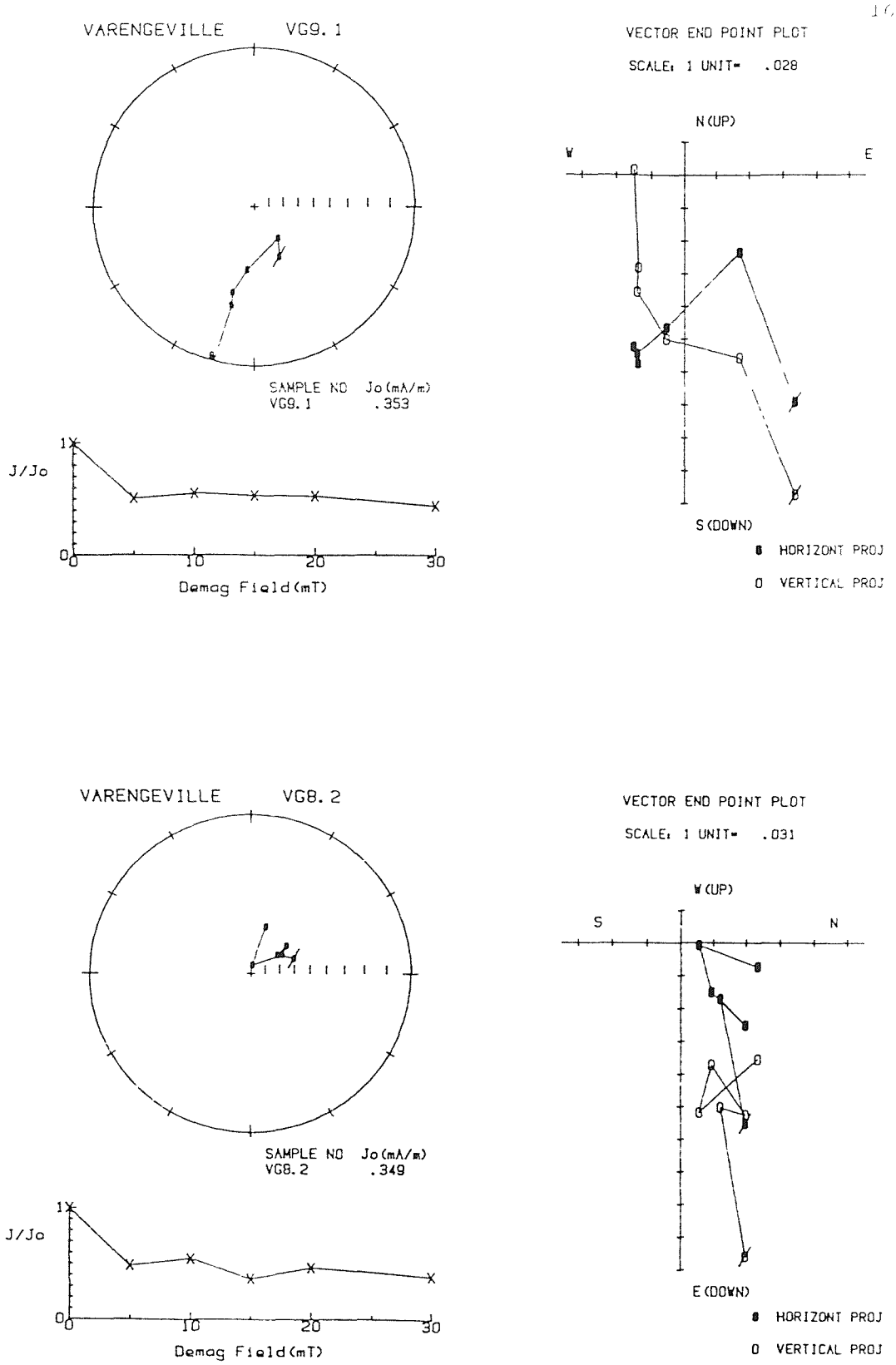

Fig 9.4 Examples of demagnetisation plots from the lower part of the Formation de Varengeville superieur at Varangeville. The upper plot shows a specimen from Division A2 with a reverse polarity and the lower plot a specimen from Division A1b with a normal polarity. For explanation of symbols see Fig 2.7.

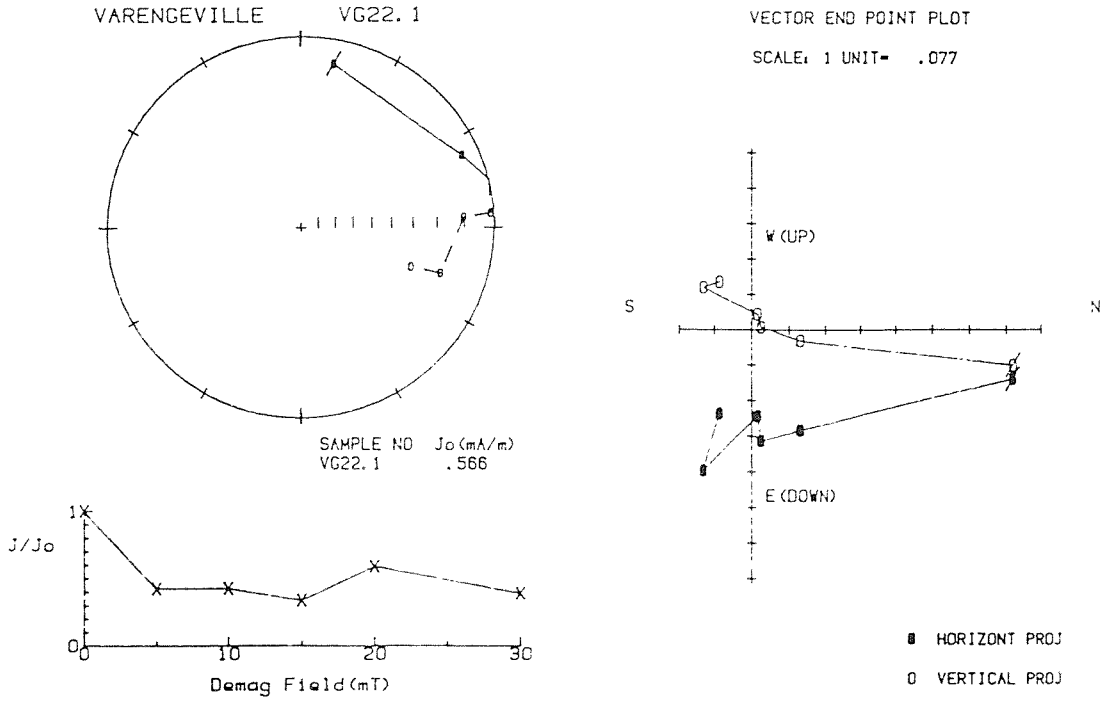

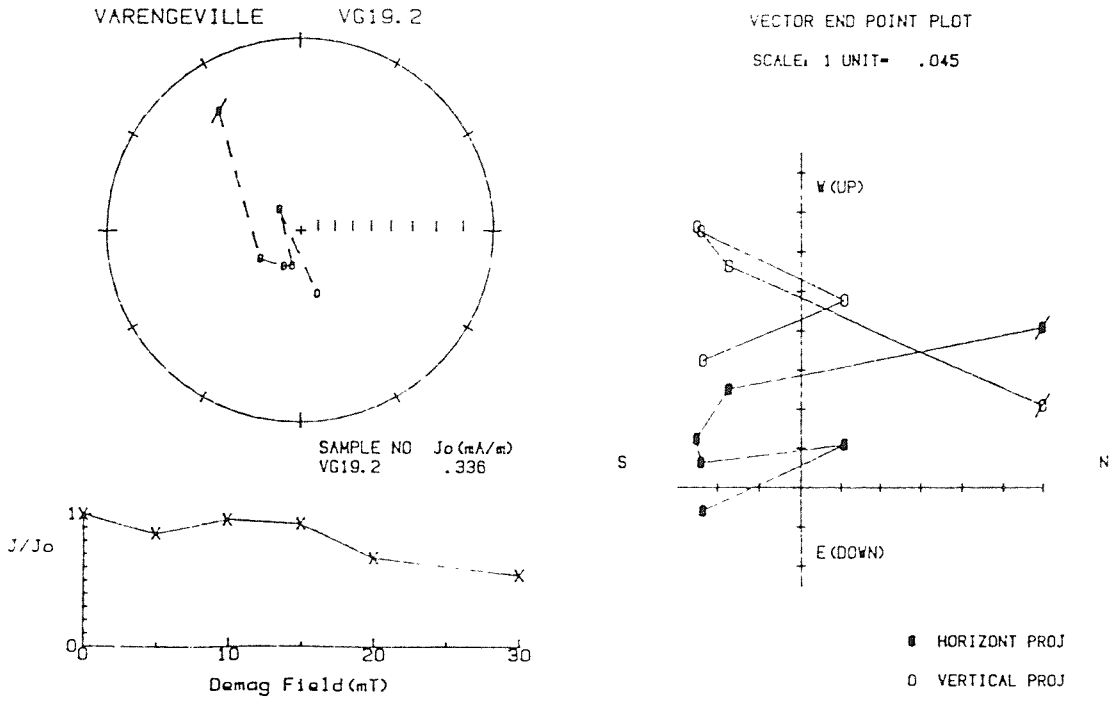

Fig 9.5 Typical reverse polarity specimens from the upper part of the Formation de Varengeville superieur at Varengeville. For explanation of symbols see Fig 2.7.

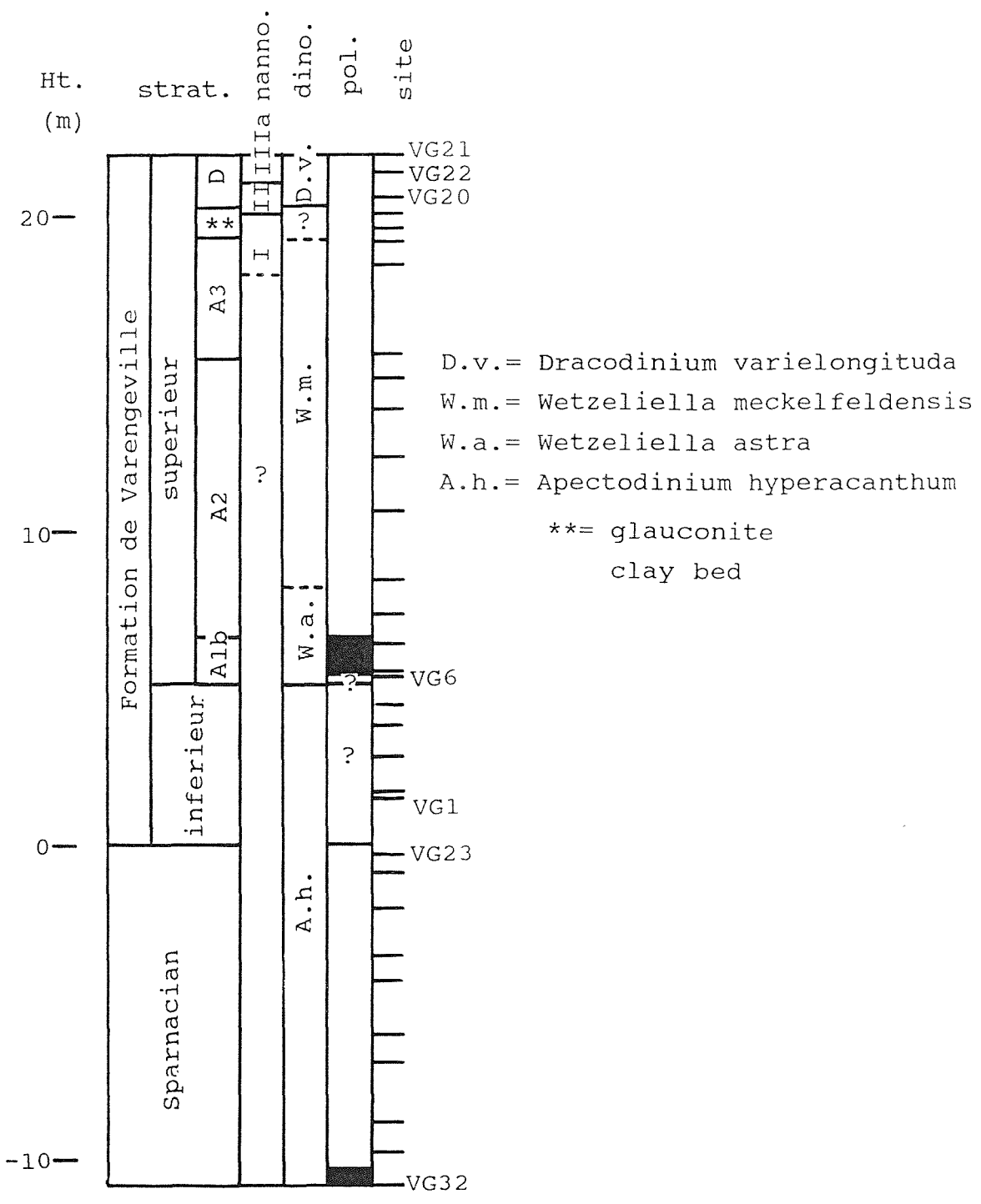

Fig 9.6 The magnetostratigraphy of the section at Varengeville.

Sparnacian, and two normal polarity sites in unit A1b. It is emphasised that the glauconitic clay bed toward the top of the section is reverse polarity.

Unfortunately, the specimens from either side of the Division A2/A3 junction do not show the marked change in NRM intensities (which can be diagnostic of changes in the magnetic mineralogy) as was observed at Sheppey (Chapter 7).

9.5.2 Therdonne

This undocumented Palaeogene outlier, just to the north of the Paris Basin, is on the northwest side of route D12, about 500m southeast of Therdonne. The section includes the upper part of the Sables de Bracheux (7.5m), the Sparnacian (9.5m), the Formation de Varengeville inferieur (0.75m), a clay bed (1m) and 5.5m of Cuisian sands (probably part of the Sables de Laon).

NRM intensities were typically in the range 0.2 to 0.5mA/m, although a few rather weak (<0.1mA/m) and strong (>2.5mA/m) specimens were encountered. The majority of the specimens were processed on the cryogenic magnetometer (demagnetisation up to 30-35 mT), with a few stronger specimens processed on the "Molspin" equipment (up to 40mT). Typical demagnetisation data are presented in Fig 9.7 and 9.8.

The magnetic polarity results are presented in Fig 9.9. The most conspicuous feature of the results is the Sparnacian part of the succession which is characterised by a high proportion of normal and indeterminate polarity levels. This is rather unusual as at all the other localities that have been investigated with similar age deposits (e.g. Varengeville and Herne Bay), these levels are dominantly reverse polarity. IRM analysis was carried out on five specimens from the Sparnacian to see if any of the levels had perhaps been magnetically altered since deposition (see Table 9.1). Specimen TD21.1, close to the base of the Sparnacian, has a very low IRM-ratio and moderately low peak IRM value, indicative of hematite.

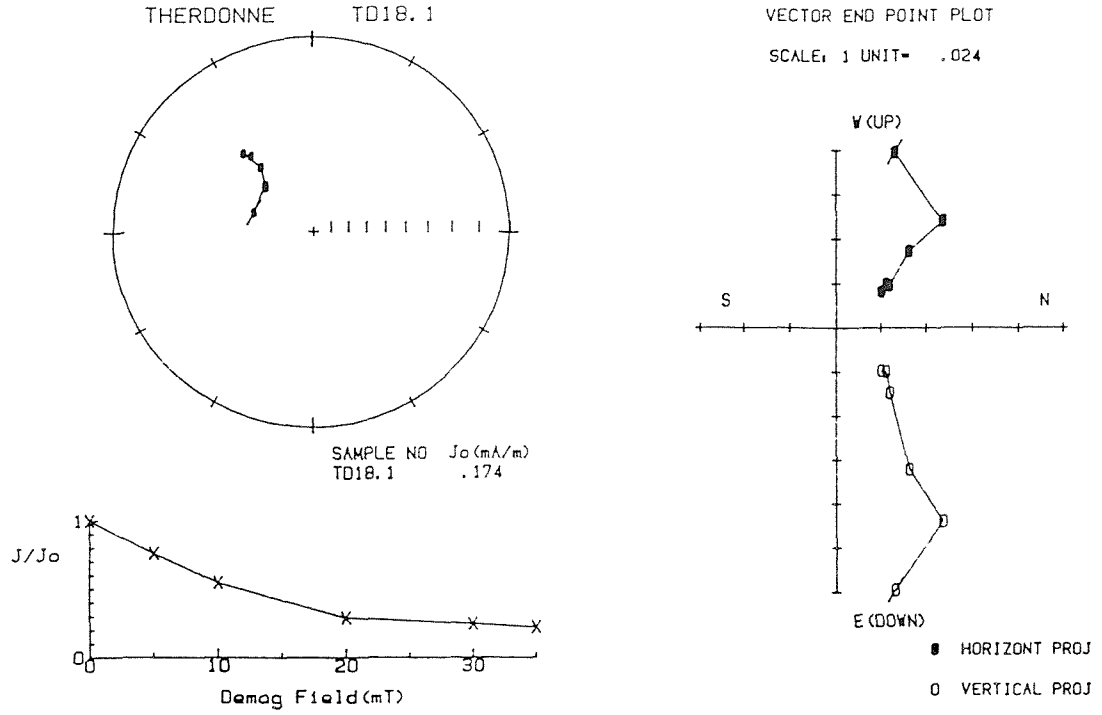

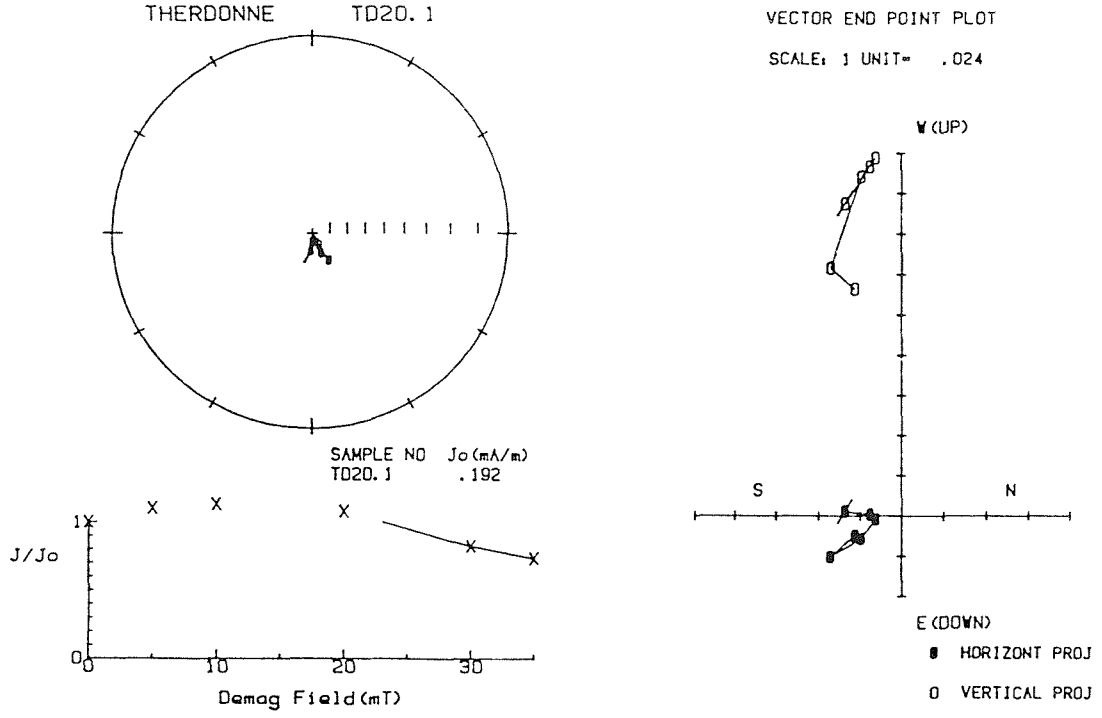

Fig 9.7 Examples of demagnetisation plots from the Sparnacian part of the section at Therdonne. The upper plot shows a specimen with a normal polarity and the lower plot a specimen with a reverse polarity. For explanation of symbols see Fig 2.7.

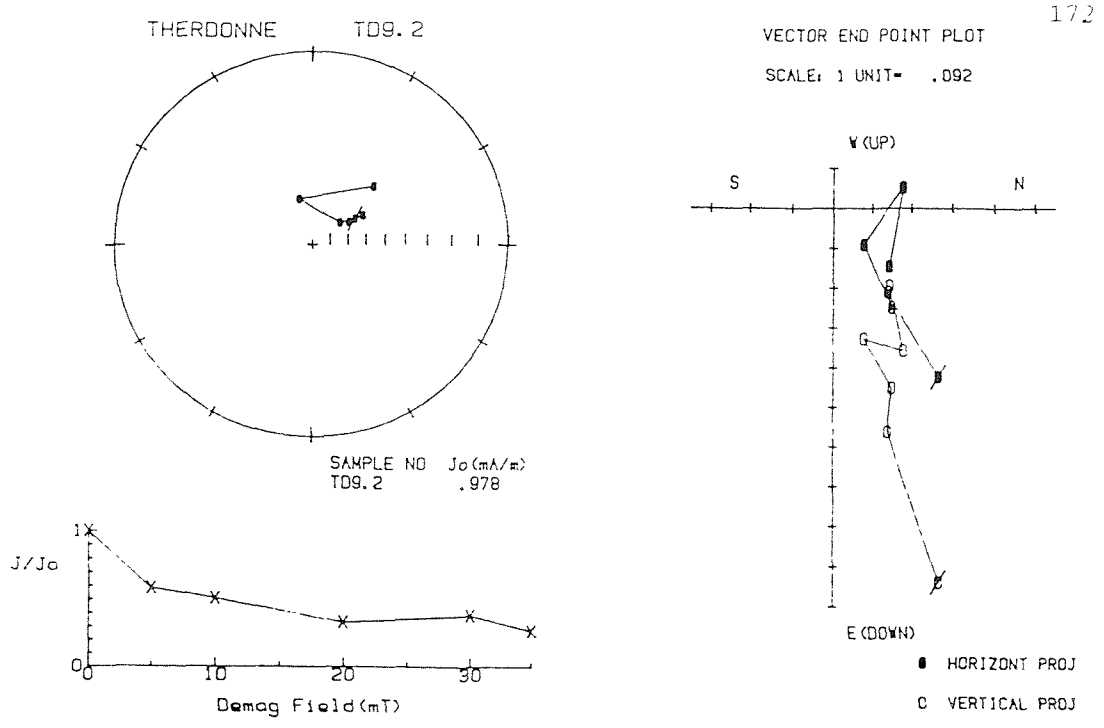

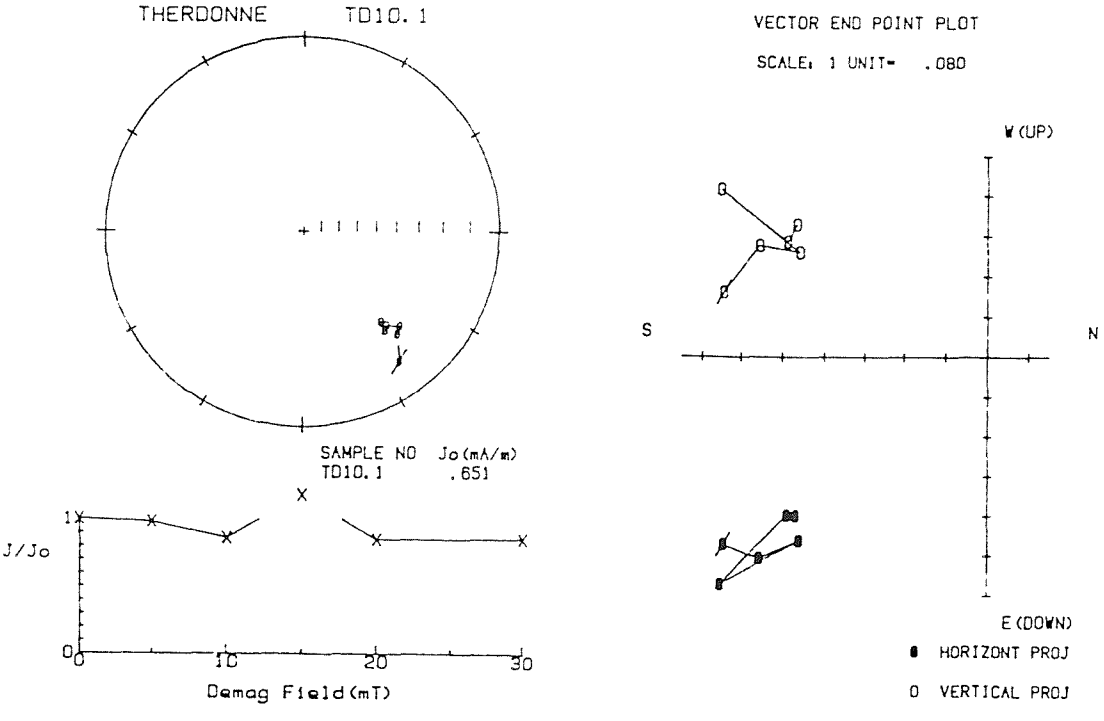

Fig 9.8 Examples of demagnetisation plots from the post-Sparnacian part of the section at Therdonne. The upper plot shows a specimen with a normal polarity and the lower plot a specimen with a reverse polarity. For explanation of symbols see Fig 2.7.

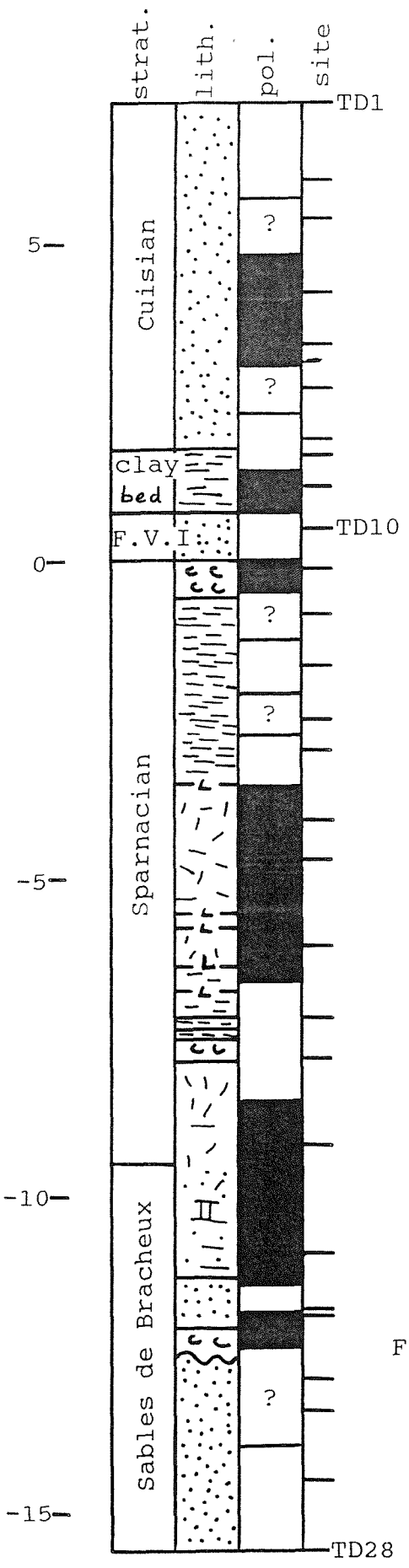

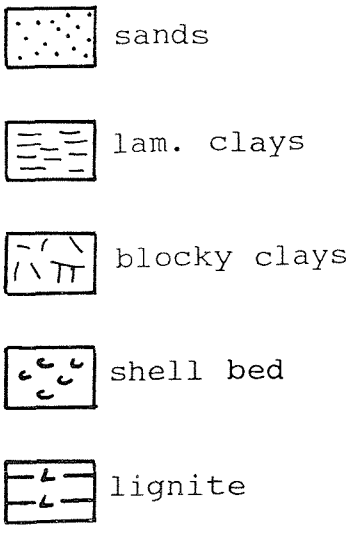

F.V.I.= Formation de Varengeville inferieur

Fig 9.9 The magnetostratigraphy of the section at Therdonne.

The four specimens above this level have IRM-ratios >0.93 but with very low peak IRM values <200 mAm^2. The remanence of these four specimens are probably carried by very low concent-rations of magnetite.

specimen	position (m)	pol	NRM mA/m	IRM ratio	peak IRM (mAm^2)
TD12.2	-0.85	?	0.20	.93	62
TD14.1	-2.50	?	0.26	.94	143
TD15.1	-3.00	R	0.70	.96	194
TD19.1	-7.21	?	0.08	.96	68
TD21.1	-9.20	N	2.15	.62	1155

Table 9.1. IRM data from the Sparnacian part of the succession at Therdonne.

There appears to be no positive link between a specimen's magnetic mineralogy and its polarity, as was the case at Wrabness, England (Chapter 6). However, 13 of the 24 specimens from the Sparnacian part of the section have NRM intensities <0.2 mA/m, and the polarity data from these specimens may be unreliable.

No biostratigraphic data are available for the post Sparnacian deposits, and so it is rather difficult to interpret the results from these levels. D. Jolly (pers. comm.) is currently investigating the dinoflagellate content of some of the palaeomagnetic specimens taken from different levels within the section.

9.5.3 The Paris Basin

Exposures of the Cuisian in the Paris Basin are almost entirely in the upper third of this unit, below the Lutetian "Glauconie grossier". This is because of the "table-topography" of the area resulting from the present day river courses, which, having cut through the hard Lutetian limestones ("Calcaire grossier"), today run across the softer Sparnacian sediments. The unconsolidated sands below the hard Lutetian cap-rock are easily dislodged and

pile-up as a thick cover, obscuring the lower part of the Cuisian.

Five sections were sampled in the spring of 1987, although a number of other exposures were visited but not sampled because they were either inaccessible, or too degraded. When combined, the sections that were sampled span the upper part of the Sables de Aizy to the top of the Argile de Laon. Steurbaut (1988, Table 1) shows that these units span a very short period of the middle part of the Ypresian (nannoplankton subzones II, IIIa and IIIb).

The remanence characterisics of specimens from the five sections are all very similar in terms of NRM intensity, the quality of the demagnetisation, and the polarity data. The dominantly sandy lithologies of the upper part of the Cuisian made it necessary to sample the sections using the palaeomagnetic boxes described in Chapter 2. The exposure was first excavated to remove weathered surface material, then a horizontal "shelf" was cut into the outcrop. Two sample boxes were then pressed into the "shelf" surface and the arrow on the box was oriented relative to North (the remanence of the specimen need only be declination corrected). The specimens were then carefully removed from the outcrop and sealed, to prevent moisture-loss.

NRM intensities were typically between 0.2 and 0.4mA/m, although specimens with intensities varying between 0.05 and 1.5mA/m were processed. One of the most remarkable features of the NRM intensity data (listed in the Appendix) is the difference in values between many sister specimens taken from the exact same stratigraphic horizon. Variations by a factor of 3-5 were not uncommon, with occasional discrepancies of a factor of 10. The deposition of microscopic size magnetic grains within a predominantly well-sorted, coarse sand has probably lead to this inhomogeneous magnetisation within particular horizons. The problem is compounded by the fact that there is large interstitial volume within these uncemented sands, and so it is less likely that all of the ferromagnetic grains which were deposited alongside the sands will be uniformly

distributed within them.

Virtuall all the specimens were processed on the cryogenic magnetometer, usually being demagnetised to between 30 or 35mT. Some specimens had MDF's less than 10mT, whilst others remained essentially unaffected by the demagnetisation. A series of typical demagnetisation plots is presented in Figs 9.10 to 9.14. Over 30% of the specimens are classified "erratic", and there was not a single specimen (from over 130) that produced a SEP direction. About 25% of the specimens carry an indeterminate polarity.

9.5.3.1 Mons-en-Laonnois

The section is in both sides of the roadcutting along the minor road leading from Bourguignon to la Cannotte, and is about 600m south of Mons-en-Laonnois. This 14m thick exposure extends down from the base of the Pierrefonds Horizon into the Sables de Aizy (Fig 9.15). The section is dominantly normal polarity, although 2 reverse and 2 indeterminate polarity levels were identified. The normal polarity sites are used to define a magnetozone BG-a.

9.5.3.2 Cinqueux

The section is in a disused sand-pit about 500m east of Cinqueux, on the main road leading to the village. C. King (who helped with the fieldwork) had previously visited this exposure in 1979, and had been able to log a 12m section from the base of the Pierrefonds Horizon down into the Sables de Aizy. The exposure today is in a very dangerous state with many overhanging trees precariously balanced. A 4.5m section was sampled, with the highest site positioned at 5.75m below the Pierrefonds Horizon. The polarity results from this section are rather poor, with three normal, two reverse and one indeterminate polarity site (Fig 9.15).

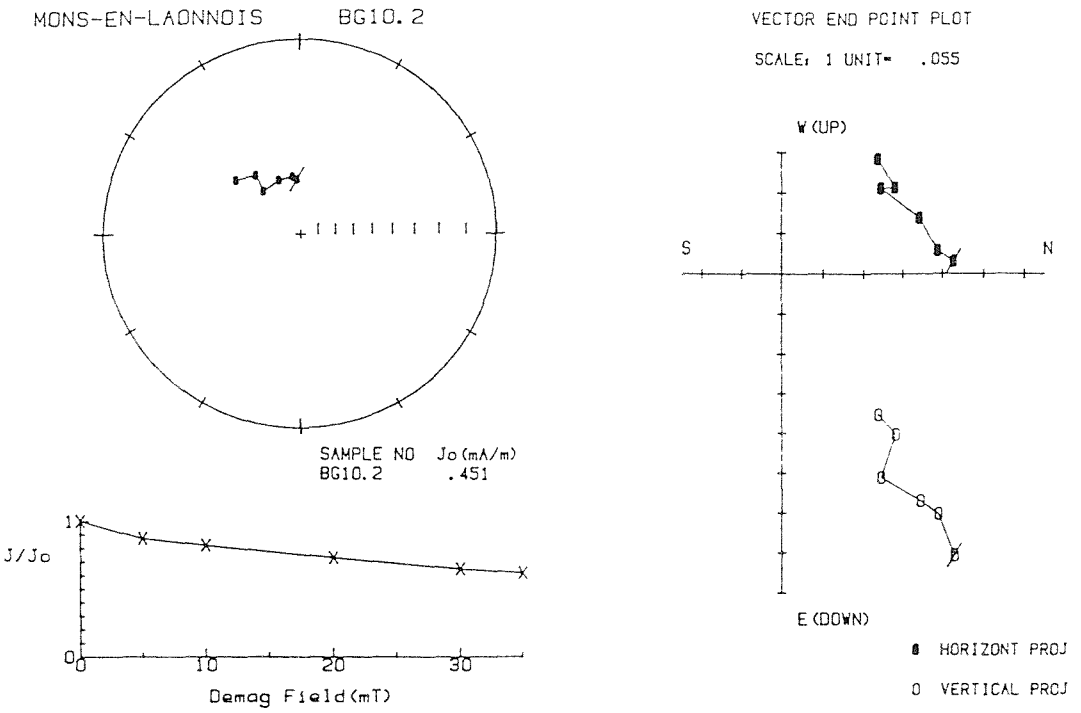

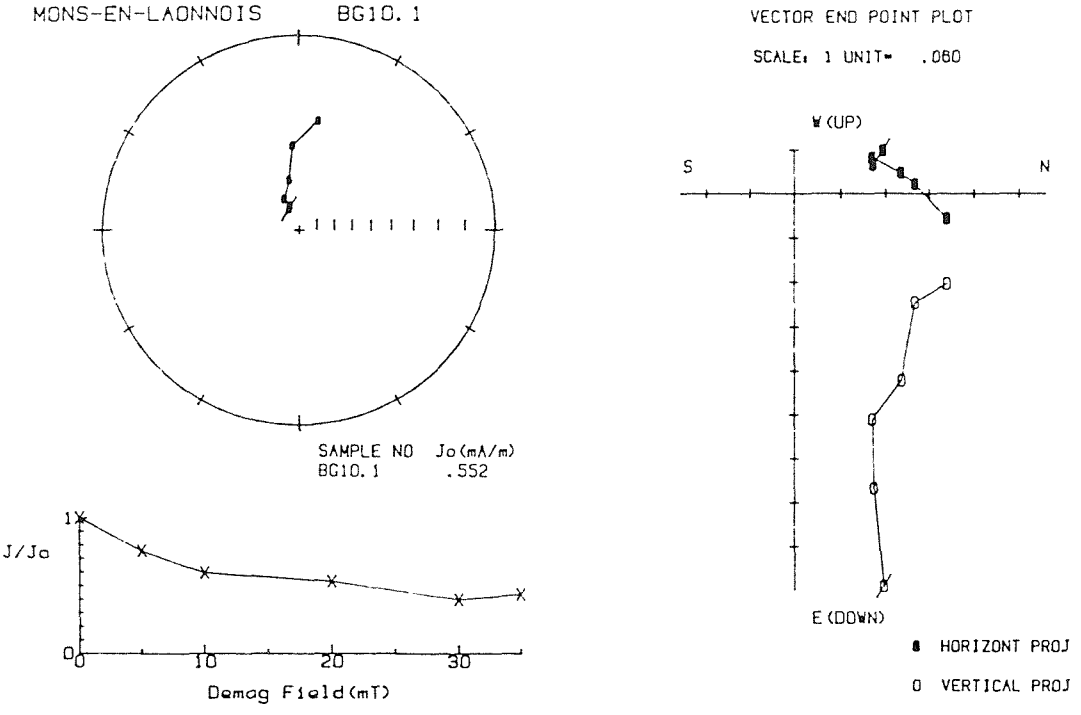

Fig 9.10 Typical normal polarity specimens from the Sables de Aizy at Mons-en-Laonnois. For explanation of symbols see Fig 2.7.

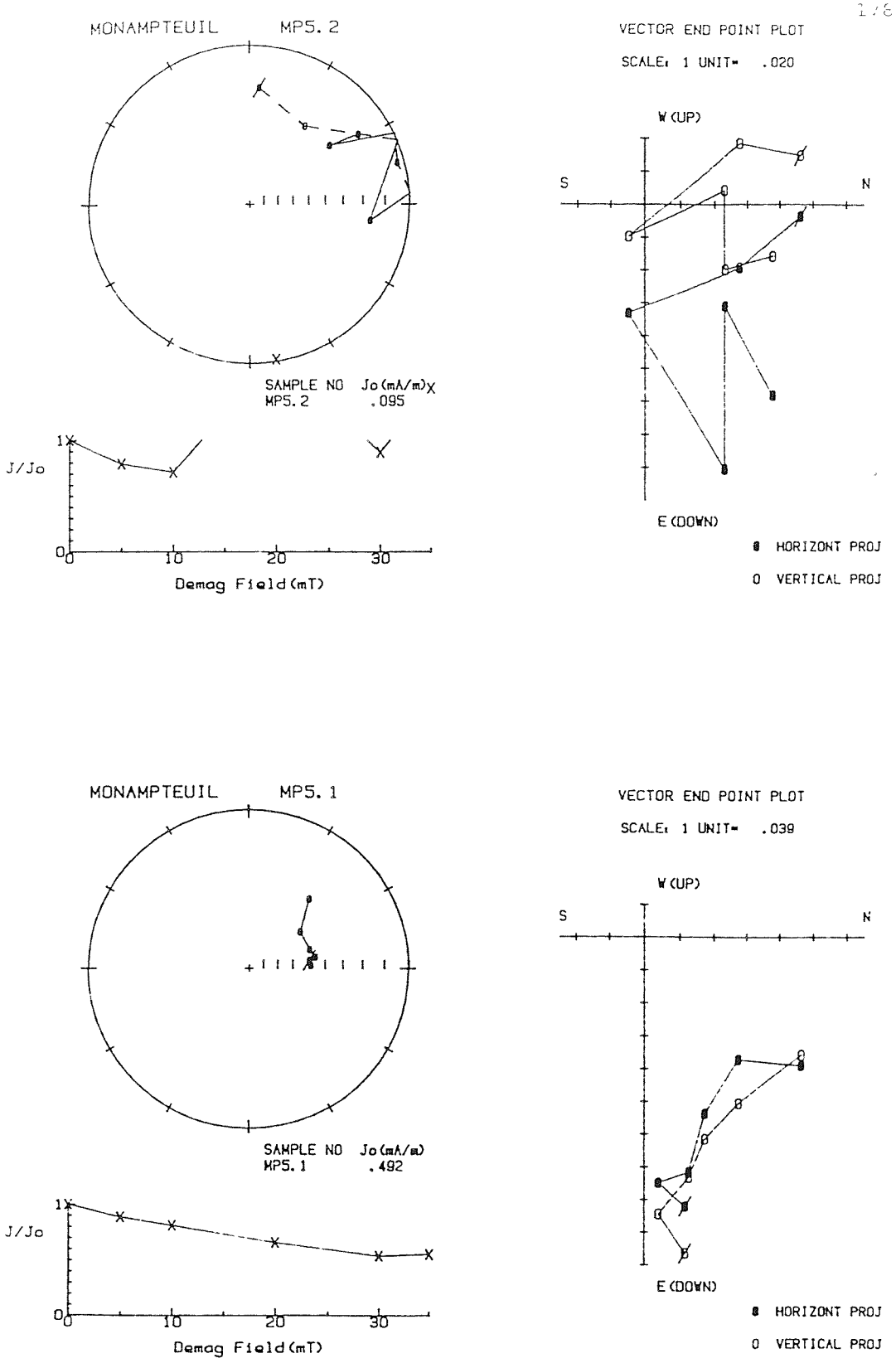

Fig 9.11 Examples of demagnetisation plots from the Sables de Aizy at Monampteuil. The upper plot shows a specimen with an indeterminate polarity and the lower plot a specimen (from the same site) with a normal polarity. Note the difference in NRM intensity. For explanation of symbols see Fig 2.7.

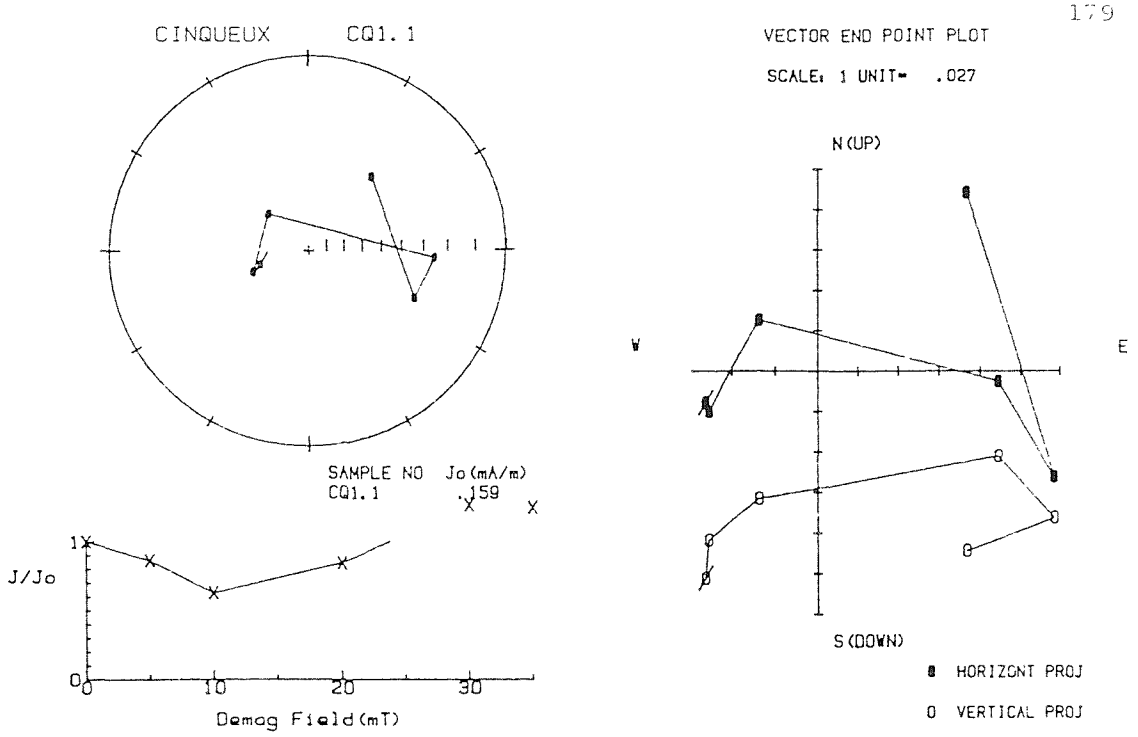

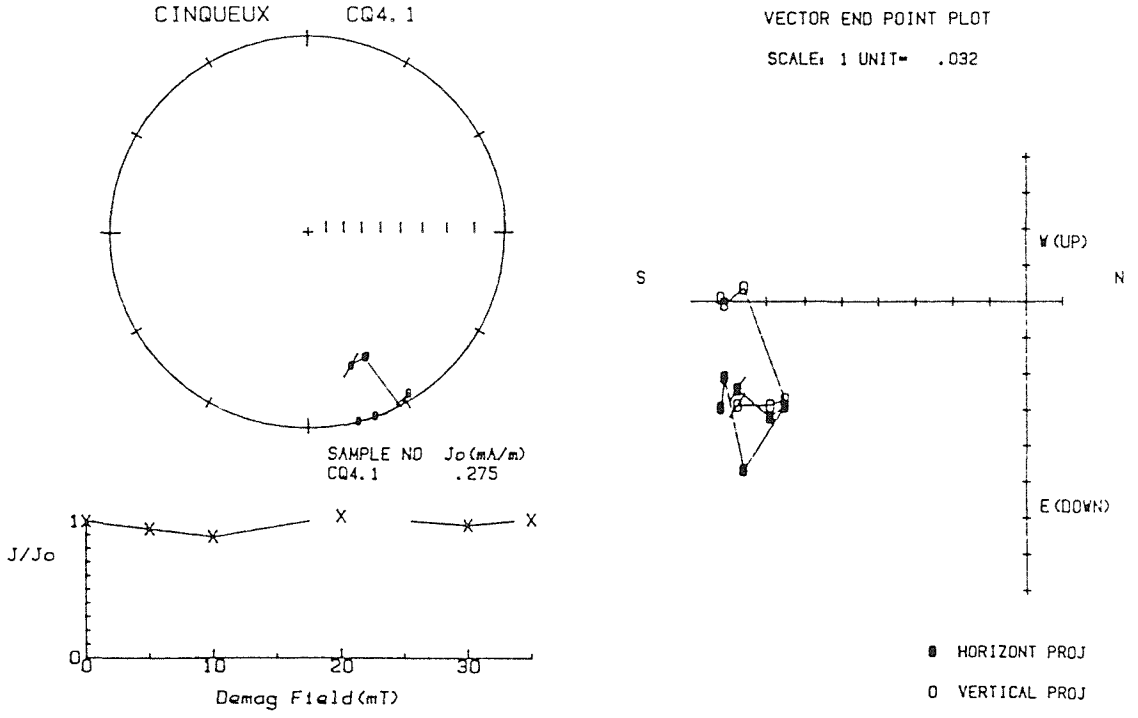

Fig 9.12 Examples of demagnetisation plots from the Sables de Aizy at Cinqueux. The upper plot shows a specimen (classified as "erratic") with a normal polarity and the lower plot a specimen with a reverse polarity. For explanation of symbols see Fig 2.7.

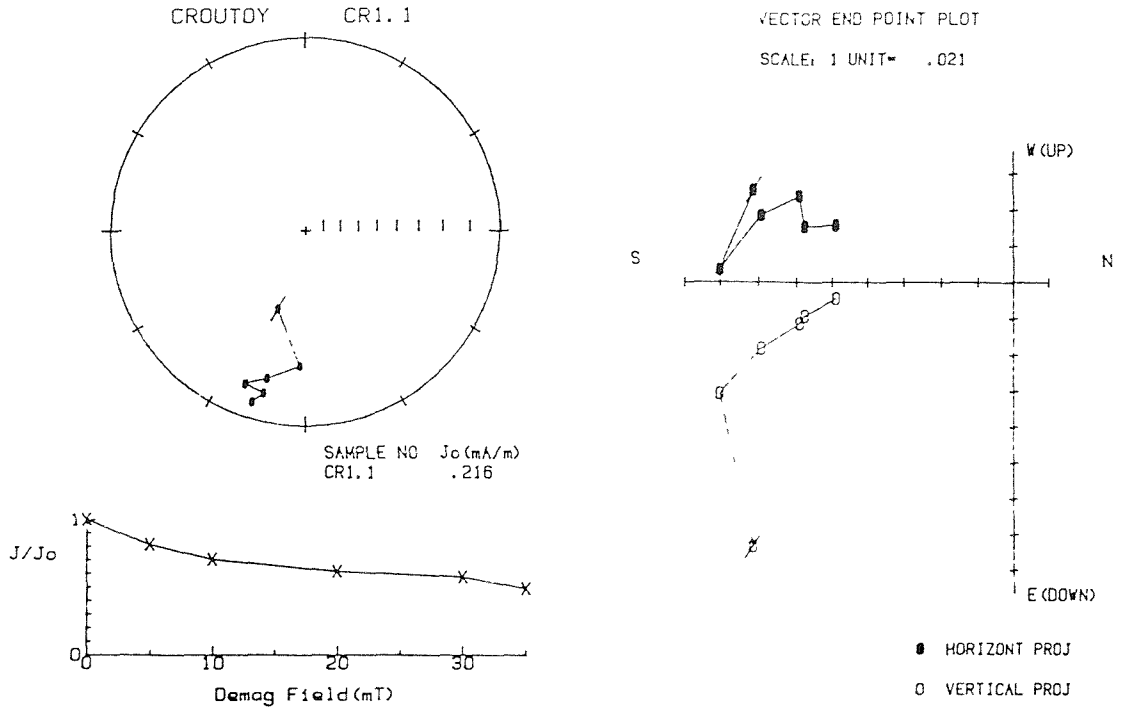

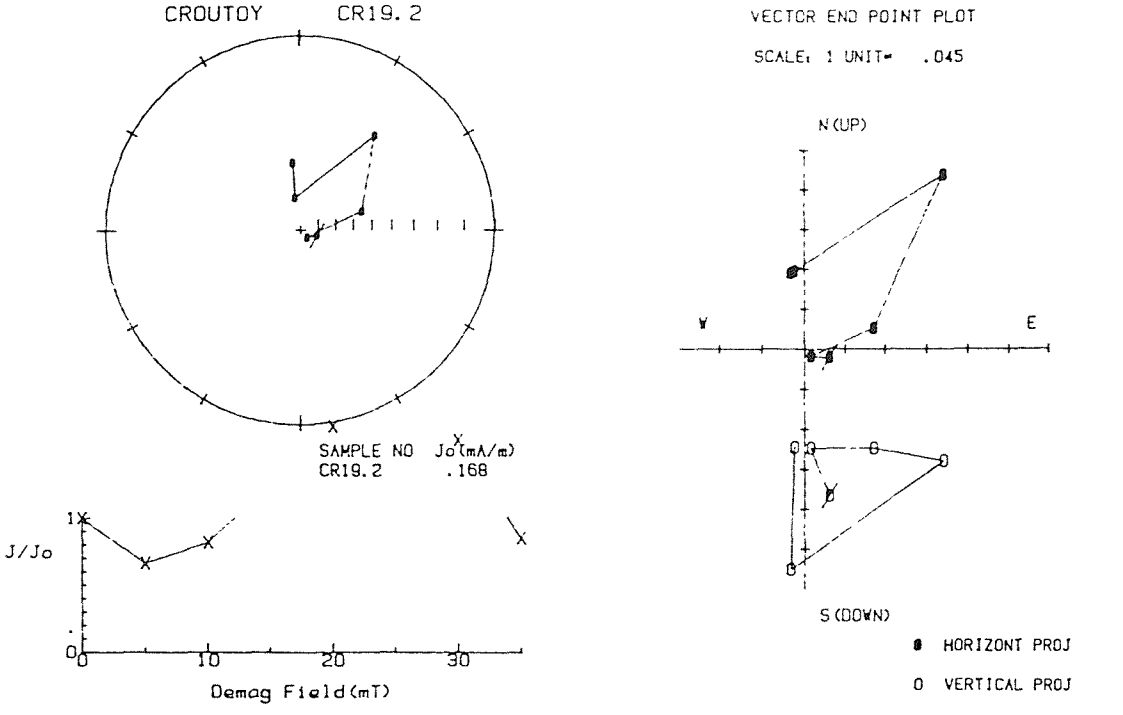

Fig 9.13 Examples of demagnetisation plots from the section at Croutoy. The upper plot shows a specimen from the Argile de Laon with with a reverse polarity. The lower plot shows a specimen from the Sables de Aizy with a normal polarity. For explanation of symbols see Fig 2.7.

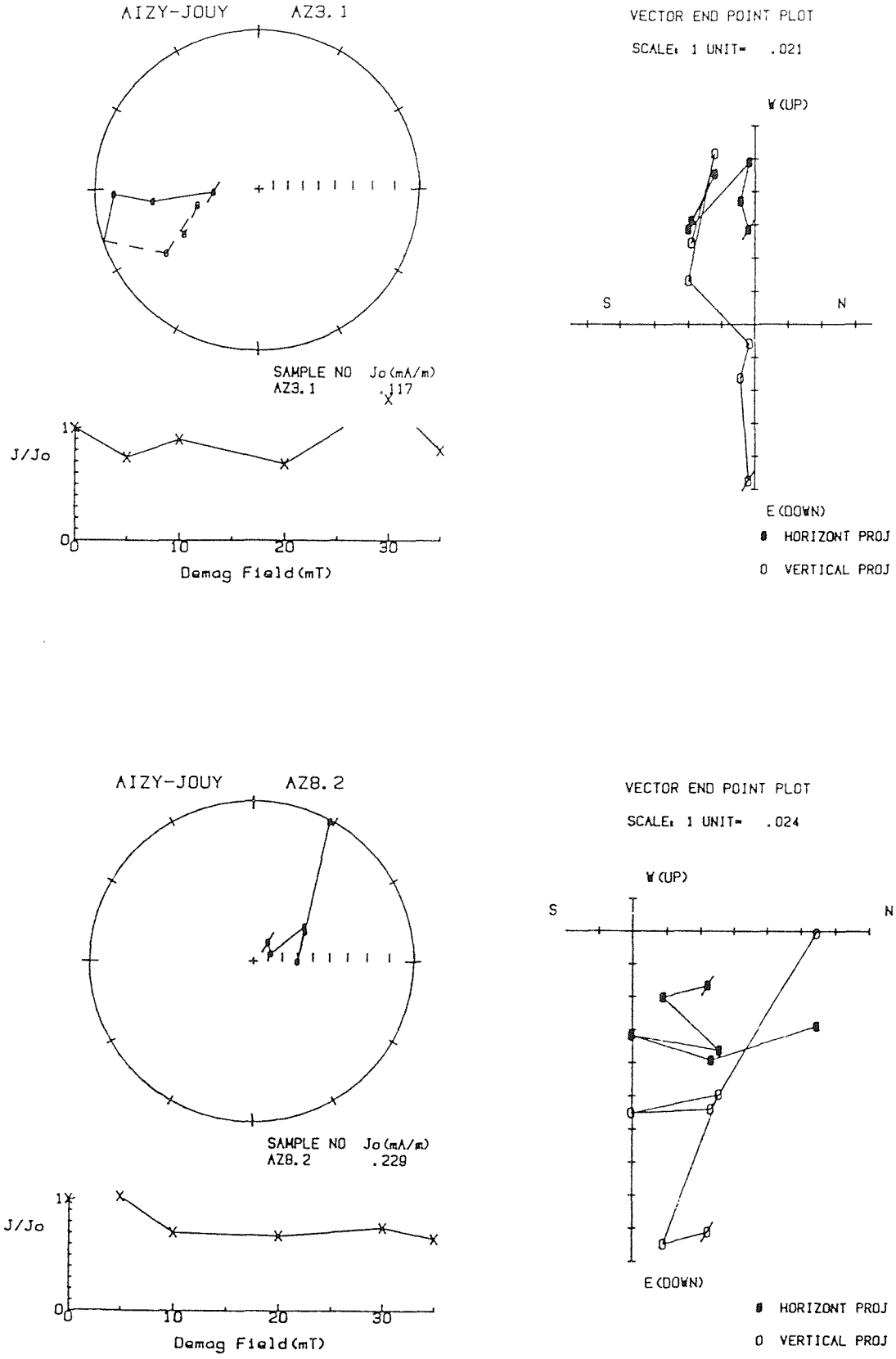

Fig 9.14 Examples of demagnetisation plots from the Argile de Laon at Aizy-Jouy. The upper plot shows a specimen with a reverse polarity and the lower plot a specimen with an indeterminate polarity. For explanation of symbols see Fig 2.7.

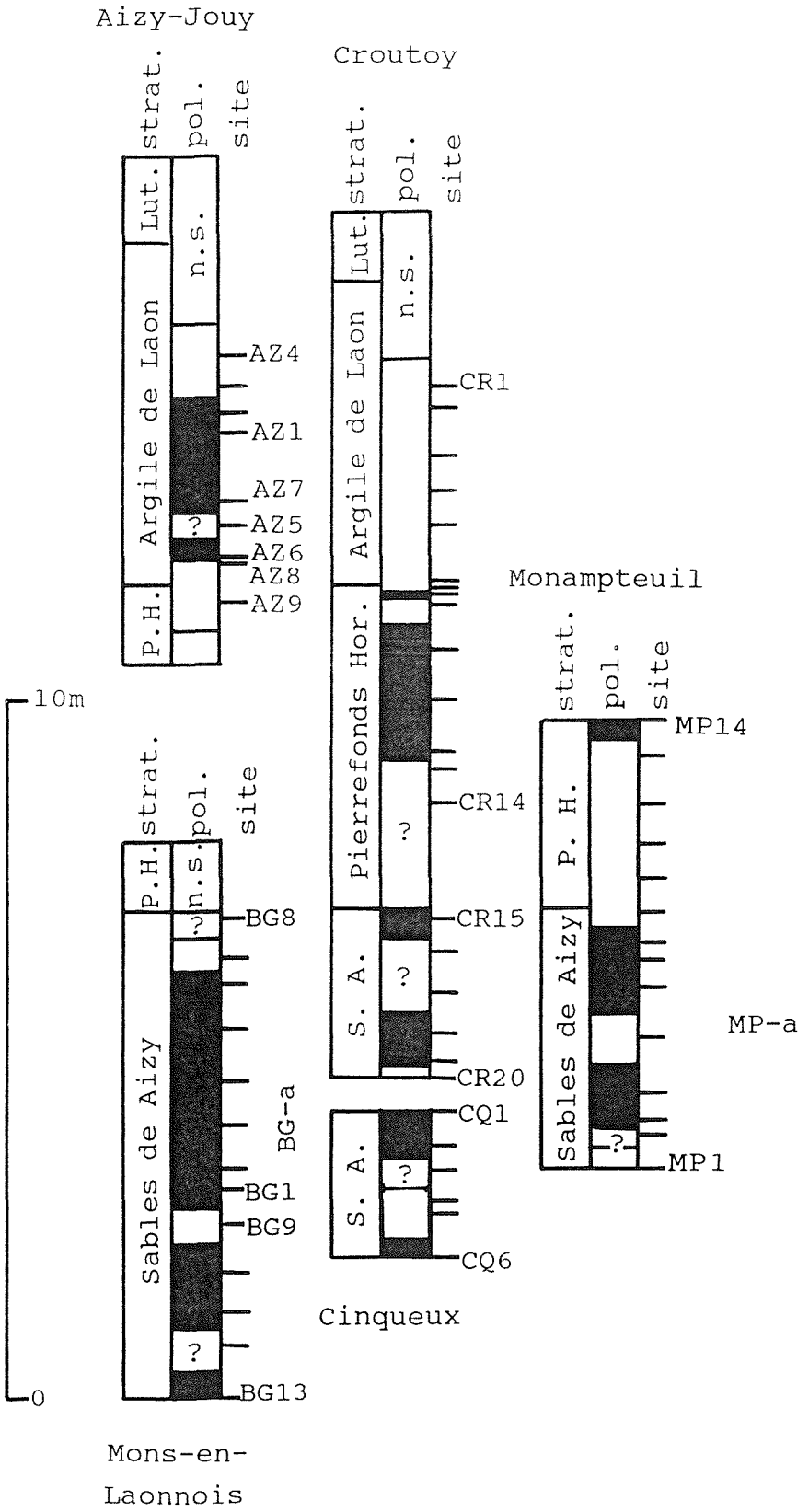

Fig 9.15 The magnetostratigraphy of the upper part of the Cuisian in the Paris Basin.

9.5.3.3 Monampteuil

The section at Monampteuil is in a sand-pit, 600m SE of the village of Urcell, at the end of a minor road. It exposes the upper part of the Sables de Aizy (7.5m) and the lower part of the Pierrefonds Horizon (5.5m). Normal polarity sites dominate the Sables de Aizy, and are used to define magnetozone MP-a, whilst the Pierrefonds Horizon is characterised by a reverse polarity.

9.5.3.4 Croutoy

Two sand-pit sections about 400m south of the crossroad on route N31, on the road leading from Attichy to Croutoy were sampled. The two pits together expose a 23m succession beneath the Lutetian "glauconie grossiere". The lower pit (which had to be dug back quite some way to extend the sampled sequence) exposes the upper 5m of the Sables de Aizy and the base of the Pierrefonds Horizon. The section in the upper pit, 50m to the North, extends from the base of the Pierrefonds Horizon to the top of the Argile de Laon. The magnetic polarity results (Fig 9.15) indicate that the Sables de Aizy are normal polarity, as is the upper half of the Pierrefonds Horizon. The sediments above this level are dominantly reverse polarity.

9.5.3.5 Aizy-Jouy

This section is exposed in the north side of the D14 road, about 500m WNW of Aizy-Jouy. Nine sites in the Argile de Laon were sampled, and the section is dominantly normal polarity.

9.5.4 Sections that were not sampled

The following sections were visited but not sampled during the spring of 1987, either because the sections were inaccessible, or too degraded: Cuise-la-Motte; Clairoix and Longuell-Annel, near Compiegene; Monchy, near Creil; Hermes; and Mercin-et-Vaux, near Soissons.

9.6 Synthesis and Correlation

The results from the section at Varengeville, and a composite section (based on results from the five localities) through the upper Cuisian in the Paris Basin are presented in Fig 9.16. The two sections are drawn in their relative stratigraphic positions. The results from the Therdonne section are not included, firstly because the polarity data from the Sparnacian part of the succession is considered too poor, and secondly, because there are no biostratigraphic data available from the Eocene part of the succession.

At Varengeville, the section from the Sparnacian up to the top of Division A3 of the Formation de Varengeville spans the *A. hyperacanthum*/ *W. meckelfeldensis* zones. As these sediments are dominantly reverse polarity the correlation of these units with Chron C24BR is proposed. The normal polarity sites in unit A1b of the Formation de Varengeville superieur can be correlated with the normal polarity sites in the London Clay Basement Bed in Kent, and the Tilehurst Member at Tilehurst (see Chapter 6).

The sediments above the glauconite clay bed are assigned to the *D. varielongituda* dinoflagellate zone and to the upper part of the NP11 nannoplankton zone. The polarity, nannoplankton and dinoflagellate data from these levels are slightly confusing. Conventionally, reverse polarity sediments assigned to NP11 would be correlated with Chron C24AR. However, since these sediments are assigned to the *D. varielongituda* dinoflagellate zone the correlation with Chron C23R is the only possible solution. The present study has, however, located reverse polarity sediments in the upper part of the NP11 zone in the Belgium Basin (Chapter 8). As these sediments are correlated with Chron C23R, a similar correlation of the reverse polarity sediments in the upper part of the Formation de Varengeville is proposed. The glauconite clay bed marks a major discontinuity, spanning Chrons C24BN up to C24AN. If deposition within this bed was very slow, and not actually marked by an hiatus, it is possible that this polarity

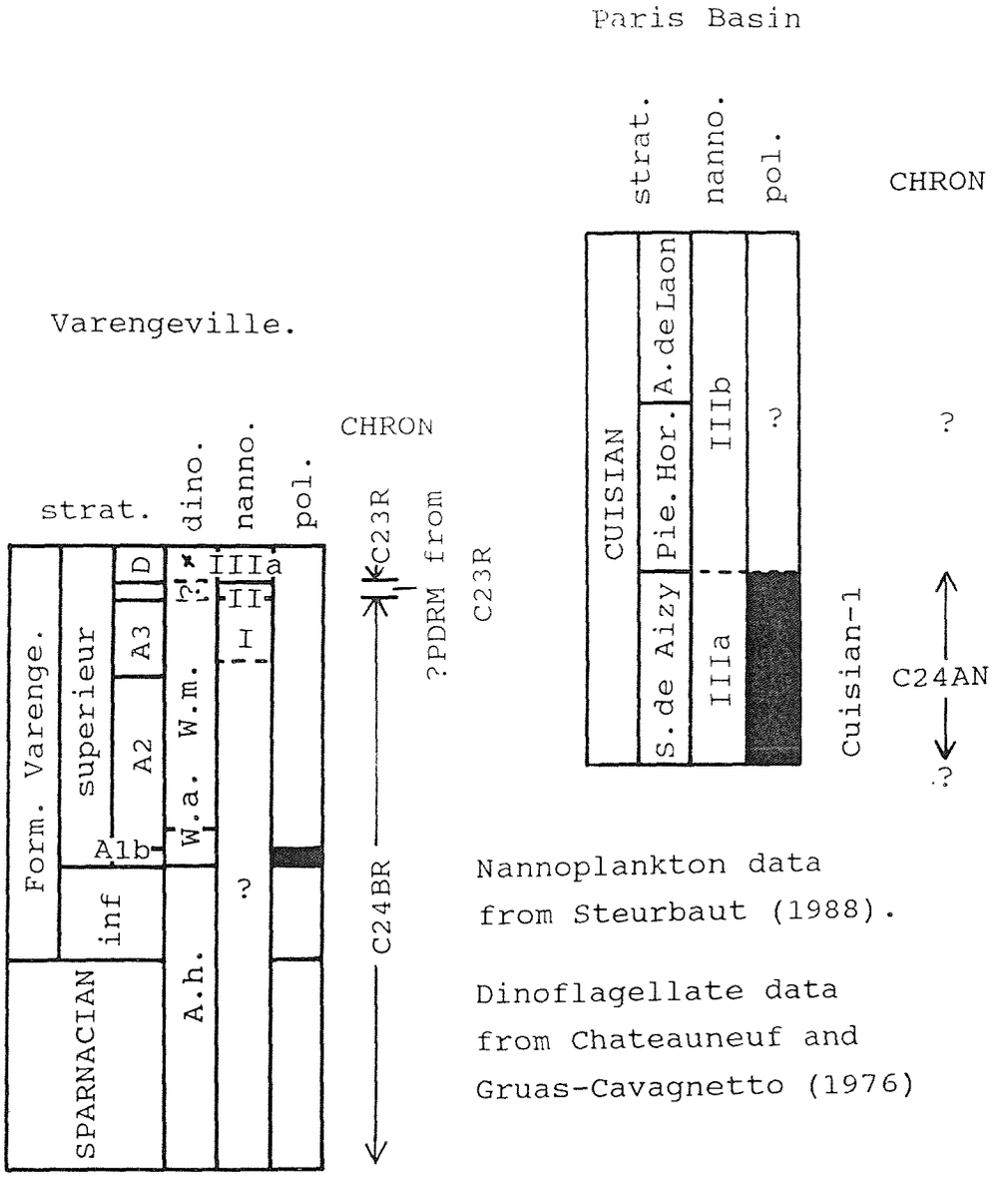

Fig 9.16 The correlation of the Lower Palaeogene deposits of the Paris basin and northern France with the geomagnetic polarity time-scale.

sequence may have been partially recorded within this horizon, but was not identified because it was sampled at just two sites. It would be interesting to continuously sample the glauconite clay bed to see what changes in the Earth's magnetic field the sediments have recorded. However, it is likely that with the very low sedimentation rates they will not have recorded the changes in polarity and, more than likely, acquired a PDRM during Chron C23R.

Dinoflagellate workers may be able to locate very accurately the Dracodinium similis and D. varielongituda zones to see if the sedimentation was continuous or intermittent whilst the glauconite bed was being deposited.

Individually the five sections through the upper part of the Cuisian have rather complicated polarity records, and it is only possible to say that certain levels within each section have a particular dominant polarity. From the results of these sections, which are all shown in Fig 9.15, a "silhouette" composite section is shown in Fig 9.16.

The Sables de Aizy are dominantly normal polarity (e.g the magnetozones BG-a and MP-a), and these sites are used to define the magnetozone Cuisian-1. The nannoplankton data from this level belong to the upper part of NP11 (unit IIIa). Normal polarity sites associated with this biozone were identified in the Belgium Basin (Chapter 8). Those levels, coded Ieper-2, were correlated with Chron C24AN. A similar correlation of Cusian-1 with Chron C24AN is proposed here.

The top of Cuisian-1 may extend possibly as high as the middle of the Argile de Laon. The polarity results from this part of the succession are very poorly defined because the two sections in which this interval was sampled carry opposing polarities.

9.7 Summary and conclusions

Most of the sediments in the Palaeogene outlier at Varengeville can be assigned to Chron C24BR, and represent a more or less uninterupted succession, very similar to the latest Palaeocene and earliest Eocene deposits in southern

England. A major hiatus is present in the upper part of this section, and this coincides with the 1m thick glauconitic clay bed. The sediments above this level are assigned to the upper part of the NP11 nannoplankton zone, and as they are reverse polarity have been correlated with Chron C23R. It is likely with such low sedimentation rates, that the remanance within the glauconite bed is a much delayed PDRM acquired during Chron C23R. The dinoflagellate zones within this unit may record a rather condensed, but complete, biostratigraphic history.

The Sables de Aizy in the Paris Basin are dominantly normal polarity. A normal polarity magnetozone, Cuisian-1, has been identified in this unit and is correlated with Chron C24AN. It has not been possible to define the upper limit of Chron 24AN in these sections. In future it would be useful to examine many more sections through the upper part of the Cuisian to accurately determine the magneto-stratigraphy of the Argile de Laon.

The following points should be considered by future workers on the magnetostratigrahy of the Paris Basin Cuisian:

1. In order to examine the lower parts of the Cuisian, borehole material will have to be used. With borehole material the major drawback is that the cores are not usually declination oriented. This makes polarity evaluations based on demagnetisation "trends" much more difficult. When one considers that not a single specimen from the Cuisian outcrops produced an SEP direction, it is clear how difficult it might be to interpret any borehole specimen data.
2. The biostratigraphic record within the lower part of the Cuisian is not only poor, presumably because of the restricted conditions at the basin margin, but also of low resolution. This would make it very difficult to correlate a magnetic polarity sequence (if one could be obtained in the first place).
3. It may be advisable to sample three (or more) specimens from each stratigraphic horizon (to overcome the problem of

the inhomogenous magnetisation within each stratigraphic level), and process only specimens with NRM intensities of say >0.25mA/m. This should make the results far more repeatable and the benefit of this would far outweigh the extra time taken up in sampling (which would be minimal anyway), and the laboratory analysis. If three specimens from a particular horizon had NRM intensities above 0.25mA/m, one could be demagnetised at 5mT steps, another at 10mT steps and the final one at the peak applied field.

Chapter 10 Results from the Late Palaeocene and Early Eocene of Denmark

10.1 Historical Background

Heilmann-Clausen et al (1985) detailed the published work carried out on the Late Palaeocene and Early Eocene succession in Denmark. Extensive lists for each of the formations were provided, dealing with the following aspects: palaeontology, biostratigraphy, palaeoenvironments, mineralogy, sedimentology and tephra chronology. Details of boreholes and outcrops were also provided.

The world famous "ash-series" (now assigned to parts of the Olst and Fur Formations) has received considerable attention. Work on the "ash-series" began in the middle of the last century (Forchammer, 1835) and a steady flow of papers folowed from the 1880's up to the first world war. Boggild (1918) established a tephra chronology for the sections now assigned to the Fur Formation, which was later extended to those of the more widespread Olst Formation (Andersen, 1937).

After the first world war attention focussed on the units now named the Holmehus, Rosnaes Clay, Lillebaelt Clay and Sovind Marl Formations (Harder, 1922; Ravn, 1928 and Odum, 1936) although Ravn had published work on some of these units at the turn of the century. Work continued after the second world war and detailed biostratigraphical studies (utilising microfossils) began in the 1960's.

A palaeomagnetic pilot study of the "ash-series" was carried out by Sharma (1969). Unfortunately the work was never followed up and a number of important flaws remain uncorrected. Sharma used a single cleaning field (30mT) and only the inclination of the remanent magnetisation was used in polarity determinations. He was therefore unable to make polarity evaluations based on directional "trends". The beds were assumed to be of Eocene age (they are in fact Late Palaeocene), and biostratigraphic information was not used to estimate the age range of the beds. Three separate normal polarity levels were identified and assumed to

represent normal chrons (they are possibly only short period magnetic "events").

Though Sharma's methods and interpretation were questionable, he showed great understanding of the potential of palaeomagnetism in Tertiary stratigraphy and many of his ideas merit further consideration. The palaeomagnetic laboratory at Aarhus University has been involved with palaeomagnetic work on the Danish Tertiary, but the author is unaware of any published information.

In recent years the stratigraphy of the Late Palaeocene and Early Eocene deposits in Denmark has been revised and the units have been formally assigned to formations (Pedersen and Surlyk, 1983 and Heilmann-Clausen et al, 1985).

10.2 The formations investigated in this study

The formations investigated in this study are discussed briefly in ascending stratigraphic order. All of the formations were defined by Heilmann-Clausen et al (1985) except for the Fur Formation which was defined by Pedersen and Surlyk (1983). The Late Palaeocene and Early Eocene exposures of Denmark are particularly important as they exhibit a similar succession to that of the eastern North Sea. Fig 10.1 summarises the stratigraphy of the Danish Palaeogene. Fig 10.2 shows the pattern of outcrop of the various formations and the localities which were sampled for this study.

10.2.1 The Holmehus Formation

The Holmehus Formation comprises non-calcareous dark greenish and brownish clays. The base of the formation overlies an unnamed unit, which in turn rests on top of the Kerteminde Marl Formation. Deposition was in an oxygenated marine environment. The formation is exposed at only a few localities, but is well-known from borehole sections. It attains a thickness of 12m (in both the LB38 borehole at Lillebaelt and the Viborg 1 borehole in central Jutland). It has been assigned to the Ceratiopsis speciosa

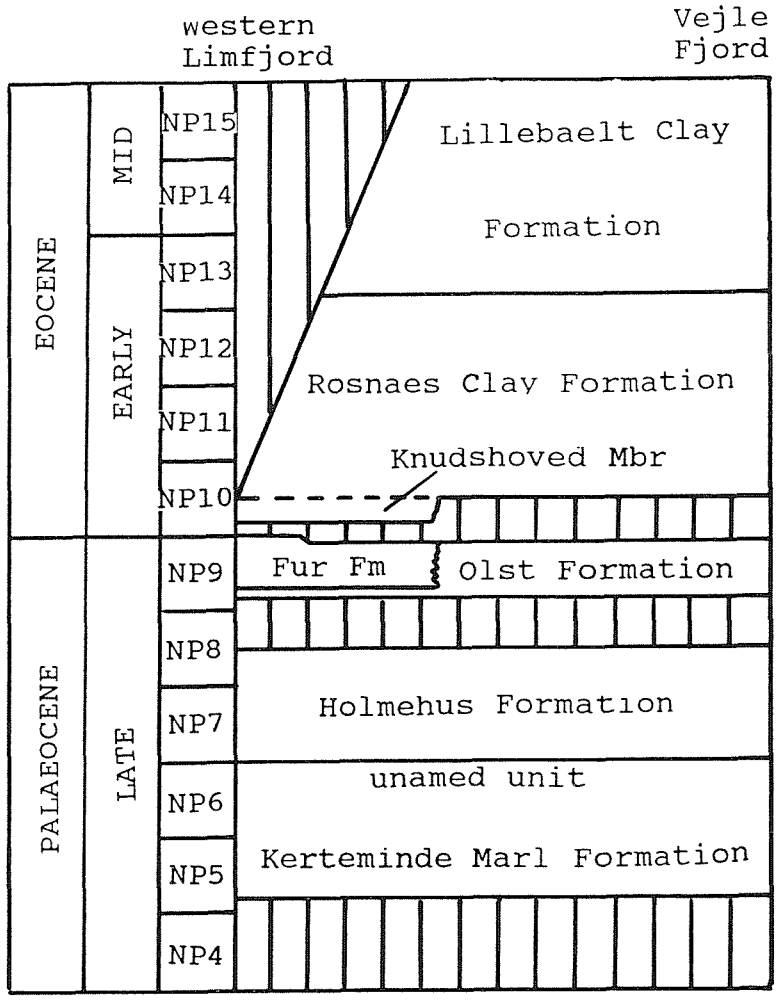

Fig 10.1 The stratigraphy of the Lower Palaeogene formations of Denmark.

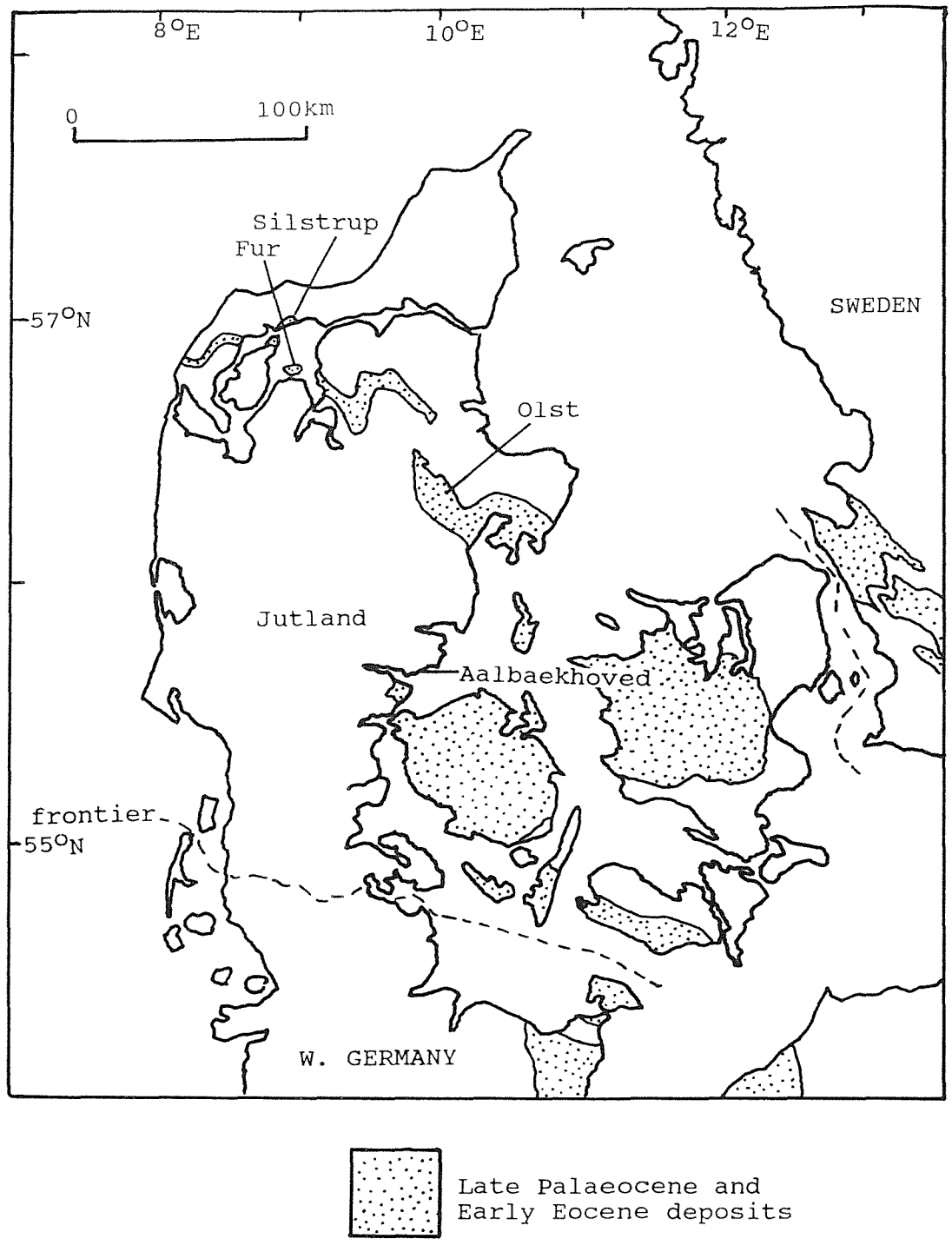

Fig 10.2 The outcrop pattern of the Danish Palaeogene formations investigated in this study.

dinoflagellate zone (Heilmann-Clausen, 1982) of the Thanetian stage.

10.2.2 The Olst Formation

A glauconite horizon, 8cm in thickness, marks the base of the Olst Formation, indicating a significant period of marine non-deposition. This formation is assigned to the Apectodinium hyperacanthum dinoflagellate zone, and is subdivided into the Haslund (lower, 20m) and Vaerum (upper, 9.1m) Members. The lower part of the Haslund Member is a very finely laminated (mm scale) black and dark green clay. The upper part of this member includes the "negative" series of ashes interbedded with dark silty clays.

The Vaerum Member includes the "positive" ash-series interbedded in a silty clay. Over 130 ash layers, varying in thickness from 1mm to over 10cm, have been documented (Andersen, 1937). Both laminated and bioturbated levels are present. Carbonate cemented levels occur, particularly at ashes +30, +77 and +86.

Volcanoes in the Skagerrak, to the north of Denmark, were thought to be the source of the ashes (Andersen, 1937). However Knox and Morton (1988) believe the source of the ashes to be the Faroe-Iceland-Greenland igneous province, based on the ash composition and their widespread distribution across the NE Atlantic and the North Sea Basin.

10.2.3 The Fur Formation

The Fur Formation, which is typically 25 to 55m thick, is an interbedded diatomite and ash sequence, restricted to the western Limfjord region (Fig 10.2). It is, for the most part, the lateral equivalent of the Olst Formation (Fig 10.3). Pedersen and Surlyk (1983) defined the Fur Formation and subdivided it into the Knudeklint ("negative" ashes) and Silstrup ("positive" ashes) Members. Heilmann-Clausen et al (1985) repositioned the base of the formation from below ash -39 to just below ash -33.

Pedersen and Surlyk (1983) proposed a model to explain

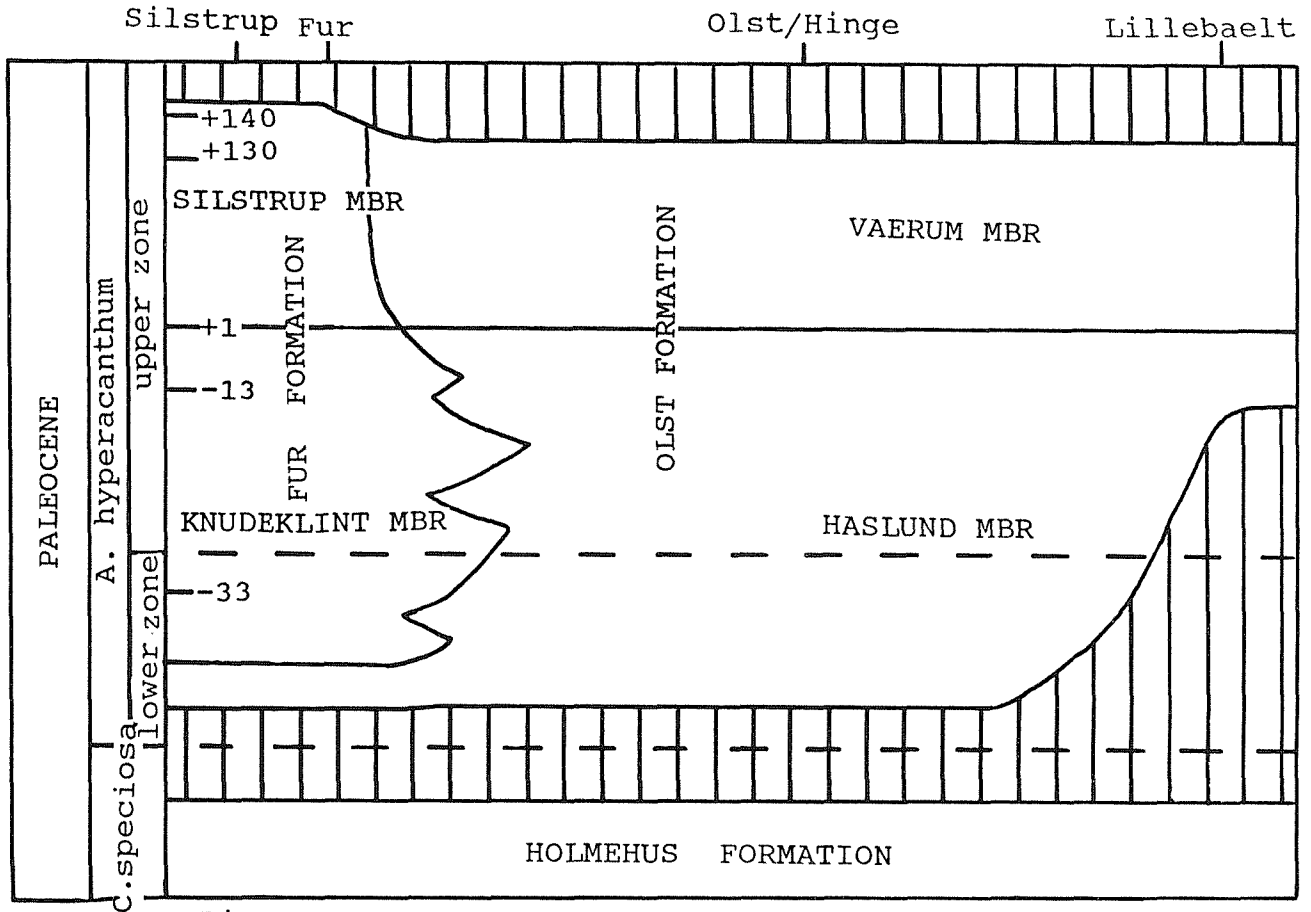

Fig 10.3 The detailed stratigraphy of the Olst and Fur Formations in Denmark (from Heilmann-Clausen et al, 1985).

the restricted extent of the diatomite. Upwelling in the western Limfjord region was constrained by a series of bathymetric highs to the west, north and east and a low to the south (see their Fig. 15). Their model has superseded Bonde's (1979) theory based on upwelling along a more extensive palaeo-coastal zone.

10.2.4 The Rosnaes Clay Formation

The Rosnaes Clay Formation is characterised by red and brown hygroscopic clays. Deposition was in a very low energy, well-oxygenated marine environment. This formation is very similar to the Unter Eozan 3 of northern Germany, and a red clay unit above the ash series in the North Sea (Knox and Harland, 1979). The locally developed Knudshoved Member of the western Limfjord area defines the base of the formation. Both the Wetzeliella astra and Wetzeliella meckelfeldensis dinoflagellate zones have been identified in the member (Heilmann-Clausen, 1982) indicating an Early Eocene age. The formation is typically 3-6m thick. However, at Aalbaekhoved in the Vejle Fjord, it exceeds 18m. Six informal lithological units (R1 to R6) have been recognised and documented. In recent unpublished work (C. Heilmann-Clausen and E.Steurbaut, pers. comm.) the Kisselovia coleothrypta and NP13 biozones were identified at the top of the formation at Aalbaekhoved.

10.2.5 The Lillebaelt Clay Formation

The basal part of the Lillebaelt Clay Formation is a non-calcareous red brown clay which contrasts sharply with the grey clay (R6) of the Rosnaes Clay Formation. However, most of the Lillebaelt Clay Formation is typically a grey and grey-green non-calcareous clay with a few ash layers in the lower parts. The formation varies greatly in thickness from about 10 to 70m. Six informal lithological units (L1 to L6) have been recognised and can be traced across wide areas with only minor lateral variations. Although the formation is essentially non-calcareous, carbonate concretions do occur, a result of carbonate mobilization

during diagenesis. The biostratigraphy is based chiefly on dinoflagellates and foraminifera although the NP14 and NP15 nannoplankton zones have been identified in the upper part of the formation (Thiede et al, 1980).

10.3 Olst

The clay pit at Olst is located 10km south of Randers, in eastern Jutland (map sheet 1315 III NV, NH 665495). One of the most complete Danish Palaeogene successions is exposed in the pit, a result of deformation during the Recent glaciations (Gry, 1940) which tilted the beds to near vertical. Sixty irregularly spaced sites were sampled, spanning the upper part of the Holmehus Formation to the base of the Lillebaelt Clay Formation (c. 25m).

10.3.1 The Holmehus and Olst Formations

Five sites in the Holmehus Formation and 26 sites in the Olst Formation were sampled. Sites in the "ash-series" were measured relative to the conspicuous layers, and the positions adjusted to Andersen's (1937) standard units. Unfortunately, due to slumping, the middle part of the Haslund Member could not be sampled. Sites close to the Holmehus/Olst Formation junction dip 63^{o} towards the NNE, whilst the upper sites dip c.90^{o} in the same direction.

A plot of NRM intensity against stratigraphic position is shown in Fig 10.4. The intensities appear to be directly related to the presence of volcanic material in the sediment. After demagnetisation, IRM measurements were carried out on six representative specimens (five from the Haslund Member and one from the Vaerum Member). The IRM plots are shown in Figs. 10.5 to 10.7. All specimens have a high IRM ratio (.94 to .99), usually indicative of magnetite; however the peak IRM values vary considerably. The three specimens from the lower and middle part of the Haslund Member have maximum values of c.50 mAm^2. Sites OL39 and OL40 (close to the top of the negative "ash-series") mark an important transition with values of 720 and 4600 mAm^2 respectively. The single specimen from the

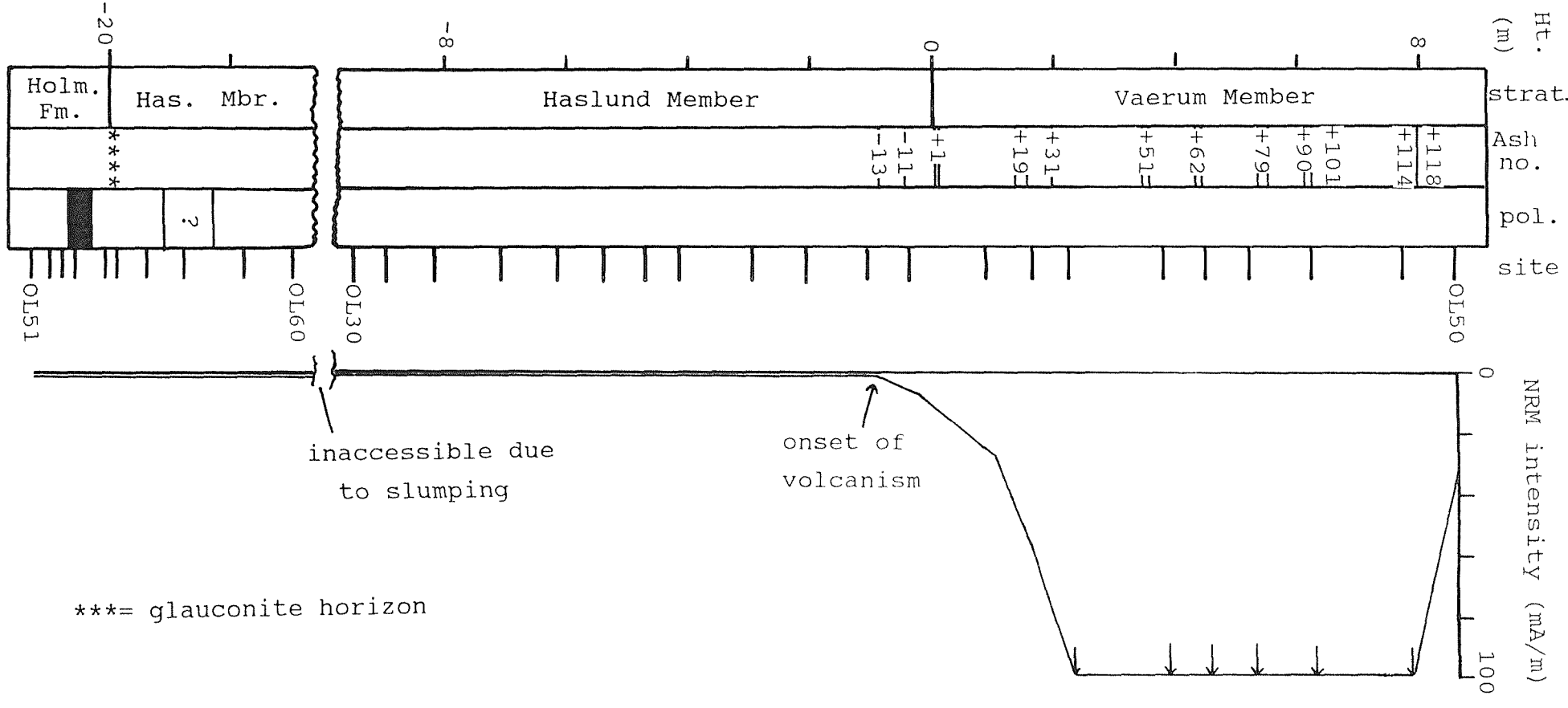

Fig 10.4 The magnetostratigraphy of the Holmehus and Olst Formations at Olst.

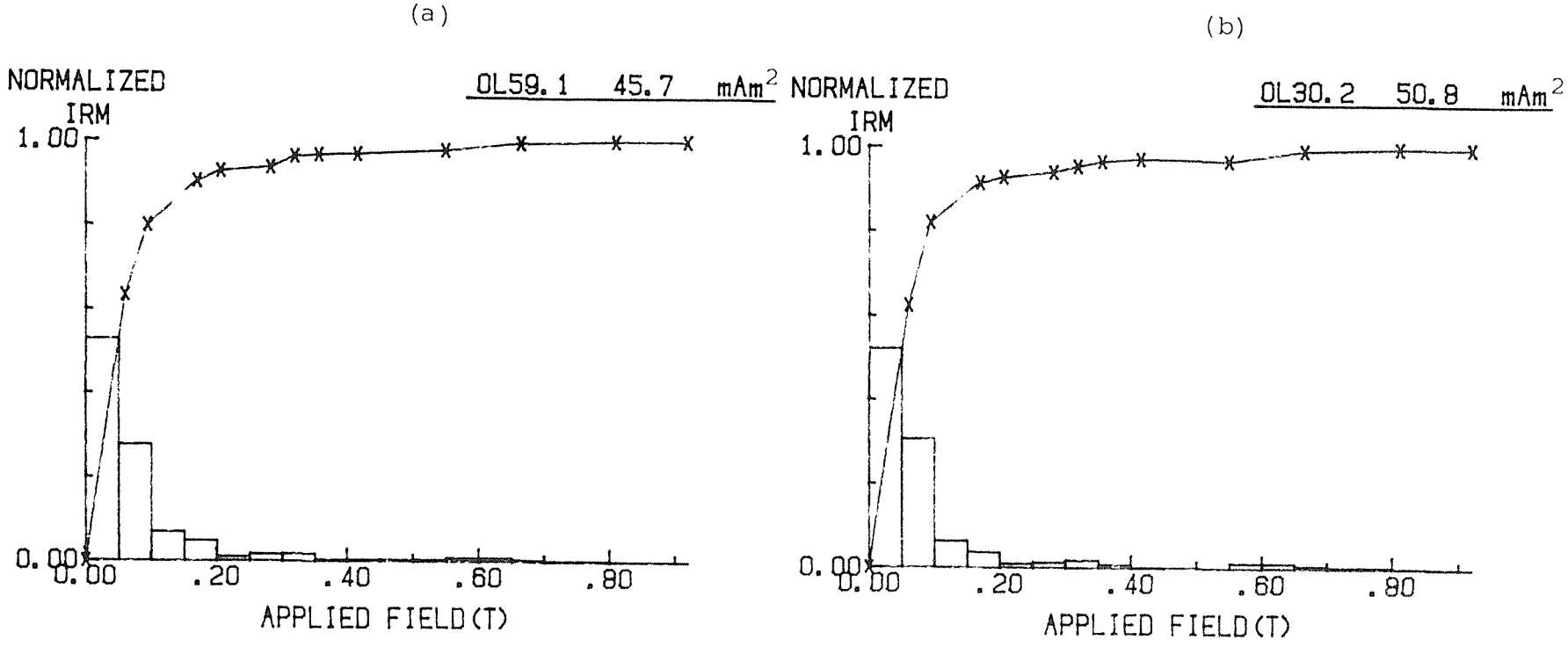

Fig 10.5 Typical IRM plots for specimens from the basal part of the section at Olst. The remanence of the upper part of the Holmehus Formation (a) and basal part of the Olst Formation (b) is carried by magnetite. However, both specimens contain only very small amounts of magnetite, because they both have very low peak IRM values.

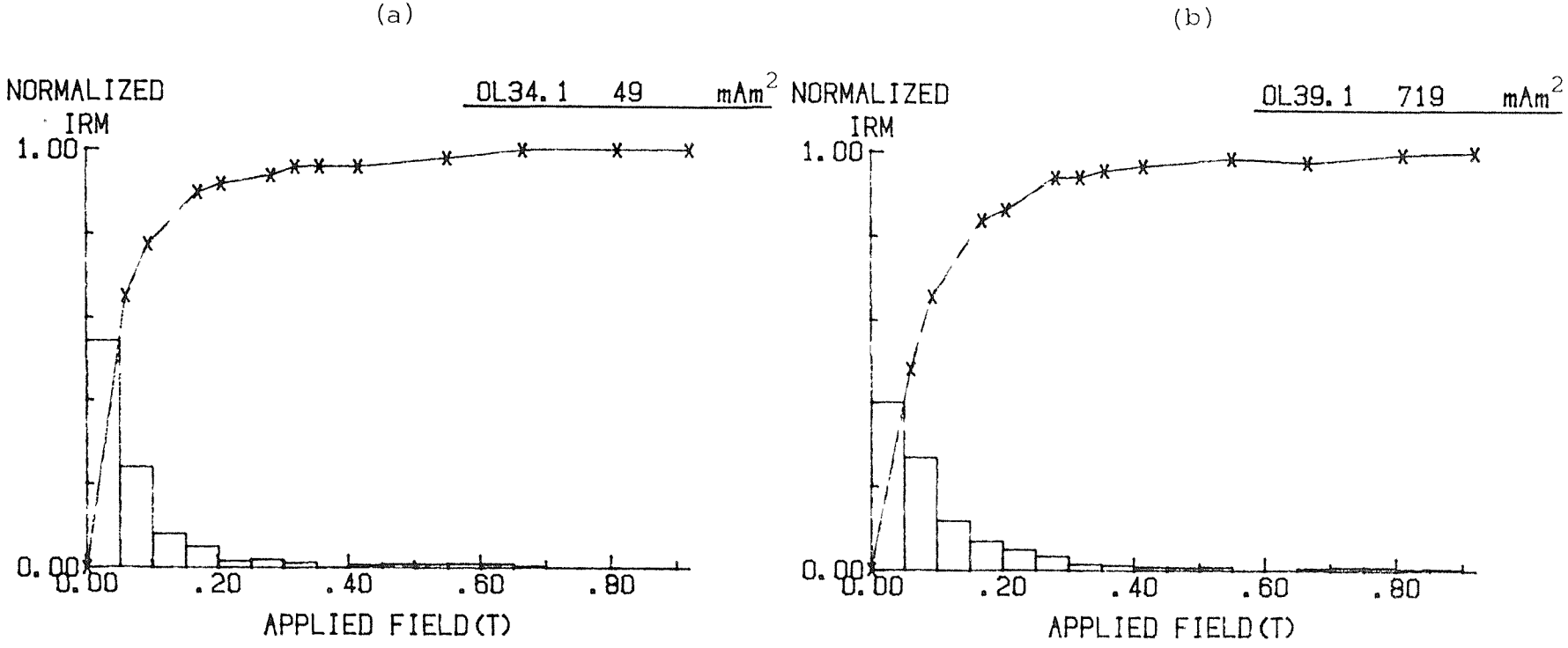

Fig 10.6 Typical IRM plots for specimens from the lower and middle parts of the Olst Formation at Olst. Both specimens have a remanence carried by magnetite, although OL39.1 (b) contains a higher proportion of magnetite (it has a much greater peak IRM).

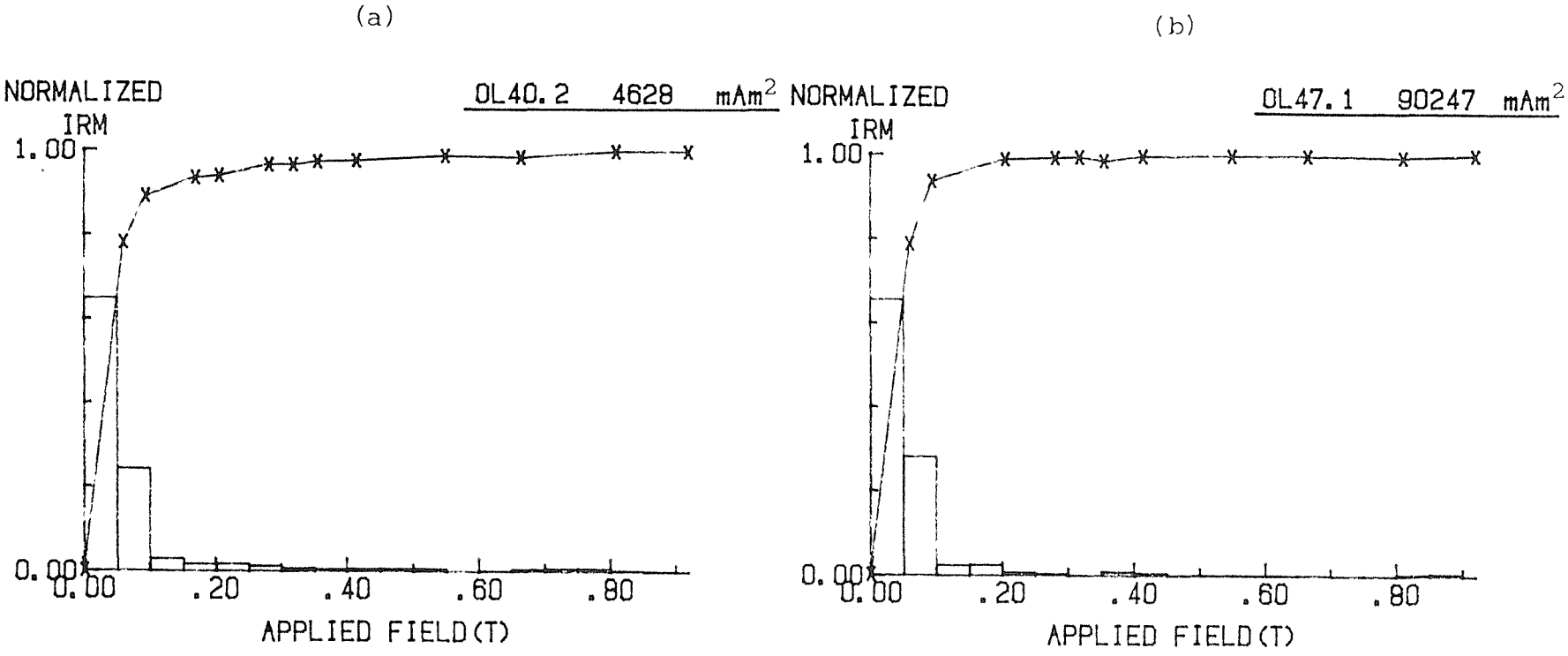

Fig 10.7 Typical IRM plots for specimens from the upper part of the Olst Formation at Olst. OL40.2 (a) is from the top part of the Haslund Member whilst OL47.1 (b) is from the middle of the Vaerum Member. Both specimens are magnetite-rich. Note the extremely high peak IRM of OL47.1.

middle of the Vaerum Member had a peak IRM of 90,000 mAm^2. The IRM data confirm the relationship between high NRM intensity and the presence of volcanic ash. The abrupt change in magnetic intensity is not related to a change in magnetic mineralogy, as is often the case, but to the onset of a major period of volcanism which dramatically increased the quantity of magnetic material being incorporated into the sediment. It must be noted that the ash-layers were not sampled, as it was assumed that the magnetism of these layers would be too unstable to yield useful results.

Typical demagnetisation data are presented in Figs 10.8 and 10.9. The magnetic polarity results from the two formations are presented in Fig 10.4. A single normal polarity site (OL54) was identified and probably represents a short period magnetic "event". The remainder of the section is reverse polarity. The hiatus separating the two formations is critical and its importance will be discussed in Section 10.7.2.

10.3.2 The Rosnaes Clay and Lillebaelt Clay Formations

A 3.3m section of the Rosnaes Clay and Lillebaelt Clay Formations was sampled in detail. The condensed sequence spans the *W. mecklefeldensis* to *K. coleothrypta* dino-flagellate zones (NP10 to NP13 nannoplankton zones). The formations have been tilted (bedding correction: 279^o,83^o) and appear disturbed, although individual beds and ash-layers can be traced easily. The inter-site spacing was 10-15cm, providing 29 sites (alternating 2 specimens/ 1 specimen per site).

Twenty-one of the specimens (taken randomly from the sampled set) were measured and demagnetised up to maximum fields of 25 to 50mT. NRM intensities were very high (30-150mA/m), again probably the result of ash material being incorporated into the sediment. The majority of the specimens carried a strong VRM (MDF c. 12mT). Care was taken to eliminate, where possible, fluctuations of the remanent magnetisation which commonly occured during the measurement cycle (these specimens were measured on the

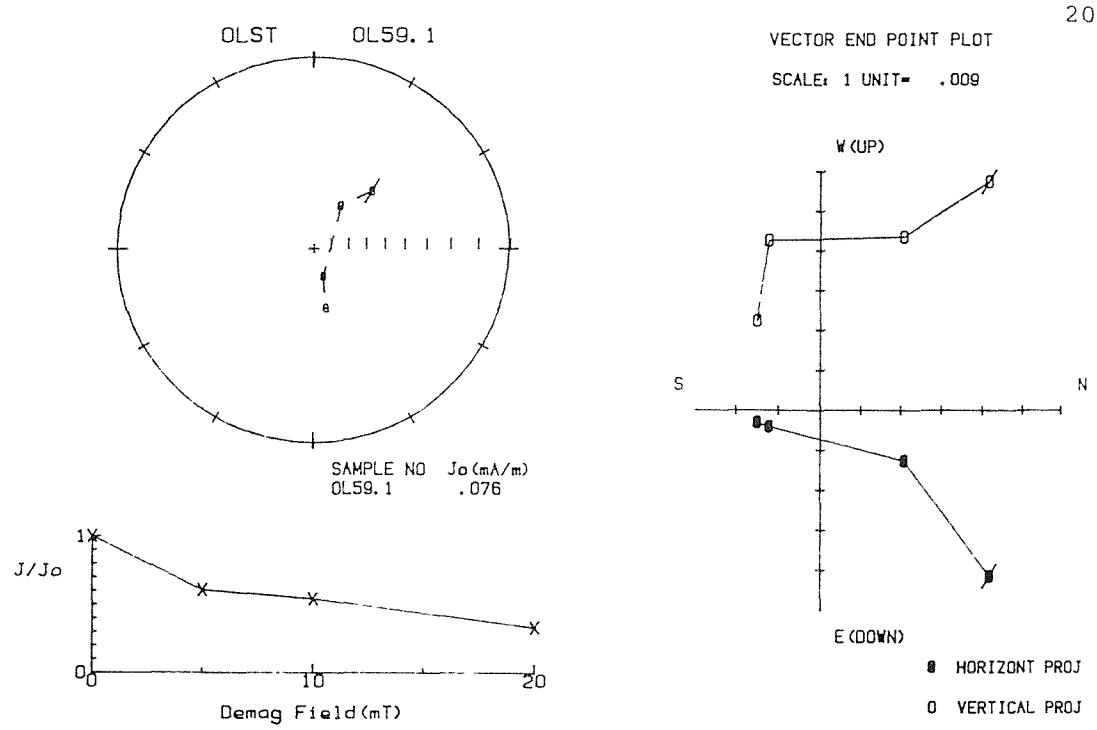

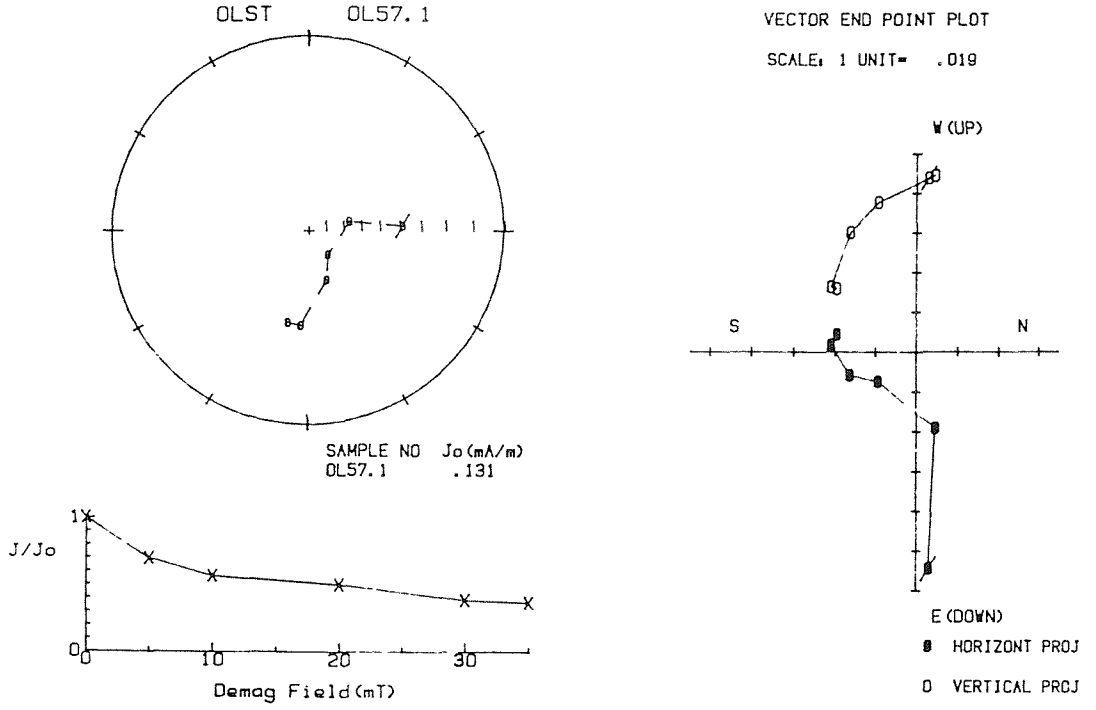

Fig 10.8 Typical reverse polarity specimens from the upper part of the Holmehus Fomation and basal part of the Olst Formation at Olst. For explanation of symbols see Fig 2.7.

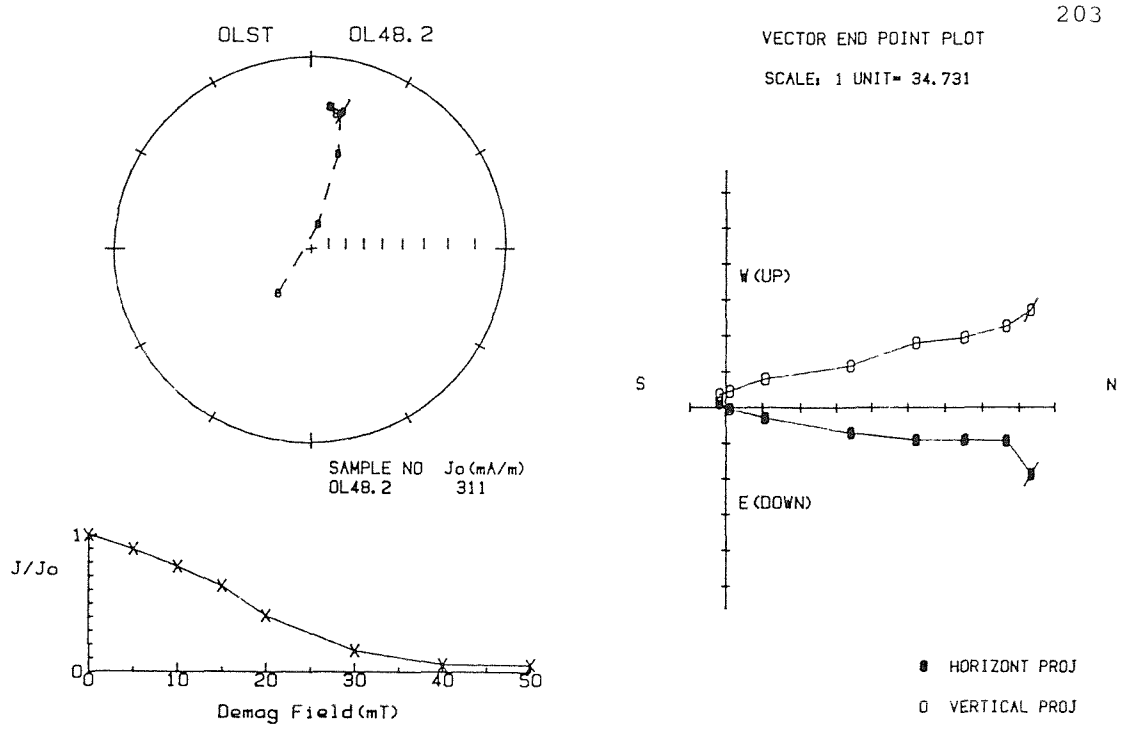

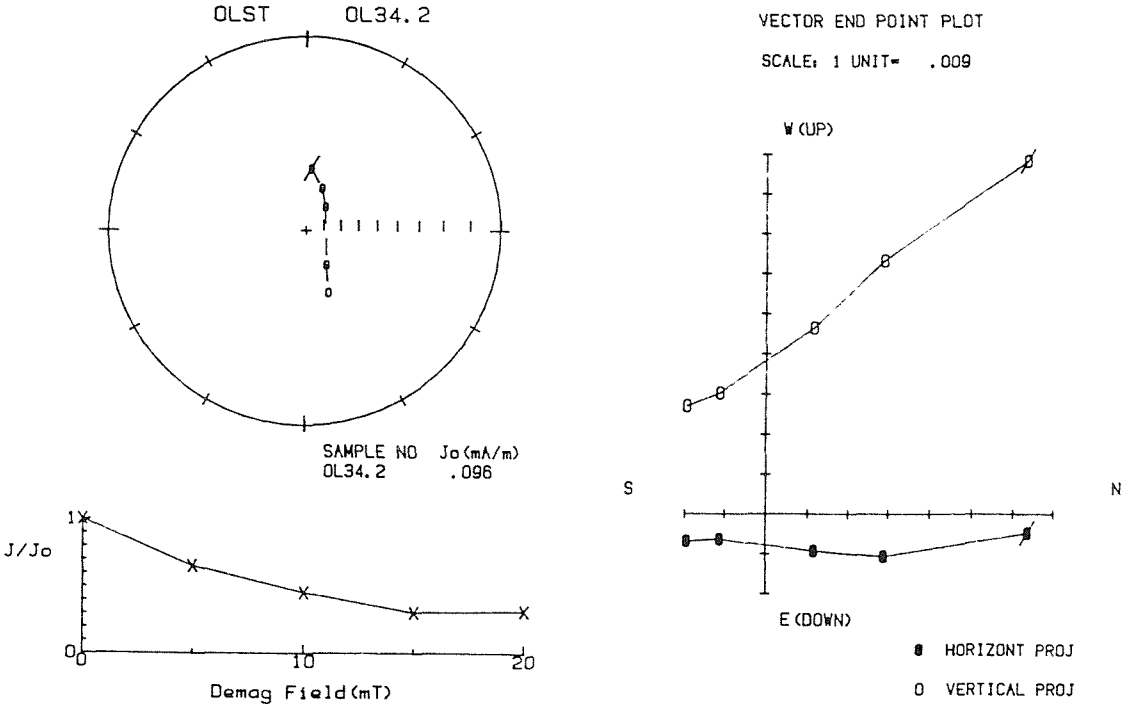

Fig 10.9 Typical reverse polarity specimens from the Olst Formation at Olst.. For explanation of symbols see Fig 2.7.

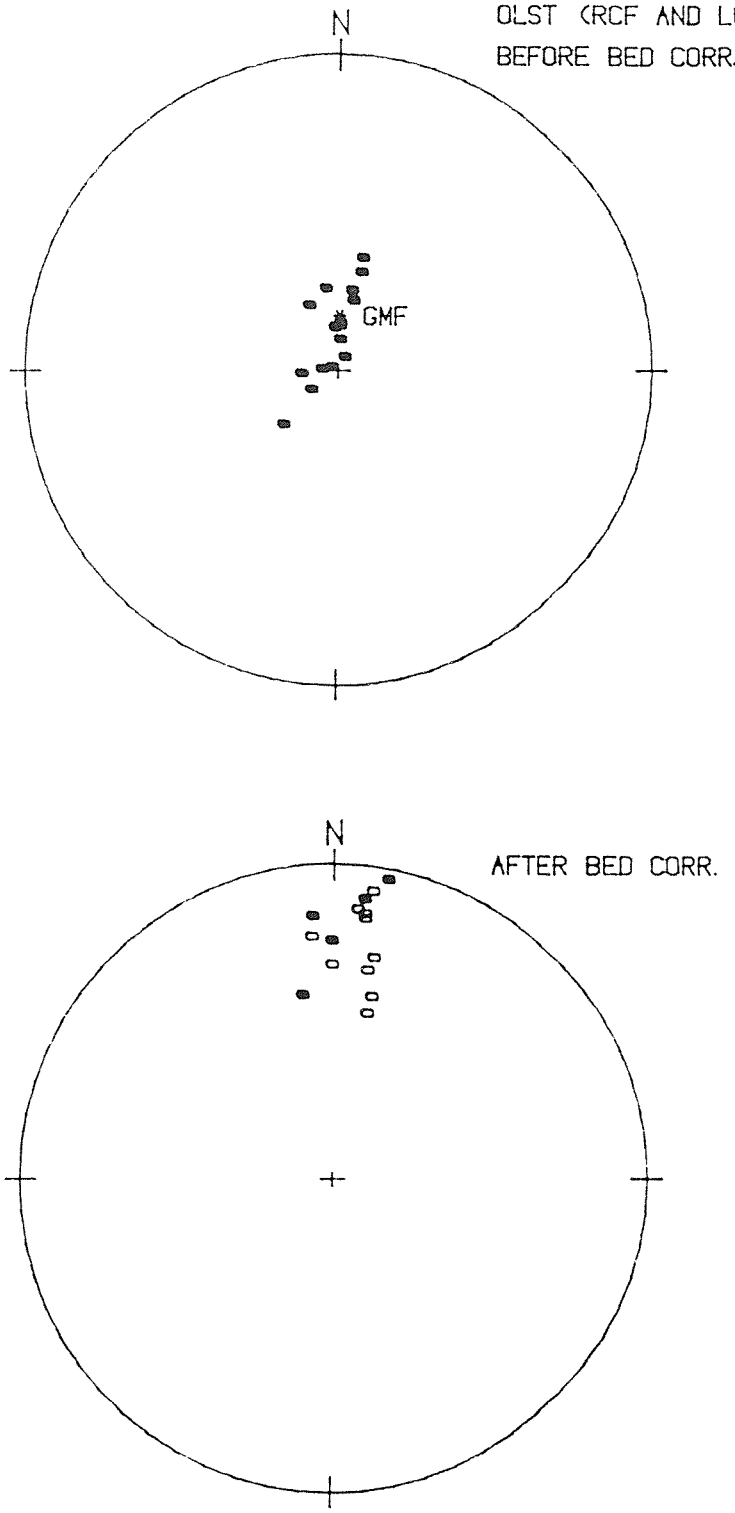

Fig 10.10 The SEP directions for the specimens from the Rosnaes Clay and Lillebaelt Clay Formations at Olst. The upper plot shows the pre-bedding corrected directions and the lower plot the bedding corrected directions (Strike= 278.7; Dip= 82.5). (* GMF= present-day geomagnetic field direction)

"Molspin" magnetometer). Sixteen of the specimens produced a SEP direction (plotted, before and after the application of the bedding correction, on a stereonet in Fig 10.10). The striking feature to emerge is the grouping of the directions about two points. The pre-corrected directions are very close to the present-day field direction in Denmark. Using the magneto- biostratigraphic scale of Berggren et al (1985), the sediments span Chrons C24BR to C22R (4 reversed and 3 normal polarity chrons). It is concluded that the remanent magnetisation must have been acquired at, or sometime after, the tilting episode. The remanent magnetisation for the five specimens showing directional "trends" during demagnetisation confirm this (the data are listed in the Appendix).

10.4 Silstrup "Sydklint"

The coastal cliff at Silstrup (map sheet 1116 INV, MJ 789087) exposes the upper part of the Silstrup Member of the Fur Formation. The exposure is very important as it is the only place where ash-layers +130 to +140 are exposed. A total of 11 sites were sampled spanning 7.8m (from just below ash +115 to 1.4m above ash +140). The Silstrup Member is overlain by a micaceous clay of Oligocene age. Part of the sampled section has been tilted by glacial tectonics and some of the sites were in beds dipping 30^{o} toward the West. NRM intensities varied significantly (0.1 to 4.3 mA/m). The stronger values appear to correspond with diatomite levels with an increased ash content.

Examples of demagnetisation plots are shown in Figs 10.11. The magnetic polarity results are presented in Fig 10.12. A single normal polarity site (SL5) was identified within an otherwise reverse polarity sequence. Unfortunately sites SL4 and SL6 are widely spaced and so the limits of this short normal polarity interval are poorly defined.

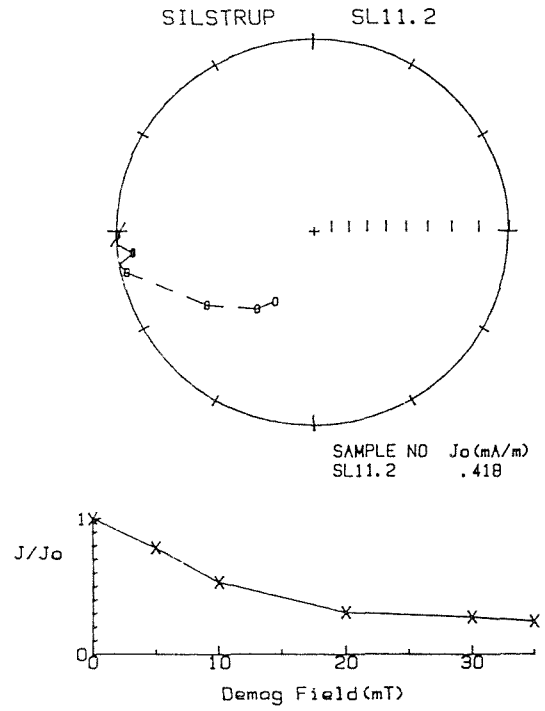

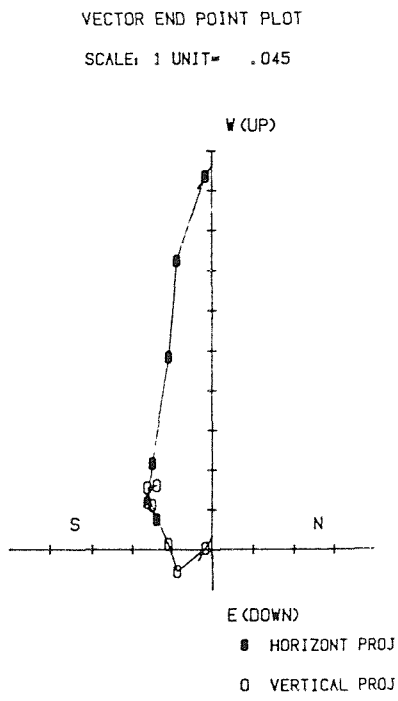

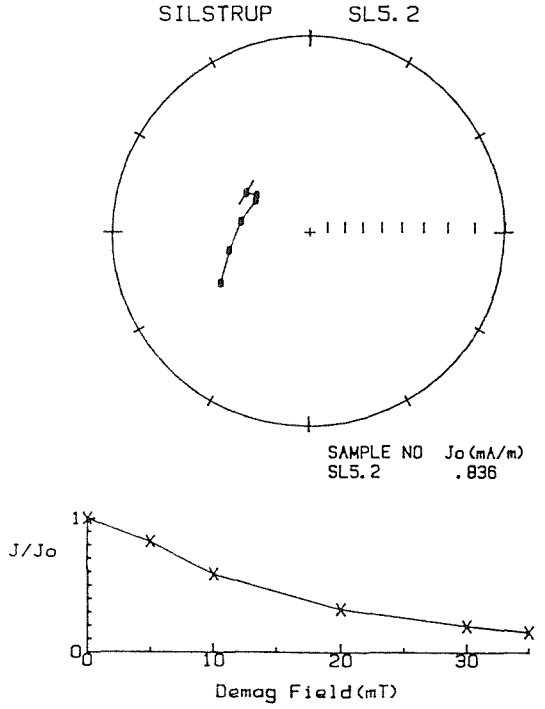

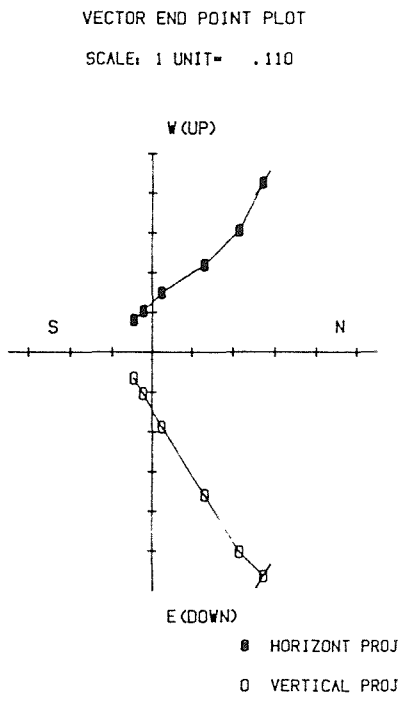

Fig 10.11 Typical reverse polarity specimens from the Silstrup Member of the Fur Formation at Silstrup "sydklint".

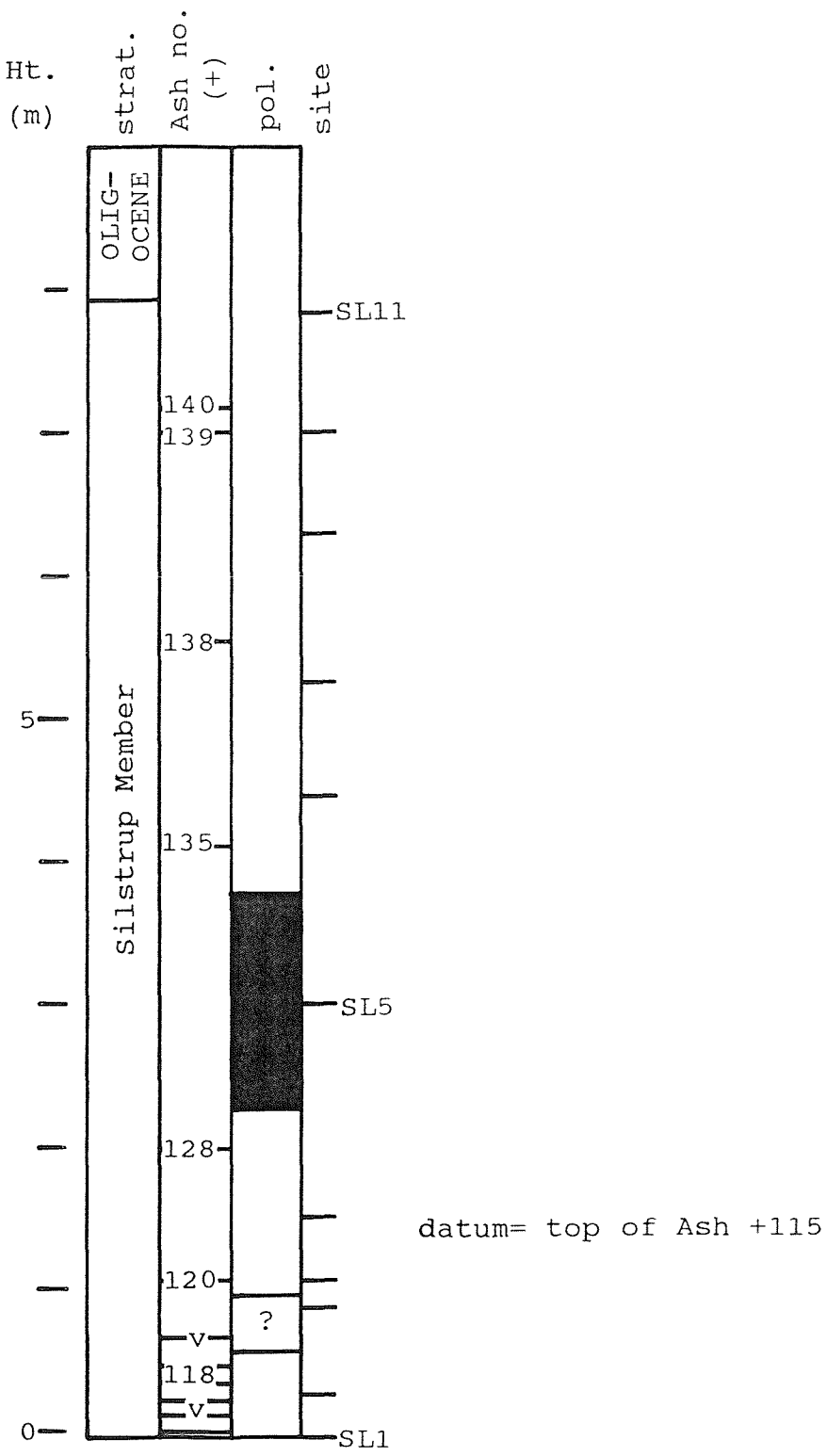

Fig 10.12 The magnetostratigraphy of the section at Silstrup "sydklint".

10.5 Fur

Two separate sections were sampled on the island of Fur in the western Limfjord.

10.5.1 Stolle Klint

Isolated sites in the lower part of the Fur Formation were sampled at Stolle Klint (map sheet 1216 VSV, MH 994 999). Sampling was restricted to the interval from below ash -33 up to ash -17. The results are poor due to the very low NRM intensities (about 0.06mA/m) however one anomalously strong specimen was encountered (FU34.1: 2.38 mA/m). Only two specimens produced a reliable polarity result (FU28.1 and FU34.1), both of which sh ed good normal polarity "trend" directions. However, it would be unwise to draw any conclusions from the limited results of this section.

10.5.2 Knuden

The Knudshoved Member of the Rosnaes Clay Formation was sampled in great detail at Knuden (map sheet 1116 ISO, MH 978996). The Member is well exposed in two synformal synclines. The W. astra and W. meckelfeldensis dinoflagellate zones have been identified in a 4m succession. Fifteen sites spanning the lower 2.68m were sampled on the north-eastern side of the synform (bedding correction: $129^{o},90^{o}$). (It must be noted that the bedding correction assumes a zero fold plunge.) Eleven representative specimens were processed (all but one up to 30mT). Eight of the specimens produced a SEP direction (which are plotted before and after bedding correction in Fig 10.13)
The W. astra and W. meckelfeldensis dinoflagellate zones are associated with the middle and upper part of Chron C24BR. Most of the bedding corrected SEP directions have declinations of about 240^{o} with generally shallow positive inclinations. The Knudshoved Member probably has a NRM which was acquired at, or sometime after, the folding episode. It is also worth noting that most of the pre-corrected directions have northerly declinations and steep

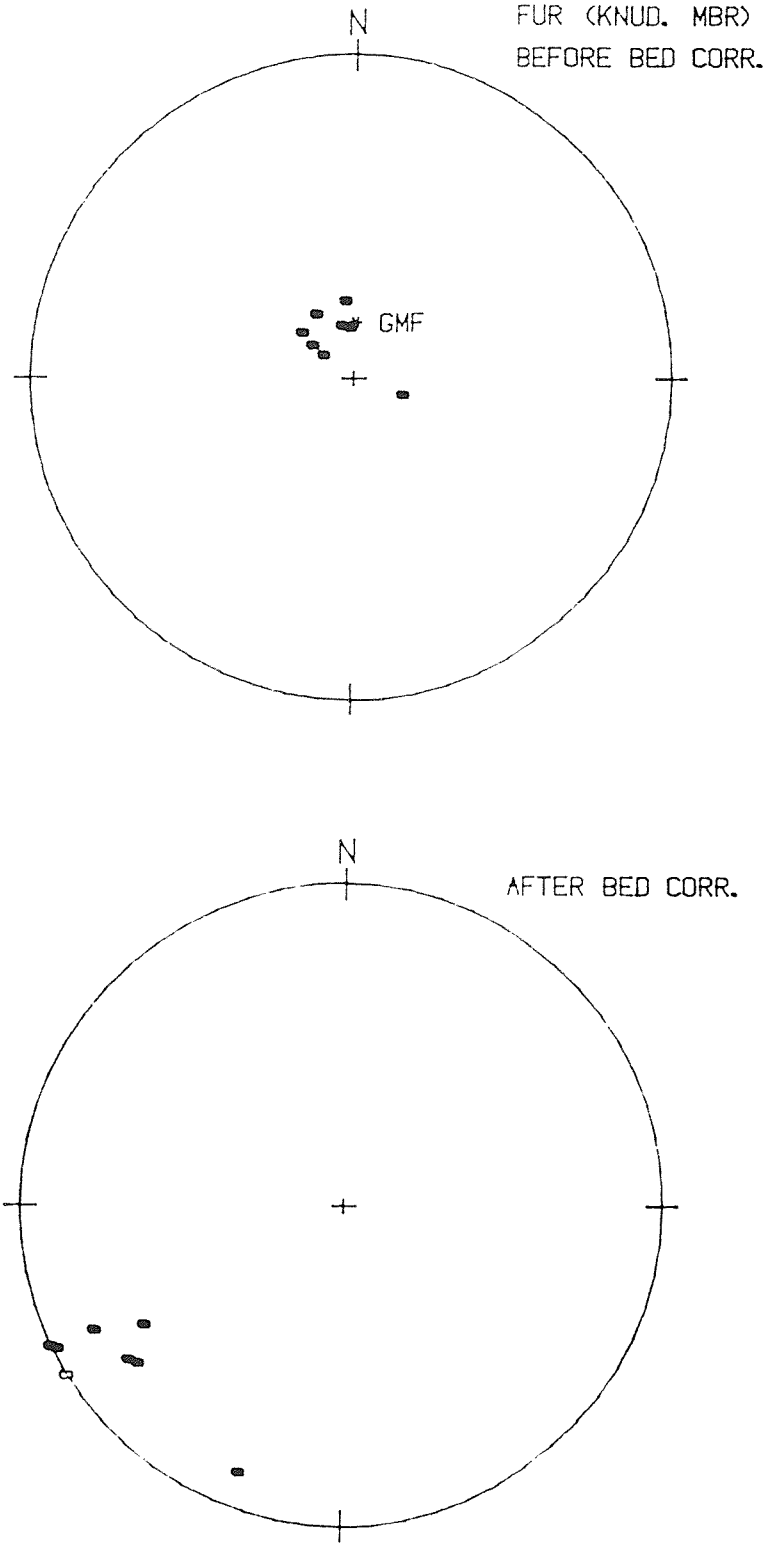

Fig 10.13 The SEP directions for specimens from the Knudshoved Member of the Rosnaes Clay Formation at Knuden, Fur. The upper plot shows the pre-bedding corrected directions and the lower plot the bedding corrected directions (Strike= 129; Dip= 90). (*GMF= present-day geomagnetic field direction)

positive inclinations, although they do not group very closely about the present-day field direction for northern Denmark.

Incidentally, had the southwestern limb of the synform been sampled, demonstrating the probable overprint would have been easier. The bedding corrected directions would have been toward the opposite side of the stereonet, close to NE. This would clearly have been discordant with a predicted reverse polarity magnetisation for these sediments.

10.6 Aalbaekhoved

The Rosnaes Clay Formation is typically 3-6m thick. The sequence is locally expanded in the Vejle Fjord area (Fig 10.1), and is best exposed in the coastal cliff at Aalbaekhoved (map sheet 1313 IVSV, NG 612728) where it is >18m thick. The basal part of the documented section is assigned to the NP11 nannoplankton zone (E. Steurbaut, pers. comm.).

During fieldwork a bed (assumed to be R1), not documented at Aalbaekhoved, was sampled (3 specimens). The bed rests directly on the Olst Formation and probably belongs to the *W. meckelfeldensis* dinoflagellate zone (?NP10). Seventy-nine other sites were sampled from the documented part of the Rosnaes Clay Formation and the basal part of the Lillebaelt Clay Formation. The beds are glacially disturbed, generally dipping towards the NE at 20^{o}-40^{o}.

NRM intensities for the succession are typically 50 to 150 mA/m, but the specimens have a very low MDF (c. 5mT). A number of typical demagnetisation plots are shown in Figs 10.14 and 10.15. The magnetic polarity results are presented in Fig 10.16. The succession is dominantly reverse polarity except for a number of single normal polarity specimens and the interval 11.75m to 16.4m which is dominantly normal polarity (coded AK-a). Sites AK46 and AK48 are arbitrarily included as part of magnetozone AK-a rather than considering them as isolated normal sites within the older reverse polarity zone.

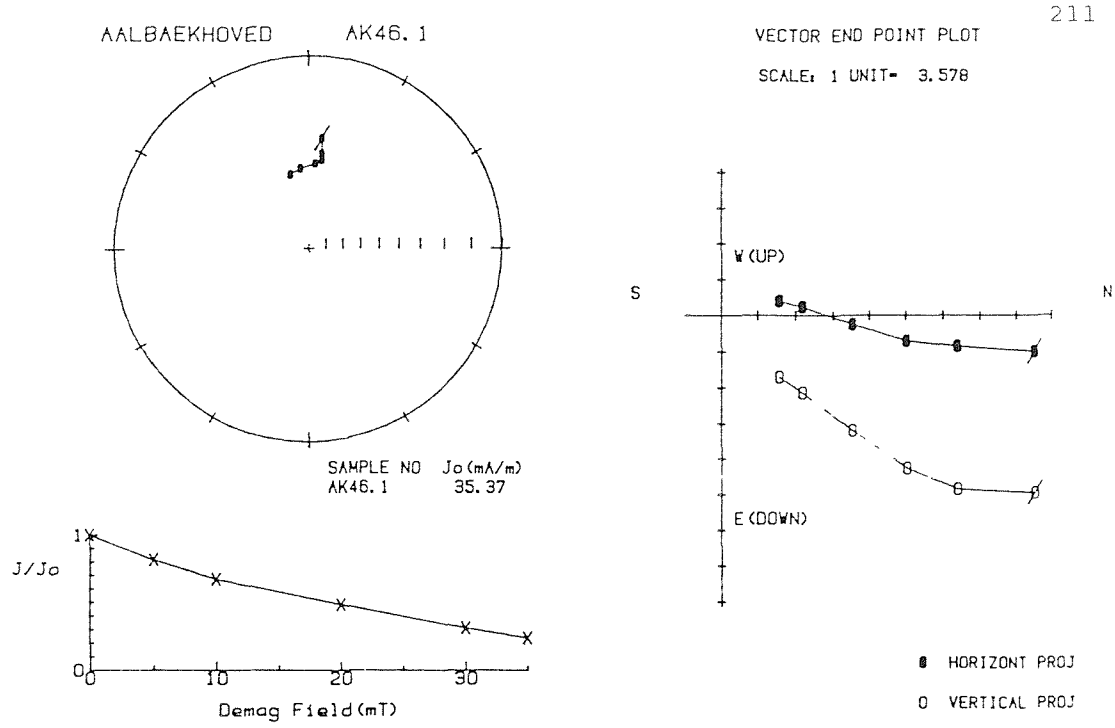

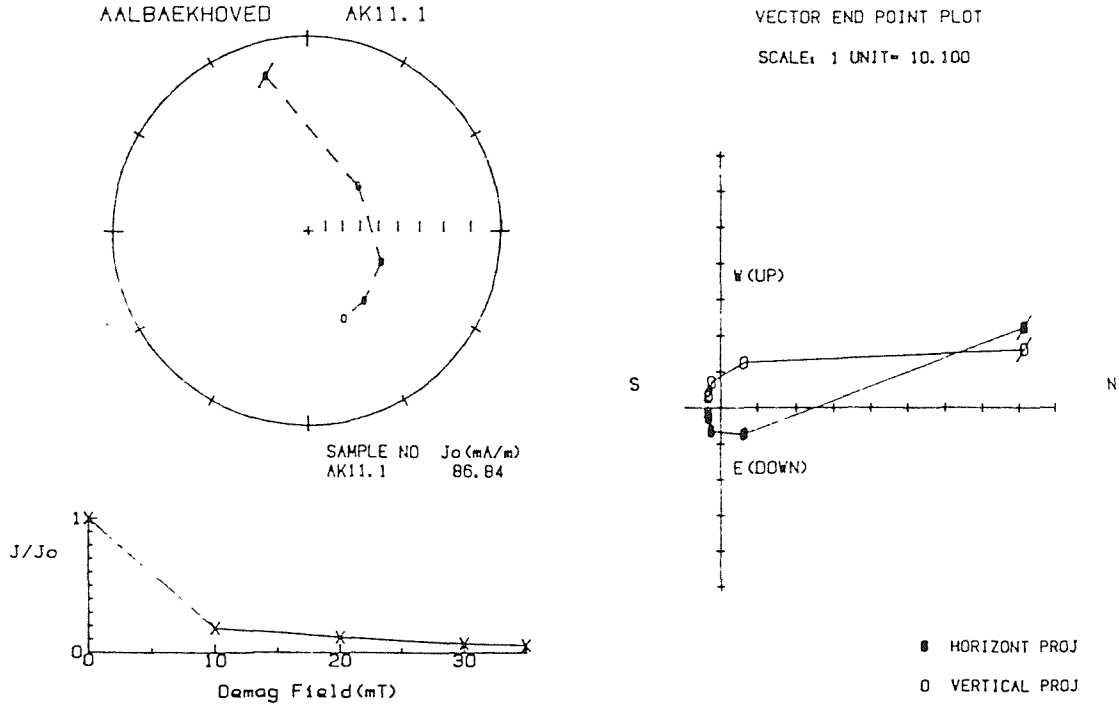

Fig 10.14 Examples of demagnetisation plots from the Rosnaes Clay Formation at Aalbaekhoved. The upper plot shows a specimen with a normal polarity and the lower plot a specimen with a reverse polarity. For explanation of symbols see Fig 2.7.

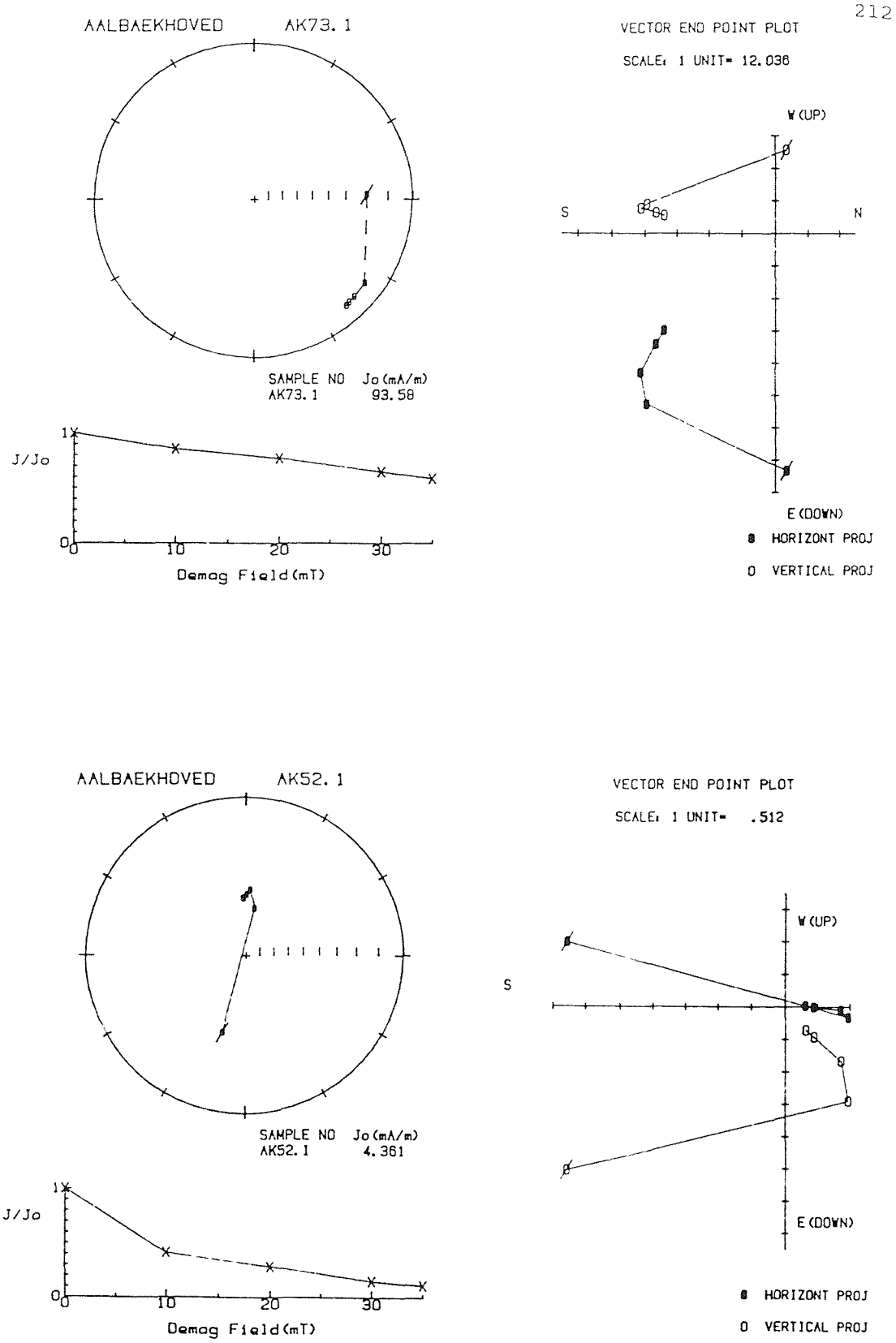

Fig 10.15 Examples of demagnetisation plots from the Rosnaes Clay Formation at Aalbaekhoved. The upper plot shows a specimen with a reverse polarity and the lower plot a specimen with a normal polarity. For explanation of symbols see Fig 2.7.

1 = E. Steurbaut (pers. comm.)

2 = C. Heilmann-Clausen (pers. comm.)

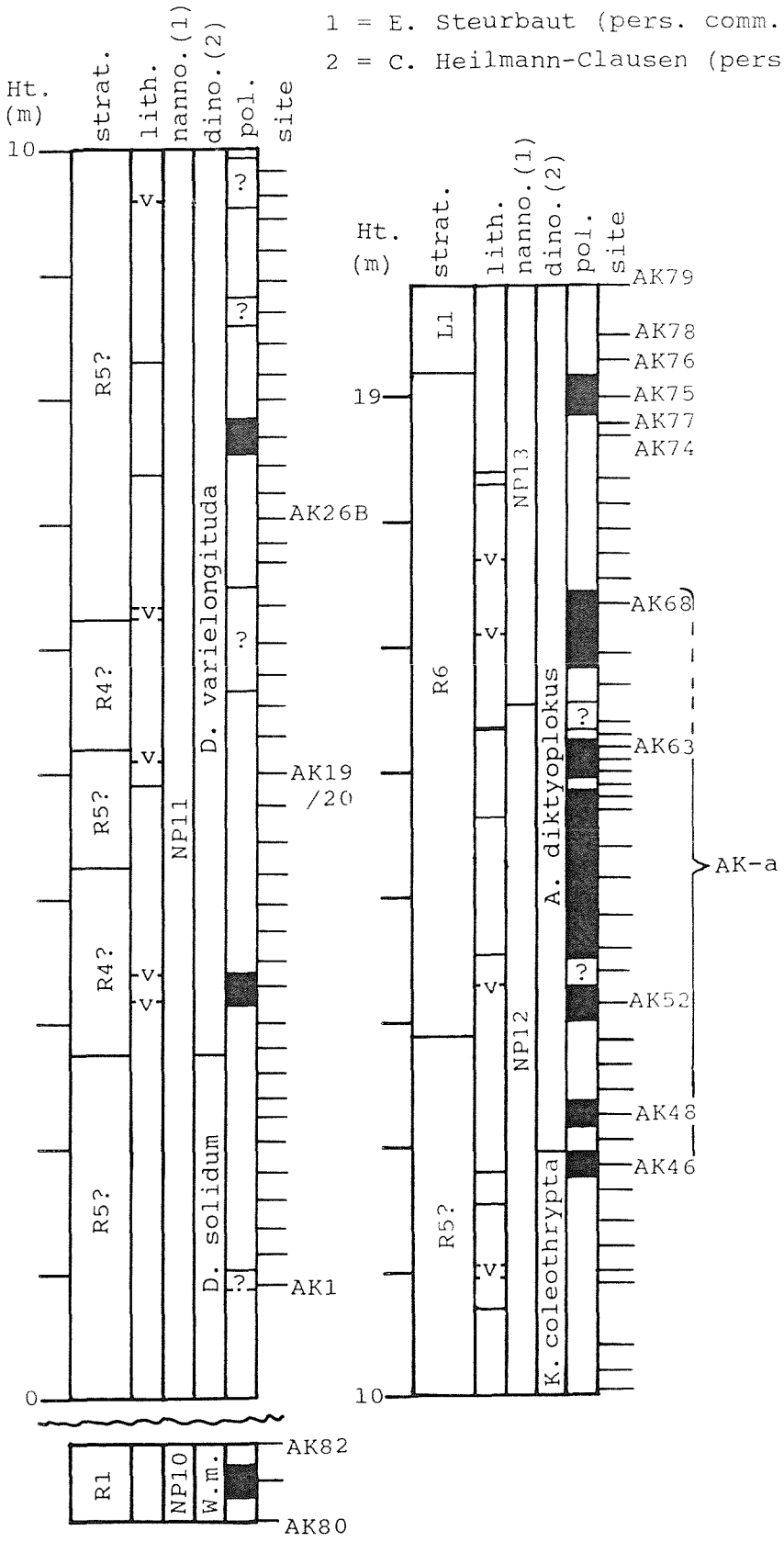

Fig 10.16 The magnetostratigraphy of the Rosnaes Clay Formation at Aalbaekhoved.

10.7 Synthesis and correlation

The magnetostratigraphic results from the four localities form a composite section which extends upwards from the top of the Holmehus Formation to the base of the Lillebaelt Clay Formation. The results are combined in Fig 10.17 with each section drawn in its relative stratigraphic position. Correlations are made with Berggren et al (1985 Figs 3 and 4)

10.7.1 The Holmehus Formation

The upper part of the Holmehus Formation was sampled at Olst. The top 1.2m of this formation is reverse polarity with the exception of a single normal polarity site. Heilmann-Clausen et al (1985) assign the Formation to the Thanetian C. speciosa dinoflagellate zone. The top of the formation is tentatively correlated with the upper part of Chron C25R.

10.7.2 The Olst Formation

The Olst Formation at the stratotype section is entirely reverse polarity. The formation is assigned to the A. hyperacanthum dinoflagellate zone and is therefore correlative with Chron C24BR. The hiatus at the base of the Olst Formation is assumed to be similar in duration to that separating the Thanet and Woolwich Formations in England, and the Lista and Sele Formations in the North Sea, as Chron C25N appears to be absent.

10.7.3 The Fur Formation

The upper part of the formation at Silstrup is reverse polarity. As the section is assigned to the A. hyperacanthum zone it can be correlated with Chron C24BR. Results from the lower part of the formation at Stolle Klint, Fur, were too poor to attempt correlation with the polarity time-scale.

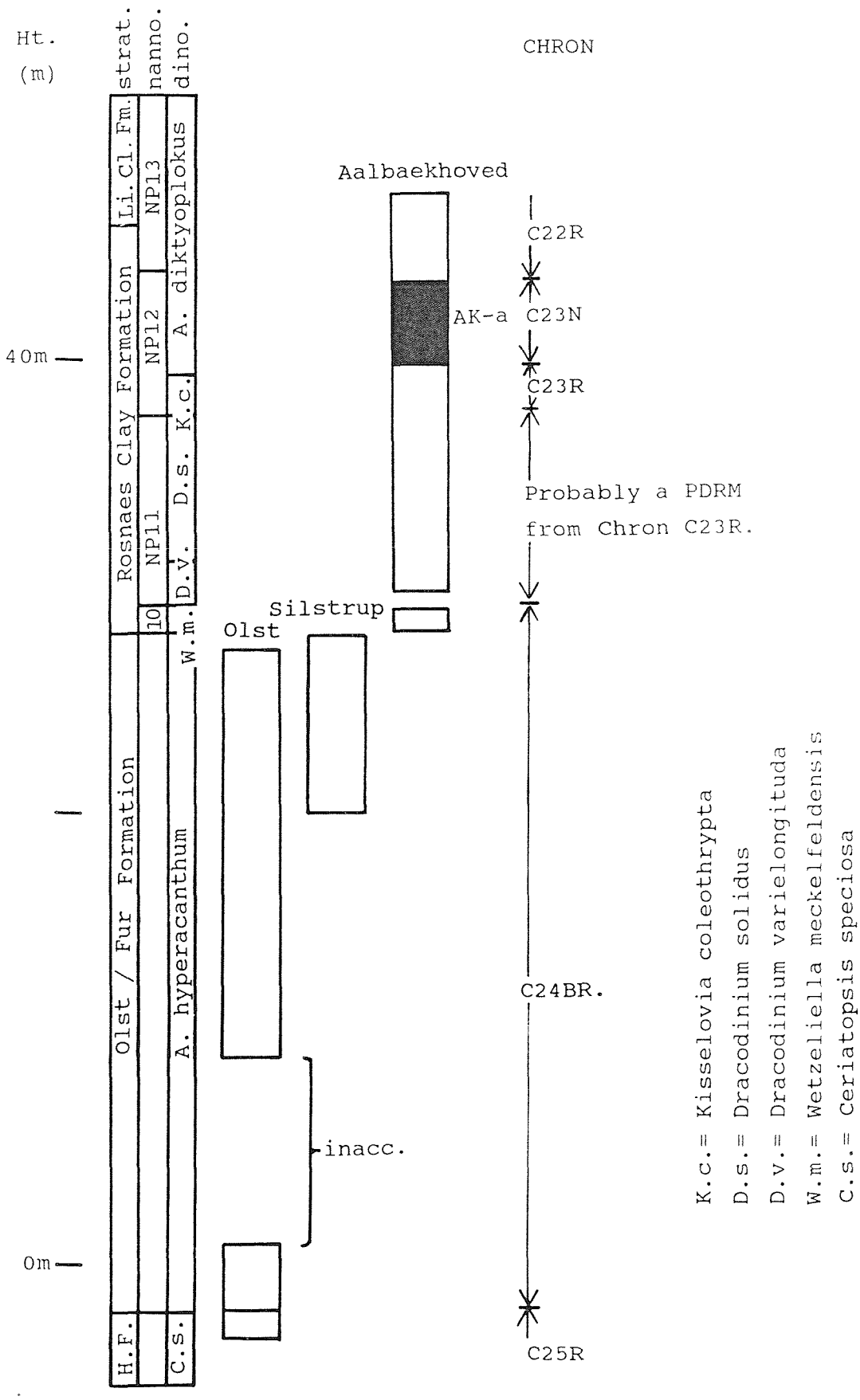

Fig 10.17 Synthesis and correlation of the Danish magnetostratigraphic results.

10.7.4 The Rosnaes Clay Formation

The Rosnaes Clay Formation was sampled at Olst, Aalbaekhoved and Knuden (on the island of Fur). The oldest sediments, sampled at Knuden, belong to the locally developed Knudshoved Member. Unfortunately, as discussed in Section 10.5.2, these sediments were probably overprinted sometime after the last glacial period.

A similar result was also obtained for the entire formation at Olst where the NRM is directed close to the present-day field direction in steeply dipping beds.

Fortunately, the section at Aalbaekhoved produced a positive result in beds dipping at 20^{o}-40^{o}. A single normal polarity magnetozone (AK-a) was identified in the interval +11.75m to +16.4m. E. Steurbaut (pers. comm.) has identified the base of NP12 at c. 10.0m in this section. C. Heilmann-Clausen (pers. comm.) positions the base of the K. coleothrypta dinocyst zone at a similar level and the FAD of Areospheridium diktyoplokus at 16.3m

Using the time-scales of both Berrgren et al (1985) and Haq et al (1987), magnetozone AK-a is correlated with Chron C23N. It must be noted that AK-a, as it is defined, continues into the base of the NP13 nannoplankton zone, whereas the top of Chron C23N is conventionally placed below this level. Thus it seems unlikely that normal polarity sites AK67 and AK68 included in AK-a are part of Chron C23N.

Nannoplankton zone NP11 has been identified in the lower part of the documented section, and the FAD of Dracodinium varielongituda is at +2.75m. Chron C24AN is normally associated with this interval and its absence at Aalbaekhoved requires an explanation.

A possible reason is that a significant hiatus is present in the section somewhere between +2.75m and +9.6m. Normally such a feature would be marked by the development of a glauconite horizon and a noticeable break in the bio-stratigraphic record, neither of which have been reported.

A second possible explanation is related to the very low accumulation rate, and hence the preservation potential

of the DRM after deposition. Sedimentation rates for the Rosnaes Clay Formation at Aalbaekhoved are of the order of 10m/m.y. It is thought very likely that Chron C24AN (which according to Berggren et al, 1985, is 0.23 m.y. in duration) has been overprinted by a PDRM from Chron C23R (0.44 m.y.). However, with such an explanation one must then question the validity of magnetozone AK-a (correlated with Chron C23N) in the same section.

10.8 Conclusion and suggestions for further work

Results from the first detailed palaeomagnetic study of five classic Danish Palaeogene localities have been presented. The succession from the Holmehus Formation up to the base of the Lillebaelt Clay Formation spans Chrons C25R up to C22R.

Chron C24AN was not identified in the lower part of the Rosnaes Clay Formation section at Aalbaekhoved, where it might have been expected (based on data from unpublished nannoplankton and dinoflagellate studies). Its absence is attributed to the NRM of the sediments at these levels being a much delayed PDRM; that is sediment was deposited during Chron C24AN but the NRM was acquired during Chron C23R.

The well-developed lithostratigraphy and dinoflagellate biostratigraphy (Heilmann-Clausen et al, 1985) affords great potential for future palaeomagnetic work on other Palaeogene sections in Denmark. The application of Steurbaut's (1988) refined nannoplankton zonation scheme to the Rosnaes Clay and Lillebaelt Clay formations would enhance work even further.

One serious drawback with the exposed sections is the possibility of magnetic overprinting as a result of the deformation of the sediments during the last glaciation. Consequently, because of these problems the superb exposures of the Rosnaes Clay Formation at Knuden and Olst are of no use to magnetostratigraphic studies. The same problem may be encountered at other localities where unlithified sediments have been intensely folded.

Further work on the Rosnaes Clay Formation would require a very close sampling interval. The Formation is typically 3m to 6m thick and spans c. 4.m.y (Chrons C24BR to C22R). A site interval of 5-10cm would be the only way to produce a high resolution magnetostratigraphy, and continuous sampling should be considered. Detailed stepwise AF demagnetisation (5mT steps) would be needed, because of the low coecivity NRM, up to at least 30-40mT. The use of borehole sections, which can be easily sampled (and resampled), and which are unaffected by near surface deformation could prove particularly useful.

Chapter 11 Summary, future work and conclusions

11.1 The correlation

The magnetic polarity history for each of the "basins" has been presented in Chapters 5-10. The detailed correlation of levels within the various formations is presented in this Chapter. The magneto- biostratigraphic time-scale is taken from Berggren *et al* (1985). For discussion purposes the time-scale is split into three portions spanning the intervals 62-58Ma, 58-55Ma and 55-51Ma.

11.1.1 The period 62 to 58Ma

This part of the time-scale, and the proposed correlation is presented in Fig 11.1. The interval of time spans the middle part of Chron C26R up to the middle part of Chron C24BR, and the younger limit is slightly older than the Palaeocene/Eocene boundary (57.8Ma). The oldest sediments that have been investigated are from the Hales and Ormesby boreholes in Norfolk, where the bases of the two sections are correlated with Chron C26R, and represent the oldest onshore Cenozoic sediments known in the southern UK. The base of the Thanet Formation (and Thanetian Stage) stratotype in Kent is younger, and correlates with part of Chron C26N. The first Palaeogene transgression across southern England is estimated to have reached Kent about 0.5 m.y. after sedimentation in Norfolk began.

The upper part of the Holmehus Formation in Denmark is reverse polarity, and these levels are correlated with Chron C25R. It is highly probable that the lower part of this formation contains a record of C26N as it has a similar biostratigraphic range to the Thanet Formation in England.

The Woolwich and Reading Formations in England and the Olst and Fur Formations of Denmark are all correlated with the lower part of Chron C24BR. A major break in sedimentation separates these formations from the underlying units. Knox *et al* (1981) using dinoflagellates identify a similar hiatus separating the Lista and Sele Formations in the

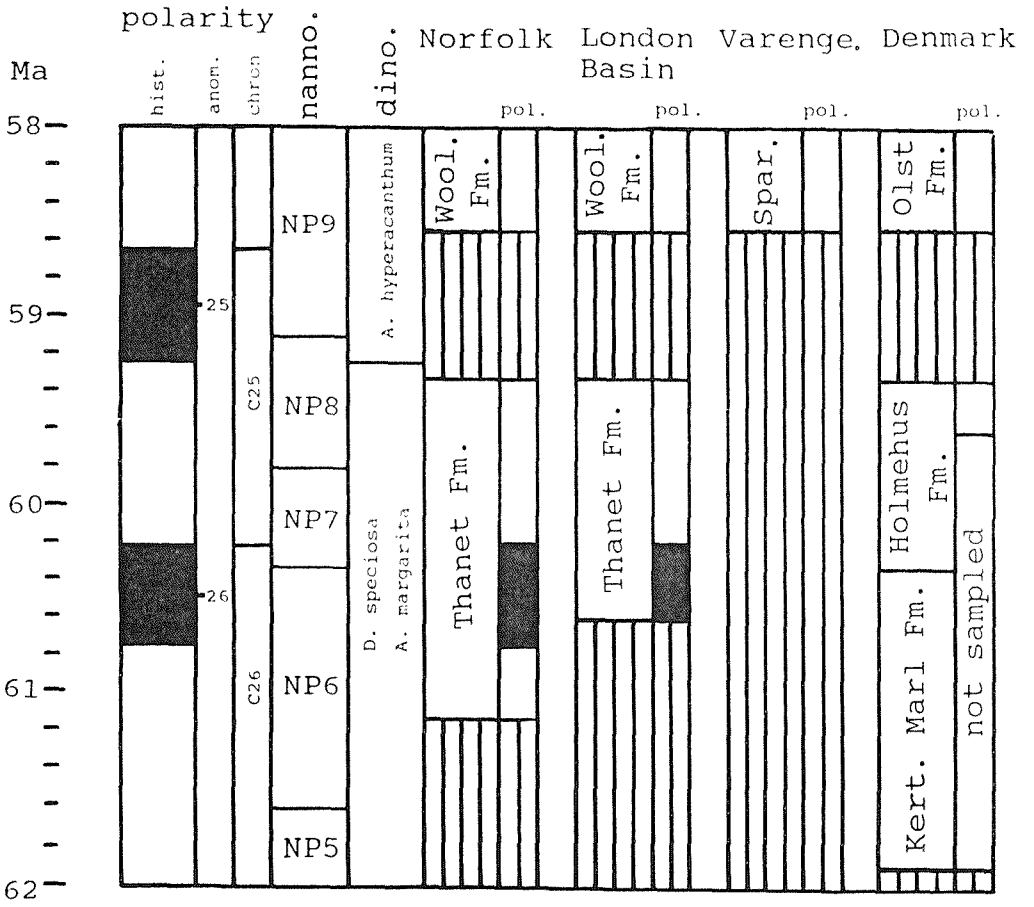

Fig 11.1 Magnetostratigraphic correlations for the period 62 to 58Ma.

North Sea sequences. This hiatus must represent at least 0.6 m.y., the duration of Chron C25N, which is absent from the English and Danish Palaeogene successions.

Thanetian age deposits are known from the Paris Basin, but these have not been investigated. At Varengeville the Sparnacian, which rests directly on the Upper Cretaceous chalk, is reverse polarity and is correlated with Chron C24BR.

11.1.2 The period 58 to 55Ma

This portion of the time-scale is presented in Fig 11.2. This interval extends from the middle part of Chron C24BR to the middle part of Chron C23R. The Palaeocene-Eocene boundary in the North Sea Basin is conventionally defined by the FAD of the dinoflagellate Wetzeliella astra (Costa et al, 1978). In Chapter 7 it is demonstrated that this datum is in part diachronous across southern England. The apparent diachroneity may either be a result of strong facies control towards the basin margin, or it could be that there are taxonomic problems in distinguishing the species from other members of the same genus. The validity of the W. astra zone needs to be reinvestigated, preferably using the palaeomagnetic specimens analysed by Townsend (1982) and in the present study. Normal polarity sites (spanning about 1m) in both the Tilehust Member and the London Clay Basement Bed (and the equivalent unit in the lower part of the Formation de Varengeville) are thought to be records of a single magnetic "event" within Chron C24BR. As they are all located within, or very close to, the W. astra zone they may be of use in helping to define the Palaeocene/Eocene boundary in southern England.

The start of Chron C24BN correlates with the base of Division B in the Hampshire and London Basins. It is not possible to determine the period separating Divisions A and B, but it is thought to be comparatively short. The end of Chron C24BN is represented within division B2 in both basins.

Chron C24A is best recorded in the Sheppey section in

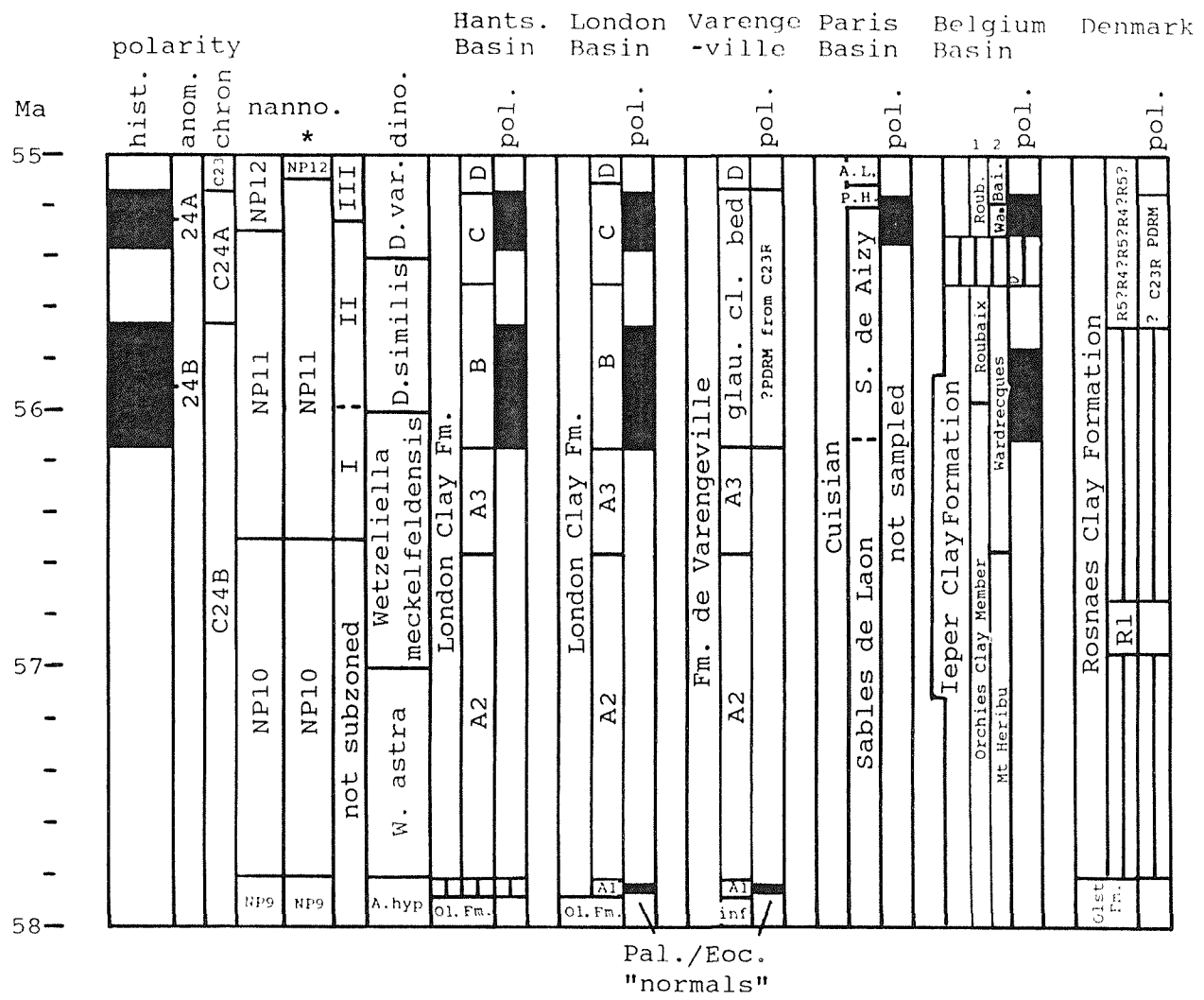

Fig 11.2 Magnetostratigraphic correlations for the period 58 to 55Ma.

*= revised position of the NP11/12 nannoplankton zone boundary.
1= Steurbaut and Nolf (1986)
2= King (in press), Palaeocene-Eocene junction at 57.8 Ma.

the eastern part of the London Basin, where it commences above the base of Division C and terminates about 8m below the base of Division D. In the Hampshire Basin the record of this magnetic chron is rather poor. It probably begins at about 5m above the base of Division C and terminates in the lower part of Division D. This implies that the base of Division D in the Hampshire Basin is older than the same horizon in the London Basin. However the results from these levels in the Whitecliff Bay section should be treated with some caution.

In the Belgium Basin, Chron C24BN is recorded in the lower part of King's (in press) Wardrecques Member. Chron C24AN is represented in the upper part of the Wardrecques Member, above King's (in press) I5 event, and continues into the lower half of the Bailluel Member. (This chron is represented in the upper part of Steurbaut and Nolf's Roubaix Clay Member.)

The end of Chron C24AN is represented just below the base of the NP12 nannoplankton zone in the Belgium Basin sections. Conventionally the base of NP12 is correlated with the late part of Chron C24AN. Two explanations are possible. The first is that the resolution of the magneto- and biostratigraphic record within this interval in the pelagic sequences on which the correlation is chiefly based is not high enough, and the relative positions of these two markers has been incorrectly fixed. Alternatively, the base of this biozone is diachronous coming from the open seas of the proto-Atlantic to the restricted seas of the North Sea Basin. The correlation of this magnetic chron and biozone should be tested in the Warden Point section on Sheppey, where the end of Chron C24AN has been identified, but which has not yet been studied for nannofossils. If a similar result is obtained there, then a reexamination of material from suitable DSDP sites in the NE Atlantic is recommended.

The upper part of the Cuisian (Sables de Aizy) in the Paris Basin contains a record of Chron C24AN. The results from the Argile de Laon, above this unit, are very poor and it is not possible to define the end of this chron.

At Varengeville there is a "massive" condensation of time in the 1m thick glauconite clay bed in the upper part of the Formation de Varengeville. The sediments above this level are reverse polarity and, as they are assigned to the Dracodinium varielongituda dinoflagelate zone, are correlated with Chron C23R. The reverse polarity magnetisation of sediments within the glauconite clay unit is thought to be a much delayed PDRM from Chron C23R. However, it may be possible to identify the upper part of the Wetzeliella meckelfeldensis and the base and top of the Dracodinium similis dinoflagellate zones in this condensed unit.

The results from the Danish Early Eocene are based on the Rosnaes Clay Formation section at Aalbaekhoved. Although the sequence there is locally expanded, it is still very condensed when compared with the equivalent successions in England and Belgium. There does not appear to be a record of the top of the W. meckelfeldensis and D. similis zones in the Rosnaes Clay Formation at the areas in Denmark where it is has been studied (e.g the Store Baelt borehole, 83101, studied by Nielsen et al, 1986). This must represent a condensed time interval equivalent in part to the glauconite clay bed at Varengeville. A record of Chron C24BN is almost certainly missing from the Danish Palaeogene because of the condensation at this level. The upper part of the NP11 and all of the NP12 nannoplankton zones are present at Aalbaekhoved. Chron C24AN is normally associated with the upper part of NP11 and the basal part of the NP12 nannoplankton zones. At Aalbaekhoved this interval is reverse polarity and the absence of a record of Chron C24AN is attributed to a PDRM from Chron C23R, due to the slow sedimentation at this level being unable to trap the older normal polarity DRM.

The D. similis dinoflagellate zone is almost certainly not diachronous across the North Sea Basin. Its apparent absence in the southern and eastern parts of the basin reflects a major condensation of sedimentation at this level in those areas. The evidence is based on the record of Chron C24BN (with which the zone is associated) which is

extremely condensed (or absent due to a PDRM from Chron C23R) at Varengeville and in the Danish Basin. As there is a complete record of Chron C24BN in the Hampshire and London Basins, this suggests that the dominant source of sediments at this time was almost certainly the British Isles to the west of the North Sea Basin.

11.1.3 The period 55 to 51Ma

This portion of the time-scale, and the magnetobiostratigraphic results are presented in Fig 11.3. The start of Chron C23N is very accurately defined in the sections of the Hampshire, London, Belgium and Danish Basins. In the Hampshire Basin this level is 2.6m below the base of the Wittering Formation, whilst in the London Basin it is 3.35m below the top of Division D. In the Belgium Basin it is recorded 1.4m above the base of the Aalbeke Clay Member, and in the exposure at Aalbaekhoved, Denmark, it is at 11.75m above the base of the Rosnaes Clay Formation.

The end of this chron is represented in the Hampshire Basin (in the middle part of Plint's (1983) unit WB6 at Whitecliff Bay). In Belgium it is recorded at, or just above, the base of the Egem Sand Member. In Denmark it has been identified at about 15.5m above the base of the Rosnaes Clay Formation at Aalbaekhoved.

The youngest sediments sampled in this study are from the upper part of the Wittering Formation at Whitecliff Bay. This section was previously studied by Townsend (1982). A reverse polarity magnetisation was found in the bed above the Whitecliff Bay Bed (a 1m thick lignite), similar to the result obtained by Townsend (1982). Aubry et al (1986) correlated the levels above the Whitecliff Bay Bed with Chron C21R, and a similar correlation is proposed from the results of the present study. There is no record of Chron C22N in the Hampshire Basin. This particular chron is associated with the NP13 nannoplankton zone. There are formations in Belgium (Vlierzelle) and Denmark (Lillebaelt Clay) which contain a more complete record of the NP13 nannoplankton zone. These should be investigated in an

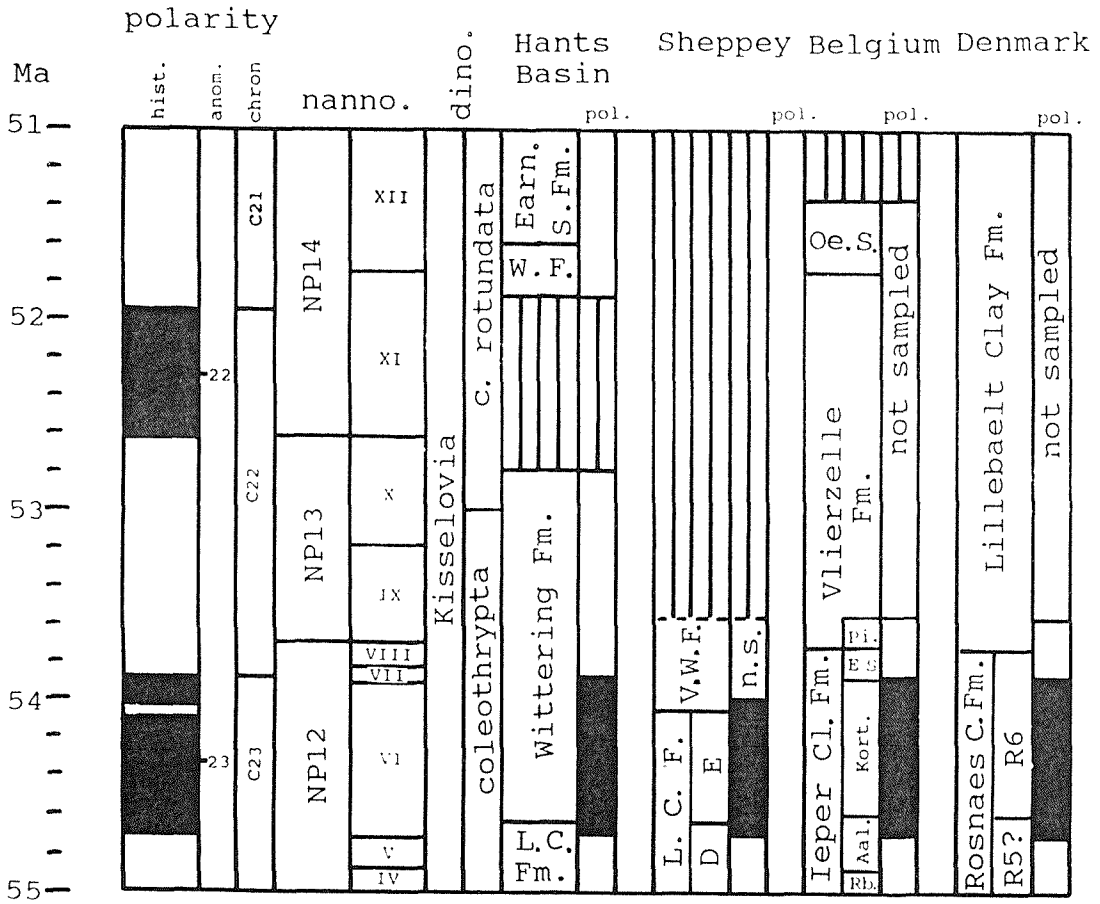

Fig 11.3 Magnetostratigraphic correlations for the period 55 to 51Ma.

Early-Middle Eocene junction at 52.0 Ma. Nannoplankton subzones (IV-XII) are from Steurbaut and Nolf (1986).

attempt to locate Chron C22N.

11.2 Comparison of the North Sea Basin sequences with the global sea-level chart

During the past decade workers at Exxon, in Texas, led by P.R. Vail and J. Hardenbol have developed a global sea-level chart for Late Mesozoic and Cenozoic times. The chart, popularly known as the "Exxon-curve", is a supposed model of eustatic sea-level changes. The "Exxon-curve" has generated a noisy debate, and has been subject to much criticism (e.g Summerhayes, 1986).

Aubry et al (1986) tried to relate hiatuses in the magneto- biostratigraphic record of the English lower Palaeogene to the "Exxon-curve" presented by Vail and Hardenbol (1979). The absence of Chrons C25N and C22N was related to sea-level falls at the base of Cycle TP2.3, and the base of Supercycle Tb respectively.

In the present study it has been shown that a record of Chron C25N is missing from the sequences in England and Denmark. This level coincides with the unconformity separating the Lista and Sele Formations in the southern and central North Sea. The most recent "Exxon-curve" was presented by Haq et al (1987). On this chart (greatly modified in Fig 11.4) a major sea-level fall is proposed at 55Ma (base of Cycle TA2.2), which is slightly younger than the date proposed by these authors for the younger limit of Chron C25N. The present author's interpretation of this "Exxon-curve" suggests that there should be a record of Chron C25N in the NW European sequences, as this corresponds to a sea-level highstand period. In this particular case the "Exxon-curve" does not appear to fit the magneto-biostratigraphic data.

The absence of a record of Chron C22N in the Hampshire Basin sequence may be associated with the major sea-level fall at the base of the Supercycle TA3.

No firm conclusions are drawn from these results. The future of the "Exxon-curve" relies very heavily on the detailed magneto- biostratigraphic studies of many

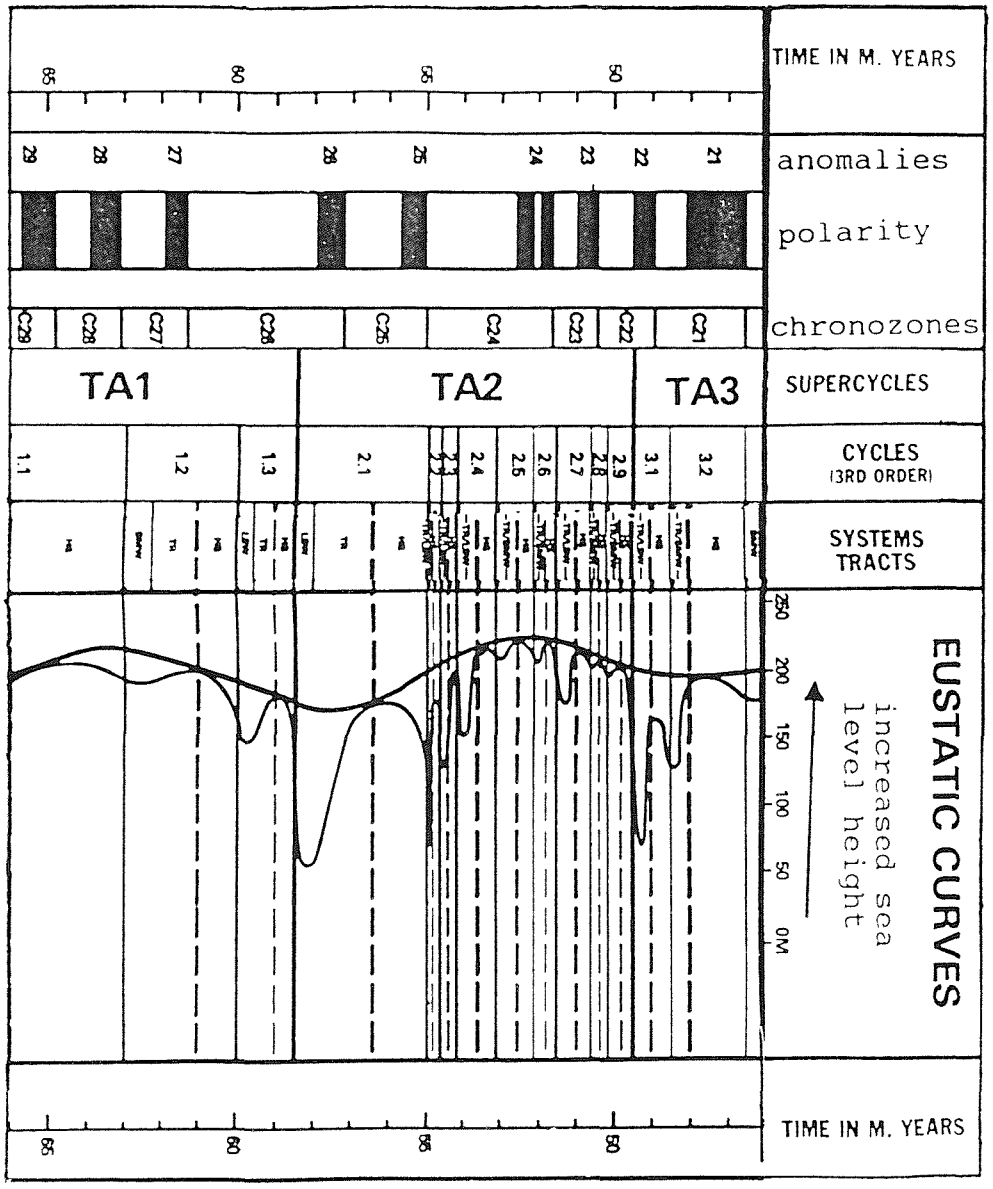

Fig 11.4 The Early Palaeogene part of Haq et al's (1987) global sea level chart.

"packets" of Cenozoic time across the globe.

11.3 Future work outside of the North Sea Basin

The magneto- biostratigraphic work carried out on the Thanetian and Ypresian age deposits of NW Europe provide a particularly good starting point from which to test the "Exxon-curve" as a model for global sea-level fluctuations for the following reasons:

1. The correlation of the North Sea Basin sequences (which include the international stage stratotypes) is now approaching a bed level resolution. This level of stratigraphic definition could be extented to other areas.
2. Steurbaut (1988) has already demonstrated that the refined nannoplankton zonation scheme presented by Steurbaut and Nolf (1986), in their work on the Ypresian in the Belgium Basin can be used to help define a world-wide "event-stratigraphy" for this period.
3. For Late Palaeocene and Early Eocene times, the geomagnetic field reversal frequency was of a similar order of magnitude to the biozone intervals. Therefore, the correlation of a particular magnetozone identified within a sequence to the geomagnetic polarity time-scale is relatively straightforward.
4. King (in press) has been able to extend the King (1981) London Clay Formation divisions to the Ieper Clay Formation. The depositional cycles that King recognises reflect either local subsidence/uplift, or eustatic fluctuations.

The aim of any future work outside of the North Sea Basin area must be to try to identify these cycles, and to see how they fit in with the established magnetobiostratigraphic framework. The most suitable areas to test global sea-level changes are in sequences deposited in a shelf environment. There, any sea level fluctuations should produce a distinct lithological signature in the depositional record. Hopefully, the sequences will also contain enough of the North Sea Basin biostratigraphic "events" to allow a direct and high resolution correlation. These fluctuations can then be put into a geochronological

framework by investigating the magnetostratigraphy.

Two areas would seem to be particularly suited for comparison with the North Sea Basin record and for testing the "Exxon-curve".

11.3.1 Southern Europe

The marine sequences in southwest France and northeast Spain are particularly suitable as they provide a direct link with the NW European and Mediterranean sequences.

The marine sediments in the Aquitaine Basin span more or less the entire Palaeogene (Curry et al, 1978). Sediments from the lower part of the succession have yielded an apparently uninterrupted series of nannoplankton zones from NP9 up to NP14 (Kapellos and Schaub, 1973 and 1975).

The exposures of the Ager Formation at Tremp and Campo in the Tremp Basin, NE Spain, are used to define the Ilerdian Stage. This stage, originally introduced by Hottinger and Schaub (1960), spans the late Palaeocene (NP9) up to the middle of the Early Eocene (NP12). These marine sequences are of the order of 1000m thick, with the potential to allow an extremely high stratigraphic resolution. Calcareous nannoplankton (Kappellos and Schaub, 1973), planktonic foraminifera (Von Hillebrandt, 1965 and 1975; Luterbacher, 1973) and dinoflagellates (Caro, 1973 and Caro et al, 1975) have been studied. Plaziatt (1975 and 1981) has helped place the Ilerdian in context with the Sparnacian and Cuisian/Ypresian Stages in NW Europe.

11.3.2 The Gulf Coast of North America

Late Palaeocene and Early Eocene deposits are present in the southern coastal states of the US and the eastern seaboard of Mexico (Fig 11.5). Work on these sequences has focused on the river-cliff exposures and borehole sections in the states of Georgia, Alabama and Mississippi. The deposits have been investigated in as great a detail as their European equivalents, and a well-defined lithostratigraphic scheme has been erected (e.g. Gibson et al,1982). The sediments have been examined for both calcareous nanno-

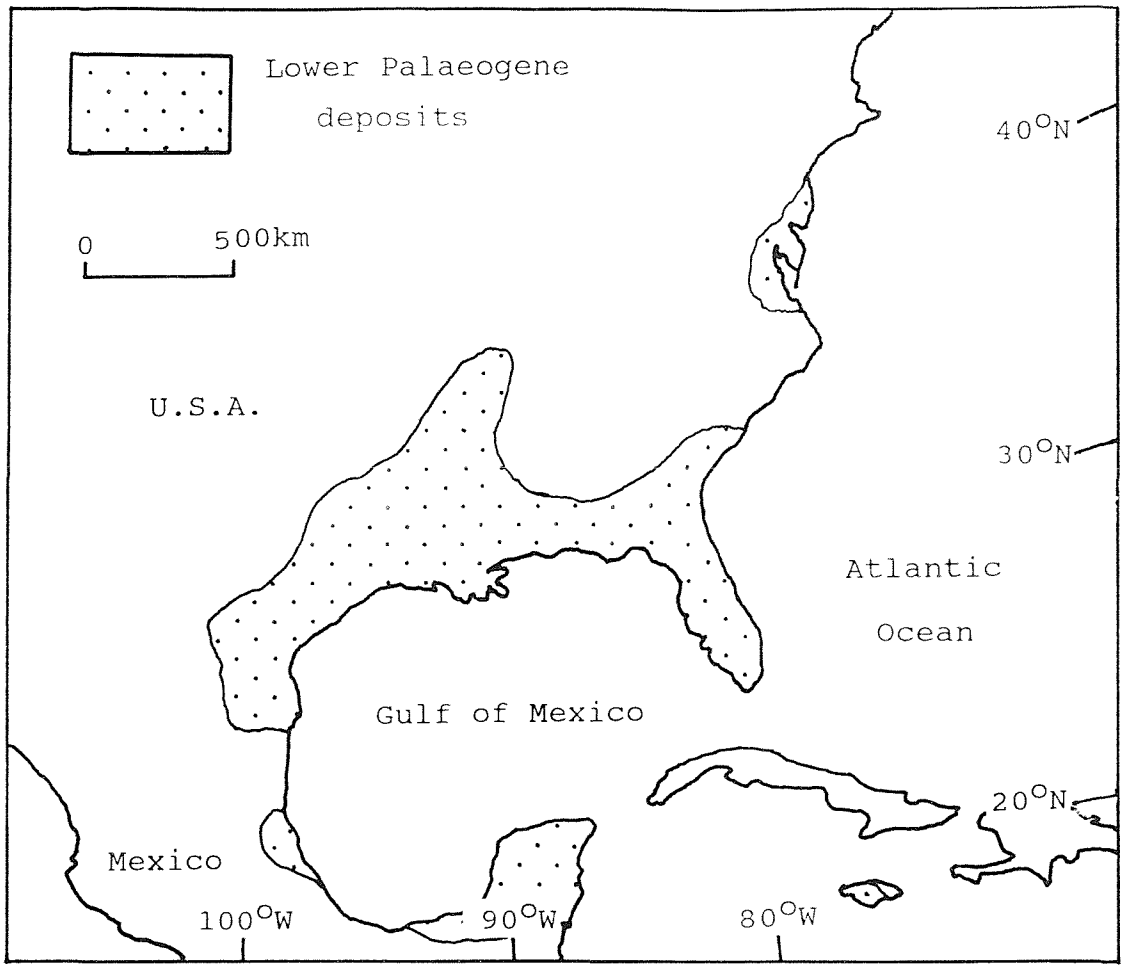

Fig 11.5 The distribution of Lower Palaeogene sediments in the Gulf Coast of North America.

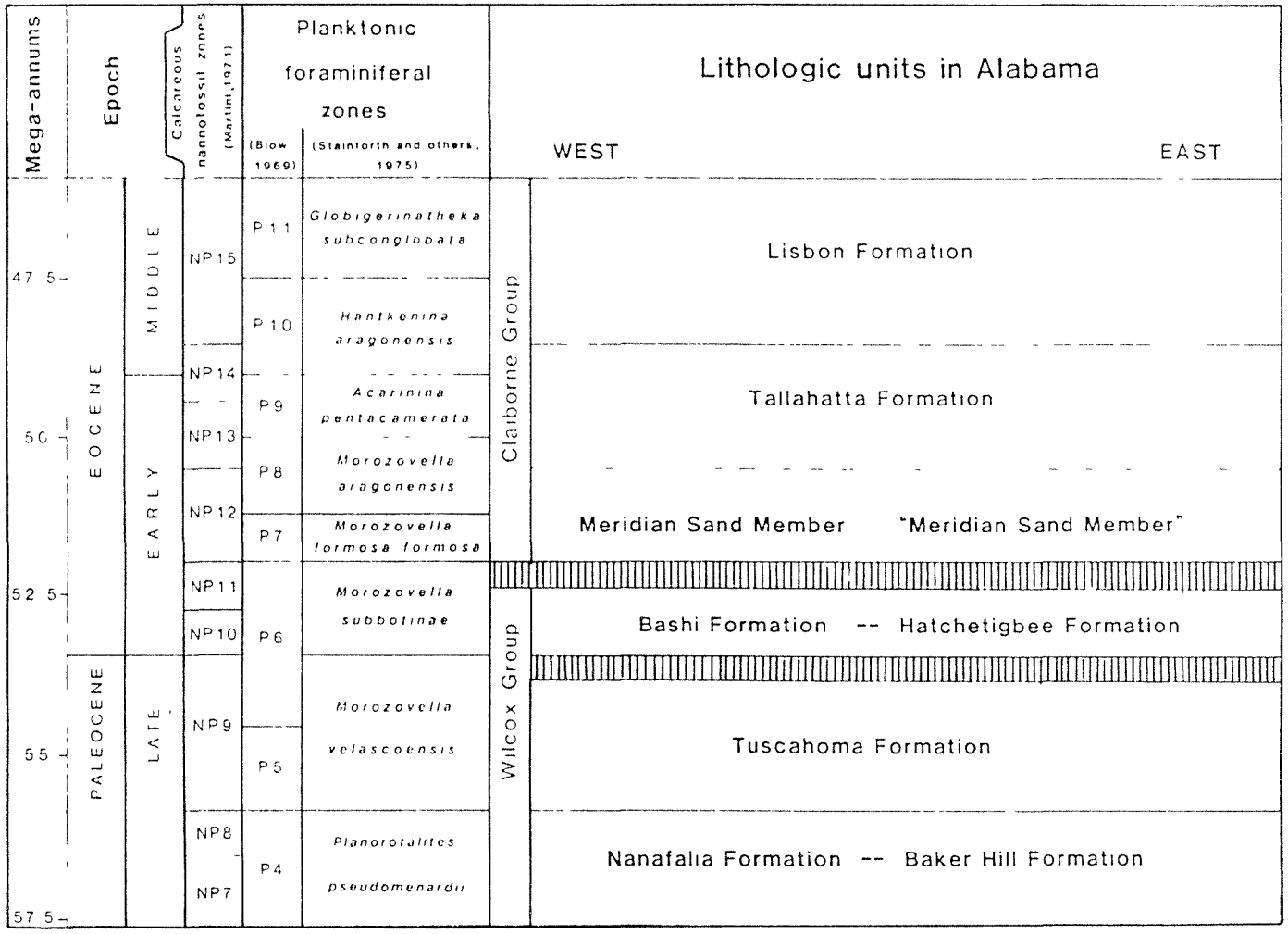

Fig 11.6 The stratigraphy of the late Palaeocene and Early Eocene deposits of Alabama. (from Bybell and Gibson, 1985).

fossils (e.g. Siesser, 1983) and planktonic foraminifers (e.g. Bybell and Gibson, 1985). The Late Palaeocene and Early Eocene stratigraphy of the eastern part of the Gulf Coast is summarised in Fig 11.6.

The formations are slightly more expanded than the Thanetian and Ypresian-age deposits in England and Belgium. Fortunately, there are no major breaks in sedimentation, or levels of marked condensation within the sequences. All of the formations contain lithologies suitable for palaeomagnetic sampling (that is, a significant proportion of fine-grained consolidated material) except for the lower half of the Nanafalia Formation and the Meridian Sand Member in the lower part of the Tallahatta Formation, which both consist predominantly of unlithified coarse-grained sands.

It is believed that the Gulf Coast is the most suitable area in which to define the magnetostratigraphy of the lower Palaeogene outside of the North Sea Basin. Apart from these being shelf-sediments (which are particularly suitable for testing the "Exxon-curve") and the fact that they are lithologically suitable for palaeomagnetic studies, the stratigraphy of these deposits also has been investigated in very fine detail for a considerable period of time. Other important sources of information on these deposits include the publications of Smith et al (1894), Loeblich and Tappan (1957), Toulmin and La Moreaux (1963), Huddlestun et al (1974) and Mancini and Oliver (1981). It is interesting to note that Sir Charles Lyell (one of the leading Tertiary stratigraphers of the last century) twice visited the Gulf Coast area in the 1840's, and published accounts on the deposits in 1846 (Lyell, 1846a and b and 1849).

11.4 Conclusions

This study has demonstrated the potential of magnetostratigraphy for the detailed correlation of sedimentary sequences deposited in a variety of environments across wide geographical areas. The magnetic polarity history of

the Thanetian and Ypresian-age deposits is now well-defined for the Anglo-Belgium Basin. The work on these deposits has enabled a high resolution correlation of the standard biozone boundaries in these deposits with the geomagnetic polarity time-scale. Hopefully the results that have been presented will be of use in helping to refine future generations of the Palaeogene time-scale.

Although further work is required on the sequences in the Paris and Danish Basins, it is believed that the next major advances will be in defining the magnetostratigraphy of similar age deposits in the Gulf Coast of North America. Such a study, when the data are fully integrated with the bio- and lithostratigraphic evidence should form the basis for a very rigorous testing of the "Exxon-curve" as a model for global eustatic sea-level changes.

Appendix

The following pages list the results of specimens collected at each locality. The localities are listed in the order in which they appear in this thesis. The following parameters may be included for each specimen:

1. Spec. No.
2. Depth/height in metres. Site positions are measured relative to lithostratigraphic markers which can easily be identified in the borehole cores or field exposures.
3. Field (F), is the peak applied demagnetising field and is expressed in milli-Tesla (mT).
4. Median Destructive Field is the value at which the specimen's magnetic intensity decreases to 50% of its original value and is also expressed in mT. "NR" is used when the specimen's intensity does not reach the 50% intensity level
5. Reliability index (RI). Each specimen's demagnetisation plot is assigned a RI, which is a guide to the quality of the data. "S" indicates a SEP, "T" indicates a "trending" direction and "E" indicates an "erratic" demagnetisation.
6. Declination/Inclination. For specimens with an RI= S, this direction is the SEP direction. For specimens with an RI= T or E, this is the direction of the remanence after the final demagnetisation step.
7. The Natural Remanent Magnetisation (NRM) is the specimen's magnetic intensity measured before demagnetisation has commenced, and is expressed in mA/m.
8. Volume Susceptibility (VS) is a dimensionless quantity and is expressed as $*10^{-4}$ SI units.
9. The IRM-ratio is a dimensionless quantity. It is the ratio of the IRM at 0.3T/IRM at 0.94T (maximum field available using the "Newport" high-field magnet in the Oceanography Department).
10. The peak IRM is expressed in mAm^2.

"*NM" - is used when a particular parameter was not measured.

HALES Spec. No.	BOREHOLE Depth (m)	F	MDF	RI	DEC	INC	pol.	NRM	IRM-rat.	peak IRM
HL1	12.04	15	7	T	84.1	32.6	N	3.00	.91	1967
HL2	12.50	15	8	S	67.2	64.2	N	1.35	.87	1076
HL3	13.02	20	3	T	294.4	14.1	N	14.06	.96	5324
HL4	13.23	30	15	S	11.8	42.3	N	20.90	.98	10685
HL101	13.33	40	15	T	328.5	-30.5	R	8.81	.98	11524
HL5	13.50	20		T	304.0	-2.2	R	22.51		
HL6	14.15	30		T	256.3	-22.4	R	17.84	.98	8882
HL7	14.50	20		T	49.6	-0.8	R	6.71		
HL8	15.00	30	12	T	335.9	-34.1	R	15.88		
HL102	15.35	40	15	T	328.5	-41.2	N	74.44		
HL9	15.52	30	15	S	346.4	74.5	N	93.90		
HL103	15.57	40	3	T	72.3	-56.5	R	20.58		
HL10	16.05	30	22	T	344.2	2.7	R	29.40		
HL11	16.50	45	23	T	313.0	-14.5	R	17.39		
HL12	17.00	20		T	153.4	-37.3	R	7.78		
HL13	17.57	30	5	T	317.5	1.7	R	1.18		
HL14	18.00	20		T	194.6	-43.2	R	3.93		
HL15	18.50	40	NR	S	26.7	-17.2	R	13.83		
HL16	19.00	20		T	66.2	-25.3	R	6.23		
HL17	19.50	20		T	258.9	-21.0	R	11.30		
HL18	20.02	40	NR	S	86.5	-25.6	R	9.54		
HL19	20.50	20		T	63.7	-13.4	R	5.02		
HL20	21.20	40	NR	S	353.6	-19.1	R	9.33		
HL21	21.50	20		T	202.9	-27.9	R	8.45		
HL22	21.97	40	NR	S	188.2	-29.6	R	8.86		
HL23	22.49	20		T	239.5	-41.3	R	6.71		
HL24	23.02	40	25	S	167.1	-41.9	R	6.82		
HL104	23.58	40	4	T	315.8	1.0	?	5.67		
HL25	23.70	20		T	48.4	30.1	N	7.19		
HL105	23.76	30	8	T	346.1	29.3	N	4.01		
HL26	24.32	50	30	T	55.4	-16.1	R	7.22		
HL27	24.70	20		T	24.8	-24.5	R	8.31		
HL28	25.00	20		T	98.9	-0.9	R	2.52		
HL29	25.50	40	NR	S	4.2	-31.1	R	14.42		
HL30	26.00	20		T	284.6	-26.7	R	11.18		
HL31	26.50	40	NR	S	326.3	-35.3	R	4.93		
HL32	26.83	20		T	282.7	-22.2	R	8.83		
HL33	27.70	40	NR	T	172.2	-29.3	R	9.98		
HL34	28.02	20	7	T	304.7	-32.8	R	1.53		
HL106	28.11	30	15	T	356.1	-31.0	R	2.60		
HL107	28.30	30	4	T	319.5	-26.1	R	1.90		
HL35	28.42	40	6	S	17.3	36.5	N	3.99		
HL36	28.68	30	NR	T	331.7	39.5	N	1.09		
HL108	28.90	30	17	S	339.1	30.4	N	10.78		
HL37	29.37	50	40	S	297.3	-15.4	R	7.30		
HL38	30.04	15	NR	T	49.2	31.1	N	0.45		
HL109	30.25	40	NR	T	328.5	8.0	?	0.27		
HL39	30.58	30	NR	E	342.2	9.0	?	0.68		
HL40	31.00	15	NR	T	286.4	-48.9	R	0.72		
HL41	31.50	30	25	S	278.1	-40.5	R	0.96		
HL42	31.80	20	20	T	270.6	-9.5	R	1.86		
HL43	32.10	20	5	T	213.8	-1.0	R	1.09		
HL44	32.40	15	NR	T	251.8	-37.9	R	4.68		
HL45	32.84	40	23	S	32.6	-52.7	R	4.87		
HL46	33.27	40	NR	S	342.6	-26.3	R	5.16		
HL47	33.88	20		T	145.1	-62.4	R	4.24		
HL48	33.90	40	NR	T	144.4	-62.3	R	3.44		
HL49	34.40	20	NR	T	148.4	-60.5	R	0.90		
HL110	34.62	50		T	206.6	-48.4	R	12.10		
HL50	34.85	30	6	S	105.9	59.6	N	8.03		
HL111	35.02	30	3	T	246.1	-54.3	R	15.79		
HL51	35.25	30	22	T	126.3	-17.9	R	6.97		

Spec. No.	Depth (m)	F	MDF	RI	DEC	INC	pol.	NRM
HL52	35.65	25	4	T	194.8	-12.3	R	5.51
HL53	37.30	20		T	155.7	-42.8	R	2.14
HL54	37.75	40	NR	S	162.5	-52.4	R	3.97
HL55	38.26	20		T	155.4	-33.9	R	8.85
HL56	38.60	40	NR	S	12.1	-31.9	R	11.36
HL57	39.00	20		T	18.4	-48.1	R	6.66
HL58	39.55	40	NR	S	169.7	-50.2	R	12.51
HL59	40.00	20		T	136.9	-55.3	R	4.15
HL60	40.50	40	NR	S	23.1	-34.6	R	9.89
HL61	41.00	20		T	34.6	-49.2	R	24.68
HL62	41.30	20		T	228.4	-36.1	R	11.22
HL63	41.90	40	NR	S	132.8	-41.0	R	4.69
HL64	42.56	40	20	S	118.3	60.3	N	17.28
HL65	43.05	40	23	S	4.9	49.4	N	28.74
HL115	43.38	40	20	S	291.9	24.7	N	31.80
HL116	43.53	30	NR	T	340.4	41.8	N	24.11
HL112	43.81	40	30	S	202.2	42.0	N	29.61
HL66	44.37	20		T	291.1	39.0	N	30.70
HL67	44.97	40	23	S	154.9	41.5	N	31.30
HL68A	45.50	20		T	98.8	46.5	N	35.50
HL68B	45.50	40	28	S	97.3	41.0	N	33.56
HL69	46.00	20		T	78.4	30.4	N	26.37
HL70	46.50	20		T	133.2	44.5	N	20.78
HL71	47.01	40	28	S	120.1	40.0	N	27.01
HL72	47.62	20		T	200.2	51.5	N	35.36
HL73	48.03	40	40	S	139.7	46.8	N	36.85
HL74	48.42	20		T	267.0	45.6	N	35.51
HL75	49.00	40	8	S	136.0	54.2	N	60.81
HL76	49.45	20		T	272.6	43.8	N	35.75
HL77	49.85	40	30	S	319.0	48.1	N	35.13
HL113	50.19	30	15	T	181.7	48.0	N	10.78
HL78	50.45	40	NR	S	320.9	-41.2	R	13.76
HL79	51.07	20		T	277.3	-31.9	R	10.69
HL80	51.50	20		T	267.4	-50.4	R	9.18
HL81	52.00	40	NR	T	342.7	-38.0	R	10.04
HL82	52.47	20		T	332.8	-38.8	R	26.03
HL83	53.00	20		T	321.8	-35.8	R	25.04
HL84	53.54	40		S	217.8	-53.1	R	14.99
HL85	54.10	40	39	S	318.9	-51.1	R	17.66
HL117	54.19	30	10	S	304.4	-47.6	R	66.55
HL118	54.39	30	18	S	300.6	-49.1	R	54.39
HL119	54.55	30	NR	T	122.3	63.3	N	7.83
HL86	55.03	20		T	75.6	-43.5	R	20.33
HL87	55.51	20		T	0.8	-37.9	R	21.62
HL88	55.95	40	NR	S	306.0	-34.4	R	18.92
HL89	56.60	20		T	294.1	-54.5	R	20.81
HL90	57.13	40	5	S	13.4	-69.9	R	16.18
HL91	57.54	15	4	T	296.5	64.5	N	7.57
HL114	57.56	30	30	S	15.0	-43.3	R	12.76

Junctions: base Thanet Fm.= 57.58m; base "unrecognised unit"= 37.2m; base Woolwich Fm.= 32.4m; base Harwich Member= 16.0m. The top of the Harwich Member is at 12.04m. Specimens with no entry under MDF were "spot demagnetised" and the intensity decreased to <50% of the NRM. The MDF value for these specimens is an inaccurate figure and is not included.

ORMESBY BOREHOLE

Spec. No.	Depth (m)	F mT	MDF mT	RI	DEC	INC	pol	NRM	IRM-rat.	peak IRM
OR110	70.67	35	NR	E	269.8	20.0	?	0.08		
OR111	71.00	35	NR	S	348.4	-67.1	R	0.53		
OR112	71.00	35	12	T	234.0	-55.7	R	0.69		
OR113	71.55	35	4	T	161.6	-46.4	R	0.36		
OR114	71.84	30	7	S	187.1	-54.2	R	0.30		
OR101	71.98	30	20	T	12.8	-30.9	R	0.55	.78	671
OR115	72.10	35	30	S	38.5	-21.2	R	0.45		
OR102	72.35	30	5	T	129.9	-61.6	R	0.64	.83	464
OR116	72.59	30	10	T	291.2	23.9	N	0.20	.76	872
OR117	72.70	35	NR	S	172.3	-25.9	R	0.21		
OR118	73.05	35	NR	T	290.6	-49.6	R	0.32		
OR119	73.46	35	22	S	218.6	-38.5	R	0.55		
OR103	78.95	40	7	S	248.1	69.0	N	17.79	.97	9594
OR104	79.62	40	12	T	166.2	30.8	N	32.52	.98	11595
OR105	83.32	40	35	S	167.3	-47.8	R	20.75		
OR106	83.56	40	12	T	26.9	-73.0	R	11.99		
OR107	107.32	40	NR	S	105.4	36.4	N	16.39		
OR108	120.16	40	17	S	213.8	-52.7	R	26.13		
OR109	120.5	40	13	S	50.1	-54.5	R	21.76		

A list of the Ormesby specimen data used in the work presented by Cox et al (1985) is provided by Johnston (1983). The data listed above represent those specimens processed by the present author.

PEGWELL BAY (Cliff End section)

Spec. No.	ht. (m)	F (mT)	MDF (mT)	RI	DEC	INC	pol.	NRM
PB101.1	0.61	35	4	S	336.7	48.0	N	12.64
PB101.2	0.61	35	8	T	212.9	84.0	N	8.83
PB102.1	1.19	35	20	S	331.2	49.7	N	9.28
PB102.2	1.19	35	4	S	332.9	50.5	N	5.46
PB103.1	3.92	35	5	E	118.0	38.0	?	5.49
PB103.2	3.92	35	4	T	185.3	-26.4	R	5.90
PB104.1	5.99	35	5	T	205.2	61.3	N	3.71
PB104.2	5.99	35	4	E	287.4	-22.3	?	4.82
PB105.1	7.27	35	6	T	121.3	32.9	N	7.48
PB105.2	7.27	35	5	T	327.2	31.0	N	2.92

Specimens PB104.1 and PB105.1 both showed good "trends" toward a normal polarity.

(Hoverport section)

Spec. No.	ht. (m)	F (mT)	MDF (mT)	RI	DEC	INC	pol.	NRM
PB111.1	1.45	35	4	T	188.3	-24.6	R	1.49
PB111.2	1.45	35	6	T	282.2	27.0	?	0.48
PB111.3	1.45	35	7	T	324.5	-10.8	R	0.51
PB106.1	2.35	35	5	T	67.8	62.7	N	2.62
PB106.2	2.35	35	5	E	87.9	27.1	N	2.42
PB107.1	3.02	35	5	T	112.0	-14.7	R	2.06
PB107.2	3.02	35	5	E	22.6	-3.4	?	3.32
PB108.1	3.56	35	6	T	112.3	23.9	R	0.66
PB108.2	3.56	35	3	T	248.3	74.6	N	3.26
PB109.1	3.97	35	8	T	57.0	-47.5	R	0.83
PB109.2	3.97	35	NR	E	39.7	-31.7	?	0.16
PB112.1	4.22	35	20	T	170.7	48.6	R	0.19
PB112.2	4.22	35	5	E	26.2	-27.0	?	1.85
PB110.1	4.68	35	4	T	14.5	41.0	N	3.70
PB110.2	4.68	35	NR	T	96.9	2.6	?	3.12
PB113.1	4.84	35	5	T	340.3	59.0	N	2.02

Spec. No.	ht. (m)	F (mT)	MDF (mT)	RI	DEC	INC	pol.	NRM
PB113.2	4.84	35	2	T	232.4	-28.6	R	0.12
PB114.1	5.55	35	4	T	86.3	-41.1	R	0.73
PB114.2	5.55	35	5	T	328.0	63.7	N	2.20

The sites in both Pegwell Bay sections are positioned relative to the lithological units defined i the paper by Siesser et al (1987).

LEVINGTON

Spec. No.	ht (m)	F mT	MDF mT	RI	DEC	INC	pol.	NRM	IRM-rat.	peak IRM
LV11.1	8.15	20	4	T	25.5	11.4	N	2.10		
LV11.2	8.15	15	15	T	13.7	57.9	N	2.11	.74	1427
LV10.1	7.35	30	10	S	14.8	64.0	N	3.86		
LV10.2	7.35	30	15	T	15.8	43.8	N	4.06		
LV9.1	6.65	20	9	T	354.9	54.7	N	43.54		
LV9.2	6.65	20	9	S	23.8	59.9	N	2.57		
LV7.1	4.65	30	9	T	305.2	56.8	N	3.09		
LV7.2	4.65	15	10	T	351.8	71.4	N	0.95		
LV6.1	3.85	30	22	S	353.1	72.2	N	5.29		
LV6.2	3.85	30	17	S	350.5	56.9	N	4.13		
LV5.1	2.85	10	2	T	195.2	55.1	?	2.17		
LV5.2	2.85	20	7	S	359.5	62.3	N	12.39	.87	3512
LV4.1	1.80	20	4	S	15.5	69.5	N	3.56		
LV12.1	1.15	40	NR	T	220.5	-50.1	R	66.48		
LV12.4	1.15	40	NR	T	193.7	-53.5	R	189.40		
LV12.5	1.15	50	33	T	213.5	-44.7	R	330.90		
LV3.3	0.82	25	6	S	349.1	69.2	N	41.31		
LV2.1	0.40	25	16	T	57.3	54.3	N	29.30		
LV2.2	0.40	25	9	S	334.5	57.6	N	30.16	.97	12502
LV1.1	0.00	30	8	S	329.2	63.8	N	136.60		
LV1.2	0.00	30	15	T	345.7	23.3	N	149.00		

Site LV12 is in the Harwich Stone Band. Specimens from site LV8 were not processed.

WALTON-ON-THE-NAZE

Spec. No.	ht. (m)	F mT	MDF mT	RI	DEC	INC	pol	NRM	IRM rat.	peak IRM
WN17.2	12.3	30	NR	T	242.2	-3.4	R	0.30		
WN16.1	11.2	30	NR	T	184.3	-30.8	R	0.07		
WN16.2	11.2	30	NR	T	265.3	-7.7	R	0.31	.73	1311
WN15.1	10.4	30	NR	T	201.0	-12.1	R	0.21		
WN15.2	10.4	30	NR	T	265.8	-16.1	R	0.11		
WN14.1	9.3	30	25	T	194.3	-2.6	R	0.26		
WN14.2	9.3	20	20	T	184.0	19.3	R	0.23		
WN13.1	8.4	20	NR	E	273.0	63.5	?	0.15		
WN13.2	8.4	30	NR	T	108.5	-24.6	R	0.22		
WN12.1	7.5	30	NR	T	254.6	2.6	R	0.23		
WN12.2	7.5	30	NR	T	215.5	32.0	R	0.22		
WN11.1	6.7	40	30	S	221.7	54.4	?	0.69		
WN11.2	6.7	30	30	T	7.1	34.2	N	0.31		
WN10.1	5.4	10	NR	T	156.0	-27.5	R	0.38	.77	1132
WN10.2	5.4	20	15	T	281.3	50.1	N	0.58		
WN9.1	4.9	50	25	T	233.2	25.4	R	1.27		
WN9.2	4.9	50	45	T	334.1	72.9	N	0.87		
WN8.1	4.5	50	45	E	288.8	16.8	?	0.99		
WN7.1	4.05	60	30	T	227.9	14.4	R	2.14		
WN7.2	4.05	50	45	T	241.2	3.0	R	1.00		
WN6.1	3.9	40	10	T	228.4	28.2	R	5.25	85	3437
WN6.2	3.9	40	15	T	320.3	69.0	N	4.18		
WN5.1	3.4	50	20	T	249.7	19.5	R	6.44		
WN5.2	3.4	40	20	E	181.7	71.8	?	17.44		

Spec. No.	ht. (m)	F mT	MDF mT	RI	DEC	INC	pol	NRM	IRM rat.	peak IRM
WN4.1	2.75	50	20	T	208.3	37.1	R	7.92	.94	8446
WN4.2	2.75	50	8	T	196.6	-8.0	R	9.32		
WN3.1	2.2	50	15	T	197.0	-6.5	R	10.95		
WN3.2	2.2	50	20	T	195.6	-25.0	R	6.39		
WN2.1	1.0	30	10	T	121.5	-37.6	R	9.51		
WN2.2	1.0	40	8	S	190.8	-37.0	R	16.55		
WN1.1	0.0	50	13	T	203.1	1.0	R	15.13	.96	1320

Junction: Harwich/Walton Member juction at 4.0m.

WRABNESS

Spec. no.	Depth (m)	pol.	NRM	VS	IRM-ratio	peak IRM
WR2.4	0.00	R	1.14	1.97	.83	682
WR2.3	0.00	R	0.86	2.33		
WR2.2	1.05	R	1.31	1.93	.74	1201
WR2.1	1.05	R	1.46	1.96		
WR1.2	1.88	N	1.82	2.24	.70	1167
WR1.1	1.88	N	1.62	2.12		
WR1.4	3.35	N	9.48	3.29		
WR1.3	3.35	N	8.57	3.42	.81	4264
WR1.6	4.40	N	2.17	1.77		
WR1.5	4.40	N	1.29	1.93		
WR1.8	5.59	N	1.10	1.88	.71	1214
WR1.7	5.59	N	1.15	2.10		
WR1.12	7.04	N	0.69	2.42		
WR1.11	7.04	N	1.47	2.47		
WR1.10	7.79	N	2.70	2.93		
WR1.9	7.79	N	1.39	2.28		
WR1.14	8.22	N	2.41	2.42	.76	1951
WR1.13	8.22	N	2.56	2.48		
WR1.15	9.12	R	1.42	2.08		
WR1.18	9.59	R	16.45	10.07		
WR1.17	9.59	R	15.14	7.26		
WR1.20	10.39	R	29.27	8.99		
WR1.19	10.39	R	26.43	11.20	.95	14749
WR1.22	10.87	R	1.64	3.56		
WR1.21	10.87	R	1.65	3.22		
WR3.1/7	11.27	R	c.600	*NM		
WR1.24	11.68	R	25.56	8.05		
WR1.23	11.68	R	30.96	10.30	.95	20920

Harwich/Walton Member junction at 1.5m BD

SHELFORD

Spec. No.	ht. (m)	F (mT)	MDF (mT)	RI	DEC	INC	pol	NRM	IRM-rat.	peak IRM
SQ1.1	0.0	30	NR	T	175.2	-57.0	R	0.20		
SQ1.2	0.0	30	NR	T	175.7	-38.0	R	0.16	.89	271
SQ1A.1	0.2	20	20	E	223.8	30.0	?	0.30		
SQ2.1	0.4	40	15	E	289.6	3.2	?	1.12		
SQ2.2	0.4	30	13	E	9.2	-7.2	?	0.51		
SQ3.2	2.7	30	NR	T	197.3	-8.2	R	0.84	.70	648
SQ4.1	3.5	40	NR	T	227.9	-14.5	R	0.59		
SQ4.2	3.5	40	35	S	235.3	30.6	?	0.48	.77	538
SQ5.1	5.2	60	3	T	278.3	66.6	N	2.12		
SQ5.2	5.2	60	20	T	305.2	47.8	N	1.80	.78	1840
SQ6.1	5.7	20	15	T	356.8	55.0	N	0.75		
SQ6.2	5.7	40	17	E	262.9	17.1	?	0.69		
SQ7.1	6.4	10	3	T	192.4	-57.7	R	0.41		
SQ7.2	6.4	30	NR	T	196.9	-14.5	R	0.22		
SQ8.1	7.35	10	7	E	150.8	14.5	R	0.37		
SQ8.2	7.35	10	NR	E	223.5	19.7	?	0.16	.83	284

Spec. No.	ht. (m)	F (mT)	MDF (mT)	RI	DEC	INC	pol	NRM
SQ9.1	8.40	30	NR	T	138.0	-65.5	R	0.31
SQ9.2	8.65	30	NR	T	148.2	-16.5	R	0.22
SQ10.1	9.25	15	8	T	150.0	-41.1	R	0.27
SQ10.2	9.25	40	NR	T	166.4	-1.6	R	0.20
SQ11.1	9.7	20	NR	T	125.7	-57.4	R	0.18
SQ11.2	9.7	10	5	T	143.9	-37.2	R	0.27
SQ12.1	10.35	30	NR	T	180.2	-50.3	R	0.38
SQ12.2	10.35	40	8	T	129.3	-44.2	R	0.59
SQ13.1	10.9	40	NR	T	103.3	-2.8	R	0.34
SQ13.2	10.9	10	2	T	176.6	-9.7	R	0.59
SQ14.1	11.65	10	3	T	88.6	-26.4	R	0.32
SQ14.2	11.65	10	3	T	188.6	-16.4	R	0.55
SQ15.1	12.3	15	3	T	50.5	-16.2	E	0.32

Junctions: Old. Fm./A1= 5.1m; A1/A2= 5.9m.

HERNE BAY

Spec.	Depth (m)	pol.	NRM	VS	IRM ratio	peak IRM
HB4.20	0.00	R	1.02	2.46	.79	789
HB4.17	1.50	R	0.80	2.46		
HB4.15	2.40	R	0.74	2.19	.76	700
HB4.13	3.60	R	1.08	2.03		
HB4.11	4.90	R	1.10	1.92	.74	881
HB4.9	6.30	R	0.87	2.06		
HB4.8	6.60	R	0.88	1.88		
HB4.5	7.40	R	1.12	1.86	.72	980
HB4.3	7.72	R	1.26	2.15		
HB4.2	7.85	R	1.07	3.40	.44	1039
HB3.25	8.35	N	9.75	3.78	.94	6159
HB3.23	9.04	N	4.52	2.35		
HB3.22	10.01	N	7.45	2.52		
HB3.19	10.61	N	15.91	10.30	.95	12441
HB3.17	11.35	N	18.68	9.44		
HB3.16	12.20	N	33.80	10.00	.96	10891
HB3.12	13.30	N	19.55	11.76		
HB3.10	13.75	N	18.89	7.80		
HB3.8	14.07	R	5.47	2.52	.86	3033
HB3.3	14.37	R	2.16	2.13		
HB3.2	14.60	R	2.55	2.39	.87	2409

Old./London Clay Fm. junction at 8.25m BD.

TILEHURST

Spec. No.	ht. (m)	F (mT)	MDF (mT)	RI	DEC	INC	pol	NRM	IRM rat	peak IRM
TH12.1	4.45	30	3	S	335.2	55.6	N	5.31	.75	1049
TH12.2	4.45	40	6	T	350.7	8.3	N	3.34		
TH11.1	4.00	40	2	E	282.8	17.6	?	1.65	.80	549
TH11.2	4.00	50	2	E	356.9	53.0	N	4.01		
TH10.1	3.50	50	6	E	112.3	72.7	?	4.55		
TH10.2	3.50	40	4	T	223.3	9.8	R	5.41	.76	890
TH9.1	2.68	30	4	T	228.7	39.1	R	8.23		
TH9.2	2.68	40	6	T	231.6	46.9	R	4.88		
TH8.1	2.32	40	3	T	24.8	33.8	N	3.54		
TH8.2	2.32	50	3	T	293.2	46.6	N	5.20		
TH7.1	1.86	50	5	T	259.7	14.9	R	7.40		
TH7.2	1.86	40	4	T	237.3	1.0	R	8.36	.82	1565
TH6.1	1.63	30	5	S	41.1	49.6	N	5.55		
TH6.2	1.63	40	3	S	2.7	48.5	N	3.22		
TH5.1	1.28	50	3	T	346.0	-77.6	?	3.61		
TH5.2	1.28	30	3	T	343.0	72.6	N	6.55		
TH4.1	0.81	30	NR	T	140.4	-12.4	R	0.53		

Spec. No.	ht. (m)	F (mT)	MDF (mT)	RI	DEC	INC	pol	NRM	IRM rat	peak IRM
TH4.2	0.81	20	3	T	157.7	9.4	R	2.04		
TH3.1	0.74	30	3	T	203.9	36.9	?	6.74		
TH3.2	0.74	30	3	T	357.9	51.1	N	10.55		
TH2.1	0.34	40	3	S	171.6	-52.3	R	7.57		
TH2.2	0.34	25	5	T	128.8	-57.3	R	38.94	.90	2396
TH1.1	-0.10	30	4	T	99.6	-12.4	R	1.40		
TH1.2	-0.10	50	3	T	202.0	57.0	?	1.85		

Junctions: Reading Fm./Tilehurst Mbr.=0.0m
Tilehurst/Walton Member= 4.0m.

HARTY BOREHOLE

Spec. No.	Depth (m)	F mT	RI	DEC	INC	pol.	NRM	VS	IRM rat.	peak IRM
IH1	9.5	20	S	285.5	52.1	N	17.86	7.76		
IH2	10.5	20	S	35.9	33.2	N	10.09	5.11	.83	4418
IH3	11.5	20	S	22.4	35.2	N	2.84	4.89		
IH4	12.5	20	T	109.6	43.1	N	15.00	7.11		
IH5	14.0	20	T	5.0	-35.2	R	15.30	10.67		
IH6	15.3	25	T	279.2	57.3	N	9.29	11.55	.95	12097
IH7	16.0	25	S	287.5	31.8	N	48.78	9.51		
IH8	17.0	25	S	157.9	47.1	N	34.30	8.64		
IH9	18.0	25	S	70.5	37.3	N	26.92	9.02		
IH10	19.0	25	S	288.2	30.3	N	31.53	10.15		
IH11	20.0	25	S	36.6	48.2	N	33.69	10.84		
IH12	21.0	20	T	52.1	70.4	N	19.96	10.00	.92	10448
IH13	22.0	25	T	197.5	44.8	N	13.52	9.91		
IH14	23.0	25	T	331.0	35.0	N	16.86	9.93		
IH15	24.0	40	T	62.8	50.4	N	20.25	9.22		
IH16	25.0	25	S	22.7	39.8	N	23.40	8.83		
IH17	27.0	20	S	64.9	35.9	N	34.95	9.81		
IH18	28.0	25	T	26.2	37.1	N	19.52	8.66	.92	8934
IH19	29.0	25	E	251.3	-2.0	?	1.05	5.88		
IH20	30.0	25	T	40.0	-47.5	R	2.11	5.76	.90	6983
IH21	31.0	25	S	307.3	-35.3	R	31.86	7.11		
IH22	32.0	25	T	29.5	-24.3	R	12.75	10.12		
IH23	33.0	35	T	61.5	-53.8	R	8.42	12.91		
IH24	34.0	25	T	118.8	-28.9	R	22.20	11.12		
IH25	34.4	25	E	191.4	2.2	?	10.72	9.20		
IH26	35.5	40	T	257.4	-30.2	R	22.67	10.15		
IH27	36.5	25	S	305.3	43.8	N	60.67	13.24	.95	16119
IH28	37.5	25	T	30.1	-33.9	R	9.42	8.45		
IH29	38.5	20	S	38.5	-29.5	R	6.62	5.15	.92	5986
IH30	39.5	15	T	264.2	-43.2	R	0.78	2.59	.71	1978
IH31	40.5	5	E	153.9	19.4	N	0.36	2.64		
IH32	41.5	10	T	319.8	-41.2	R	0.52	2.26		
IH33	42.5	8	E	162.8	31.2	N	0.33	2.34	.76	613
IH34	43.5	25	T	278.8	-12.7	R	0.47	1.84		
IH35	44.5	10	E	96.7	-34.9	R	0.54	2.48	.74	943
IH36	45.5	20	T	29.4	-14.9	R	0.57	2.11		
IH37	46.5	25	T	55.8	-27.6	R	0.94	2.04	.75	1028
IH38	47.2	5	E	6.7	8.9	?	0.32	2.00		
IH39	48.5	20	E	322.2	-47.5	R	0.27	1.89		
IH40	49.5	8	E	344.2	-21.0	R	0.44	1.91	.86	2673
IH41	50.5	25	E	31.0	-44.5	R	0.74	3.10		
IH42	51.0	25	T	81.4	32.2	N	17.08	19.70	.97	31834
IH43	51.5	20	T	343.0	23.2	N	5.54	3.40	.96	5440

Junctions: Old. Fm./A1= 51.26m; A1/A2= 50.64m;
A2/A3= 38.50m; A3/B= 28.50m

WARDEN BAY BOREHOLE

Spec. No.	Depth (m)	F (mT)	RI	DEC	INC	pol	NRM	VS	IRM rat	peak IRM
WB1	8.0	20	S	303.3	51.5	N	1.78	2.73	.60	2279
WB2	8.9	30	S	212.2	54.0	N	2.63	2.83		
WB3	10.3	30	T	28.1	61.5	N	1.44	2.74	.68	2307
WB4	11.0	30	T	131.4	43.7	N	20.27	9.37		
WB5	12.6	35	T	91.0	38.8	N	26.69	10.50		
WB6	13.45	35	T	78.4	56.7	N	13.94	10.99		
WB7	15.5	35	T	302.9	25.7	N	23.98	10.62	.95	15069
WB8	16.4	40	T	162.1	12.4	N	22.97	11.89		
WB9	17.6	35	T	64.1	35.1	N	55.43	10.76		
WB10	18.5	30	S	28.9	23.3	N	31.52	9.75		
WB11	19.65	30	T	139.3	26.0	N	16.72	12.12		
WB12	20.5	30	T	265.1	36.5	N	21.66	13.24	.94	13816
WB13	21.6	30	E	192.6	5.6	?	11.70	12.64		
WB14	22.65	20	T	348.6	24.9	N	8.12	12.19		
WB15	23.5	35	S	288.7	46.9	N	17.42	10.17		
WB16	24.5	30	S	137.0	38.8	N	23.80	9.28		
WB17	25.5	25	T	69.5	21.7	N	12.20	12.54	.92	14116
WB18	26.5	20	T	0.8	28.8	N	9.85	12.19		
WB19	27.5	50	T	318.9	-13.0	R	10.83	11.85		
WB20	28.5	50	S	224.2	-26.5	R	12.14	9.92		
WB21	29.55	30	T	101.6	23.1	N	23.93	11.00	.93	12976
WB22	30.5	50	S	204.6	31.4	N	34.81	10.46		
WB23	31.5	25	S	109.5	-31.3	R	7.31	12.91		
WB24	32.7	50	T	173.0	-19.0	R	3.00	*NM		
WB25	33.5	40	T	127.9	-11.0	R	6.94	*NM		
WB26	34.5	25	T	286.1	-22.1	R	10.40	10.31		
WB27	35.5	30	S	115.1	-21.6	R	23.94	11.00	.94	11364
WB28	36.5	30	T	77.9	-29.9	R	7.06	11.04		
WB29	38.6	35	T	278.1	-11.0	R	7.45	*NM		
WB30	39.5	50	T	266.9	-1.9	R	9.16	*NM		
WB31	40.55	40	T	141.8	-3.6	R	14.10	8.50		
WB32	41.5	20	T	97.9	49.9	N	62.23	11.23	.94	13061
WB33	42.5	40	T	351.8	32.4	N	16.58	10.30		
WB34	43.5	35	S	215.2	52.6	N	28.54	11.12		
WB35	44.5	30	T	309.2	37.3	N	70.60	9.16		
WB36	45.5	30	S	138.6	29.2	N	28.42	9.16		
WB37	46.5	30	T	273.8	16.6	N	87.42	11.23	.93	11735
WB38	47.5	40	S	291.6	31.5	N	76.03	11.00		
WB39	48.5	40	S	241.0	30.6	N	34.83	10.96		
WB40	49.5	40	S	234.8	32.9	N	38.92	9.28		
WB41	50.5	40	T	251.2	31.7	N	34.64	9.90		
WB42	51.5	40	T	289.7	19.4	N	82.62	9.90	.93	10790
WB43	52.5	40	S	239.4	49.6	N	39.36	8.86		
WB44	53.5	25	T	345.1	35.1	N	14.63	10.77		
WB45	54.6	35	S	308.5	31.8	N	21.53	9.75		
WB46	55.5	30	T	157.3	43.5	N	16.52	10.76		
WB47	56.5	35	T	297.3	35.8	N	59.89	11.19	.94	12166
WB48	57.5	40	T	201.7	33.3	N	29.95	8.42		
WB49	58.3	35	T	295.7	42.5	N	26.18	9.97		

Junction: B/C= 34.0m

WARDEN POINT

Spec. No.	ht. (m)	F mT	RI	DEC	INC	pol	NRM	VS	IRM rat	peak IRM
WP101.1	0.0	50	T	9.9	83.4	N	32.51	11.83	.94	16859
WP101.2	0.0	50	S	7.5	53.3	N	23.38	11.31		
WP102.1	1.0	40	T	347.1	36.3	N	31.38	9.09		
WP102.2	1.0	50	S	3.7	41.7	N	31.18	11.04		
WP103.1	1.2	50	S	288.6	57.7	N	22.55	12.61		
WP103.2	1.2	50	S	15.6	44.4	N	40.80	10.02		
WP104.1	2.6	30	T	13.2	23.6	N	33.51	11.46		

Spec. No.	ht. (m)	F mT	RI	DEC	INC	pol	NRM	VS	IRM rat	peak IRM
WP104.2	2.6	50	T	8.3	45.0	N	31.91	11.83		
WP105.1	2.8	25	T	69.4	60.5	N	10.82	11.04		
WP105.2	2.8	30	T	354.6	13.9	N	10.82	10.53		
WP106.1	4.3	30	T	178.7	30.9	?	27.11	10.56		
WP106.2	4.3	30	T	144.4	1.6	R	17.19	9.43		
WP107.1	5.5	50	T	187.8	-25.9	R	16.11	11.04	.94	14755
WP107.2	5.5	30	T	131.8	-12.2	R	12.40	10.08		
WP108.1	6.6	30	T	124.7	-23.3	R	20.67	11.97		
WP108.2	6.6	50	S	174.4	-25.8	R	14.60	12.33		
WP109.1	7.5	50	S	168.2	-39.3	R	13.01	9.31		
WP109.2	7.5	30	T	128.3	-18.6	R	5.26	9.90		
WP110.1	7.8	30	T	170.4	-11.3	R	15.54	9.36		
WP110.2	7.8	40	T	195.8	-5.2	R	19.57	12.06		

Base of the exposed Sheppey section is taken as King's (1984) nodule band "A". Site WP101 is positioned at this level.

EASTCHURCH GAP

Spec. No.	ht. (m)	F mT	RI	DEC	INC	pol	NRM	VS	IRM rat.	peak IRM
EG10.2	8.6	40	E	60.6	2.6	?	14.06	10.26		
EG10.2	8.6	40	T	184.0	23.6	?	8.87	10.80		
EG9.1	10.6	50	T	221.5	-22.5	R	25.18	10.56		
EG9.2	10.6	50	T	189.5	-19.5	R	26.03	11.04	.95	17573
EG8.1	11.3	40	T	197.9	-28.8	R	13.46	11.01		
EG8.2	11.3	40	S	192.4	-21.4	R	8.89	9.40		
EG7.1	12.3	40	T	172.2	14.9	R	7.26	9.57		
EG7.2	12.3	50	T	207.0	-31.0	R	35.09	12.06		
EG6.1	13.9	50	T	265.3	-41.9	R	11.44	12.61		
EG5.1	14.8	50	T	240.6	-37.3	R	18.72	11.57		
EG5.2	14.8	40	T	179.7	-24.2	R	7.08	11.56	.93	14638
EG4.1	15.8	30	T	191.6	-4.0	R	9.19	9.99		
EG4.2	15.8	40	S	230.9	-43.3	R	20.70	11.88		
EG3.1	16.9	50	T	180.9	-0.2	R	26.16	8.30		
EG3.2	16.9	50	T	177.0	-0.6	R	19.17	8.30		
EG2.1	18.3	50	T	170.1	-42.2	R	13.37	5.72		
EG2.2	18.3	30	T	164.3	-16.2	R	7.38	7.04		
EG1.1	19.45	50	T	199.3	-32.5	R	13.54	8.29		
EG1.2	19.45	30	T	179.5	17.8	R	6.84	7.74		

Junction: C/D= 12.3m

PADDY POINT

Spec. No.	ht. (m)	F mT	RI	DEC	INC	pol	NRM	VS	IRM rat.	peak IRM
PP60.1	18.45	30	S	168.4	-11.1	R	11.87	7.41		
PP60.2	18.45	40	T	173.9	9.1	R	9.79	7.04		
PP59.1	19.85	40	T	206.9	-26.8	R	21.04	9.92	.92	14525
PP59.2	19.85	50	T	189.0	0.4	R	16.90	10.30		
PP58.1	20.75	50	T	150.2	-12.8	R	5.18	11.56		
PP57.1	21.85	40	T	134.1	-8.2	R	13.71	10.56		
PP57.2	21.85	15	T	68.4	-60.8	R	16.88	10.30		
PP56.1	22.75	50	T	159.5	-21.2	R	29.95	8.67		
PP56.2	22.75	50	S	194.6	-8.6	R	51.71	10.74		
PP55.1	23.35	40	T	192.3	31.9	R	19.90	6.90		
PP55.2	23.35	30	T	140.8	-8.8	R	10.31	7.20		
PP54.1	23.95	50	S	138.9	-7.2	R	24.53	7.07		
PP54.2	23.95	50	T	194.1	-32.2	R	33.30	8.27	.95	14321
PP53.2	24.5	50	T	203.6	-11.7	R	18.87	6.97		
PP52.1	25.7	50	T	33.6	58.8	N	11.07	4.86		
PP52.2	25.7	30	T	10.8	29.8	N	11.21	4.95		
PP51.2	26.4	50	S	357.1	40.7	N	23.23	5.67		

Spec. No.	ht. (m)	F mT	RI	DEC	INC	pol	NRM	VS	IRM rat.	peak IRM
PP51.1	26.4	50	T	347.6	37.2	N	39.33	6.74		
PP50.1	27.05	50	T	23.8	44.4	N	64.14	9.47		
PP50.2	27.05	40	S	23.2	46.1	N	28.00	8.28		
PP49.1	28.45	40	S	24.6	40.7	N	17.43	7.39		
PP49.2	28.45	50	T	28.1	35.2	N	20.31	9.06	.94	12330
PP48.1	29.65	30	T	359.6	24.1	N	15.81	7.23		
PP48.2	29.65	40	T	24.3	29.7	N	17.86	7.04		
PP47.1	30.3	50	S	10.3	34.0	N	24.13	5.63		
PP47.2	30.3	50	S	10.5	29.1	N	39.40	7.58		
PP46.1	31.75	50	S	10.1	49.5	N	22.11	8.27		
PP46.2	31.75	50	S	18.5	42.3	N	43.19	8.27		
PP45.1	32.5	50	S	11.3	48.4	N	43.95	9.71		
PP45.2	32.5	50	T	14.2	43.2	N	45.49	11.04		
PP44.1	33.65	50	S	18.0	40.7	N	45.07	8.33		
PP44.2	33.65	50	T	38.1	34.6	N	41.22	8.03	.93	10967
PP43.1	34.65	50	S	22.1	26.5	N	27.27	6.45		
PP43.2	34.65	50	S	10.9	30.0	N	26.86	7.36		
PP42.2	35.8	50	T	46.8	45.0	N	53.21	11.04		
PP18	36.9	30	T	11.1	43.5	N	25.49	9.81	.95	16987
PP19	38.3	30	T	30.2	14.4	N	34.28	9.06		
PP21	40.7	30	T	31.8	27.7	N	6.59	*NM		
PP22	41.9	30	T	9.5	41.3	N	17.31	3.48		
PP23	43.5	30	T	294.5	1.2	?	18.38	4.50	.95	6502
PP24	44.5	30	E	60.0	-37.8	?	18.78	4.35		
PP25	45.6	30	S	19.6	38.5	N	10.70	3.87		
PP26	46.6	30	S	29.4	20.7	N	15.58	8.29		
PP28	48.5	30	T	11.1	1.8	?	6.81	3.52	.89	3819
PP29	49.3	30	T	36.7	13.1	N	15.98	*NM		
PP30	50.3	30	T	357.3	51.4	N	12.50	6.04		
PP31	51.8	30	T	16.9	15.0	N	2.01	4.58	.90	4505
PP33	55.5	30	T	347.3	28.6	N	1.55	1.78		
PP41.1	55.8	30	S	347.7	68.2	N	10.33	2.59		
PP41.2	55.8	30	T	62.5	71.8	N	17.84	3.09		
PP40.1	56.3	25	S	20.8	70.5	N	11.57	3.45		
PP40.2	56.3	30	T	45.9	54.6	N	9.25	*NM		
PP39.2	57.3	30	T	336.3	14.7	N	1.42	*NM		
PP38.1	59.05	35	T	20.7	46.4	N	3.59	*NM		
PP37.1	59.6	35	T	9.9	21.4	N	1.12	*NM		
PP37.2	59.6	30	E	192.7	79.8	?	2.38	*NM		
PP36.1	60.55	20	T	355.0	53.9	N	1.55	*NM		
PP36.2	60.55	20	T	328.4	44.1	N	1.11	*NM		
PP35.2	61.3	25	T	331.9	49.5	N	1.34	*NM		

Junctions: D/E= 28.45m; E/Virginia Water Fm.= 53.55m

<u>WHITECLIFF BAY</u> (lower section)

Spec. No.	ht. (m)	F (mT)	MDF (mT)	RI	DEC	INC	pol.	NRM
WH38.1	0.02	35	NR	T	179.4	-0.4	R	0.42
WH38.2	0.02	35	NR	T	142.4	1.5	R	1.28
WH39.1	1.40	35	NR	S	203.0	-43.0	R	1.47
WH39.2	1.40	35	NR	T	163.2	-38.7	R	1.74
WH40.1	1.97	35	28	T	237.8	-59.0	R	1.38
WH41.1	2.80	35	10	T	201.6	12.4	R	2.87
WH41.2	2.80	35	12	T	193.5	-17.2	R	1.62
WH42.1	4.35	35	NR	T	179.3	-22.7	R	2.14
WH42.2	4.35	35	5	T	247.7	-2.1	R	3.61

Junctions: base Tilehurst Member= 0.0m;
base Walton Member= 2.80m.

(upper section)

Spec. No.	ht. (m)	F (mT)	MDF (mT)	RI	DEC	INC	pol.	NRM
WH1.1	-0.50	35	6	T	209.8	35.2	R	2.02
WH2.1	0.15	35	6	T	143.0	-41.1	R	0.87
WH2.2	0.15	35	6	E	6.4	-56.1	?	2.47
WH3.1	1.15	35	NR	T	66.8	22.6	?	1.40
WH3.2	1.15	35	6	T	2.5	62.7	R	4.57
WH4.1	2.15	35	8	T	161.3	61.0	R	3.47
WH4.2	2.15	30	8	T	24.1	15.3	N	6.66
WH5.1	9.60	35	8	T	72.8	-58.7	R	3.90
WH5.2	9.60	30	8	T	22.7	35.1	N	2.73
WH6.2	11.90	35	9	T	131.9	-88.9	R	0.68
WH7.1	15.50	30	18	T	17.9	-8.6	?	0.71
WH7.2	15.50	35	13	T	12.7	-16.4	?	0.90
WH8.1	16.80	30	NR	T	120.1	-42.5	R	0.25
WH8.2	16.80	35	4	T	45.3	29.5	R	0.44
WH9.1	17.90	35	15	T	10.0	-23.2	R	0.43
WH9.2	17.90	35	NR	E	46.6	-14.2	?	0.17
WH10.1	21.50	35	15	E	312.5	-24.7	?	0.60
WH10.2	21.50	30	NR	T	38.5	-8.8	?	0.17
WH11.1	32.10	35	17	T	185.0	31.8	R	0.86
WH11.2	32.10	35	NR	T	89.9	-18.1	R	0.30
WH12.1	33.30	35	14	T	342.5	37.5	N	0.46
WH12.2	33.30	30	NR	T	9.1	28.4	N	0.27
WH13.1	36.50	30	18	T	30.7	-37.7	?	0.55
WH13.2	36.50	35	9	T	339.8	-21.7	N	0.59
WH14.1	38.10	30	8	T	22.1	-11.0	?	0.25
WH14.2	38.10	35	NR	T	196.9	9.6	R	0.14
WH15.1	51.80	35	6	E	281.1	16.2	?	0.53
WH15.2	51.80	30	NR	T	148.0	-25.1	R	0.51
WH16.1	53.80	35	6	T	165.8	-55.4	R	0.81
WH16.2	53.80	30	12	T	93.5	1.1	R	0.44
WH17.1	56.00	35	7	T	124.5	-52.9	R	0.58
WH17.2	56.00	35	9	E	304.4	64.9	N	0.40
WH18.1	57.60	35	7	E	65.4	-10.6	?	0.57
WH18.2	57.60	30	8	T	244.1	-25.6	R	0.60
WH19.1	61.00	35	NR	S	30.4	22.1	N	0.33
WH19.2	61.00	30	20	T	8.7	0.0	N	0.70
WH20.1	61.20	30	10	E	17.5	-1.1	N	0.60
WH20.2	61.20	35	18	T	309.7	-3.9	?	0.75
WH21.1	61.40	30	12	T	335.2	14.5	N	0.72
WH21.2	61.40	35	8	T	350.3	52.5	N	0.65
WH22.1	62.00	30	12	T	3.6	69.6	N	0.69
WH22.2	62.00	35	9	S	4.8	56.2	N	0.75
WH23.1	69.60	35	25	T	345.1	-3.0	N	0.77
WH23.2	69.60	30	15	T	32.1	-33.2	?	0.80
WH24.1	74.00	30	8	T	23.8	-0.8	N	0.56
WH24.2	74.00	35	18	T	18.7	49.1	N	0.70
WH25.1	82.80	35	8	T	358.6	-5.8	N	0.78
WH25.2	82.80	35	6	E	135.6	19.5	?	0.43
WH26.1	84.60	35	33	T	274.4	35.7	N	0.15
WH26.2	84.60	30	8	E	10.1	-44.7	?	0.13
WH27.1	89.70	30	9	E	107.1	36.2	?	0.19
WH27.2	89.70	35	20	T	39.7	17.7	N	0.22
WH28.1	95.00	35	18	T	267.7	-38.4	R	0.20
WH28.2	95.00	30	NR	T	265.6	-18.0	R	0.22
WH29.1	99.80	35	8	T	108.4	-16.3	R	0.22
WH29.2	99.80	30	25	T	292.7	-31.5	R	0.09
WH30.1	100.20	35	17	T	131.5	-7.9	R	0.15
WH30.2	100.20	35	NR	T	150.2	-12.8	R	0.19
WH31.1	101.20	10	8	E	124.5	-65.1	?	0.04
WH31.2	101.20	35	8	T	85.4	-46.5	R	0.18
WH32.1	103.80	35	22	T	170.1	-40.1	R	0.18
WH32.2	103.80	35	12	T	77.6	29.4	R	0.92

Spec. No.	ht. (m)	F (mT)	MDF (mT)	RI	DEC	INC	pol.	NRM
WH33.1	105.00	35	15	T	92.9	-37.7	R	0.17
WH33.2	105.00	35	10	E	116.2	30.0	?	0.13
WH34.1	105.60	35	NR	E	76.2	-3.3	?	0.03
WH34.2	105.60	30	12	E	45.5	-19.0	?	0.05
WH35.1	109.00	35	7	E	84.3	-30.2	?	0.11
WH35.2	109.00	30	11	T	227.6	-35.6	R	0.12
WH36.1	111.80	35	6	T	183.4	-30.9	R	0.10
WH36.2	111.80	35	7	T	231.0	16.9	R	0.07
WH37.1	114.80	35	6	E	88.4	-16.5	?	0.12
WH37.2	114.80	35	8	T	121.3	1.6	R	0.13

Junctions: The base of King's (1981) London Clay Formation Division C is used as datum. The base of the other major lithostratigraphic units are as follows: C2= 9.6m; D= 31.6m; WB1= 51.1m; Wittering Formation= 62.0m. The top of the Wittering Formation is at 114.8m.

FLINES-LES-RACHES

Spec. No.	ht. (m)	F (mT)	MDF (mT)	RI	DEC	INC	pol.	NRM
FL4.1	15.7	40	25	T	14.8	29.2	N	1.07
FL4.2	15.7	30	3	E	34.9	27.1	N	0.88
FL3.1	15.2	40	3	T	242.0	38.3	?	0.54
FL3.2	15.2	40	20	T	29.8	40.3	N	0.57
FL2.1	14.6	30	NR	T	129.5	-5.6	R	0.35
FL1.1	14.0	30	8	T	220.9	32.4	?	0.56
FL1.2	14.0	10	30	E	125.5	-21.1	R	0.52
FL13.1	13.5	35	NR	T	70.4	39.6	N	0.09
FL13.2	13.5	35	25	T	50.4	4.3	?	0.39
FL12.1	11.8	35	NR	T	102.5	31.9	?	0.09
FL12.2	11.8	35	20	T	49.6	41.4	N	0.36
FL11.1	10.2	35	28	E	2.3	-6.0	?	0.17
FL11.2	10.2	35	30	E	272.0	-13.0	?	0.09
FL9.1	8.5	35	NR	T	205.9	63.1	N	0.12
FL9.2	8.5	35	NR	E	120.5	-59.1	R	0.08
FL8.1	6.5	35	NR	E	15.0	71.0	N	0.06
FL8.2	6.5	35	NR	E	84.0	-4.0	R	0.11
FL7.1	2.65	35	12	E	41.7	-42.4	?	0.22
FL6.1	0.9	35	NR	E	122.6	26.8	R	0.14
FL6.2	0.9	35	NR	T	138.8	69.3	N	0.23
FL5.1	0.0	35	28	T	33.9	-37.4	?	0.20
FL5.2	0.0	35	28	E	31.0	79.1	N	0.10

Junction:Landen/Ieper Clay Fm.=13.75m.

LE FOREST

Spec. No.	ht. (m)	F (mT)	MDF (mT)	RI	DEC	INC	pol.	NRM
LF1.1	0.0	30	8	T	11.2	23.5	N	0.64
LF1.2	0.0	0	NR	E	2.2	-9.9	?	0.32
LF2.1	1.0	40	NR	E	154.5	38.5	?	0.37
LF2.2	1.0	40	5	T	84.8	14.4	N	0.92
LF3.1	1.72	30	NR	T	188.2	-80.1	R	0.15
LF3.2	1.72	10	NR	E	214.2	77.9	?	0.31
LF4.1	2.8	10	NR	E	279.7	-10.8	?	0.14
LF4.2	2.8	10	4	T	342.2	28.6	N	0.53
LF5.1	3.7	40	8	T	42.9	39.7	N	0.58
LF5.2	3.7	30	10	T	357.4	50.4	N	1.50
LF6.1	4.4	30	NR	T	211.5	2.8	R	0.28
LF6.2	4.4	30	NR	T	196.0	-1.9	R	0.53
LF7.1	4.5	30	NR	S	145.6	-6.6	R	0.63
LF7.5	4.5	30	28	T	148.7	-7.3	R	0.50

Site LF7 is in the concretion band marking the top of King's (in press) Mt Heribu Member.

WARDRECQUES

Spec. No.	ht. (m)	F (mT)	MDF (mT)	RI	DEC	INC	pol.	NRM	IRM rat	peak IRM
WQ1.1	0.0	30	17	S	161.9	-19.8	R	2.54	.88	2460
WQ1.2	0.0	30	26	T	152.2	-19.0	R	1.17		
WQ2.1	1.1	30	25	E	217.5	54.0	?	0.80		
WQ2.2	1.1	35	12	T	41.2	29.2	N	0.95		
WQ3.1	2.2	20	8	S	346.6	29.4	N	0.63		
WQ3.2	2.2	15	8	T	60.0	56.5	N	0.55		
WQ4.1	3.4	20	NR	S	354.5	56.3	N	1.91		
WQ4.2	3.4	30	22	S	37.4	59.8	N	1.74	.86	2631
WQ5.1	5.35	30	27	S	346.0	37.2	N	11.47		
WQ5.1	5.35	40	28	S	322.4	50.2	N	13.94		
WQ6.1	6.35	40	31	S	7.0	34.9	N	19.95		
WQ6.2	6.35	30	27	S	341.9	51.3	N	14.88		
WQ7.1	7.15	40	20	S	6.9	56.3	N	17.52		

Spec. No.	ht. (m)	F (mT)	MDF (mT)	RI	DEC	INC	pol.	NRM	IRM rat	peak IRM
WQ7.2	7.15	30	23	S	8.5	49.3	N	20.53		
WQ8.1	8.15	40	25	S	355.9	58.3	N	34.40	.94	9838
WQ8.2	8.15	30	20	S	11.3	54.2	N	28.44		
WQ9.1	8.85	40	28	S	358.6	53.3	N	27.10		
WQ9.2	8.85	30	26	S	4.4	51.9	N	25.94		
WQ10.1	9.30	40	23	S	9.5	51.2	N	29.39		
WQ10.2	9.30	30	25	S	23.1	54.0	N	29.62		
WQ11.1	9.90	30	22	S	16.4	54.1	N	21.44		
WQ11.2	9.90	40	25	S	3.7	43.0	N	22.91		
WQ12.1	10.30	40	23	S	350.4	60.4	N	4.30		
WQ12.2	10.30	30	23	S	1.7	70.4	N	16.04		
WQ13.1	12.00	30	27	S	4.0	52.8	N	27.59	.93	8639
WQ13.2	12.00	40	26	T	351.1	43.5	N	29.39		
WQ14.1	13.45	0	NR	E	6.3	46.4	N	13.59		
WQ14.2	13.45	40	30	S	347.7	37.1	N	11.28		
WQ15.1	14.40	30	18	S	358.8	48.5	N	10.79		
WQ15.2	14.40	30	18	S	356.1	57.5	N	14.94		
WQ16.1	15.55	40	10	T	347.9	27.2	N	8.87		
WQ16.2	15.55	30	20	T	347.2	34.7	N	19.90		
WQ17.1	16.50	30	25	S	328.9	49.2	N	9.13	.93	6099
WQ17.2	16.50	40	23	T	339.7	33.1	N	13.16		
WQ18.1	17.50	20	14	T	36.6	45.1	N	2.26		
WQ18.2	17.50	20	8	S	17.5	33.9	N	4.36		
WQ19.1	18.60	10	NR	E	8.3	-54.5	?	0.13		
WQ19.2	18.60	30	NR	T	109.4	-52.0	R	0.15		
WQ20.1	19.40	20	15	T	322.0	38.0	N	1.38	.78	2965
WQ20.2	19.40	20	17	S	60.3	62.0	N	1.04		
WQ21.1	20.50	10	10	E	179.6	46.1	?	0.53		
WQ21.2	20.50	30	NR	T	169.9	-62.3	R	0.22		
WQ22.1	21.65	30	NR	T	181.2	-61.1	R	0.67		
WQ22.2	21.65	30	5	T	39.6	-50.4	?	0.23		
WQ23.1	22.75	30	18	T	19.3	-32.9	?	0.28		
WQ23.2	22.75	0	NR	E	160.1	-50.5	R	0.28		
WQ24.1	23.70	20	4	S	205.9	-73.2	R	1.24		
WQ24.2	23.70	30	NR	T	160.5	-54.4	R	0.66		
WQ25.1	24.50	20	NR	S	8.7	48.1	N	1.38		
WQ26.1	25.60	20	13	S	20.6	72.2	N	1.95		
WQ26.2	25.60	20	17	S	17.3	65.9	N	1.74		
WQ27.1	26.30	20	18	T	349.3	60.7	N	2.00	.73	1679
WQ27.2	26.30	20	NR	S	10.0	51.6	N	1.49		

Junctions: Wardrecques/Bailluel Member= 25.1m. An impersistent tabular band, which is a useful stratigraphic marker, is at 9.8m.

MOEN CANAL BANK

Spec. No.	ht. (m)	F (mT)	MDF (mT)	RI	DEC	INC	pol.	NRM
MO1.1	1.02	50	12	T	232.8	10.5	?	15.65
MO2.1	2.28	25	13	S	334.5	63.8	N	7.29
MO2.2	2.28	30	14	T	316.3	55.0	N	4.33
MO3.1	3.37	25	8	S	49.9	51.3	N	6.52
MO3.2	3.37	30	18	S	236.3	79.1	?	3.95
MO4.1	4.02	20	6	T	14.2	66.9	N	4.96
MO4.2	4.02	35	7	T	331.1	17.3	N	3.43
MO5.1	4.69	35	15	S	350.5	49.8	N	1.77
MO5.2	4.69	25	8	S	328.6	53.9	N	4.50
MO6.1	5.41	35	NR	T	188.7	-61.7	R	1.17
MO6.2	5.41	35	NR	S	158.7	-71.1	R	0.48
MO7.1	5.87	35	15	S	337.4	41.7	N	1.06
MO8.2	6.10	35	NR	S	32.4	46.2	N	1.57
MO9.1	6.36	35	NR	E	298.4	55.9	N	0.78
MO9.2	6.36	35	12	T	298.9	55.9	N	0.91

Spec. No.	ht. (m)	F (mT)	MDF (mT)	RI	DEC	INC	pol.	NRM
MO10.1	7.66	35	NR	S	210.3	81.1	?	1.22
MO10.2	7.66	35	15	T	359.3	31.5	N	1.07
MO11.1	8.43	35	6	E	323.6	-9.7	?	0.61
MO11.2	8.43	35	6	T	147.9	51.0	?	0.59
MO12.1	9.23	35	7	E	310.6	-15.3	?	0.61
MO12.2	9.23	35	10	T	215.2	-22.2	R	0.30
MO13.1	9.88	35	NR	S	146.8	-8.4	R	0.49
MO14.1	10.68	30	NR	T	212.6	-25.5	R	0.59
MO14.2	10.68	30	NR	T	206.8	-32.3	R	0.49
MO15.1	11.61	35	NR	T	214.1	-26.6	R	0.91
MO16.1	12.28	35	NR	E	0.7	-32.8	?	0.27
MO16.2	12.28	35	NR	T	200.8	-61.3	R	0.30
MO17.1	12.87	35	5	T	204.6	-42.4	R	0.32
MO18.1	13.65	40	15	T	201.8	-11.7	R	6.31
MO18.2	13.65	30	12	T	196.1	-3.7	R	5.36

Junction: King's (in press) Wardrecques/Bailluel Member= 6.0m.

MARKE

Spec. No.	ht. (m)	F (mT)	MDF (mT)	RI	DEC	INC	pol.	NRM
MK14.1	1.6	15	13	E	86.8	50.2	?	0.25
MK14.2	1.6	10	NR	T	154.7	4.6	R	0.17
MK13.1	0.6	15	NR	T	181.7	-25.4	R	0.19
MK13.2	0.6	10	NR	E	201.3	46.8	?	0.12
MK12.1	-0.4	30	6	T	237.4	-53.6	R	0.73
MK12.2	-0.4	30	NR	T	164.1	9.2	R	0.21
MK11.1	-1.4	30	NR	S	242.5	-59.0	R	4.63
MK11.2	-1.4	40	NR	S	265.7	-67.1	R	2.97
MK10.1	-2.4	30	20	T	156.7	-59.9	R	1.15
MK10.2	-2.4	30	NR	S	238.6	-69.7	R	1.05
MK9.1	-3.4	10	3	T	75.0	-58.7	R	0.50
MK8.1	-4.4	30	NR	T	188.9	-46.3	R	0.69
MK8.2	-4.4	30	15	T	96.2	-57.7	R	0.38
MK7.1	-5.4	40	5	T	94.1	-66.3	R	0.90
MK6.1	-6.5	30	NR	T	194.0	-54.3	R	2.18
MK6.2	-6.5	30	NR	S	191.9	-61.4	R	1.13
MK5.1	-7.6	30	4	T	206.9	-44.0	R	0.61
MK5.2	-7.6	30	NR	T	174.1	-49.5	R	0.67
MK22.1	-8.1	30	10	E	347.8	2.3	?	0.31
MK22.2	-8.1	30	NR	T	174.5	-60.9	R	0.36
MK4.1	-8.6	30	18	T	211.5	-31.0	R	0.92
MK4.2	-8.6	30	14	T	200.7	-52.2	R	0.68
MK3.1	-9.6	30	30	T	181.6	-43.2	R	0.70
MK3.2	-9.6	30	8	E	194.2	26.0	?	0.56
MK21.1	-9.7	30	NR	T	90.4	-1.1	R	0.39
MK21.2	-9.7	40	NR	E	151.3	33.3	?	0.15
MK2.1	-10.6	30	6	T	136.0	-7.0	R	0.99
MK2.2	-10.6	20	5	T	178.0	-37.0	R	1.71
MK20.1	-10.65	30	NR	T	12.3	38.7	N	0.68
MK20.2	-10.65	30	NR	T	10.3	30.1	N	0.47
MK1.1	-11.4	30	5	E	95.7	9.7	?	0.70
MK1.2	-11.4	15	6	T	328.3	24.2	N	0.62
MK19.2	-11.55	40	NR	T	69.2	52.7	N	0.65
MK18.1	-12.25	30	NR	T	41.6	68.1	N	0.57
MK18.2	-12.25	30	NR	S	26.9	45.3	N	1.38
MK17.1	-12.6	40	40	T	308.2	72.0	N	0.67
MK17.2	-12.6	40	NR	E	93.6	51.3	?	0.57
MK16.2	-12.75	40	12	T	66.3	70.5	N	1.19

Spec. No.	ht. (m)	F (mT)	MDF (mT)	RI	DEC	INC	pol.	NRM
MK15.1	-13.2	30	15	S	352.3	53.4	N	1.41
MK15.2	-13.2	20	12	T	330.5	50.3	N	1.05

Junctions: Wardrecques/Bailluel Member= -12.70; Bailluel/Aalbeke Member= 0.0m.

HEERSTERT

Spec. No.	ht. (m)	F (mT)	MDF (mT)	RI	DEC	INC	pol.	NRM
AA1.1	0.0	20	5	T	120.2	16.6	R	0.97
AA1.2	0.0	40	NR	E	104.8	45.9	?	0.07
AA2.1	1.0	10	NR	T	203.9	1.1	R	0.23
AA2.2	1.0	15	NR	T	253.1	-30.2	R	0.24
AA3.1	1.8	10	NR	T	315.1	43.0	N	0.23
AA3.2	1.8	15	NR	T	56.3	69.9	N	0.17
AA4.1	2.65	O	NR	E	13.1	-12.5	?	0.20
AA4.2	2.65	20	NR	T	337.9	13.0	N	0.18
AA5.1	3.4	15	NR	T	63.3	27.8	N	0.28
AA5.2	3.4	30	20	T	8.3	44.7	N	0.31
AA6.1	4.2	30	NR	T	70.8	58.3	N	0.16
AA6.2	4.2	20	12	T	326.6	71.2	N	0.16

Junction: base of Aalbeke Clay at 0.0m.

MOUSCRON

Spec. No.	ht. (m)	F (mT)	MDF (mT)	RI	DEC	INC	pol.	NRM
MU5.1	8.22	30	NR	T	48.7	52.4	N	1.20
MU5.2	8.22	30	5	T	49.1	63.4	N	1.40
MU4.1	7.62	30	20	T	21.7	63.2	N	0.49
MU4.2	7.62	20	19	E	92.0	63.9	?	0.30
MU3.1	6.62	30	10	E	79.2	35.4	?	0.44
MU3.2	6.62	20	18	T	34.1	47.0	N	0.24
MU2.1	5.67	20	10	T	308.6	28.7	N	0.56
MU2.2	5.67	20	12	T	8.7	7.5	N	0.48
MU6.1	5.02	30	15	T	15.8	28.9	N	0.69
MU6.2	5.02	30	13	T	14.8	8.1	N	0.43
MU1.1	4.92	40	15	T	33.4	42.4	N	2.41
MU1.2	4.92	40	15	T	35.4	56.2	N	3.28
MU7.1	3.96	30	22	T	12.3	39.0	N	1.05
MU7.2	3.96	30	20	S	13.7	53.1	N	2.17
MU8.1	3.06	30	18	T	56.2	7.0	N	0.74
MU8.2	3.06	30	15	T	49.0	5.0	N	0.62
MU9.1	1.59	20	NR	T	3.2	17.1	N	0.29
MU9.2	1.59	20	NR	T	339.6	52.5	N	0.36
MU10.1	0.00	20	15	T	321.1	42.8	N	0.42
MU10.2	0.00	20	17	T	26.9	32.7	N	0.30

Junctions:Aalbeke Clay/Panisel Sand Mbr= 8.15m. A conspicuous oxidation band spans the interval 3.68 to 4.92m.

Ronse

Spec. No.	ht. (m)	F (mT)	MDF (mT)	RI	DEC	INC	pol.	NRM
RN1.1	0.0	50	24	T	2.8	56.7	N	1.07
RN1.2	0.0	30	10	T	260.0	-26.0	R	0.60
RN2.1	0.9	40	10	S	10.3	57.8	N	6.89
RN2.2	0.9	50	6	T	226.3	-65.0	R	6.88
RN3.1	1.1	40	23	T	188.9	-44.6	R	2.14
RN3.2	1.1	50	12	?	82.0	23.5	?	1.80
RN4.1	3.5	20	8	T	174.0	50.0	?	0.59
RN4.2	3.5	30	NR	T	107.4	-30.0	R	0.45
RN5.1	4.2	40	NR	E	236.7	63.5	?	1.20

Spec. No.	ht. (m)	F (mT)	MDF (mT)	RI	DEC	INC	pol.	NRM
RN5.2	4.2	40	9	E	330.3	-45.3	?	0.73
RN6.2	4.8	30	8	E	321.4	17.8	?	0.41
RN7.2	5.5	0	NR	E	?	?	?	0.15

Junction: Mons-en-Pevele Sand/Aalbeke Clay Member= 5.4m.

KORTEMARK

Spec. No.	Ht. (m)	F (mT)	MDF (mT)	RI	DEC	INC	pol.	NRM
KM1.1	0.0	20	3	T	5.3	66.5	N	2.10
KM2.2	0.67	15	2	T	45.8	44.6	N	0.86
KM3.1	1.78	15	4	T	32.7	36.8	N	1.12
KM4.1	2.63	15	2	T	12.5	31.9	N	1.50
KM5.1	3.30	20	4	S	359.1	7.3	N	1.59
KM6.1	4.24	20	4	T	13.4	51.5	N	1.84
KM7.1	5.20	30	3	S	7.0	57.7	N	2.26
KM8.1	5.93	30	5	T	36.4	67.5	N	2.32
KM9.1	6.65	30	4	S	332.2	52.0	N	3.28
KM10.1	7.83	30	4	T	349.1	37.6	N	6.71
KM11.2	8.67	30	17	T	21.4	56.3	N	0.64
KM12.2	9.73	30	4	S	40.8	44.4	N	9.60
KM13.1	10.32	20	3	E	3.0	-33.7	?	10.05
KM13.2	10.32	30	3	T	68.6	44.3	N	12.45
KM14.1	11.08	30	4	S	128.6	59.2	?	12.58
KM14.2	11.08	30	4	T	46.3	52.1	N	11.06
KM15.2	12.14	30	4	T	37.5	56.9	N	16.57
KM16.1	13.08	30	4	T	14.7	68.4	N	14.57
KM17.2	13.73	30	4	T	355.9	36.6	N	7.32
KM18.1	14.37	30	3	T	42.7	65.1	N	9.28
KM19.2	15.49	30	3	T	28.5	53.8	N	8.32
KM20.2	16.37	30	3	T	8.2	32.6	N	19.03
KM21.2	17.37	30	4	T	351.4	48.5	N	25.09
KM22.1	18.49	30	3	T	66.6	38.9	N	17.65
KM23.1	19.60	50	4	T	44.9	7.9	N	30.80
KM24.1	20.66	30	5	T	17.2	55.5	N	6.99
KM25.1	21.84	30	3	T	57.6	40.7	N	14.63
KM26.1	22.54	30	9	T	322.5	38.9	N	1.58
KM27.1	23.84	30	3	T	65.5	64.1	N	5.21
KM28.2	24.78	30	5	S	345.5	27.8	N	1.35
KM29.2	25.89	30	3	T	327.8	58.8	N	3.56
KM30.2	27.13	30	4	T	56.1	42.3	N	3.17
KM31.2	27.65	30	4	T	355.5	36.3	N	5.24

Junctions: Aalbeke Clay/ Kortemark Silt Member= 3.0m; Kortemark Silt/ Egem Sand Member= 27.0m.

EGEM

Spec. No.	Ht. (m)	F (mT)	MDF (mT)	RI	DEC	INC	pol.	NRM
EM1.1	-5.14	40	25	S	222.9	-43.9	R	1.16
EM1.2	-5.14	40	15	S	157.2	-40.4	R	0.95
EM2.1	-4.86	30	4	T	99.6	-40.0	R	1.89
EM2.2	-4.86	35	15	T	129.9	-69.9	R	1.58
EM3.1	-4.23	35	10	E	323.6	-32.7	?	0.87
EM3.2	-4.23	40	5	T	152.4	-36.9	R	1.69
EM4.1	-3.74	30	7	T	117.1	18.3	R	1.37
EM4.2	-3.74	40	7	T	22.9	20.0	N	1.57
EM5.1	-3.04	35	4	T	338.3	-49.1	R	0.08
EM5.2	-3.04	40	7	T	208.2	24.7	R	0.91
EM6.1	-1.85	40	7	T	81.3	-19.5	R	0.91
EM6.2	-1.85	40	11	T	16.9	12.0	N	1.00
EM7.2	-1.09	40	5	T	25.0	38.9	N	1.54

Spec. No.	Ht. (m)	F (mT)	MDF (mT)	RI	DEC	INC	pol.	NRM
EM8.1	-0.05	40	NR	T	9.2	51.7	N	0.81
EM8.2	-0.05	40	12	T	3.9	56.5	N	1.17
EM9.1	1.00	40	30	T	307.9	27.1	N	0.55
EM9.2	1.00	35	NR	T	204.0	-22.7	R	0.16
EM10.1	1.60	35	12	T	338.1	58.7	N	0.45
EM10.2	1.60	40	NR	T	84.0	23.6	?	0.54
EM11.1	2.36	40	20	T	38.1	74.2	N	0.52
EM11.2	2.36	35	NR	T	53.8	11.7	N	0.25
EM17.1	3.00	35	NR	E	78.8	26.2	?	0.11
EM17.2	3.00	35	10	E	91.9	-29.4	?	0.22
EM16.1	4.00	40	40	T	5.4	50.9	N	0.65
EM16.2	4.00	35	8	E	285.1	-67.6	?	0.25
EM15.2	4.74	30	NR	T	1.0	34.0	N	0.65
EM18.1	10.50	50	12	T	142.0	46.6	?	0.63
EM18.2	10.50	40	18	E	63.5	9.3	?	0.68
EM12.2	12.50	35	32	T	153.9	-2.5	R	0.32
EM13.1	12.70	30	22	T	19.8	35.2	N	0.61
EM14.1	13.03	35	25	T	29.9	77.1	N	0.51
EM14.2	13.03	25	35	E	6.9	-0.6	?	0.14
EM19.1	13.39	35	35	T	291.8	29.0	?	0.19
EM19.2	13.39	35	10	T	141.7	-68.7	R	0.24
EM20.1	14.39	35	NR	E	78.0	5.3	?	0.07
EM20.2	14.39	35	22	T	212.2	-62.8	R	0.11
EM21.1	14.93	35	NR	T	92.4	51.8	?	0.21
EM21.2	14.93	35	NR	E	58.9	-11.0	?	0.12
EM121.1	15.10	35	NR	E	359.4	-66.6	?	0.32
EM121.2	15.10	35	NR	E	13.0	-20.4	?	0.14
EM121.3	15.10	35	NR	T	309.4	36.4	N	0.18
EM22.1	15.30	35	NR	E	52.2	10.7	?	0.04
EM22.2	15.30	35	NR	T	213.3	-14.7	R	0.07
EM23.2	16.50	35	10	E	338.3	-8.0	?	0.10
EM24.1	17.45	35	12	T	13.7	17.4	?	0.12
EM24.2	17.45	35	NR	T	249.3	3.2	R	0.11
EM25.1	17.75	35	15	T	35.4	-51.5	?	0.06
EM25.2	17.75	35	5	T	176.6	4.9	R	0.12
EM26.1	18.35	30	20	T	282.1	50.4	?	0.34
EM26.2	18.35	35	22	T	14.0	36.0	N	0.20
EM27.1	19.45	20	12	T	1.1	44.7	N	0.78
EM27.2	19.45	35	10	T	323.1	70.0	N	0.66

Junctions: Kortemark Silt/Egem Sand Member= 5.0m; Egem Sand Member/Pittem Clay Member (Vlierzelle Fm.) =15.0m. It is possible that the Egem Sand Member, as defined by Steurbaut and Nolf (1986), may infact be positioned at 0.0m in this section. The base of the Egem Sand Member as defined by these authors is not marked by a sharp transition from silts to sands, and it may have been mistakenly located. However, the sites are all accurately positioned relative to the shelly sandstone marking the base of the Vlierzelle Formation.

VARENGEVILLE

Spec. No.	ht. (m)	F (mT)	MDF (mT)	RI	DEC	INC	pol.	NRM
VG32.1	-10.42	30	5	S	341.1	73.4	N	0.80
VG32.2	-10.42	40	NR	T	339.8	77.9	N	0.60
VG31.1	-9.75	0	NR	E	261.9	-17.1	?	0.03
VG31.2	-9.75	0	NR	E	199.1	30.0	?	0.04
VG30.1	-8.77	35	3	E	309.6	25.0	?	0.22
VG30.2	-8.77	30	12	T	199.9	38.1	?	0.07
VG29.1	-6.90	35	8	T	219.3	-41.8	R	0.18
VG29.2	-6.90	30	8	T	210.3	-72.7	R	0.12
VG28.1	-5.97	30	NR	E	266.0	-4.0	?	0.03
VG28.2	-5.97	30	10	T	210.2	-71.9	R	0.13
VG27.1	-4.34	40	32	T	215.9	46.6	?	0.51
VG27.2	-4.34	30	NR	S	166.3	-56.4	R	1.03
VG26.1	-3.50	30	30	T	145.1	-60.9	R	0.66
VG26.2	-3.50	30	NR	T	167.7	-60.0	R	0.20
VG25.1	-2.00	30	NR	T	190.3	-27.2	R	0.32
VG25.2	-2.00	30	28	S	178.7	-49.8	R	0.32
VG24.1	-0.92	40	NR	S	179.4	-37.1	R	11.18
VG24.2	-0.92	40	NR	S	178.3	-33.2	R	8.54
VG23.1	-0.30	30	NR	S	181.8	-40.2	R	0.46
VG23.1	-0.30	30	20	T	158.1	-42.6	R	0.42
VG1.1	1.50	35	8	E	263.6	84.8	?	0.52
VG2.1	1.70	35	NR	T	108.6	56.3	?	0.50
VG2.2	1.70	35	NR	T	211.2	80.7	?	0.27
VG4.1	3.80	35	NR	S	159.5	60.0	?	0.23
VG6.1	5.35	35	NR	T	64.2	18.9	R	0.24
VG6.2	5.35	35	NR	T	283.1	11.3	R	0.24
VG7.1	5.50	10	NR	E	310.9	60.5	N	0.22
VG7.2	5.50	30	4	E	323.2	-44.2	?	0.29
VG8.1	6.43	20	NR	T	350.4	40.2	N	0.50
VG8.2	6.43	30	12	T	17.4	55.5	N	0.35
VG9.1	7.33	30	15	T	196.1	-1.7	R	0.35
VG9.2	7.33	30	11	T	226.4	15.2	R	0.43
VG10.1	8.38	30	20	T	209.6	30.6	R	0.72
VG10.2	8.38	30	8	T	191.9	48.7	R	0.66
VG11.1	10.60	30	20	T	258.0	-7.5	R	0.56
VG11.2	10.60	30	27	T	226.4	40.8	R	0.32
VG12.1	12.35	40	NR	T	255.5	-69.4	R	0.78
VG12.2	12.35	30	NR	T	244.8	-52.4	R	0.36
VG13.1	13.75	10	NR	T	184.4	14.3	R	0.24
VG13.2	13.75	30	NR	T	162.2	-41.7	R	1.02
VG14.1	14.80	30	NR	T	115.4	-62.4	R	0.07
VG14.2	14.80	30	20	E	65.0	3.0	?	0.14
VG15.1	15.50	30	15	T	210.3	9.5	R	0.39
VG15.2	15.50	30	8	E	186.6	38.8	?	0.33
VG16.1	18.40	35	30	T	202.2	-13.8	R	0.27
VG16.2	18.40	30	NR	T	167.9	-57.5	R	0.29
VG17.1	19.10	30	NR	T	191.0	-47.8	R	0.13
VG17.2	19.10	30	NR	S	147.7	-59.1	R	0.20
VG18.1	19.50	30	NR	S	186.8	-25.2	R	0.23
VG18.2	19.50	30	3	T	220.3	-5.5	R	0.49
VG19.1	20.04	30	NR	T	178.0	-22.2	R	0.19
VG19.2	20.04	30	NR	T	165.8	-53.0	R	0.34
VG20.1	20.64	30	NR	T	130.7	-38.6	R	0.26
VG20.2	20.64	30	25	E	90.7	72.0	?	0.35
VG22.1	21.30	30	3	T	109.9	-28.1	R	0.57
VG22.2	21.30	30	NR	T	156.9	-32.5	R	0.23
VG21.1	21.88	30	NR	T	207.9	-0.9	R	0.32
VG21.2	21.88	30	NR	T	154.6	-43.0	R	0.25

Junctions: base Fm. de Varengeville inferieur= 0.0m; base Fm. V. superieur = 5.30m; A2/A3= 15.20m. The glauconitic clay bed spans the interval 18.80-19.80m.

THERDONNE

Spec. No.	ht. (m)	F (mT)	MDF (mT)	RI	DEC	INC	pol.	NRM	IRM rat	peak IRM
TD28.1	-15.58	35	32	T	21.0	-51.7	R	0.09		
TD28.2	-15.58	30	NR	T	301.9	24.7	N	0.24		
TD27.1	-14.50	35	NR	T	69.6	-41.3	R	0.02		
TD27.2	-14.50	30	NR	T	354.3	9.4	N	0.08		
TD26.1	-13.40	35	NR	T	71.6	-38.3	R	0.02		
TD26.2	-13.40	35	NR	E	45.6	-13.6	?	0.04		
TD25.1	-12.93	35	18	T	162.7	23.9	R	0.11		
TD25.2	-12.93	35	NR	T	90.1	-33.7	R	0.08		
TD24.1	-11.80	35	NR	S	314.1	48.8	N	0.36		
TD24.2	-11.80	35	NR	E	95.8	-40.6	R	0.04		
TD23.1	-11.77	35	15	T	60.2	33.3	?	0.29		
TD23.2	-11.77	30	25	T	92.8	-59.4	R	0.12		
TD22.1	-10.90	30	NR	T	355.6	73.2	N	0.85		
TD22.2	-10.90	30	9	T	20.4	38.6	N	0.42		
TD21.1	-9.20	40	NR	T	5.8	63.6	N	2.75	.62	1155
TD21.2	-9.20	40	NR	T	345.2	71.0	N	2.73		
TD20.1	-7.85	35	NR	T	156.7	-77.6	R	0.19		
TD20.2	-7.85	30	NR	T	119.3	-82.7	R	0.16		
TD19.1	-7.21	35	20	E	295.8	12.9	?	0.08	.96	68
TD19.2	-7.21	30	15	E	256.9	10.4	R	0.09		
TD18.1	-6.05	35	15	T	320.8	37.0	N	0.17		
TD18.2	-6.05	30	15	T	335.2	53.7	N	0.20		
TD17.1	-4.73	35	20	T	343.2	49.5	N	0.20		
TD17.2	-4.73	30	15	T	306.7	72.5	N	0.38		
TD16.1	-4.10	30	12	T	301.9	46.6	N	0.23		
TD16.2	-4.10	30	25	T	300.2	52.2	N	0.15		
TD15.1	-3.00	30	5	T	193.7	33.2	R	0.70	.96	197
TD15.2	-3.00	35	8	T	240.8	65.4	?	0.73		
TD14.1	-2.50	35	10	E	5.0	4.0	?	0.26	.94	143
TD14.2	-2.50	30	8	T	298.5	83.5	?	0.26		
TD13.1	-1.65	35	10	T	134.7	-53.1	R	0.16		
TD13.2	-1.65	30	8	E	254.3	46.0	?	0.23		
TD12.1	-0.85	35	NR	E	11.0	-67.3	?	0.04		
TD12.2	-0.85	30	30	T	77.0	33.8	?	0.20	.93	62
TD11.1	-0.12	35	15	T	282.9	54.6	N	0.13		
TD11.2	-0.12	30	30	T	317.7	56.8	N	0.84		
TD10.1	0.50	30	NR	S	139.4	-28.1	R	0.65		
TD10.2	0.50	30	NR	T	126.2	-32.0	R	0.71		
TD9.1	1.14	35	5	T	45.6	43.7	N	1.28		
TD9.2	1.14	35	10	T	37.0	25.0	N	1.22		
TD8.1	1.65	35	10	E	45.8	6.5	?	0.43		
TD8.2	1.65	35	5	T	155.1	-35.5	R	0.48		
TD7.1	1.90	35	10	T	223.0	-32.6	R	0.56		
TD7.2	1.90	35	8	T	221.9	-63.9	R	0.26		
TD6.1	2.70	35	15	T	343.1	74.8	N	0.35		
TD6.2	2.70	30	15	T	161.7	12.3	R	0.93		
TD5.1	3.40	35	NR	E	254.5	1.7	R	0.64		
TD5.2	3.40	35	NR	T	7.0	38.3	N	0.44		
TD4.1	4.18	35	35	T	230.6	23.0	R	0.26		
TD4.2	4.18	35	NR	T	329.5	39.0	N	0.11		
TD3.1	5.38	35	10	E	148.7	32.9	?	0.15		
TD3.2	5.38	30	NR	E	44.7	-8.5	?	0.11		
TD2.1	5.98	35	35	T	272.5	-30.3	R	0.16		
TD2.2	5.98	30	NR	E	81.5	37.7	?	0.25		
TD1.1	7.18	35	10	T	135.0	-26.3	R	0.21		
TD1.2	7.18	35	10	T	159.5	-18.7	R	0.25		

Junctions: Sables de Bracheux/Sparnacian= -9.5m; base Fm. Varengeville inf.= 0.0m; base of clay bed= 0.75m; base Cuisian Sands (Sables de Laon) = 1.75m.

MONS-EN-LAONNOIS

Spec. No.	Depth (m)	MDF (mT)	RI	DEC	INC	pol.	NRM
BG8.1	0.24	NR	T	90.6	45.2	N	0.20
BG8.2	0.24	NR	T	43.6	-40.3	R	0.09
BG7.1	1.33	NR	T	154.3	29.2	R	0.19
BG7.2	1.33	NR	E	58.3	-9.2	?	0.16
BG6.1	2.25	20	T	72.9	22.1	N	1.51
BG6.2	2.25	35	T	25.8	-6.3	?	0.29
BG5.1	3.40	32	T	285.6	57.0	N	0.28
BG5.2	3.40	20	E	43.0	-7.2	?	0.28
BG4.1	4.87	NR	T	314.1	56.9	N	0.27
BG4.2	4.87	25	T	13.0	20.7	N	0.55
BG3.1	6.15	32	T	331.9	22.8	N	0.42
BG3.2	6.15	10	E	64.9	-64.7	?	0.23
BG2.1	7.40	25	T	354.0	24.9	N	0.28
BG2.2	7.40	4	E	152.7	-10.6	?	0.16
BG1.1	8.00	4	E	56.0	-18.2	?	0.24
BG1.2	8.00	11	T	328.8	67.6	N	0.53
BG9.1	9.02	25	T	194.5	60.9	?	0.42
BG9.2	9.02	15	T	332.1	19.1	?	0.38
BG10.1	10.40	25	T	9.4	30.7	N	0.55
BG10.2	10.40	NR	T	309.6	43.8	N	0.45
BG11.1	11.50	NR	E	306.6	-15.7	?	0.22
BG11.2	11.50	12	T	23.7	36.9	N	0.51
BG12.1	12.50	NR	T	65.4	63.0	N	0.32
BG12.2	12.50	32	T	192.6	16.7	?	0.29
BG13.1	14.00	NR	T	175.7	23.0	?	0.16
BG13.2	14.00	28	T	320.6	71.4	N	0.61

All specimens were demagnetised to 35mT. All sites are within the Sables de Aizy and are positioned relative to the base of the Pierrefonds Horizon.

CINQUEUX

Spec. No.	Depth (m)	F (mT)	MDF (mT)	RI	DEC	INC	pol.	NRM
CQ1.1	0.0	35	NR	E	39.7	37.7	N	0.16
CQ1.2	0.0	35	NR	E	88.0	14.4	?	0.11
CQ2.1	1.25	35	33	T	311.2	14.6	N	0.23
CQ2.2	1.25	30	NR	T	35.3	27.8	N	0.15
CQ3.1	1.65	35	NR	E	32.2	-3.2	?	0.06
CQ3.2	1.65	30	15	E	249.1	60.5	?	0.28
CQ4.1	2.45	35	NR	T	160.3	-0.6	R	0.28
CQ4.2	2.45	35	NR	E	57.1	31.9	?	0.03
CQ5.1	3.25	35	15	T	240.8	-71.9	R	0.29
CQ5.2	3.25	35	10	E	240.5	25.0	R	0.07
CQ6.1	4.25	35	25	E	337.1	3.3	N	0.28
CQ6.2	4.25	35	NR	E	57.8	18.2	N	0.36

Site CQ1 is 5.75m below the base of the Pierrefonds horizon.

MONAMPTEUIL

Spec. No.	Ht. (m)	F (mT)	MDF (mT)	RI	DEC	INC	pol.	NRM
MP14.1	12.92	35	3	T	343.0	36.7	N	0.99
MP14.2	12.92	35	NR	E	240.1	74.4	?	0.07
MP13.1	11.92	35	NR	T	86.3	44.1	?	0.15
MP13.2	11.92	35	15	T	75.8	-45.1	R	0.18
MP12.1	10.52	35	10	T	109.7	-24.4	R	0.12
MP12.2	10.52	35	7	T	203.9	-36.8	R	0.14
MP11.1	9.42	35	7	E	108.9	35.4	?	0.21
MP11.2	9.42	35	25	T	303.4	-72.8	R	0.14

Spec. No.	Ht. (m)	F (mT)	MDF (mT)	RI	DEC	INC	pol.	NRM
MP10.1	8.42	35	NR	T	118.0	-15.9	R	0.06
MP10.2	8.42	30	5	E	56.0	-0.1	?	0.16
MP9.1	7.40	35	7	T	220.6	-38.6	R	0.21
MP9.2	7.40	35	NR	T	95.6	13.3	?	0.44
MP8.1	6.52	30	7	E	121.1	-20.9	?	0.20
MP8.2	6.52	30	15	T	324.4	38.0	N	0.24
MP7.1	5.82	30	5	T	16.3	29.2	N	0.31
MP7.2	5.82	35	NR	T	72.3	-15.9	?	0.27
MP6.1	4.82	35	NR	T	341.4	43.8	N	0.72
MP6.2	4.82	35	35	E	201.6	57.1	?	0.20
MP4.2	3.86	35	NR	T	212.3	4.1	R	0.80
MP5.1	2.10	35	NR	T	40.0	30.5	N	0.49
MP5.2	2.10	35	NR	T	57.0	12.8	N	0.10
MP3.1	1.40	35	32	T	90.3	44.8	?	0.15
MP3.2	1.40	35	NR	T	82.3	19.8	?	0.48
MP2.1	1.01	35	NR	T	321.2	51.4	N	0.26
MP2.2	1.01	35	NR	T	186.6	28.1	R	0.25
MP1.1	0.00	35	NR	E	79.0	-50.4	?	0.09
MP1.2	0.00	35	NR	T	165.4	-50.0	R	0.10

Junction: base of Pierrefonds Horizon at 7.52m.

CROUTOY

Spec. No.	Depth (m)	F (mT)	MDF (mT)	RI	DEC	INC	pol.	NRM
CR1.1	2.95	35	33	T	197.9	5.0	R	0.22
CR1.2	2.95	35	5	T	117.6	53.6	?	0.76
CR2.1	3.55	35	NR	T	267.5	18.0	R	0.23
CR2.2	3.55	35	15	T	261.9	45.7	R	0.20
CR3.1	4.95	35	NR	E	29.8	-21.2	?	0.10
CR4.1	5.95	35	32	T	173.0	-6.2	R	0.12
CR4.2	5.95	35	8	E	75.7	20.7	?	0.15
CR5.1	6.95	35	20	E	351.0	14.5	?	0.11
CR5.2	6.95	30	20	T	142.9	-53.4	R	0.33
CR6.1	8.65	35	NR	T	110.6	-16.1	R	0.06
CR6.2	8.65	30	NR	E	71.7	30.0	?	0.23
CR7.1	8.89	20	20	T	226.7	-49.8	R	0.07
CR7.2	8.89	30	20	E	277.5	43.5	?	0.13
CR8.1	9.00	35	NR	T	67.9	30.2	N	0.48
CR8.2	9.00	35	NR	T	113.9	72.4	?	0.45
CR9.1	9.35	35	15	T	240.1	36.5	R	0.27
CR9.2	9.35	30	10	T	304.0	16.7	N	0.21
CR10.1	10.60	35	8	E	87.2	-23.2	R	0.19
CR10.2	10.60	30	NR	N	344.5	17.8	N	0.22
CR11.1	12.00	35	NR	N	316.4	36.8	N	0.16
CR11.2	12.00	30	NR	T	282.4	29.1	?	0.15
CR12.1	13.52	30	25	T	353.7	38.0	N	0.29
CR12.2	13.52	30	20	T	56.3	7.3	?	0.18
CR13.1	14.96	35	NR	T	203.4	-65.4	R	0.17
CR13.2	14.96	30	NR	T	341.3	30.9	N	0.47
CR14.1	15.96	35	NR	E	56.5	-37.4	?	0.08
CR14.2	15.96	30	NR	E	12.5	15.4	N	0.14
CR15.1	18.33	35	NR	T	343.6	38.4	N	0.25
CR15.2	18.33	30	NR	T	6.3	46.8	N	0.18
CR16.1	19.18	35	20	E	89.3	36.5	?	0.38
CR16.2	19.18	30	25	E	4.4	7.8	N	0.26
CR17.1	20.40	35	32	T	163.6	9.5	R	0.13
CR17.2	20.40	30	NR	E	354.7	-2.0	?	0.08
CR18.1	21.55	30	NR	T	345.7	52.5	N	0.28
CR18.2	21.55	30	NR	E	324.5	-32.9	?	0.10
CR19.1	22.30	35	NR	E	73.1	-54.9	?	0.12
CR19.2	22.30	35	NR	T	353.1	51.8	N	0.17

Spec. No.	Depth (m)	F (mT)	MDF (mT)	RI	DEC	INC	pol.	NRM
CR20.1	22.90	35	NR	E	228.5	56.7	?	0.08
CR20.2	22.90	30	30	E	113.1	-26.5	R	0.13

Junctions: base Pierrefonds Horizon= 18.15; base Argile de Laon= 9.35m; base of Lutetian= 0.0m. Site CR19 is from a glauconite bed (0.15m thick) which is another useful stratigraphic marker.

AIZY-JOUY

Spec. No.	Ht (m)	F (mT)	MDF (mT)	RI	DEC	INC	pol.	NRM
AZ4.1	2.40	35	NR	E	38.1	-14.4	?	0.15
AZ4.2	2.40	35	NR	E	293.3	-16.5	R	0.06
AZ3.1	1.50	35	NR	T	238.1	-33.8	R	0.12
AZ3.2	1.50	35	NR	T	260.8	-55.9	R	0.10
AZ2.1	0.70	30	10	T	310.3	73.0	N	0.46
AZ2.2	0.70	30	30	E	27.7	9.5	?	0.22
AZ1.1	0.10	35	12	T	64.4	59.8	N	0.22
AZ1.2	0.10	35	25	T	56.5	66.1	N	0.41
AZ7.1	-1.80	35	NR	T	35.5	48.2	N	0.19
AZ7.2	-1.80	35	NR	T	115.0	66.8	?	0.29
AZ6.1	-2.50	35	10	E	29.9	-6.3	?	0.16
AZ6.2	-2.50	35	18	E	308.3	-39.9	?	0.09
AZ8.1	-3.60	30	NR	T	161.6	8.1	R	0.14
AZ8.2	-3.60	35	NR	E	28.1	0.6	?	0.23
AZ9.1	-4.70	35	4	T	186.7	-59.7	R	0.26
AZ9.2	-4.70	35	18	T	105.3	-34.9	R	0.32

Junctions: base Argile de Laon= -4.43m; base Lutetian= 4.00m.

OLST (Holmehus and Olst Formations)

Spec. No.	ht. (m)	F mT	MDF mT	RI	DEC	INC	pol.	NRM	IRM rat.	peak IRM
OL51.1	-21.28	30	12	T	304.3	-68.7	R	0.27		
OL51.2	-21.28	35	8	E	299.8	-15.5	?	0.40		
OL52.1	-21.00	30	15	T	189.8	-47.7	R	0.24		
OL52.2	-21.00	30	NR	T	268.3	-1.6	R	0.09		
OL53.1	-20.78	35	35	T	264.6	-69.5	R	0.09		
OL53.2	-20.78	30	20	T	313.6	-42.6	?	0.17		
OL54.1	-20.58	35	10	T	1.5	15.4	N	0.19		
OL55.1	-20.58	30	10	T	340.3	11.3	N	0.14		
OL55.1	-20.08	35	15	T	242.8	-41.8	R	0.54		
OL55.2	-20.08	30	12	T	205.7	-38.0	R	0.17		
OL56.1	-19.92	35	15	T	348.7	-8.0	?	1.03		
OL56.2	-19.92	35	25	T	337.2	-62.9	R	0.75		
OL57.1	-19.42	35	20	T	193.5	-41.6	R	0.13		
OL57.2	-19.42	30	18	T	67.9	-66.8	R	0.15		
OL58.1	-18.78	30	10	T	325.5	-8.8	?	0.05		
OL59.1	-17.78	20	12	T	168.5	-55.3	R	0.08	.95	46
OL60.1	-17.00	20	10	T	187.7	-62.4	R	0.04		
OL30.1	-9.55	30	10	T	199.4	-37.6	R	0.08		
OL30.2	-9.55	30	8	T	107.3	-40.5	R	0.09	.95	51
OL31.1	-9.05	35	5	E	45.3	-4.9	?	1.05		
OL31.2	-9.05	30	8	T	155.4	-43.0	R	0.09		
OL32.1	-8.20	30	15	T	158.9	-43.0	R	0.11		
OL32.2	-8.20	30	8	T	142.2	-16.6	R	0.12		
OL33.2	-7.15	20	8	E	285.6	18.7	?	0.05		
OL34.1	-6.20	35	5	E	83.9	12.6	?	0.12	.95	49
OL34.2	-6.20	20	10	T	160.7	-52.6	R	0.10		
OL35.1	-5.45	35	10	T	263.7	-56.7	R	0.13		
OL35.2	-5.45	20	5	T	65.4	-63.0	R	0.12		
OL36.1	-4.75	35	10	T	99.4	-38.7	R	0.11		
OL37.1	-4.20	35	5	E	53.3	-21.8	?	0.13		
OL37.2	-4.20	30	10	R	165.6	-31.4	R	0.08		
OL38.1	-3.00	30	8	T	178.6	-23.1	R	0.09		
OL38.2	-3.00	35	10	T	183.1	-18.8	R	0.10		
OL39.1	-2.10	35	10	T	65.3	-55.8	R	0.90	.94	719
OL40.1	-1.10	30	20	T	66.4	-74.6	R	1.63		
OL40.2	-1.10	40	20	E	16.1	-37.3	?	13.21	.97	4628
OL41.1	-0.40	40	18	T	45.4	-29.2	R	8.37		
OL41.2	-0.40	40	15	T	317.9	-47.0	R	1.35		
OL42.1	0.85	50	25	T	9.5	-62.7	R	27.70		
OL42.2	0.85	40	15	T	345.1	-72.7	R	35.11		
OL43.1	1.60	50	17	T	54.3	-65.5	R	59.12		
OL43.2	1.60	40	16	T	13.0	-42.4	R	69.15		
OL44.1	2.20	40	15	E	17.0	-32.2	?	115.90		
OL44.2	2.20	40	12	T	111.4	-61.0	R	110.00		
OL45.1	3.75	40	20	T	61.0	-54.4	R	169.80		
OL45.2	3.75	40	18	T	63.5	-57.2	R	164.90		
OL46.1	4.45	40	25	T	98.2	-62.7	R	127.30		
OL46.2	4.45	40	22	T	68.0	-54.4	R	186.80		
OL47.1	5.20	40	17	T	103.0	-81.8	R	216.30		
OL47.2	5.20	40	15	T	57.9	-71.0	R	280.70	.99	90247
OL48.1	6.20	40	15	T	89.6	-72.2	R	204.20		
OL48.2	6.20	50	17	T	216.0	-58.4	R	311.20		
OL49.1	7.70	40	18	T	275.4	-37.6	R	108.00		
OL49.2	7.70	50	17	T	278.0	-35.6	R	64.74		
OL50.1	8.55	50	20	T	334.1	-65.4	R	32.20		
OL50.2	8.55	50	15	T	169.2	-67.7	R	43.90		

Junctions: Holmehus Fm./Haslund Mbr. (Olst Fm.)= -20.0m; Haslund/Vaerum Member= 0.0m. Top of the Olst Formation is at 9.1m.

OLST (Rosnaes Clay and Lillebaelt Clay Formations)
These formations at Olst acquired a CRM sometime after the folding episode which tilted the beds to near vertical. The bedding correction is Strike= 278.7°, Dip= 82.5°.

Spec. No.	ht. (m)	NRM	F (mT)	MDF (mT)	RI	Before Dec	Before Inc	After Dec	After Inc
OL1.2	0.04	17.52	40	10	S	10.0	60.6	10.0	-21.9
OL3.2	0.25	32.80	40	15	S	3.2	72.3	7.0	-10.1
OL4.1	0.33	42.50	40	19	S	13.8	54.0	12.1	-28.4
OL5.2	0.43	85.70	50	10	S	12.8	63.8	10.6	-18.6
OL6.1	0.59	163.90	40	17	S	267.8	76.7	355.4	9.8
OL7.2	0.75	166.30	50	15	S	236.0	78.2	359.7	15.4
OL9.1	0.93	67.40	40	15	T	4.8	-22.5	202.4	-74.5
OL10.1	0.99	61.10	40	15	S	1.0	-19.1	352.9	-62.3
OL11.2	1.04	56.30	40	15	T	337.4	-58.8	207.5	-33.4
OL12.1	1.10	68.50	40	9	S	225.9	63.1	350.6	28.3
OL13.1	1.19	15.54	50	12	T	216.8	43.7	339.2	46.3
OL14.1	1.34	15.49	25	12	T	310.3	62.8	345.6	-7.0
OL15.2	1.49	64.90	40	12	S	2.8	73.3	7.0	-9.1
OL17.2	1.80	53.50	40	12	S	26.9	83.9	10.6	1.7
OL18.1	1.95	30.00	40	12	S	351.7	60.1	359.7	-21.1
OL20.1	2.22	58.80	40	10	S	280.3	84.2	2.9	7.3
OL23.1	2.61	56.80	40	15	S	311.2	87.4	6.5	6.1
OL24.1	2.82	58.10	40	14	S	5.3	78.1	8.0	-4.4
OL27.1	3.15	1.31	30	5	S	356.5	73.9	5.3	-8.2
OL27.2	3.15	20.74	40	20	S	336.4	64.2	354.8	-14.3
OL28.1	3.25	12.40	40	8	S	12.7	49.3	11.8	-33.1
OL29.1	3.47	38.90	40	9	T	321.5	65.7	350.9	-9.1

Junctions: base Rosnaes Clay Formation at 0.0m; base Lillebaelt Clay Formation at 3.25m.

Stolle Klint, Fur (Knudeklint Mbr. of the Fur Fm.)
The results from this unit at Fur were too poor (due to the specimen's weak magnetisation) to construct a polarity log. The results from this section are listed below for completeness.

Spec. No.	ht. (m)	F (mT)	MDF (mT)	RI	DEC	INC	pol.	NRM
FU34.1	-3.0	35	15	T	15.9	58.0	N	2.74
FU35.1	-4.0	30	8	E	309.0	-7.9	?	0.07
FU36.1	-5.0	30	7	E	141.0	27.8	?	0.10
FU21.1	-12.6	35	8	E	262.1	57.2	?	0.10
FU20.1	-13.2	20	7	E	234.9	-29.0	?	0.05
FU22.1	-13.7	10	8	E	334.1	51.3	?	0.01
FU23.1	-14.3	20	8	E	323.4	29.8	?	0.05
FU24.1	-15.0	10	7	E	99.8	48.3	?	0.05
FU25.1	-15.9	10	NR	E	266.9	52.9	?	0.04
FU26.1	-15.7	0	NR	E	286.5	32.7	?	0.03
FU27.1	-16.1	0	NR	E	294.9	36.7	?	0.02
FU28.1	-16.8	20	8	T	308.2	49.2	?	0.10
FU29.1	-16.8	0	NR	E	340.2	74.5	?	0.08
FU30.1	-17.4	0	NR	E	338.1	61.1	?	0.08

Datum: Ash layer -17 in the Knudeklint Member.

Knuden, Fur (Knudshoved Mbr of the Rosnaes Clay Fm.)
This unit at Knuden acquired a CRM sometime after the folding episode which tilted the beds to vertical. The bedding correction is Strike= 129°, Dip= 90°.

Spec. No.	ht. (m)	NRM	F (mT)	MDF (mT)	RI	Before Dec	Before Inc	After Dec	After Inc
FU1.1	0.02	0.84	40	33	S	311.4	65.4	243.6	1.0
FU2.1	0.20	0.62	30	12	S	309.0	71.0	244.4	0.2
FU4.1	0.55	1.58	30	8	T	277.0	88.1	220.6	-1.0
FU5.2	0.62	1.65	30	5	S	353.9	62.4	239.3	19.1
FU7.1	0.94	1.88	30	5	S	106.9	71.1	201.4	7.0
FU8.1	1.12	1.43	30	17	S	355.9	71.7	232.6	13.0
FU10.1	1.44	1.15	15	3	T	73.0	69.8	207.4	16.6
FU11.2	1.61	2.34	30	3	S	347.4	70.6	234.4	11.9
FU13.1	2.16	0.94	30	12	T	203.5	77.1	215.5	-12.4
FU14.1	2.45	1.44	30	12	S	308.3	76.2	238.5	-0.1
FU15.1	2.68	2.35	30	12	S	329.6	63.9	243.6	8.9

Datum: Base of Knudshoved Member at 0.0m.

SILSTRUP (upper part of the Silstrup Mbr. of the Fur Fm.)

Spec. No.	ht. (m)	F (mT)	MDF (mT)	RI	DEC	INC	pol.	NRM
SL1.1	-0.05	30	5	T	228.0	-22.0	R	4.30
SL2.1	0.25	30	5	T	267.4	-21.7	R	4.32
SL2.2	0.25	30	5	T	187.0	-43.0	R	1.14
SL3.1	0.87	40	12	T	323.6	58.1	N	4.00
SL3.2	0.87	30	10	T	256.8	-4.8	R	0.41
SL4.1	1.05	35	18	T	241.7	15.9	R	0.11
SL4.2	1.05	35	20	T	258.8	79.9	?	0.26
SL5.1	1.50	40	20	T	271.8	17.3	R	1.22
SL5.2	1.50	35	13	T	240.0	35.1	R	0.84
SL6.1	3.00	35	10	T	332.2	67.8	N	0.38
SL6.2	3.00	30	10	T	281.3	59.4	?	0.59
SL7.1	4.44	35	10	T	254.6	34.2	R	2.65
SL7.2	4.44	35	10	T	255.9	25.7	R	1.57
SL8.1	5.25	30	10	T	187.4	-3.5	R	0.06
SL8.2	5.25	30	4	E	284.6	-12.1	R	0.28
SL9.1	6.28	30	8	E	6.2	-18.8	?	0.11
SL9.2	6.28	30	8	T	263.0	-43.5	R	0.11
SL10.1	7.00	30	NR	T	197.8	-40.4	R	0.08
SL10.2	7.00	35	10	T	227.9	-43.1	R	0.19
SL11.1	7.85	30	8	T	168.2	-25.5	R	0.08
SL11.2	7.85	35	12	T	208.6	-45.4	R	0.42

Datum: top of Ash +115.

Aalbaekhoved

Spec. No.	ht. (m)	F (mT)	MDF (mT)	RI	DEC	INC	pol.	NRM
AK80.1	0.05	35	5	T	238.0	12.9	R	436.5
AK81.1	0.35	35	3	T	333.9	12.7	N	276.5
AK82.1	0.65	35	3	T	111.8	-24.7	R	105.7
AK1.1	0.80	35	3	T	281.6	-13.4	?	154.9
AK2.1	1.15	35	2	T	246.5	-4.7	R	100.6
AK3.1	1.35	30	5	T	250.6	-13.3	R	151.8
AK4.1	1.60	35	5	T	212.8	-17.0	R	186.8
AK5.1	1.80	35	3	T	275.8	0.7	R	138.2
AK6.1	2.05	35	3	T	167.4	-13.2	R	66.6
AK7.1	2.25	35	3	T	132.6	21.0	R	94.4
AK8.1	2.40	35	3	T	266.8	-10.5	R	79.3
AK9.1	2.60	35	12	T	278.8	34.0	R	42.9
AK10.1	2.80	35	3	T	194.5	-41.7	R	132.6

Spec. No.	ht. (m)	F (mT)	MDF (mT)	RI	DEC	INC	pol.	NRM
AK11.1	3.00	35	3	T	157.9	-31.4	R	226.3
AK12.1	3.30	35	3	T	324.2	59.2	N	40.3
AK13.1	3.50	35	3	T	226.3	6.0	R	90.5
AK14.1	3.75	35	3	T	220.7	14.1	R	154.2
AK15.1	3.95	35	3	T	210.4	7.3	R	133.8
AK16.1	4.20	35	3	T	194.5	-8.0	R	139.6
AK17.1	4.45	35	4	T	196.4	-9.2	R	125.7
AK18.1	4.75	35	3	T	196.8	16.0	R	63.4
AK19.1	5.00	35	4	T	151.2	-3.2	R	48.7
AK20.1	5.00	35	3	T	248.9	-8.2	R	52.3
AK21.1	5.30	35	5	T	240.7	-6.8	R	158.5
AK22.1	5.55	35	3	T	189.4	-10.1	R	88.5
AK23.1	5.80	35	3	T	85.0	17.1	?	125.4
AK24.1	6.05	35	2	T	123.4	19.5	?	293.8
AK25.1	6.35	35	2	T	357.0	7.8	?	186.6
AK26.1	6.70	35	3	E	217.6	38.1	?	173.2
AK26.2	6.70	35	3	T	251.1	-10.0	R	137.9
AK26B	7.05	35	3	S	235.9	-20.7	R	142.2
AK26C	7.25	35	4	S	233.9	-23.7	R	179.3
AK27.1	7.45	35	3	S	223.2	-11.0	R	104.9
AK28.1	7.70	35	5	T	353.1	20.9	N	144.5
AK29.1	8.00	35	3	T	103.4	19.9	R	117.7
AK30.1	8.20	35	3	T	285.0	-6.0	R	201.2
AK31.1	8.45	35	3	T	121.6	7.4	R	138.9
AK32.1	8.70	35	3	T	73.3	44.1	?	90.4
AK33.1	8.95	35	3	T	234.8	0.2	R	125.4
AK34.1	9.20	35	3	T	253.8	3.0	R	157.6
AK35.1	9.45	35	3	T	248.3	-7.1	R	152.7
AK36.1	9.65	35	3	E	294.3	78.5	?	144.5
AK37.1	9.85	35	3	E	249.5	74.3	?	71.2
AK38.1	10.05	35	3	T	259.2	-71.6	?	144.1
AK39.1	10.20	35	3	T	183.0	-8.6	R	91.3
AK40.1	10.40	35	7	T	221.1	23.4	R	93.1
AK42.1	11.00	35	6	T	269.3	3.9	R	50.3
AK43.1	11.20	35	10	T	219.4	73.6	R	57.5
AK44.1	11.40	35	3	T	282.3	17.8	R	78.1
AK45.1	11.65	35	2	T	183.6	-2.1	R	1.2
AK46.1	11.85	35	4	T	345.5	46.5	N	64.5
AK47.1	12.05	35	7	T	158.4	-7.3	R	60.8
AK48.1	12.25	35	11	T	350.5	45.7	N	41.9
AK49.1	12.45	35	5	T	68.6	43.1	R	78.7
AK49.2	12.45	35	10	T	166.7	18.3	R	43.9
AK50.1	12.65	35	7	T	111.8	-24.7	R	17.0
AK51.1	12.85	35	4	T	299.8	11.1	R	100.5
AK52.1	13.15	35	3	T	357.1	49.6	N	11.3
AK53.1	13.40	35	4	T	306.7	-0.7	?	87.0
AK54.1	13.60	35	3	T	346.4	24.0	N	214.1
AK55.1	13.85	35	12	T	22.4	44.8	N	74.4
AK56.1	14.15	35	18	T	22.6	45.2	N	35.2
AK57.1	14.40	35	25	T	23.3	21.7	N	41.6
AK58.1	14.70	35	9	S	2.2	34.5	N	70.4
AK59.1	14.80	35	10	T	323.5	37.6	N	7.7
AK60.1	14.90	35	4	T	148.7	23.6	R	57.4
AK61.1	15.00	35	25	S	36.2	39.2	N	36.5
AK62.1	15.10	35	3	T	5.7	67.9	N	132.2
AK63.1	15.20	35	3	S	15.8	31.9	N	124.8
AK64.1	15.30	35	5	T	113.6	4.0	R	185.0
AK65.1	15.40	35	5	T	99.9	43.8	?	136.6
AK66.1	15.70	35	5	T	235.2	11.2	R	119.7
AK67.1	15.95	35	5	T	28.5	27.4	N	74.6
AK68.1	16.35	35	3	T	10.7	45.2	N	213.7
AK70.1	16.75	35	3	T	136.1	-41.9	R	157.9
AK71.1	16.95	35	6	T	103.9	-5.9	R	73.4

Spec. No.	ht. (m)	F (mT)	MDF (mT)	RI	DEC	INC	pol.	NRM
AK72.1	17.15	35	3	T	99.3	13.8	R	85.1
AK73.1	17.35	35	10	T	138.9	-7.0	R	164.8
AK74.1	17.70	35	3	E	72.9	25.9	?	320.4
AK77.1	17.80	35	3	T	158.2	60.8	R	109.0
AK75.1	18.00	35	5	T	353.7	63.5	N	166.8
AK76.1	18.30	35	3	T	131.2	-9.7	R	105.5
AK78.1	18.50	35	3	T	223.7	11.7	R	94.0
AK79.1	18.90	35	3	T	230.7	54.8	R	100.4

The position of Sites AK1 to AK79 can be directly related to the Rosnaes Clay Fm. log presented by Heilmann-Clausen et al (1985: Fig 12). Sites AK80 to AK82 are from the base of the same formation (resting directly on top of the Olst Fm.), which has not, as yet, been documented.

BIBLIOGRAPHY

ANDERSEN, S.A. 1937. De vulkanske Askelag i Vejgennemskaeringen ved Olst og deres Udbredelse i Danmark. Danm. Geol. Unders. 59(3). 50pp.

AS, J.A. 1960. Instruments and measuring methods in palaeomagnetic research. Med. Verh. Kon. Ned. Metereol. Instit. No.78, 56pp.

AS, J.A. and ZIJDERVELD, J.D.A. 1958. Magnetic cleaning of rocks in palaeomagnetic research. Geophys. J. R. Astr. Soc. 1:308-19.

AUBRY, M.-P. 1983. Biostratigraphie du Palaeogene epicontinental de l'Europe du Nord-ouest. Etude fondee sur les nannofossiles calcaires. Documents des laboratories de geologie de Lyon. 89.

AUBRY, M.-P. 1986. Palaeogene calcareous nannoplankton biostratigraphy of northwestern Europe. Palaeogeogr. Palaeoclim. Palaeoecol. 55:267-334.

AUBRY, M.-P., HAILWOOD, E. A. and TOWNSEND, H.A. 1986. Magnetic and calcareous-nannofossil stratigraphy of the lower Palaeogene formations of the Hampshire and London Basins. J. Geol. Soc. Lond. 143:729-35.

BARTON, C.E. and McELHINNY, M.W. 1979. Detrital remanent magnetisation in five slowly redeposited long cores of sediment. Geophys. Res. Letters. 6:229-32.

BERGGREN, W.A. 1969. Cenozoic chronostratigraphy, planktonic foramaniferal zonation and the radiometric timescale. Nature. 224:1072-75.

BERGGREN, W.A., KENT, D.V and FLYNN, J.J. 1985. Palaeogene geochronology and chronostratigraphy. In: SNELLING, N.J. (ed.). Geochronology of the geological record. Mem. Geol. Goc. Lond. No.10:141-95.

BIGNOT, G. 1980. Sparnacian. In: CAVALIER, C. and ROGER, J. (eds.). Les etages Francais et leurs stratotypes. Mem. Bur. Rech. Geol. Min. No.109:198-203.

BIGNOT, G. 1981. Cuisian. In: POMEROL, C (ed.). Stratotypes of Paleogene stages. Bull. Inf. Geol. Bass. Paris Mem. h.s. 2:63-75.

BLONDEAU, A., GRUAS-CAVAGNETTO, C., LE CALVEZ, Y. and LEZAUD, L. 1976. Etude palaeontologique du sondage de Cuise (Oise). Bull. Inf. Geol. Bass. Paris. 13(2):3-31.

BLOW, W.H. 1969. Late Middle Eocene to Recent foraminiferal biostratigraphy. In: BRONNIMAN, P. and RENZ, H.H. (eds.). Proc. first intrn. conf. planktonic microfossils. Geneva. 1967. E.J. BRILL. Leiden. 199-422.

BOLLI, H.M. 1957a. The genera Globigerina and Globorotalia in the Palaeocene-Lower Eocene Lizzard Springs Formation of Trinidad, B.W.I. Bull. U.S. Nat. Mus. 215:61-81.

BOLLI, H.M. 1957b. Planktonic foraminifera from the Oligocene-Miocene Cipero and Lengua Formations of Trinidad, B.W.I. Bull. U.S. Nat. Mus. 215:97-123.

BOLLI, H.M. 1957c. Planktonic foraminifera from the Eocene Navet and San Fernando Formations of Trinidad, B.W.I. Bull. U.S. Nat. Mus. 215:155-72.

BOLLI, H.M. 1966. Zonation of Cretaceous to Pliocene marine sediments based on planktonic foraminifera. Boln. inf. assoc. Venez. Geol. Min. Petrol. 9:3-32.

BONDE, N. 1979. Palaeoenvironment in the "North Sea" as indicated by the fish bearing Mo-clay deposit (Palaeocene/Eocene), Denmark. Meded. Werkgr. Tert. Kwart. Geol. 16(1):3-16.

BOGGILD, O.B. 1918. Den vulkanske Aske i Moleret samt en Oversight over Danmarks aeldre Tertiaerjaegarter. Danm. Geol. Unders. 33(2). 159pp.

BROCK, A. 1971. An experimental study of palaeosecular variation. Geophys. J. R. Astr. Soc. 24:303-17.

BROCK, A. and ILES, W. 1974. Some observations of rotational remanence magnetisation. Geophys. J. R. Astr. Soc. 38:431-3.

BUJAK, J.P. DOWNIE, C., EATON, G.L. and WILLIAMS, G.L. 1980. Dinoflagellate cysts and acritarchs from the Eocene of southern England. Spec. papers on palaeontology. No.24.

BUKRY, D. 1973. Low-latitude coccolith biostratigraphic zonation. In: EDGAR, SAUNDERS et al Init. Rep. D.S.D.P. 15(16):685-703.

BYBELL, L.M. and GIBSON, T.G. 1985. The Eocene Tallahata Formation of Alabama and Georgia: Its lithostratigraphy, biostratigraphy, and bearing on the age of the Claibonian Stage. US Geol. Surv. Bull. 1615:1-20.

CARO, Y. 1973. Contribution a la connaisssance des dinoflagellates du Paleocene-Eocene des Pyrenees Espagnoles. Rev. Espan. Micropal. 5:329-72.

CARO, Y., LUTERBACHER, H., PERCH-NIELSEN, K., PREMOLI-SILVA, I., RIEDEL, W.R., and SANFILIPPO, A. 1975. Zonations a l'aide de microfossiles du Palaeocene superieur et de l'Eocene inferieur. Bull. Soc. Geol. Fr. 17(7):125-47.

CHATEAUNEUF, J.J. and GRUAS-CAVAGNETTO, C. 1978. Les zones de Wetzeliellaceae (Dinophyceae) du Bassin de Paris. Comparison et correlations avec les zones du Paleogene des bassins du Nord-Ouest de l'Europe. Bull. Bur. Rech. Geol. Min. Ser 2, sect. IV, No.2:59-93.

COLLINSON, D.W. 1965. The remanent magnetism and magnetic properties of red sediments. Geophys. J. R. Astr. Soc. 10:105-26.

COLLINSON, D.W. 1967. The variation of magnetic properties among red sediments. Geophys. J. R. Astr. Soc. 12:197-207.

COLLINSON, D.W. 1983. Methods in palaeomagnetism and rock magnetism. Chapman and Hall, London. 503pp.

COSTA, L.I., DENISON, C and DOWNIE, C. 1978. The Palaeocene/Eocene boundary in the Anglo-Paris Basin. J. Geol. Soc. Lond. 135:261-4.

COSTA, L.I. and DOWNIE, C. 1976. The distribution of the dinoflagellate Wetzeliella in the Palaeogene of north-western Europe. Palaeontology 19:591-614.

COSTA, L.I. and MULLER, C. 1978. Correlation of Cenozoic dinoflagellate zones from the NE Atlantic and NW Europe. Newsl. Stratigr. 7:65-72.

COX, A. 1970. Latitude dependence of the angular dispersion of the geomagnetic field. Geophys. J. R. Astr. Soc. 20:253-69.

COX, A.V., DOEL, R.R. and DALRYMPLE, G.B. 1965. Quaternary palaeomagnetic stratigraphy. In: The Quaternary of the United States, a second volume. Princeton University Press, Princeton, NJ, USA.

COX, F.C., HAILWOOD, E.A., HARLAND, R. HUGHES, M.J. JOHNSTON, N. and KNOX, R.W.O'B. 1985. Palaeocene sedimentation and stratigraphy in Norfolk, England. Newsl. Stratigr. 14(3):169-85.

CURRY, D. 1965. The Palaeogene Beds of SE England. Proc. Geol. Assoc. 77:437-467.

CURRY, D. 1981. Thanetian. In: Pomerol, C. (ed.) Stratotypes of Palaeogene Stages. Bull. Inf. Geol. Bass. Paris. Mem. h.s. 2:255-65.

CURRY, D., ADAMS, C.G., BOULTER, M.M., DILLEY, F.C., EAMES, F.E., FUNNEL, B.M and WELLS, M.K. 1978. A correlation of Tertiary rocks in the British Isles. Special report of the Geol. Soc. Lond. No.12. 72pp.

DAVIS, A.G. 1936. The London Clay of Sheppey and the location of its fossils. Proc. Geol. Assoc. 47:328-45.

DESTOUMBES, P., GAMBLE, H.H, JUIGNET, P. and OWEN, H.G. 1977. Cretatceous and lower Tertiary of Seine-Maritime, France: a guide to key localities. Proc. Geol. Assoc. 83:471-8.

DOLFUSS, G.F. 1880. Essai sur l'extension des terrains Tertiaries dans le Bassin Anglo-Parisien. Bull. Soc. Geol. Normandie. t. 6(1879):585-605.

DUMONT, A. 1849. Rapport ssur la carte geologique de la Belgique. Bull. Acad. Roy. Sci Letter. B-A. Belg. 16(2):351-73.

EDWARDS, R.A. and FRESHNEY, E.C. 1987. Lithostratigraphical classification of the Hampshire Basin Palaeogene deposits (Reading Formation to Headon Formation). Tertairy Res. 8(2):43-73.

FEUGEUR, L. 1963. L'Ypresien du Bassin de Paris. Mem. Serv. Carte geol. det. Fr. Paris.

FISHER, O. 1862. On the Bracklesham Beds of the Isle of Wight Basin. Q. J. Geol. Soc. Lond. 18:65-94.

FISHER, R.A. 1953. Dispersion on a sphere. Proc. Roy. Soc. Lond. A217:295-305.

FORCHAMMER, G. 1835. Danmarks geognostiske forhold, forsaavidt som de ere afhaengige af Dannelser de ere sluttede. 112pp. Copenhagen.

GIBSON, T.G., MANCINI, E.A. and BYBELL, L.M. (1982). Paleocene to Middle Eocene stratigraphy of Alabama. Trans. Gulf Coast Assoc. Geol. Soc. 32:449-58.

GEORGE, T.N. and twelve others. 1968. International Geological Programme: United Kingdom contribution. Roy. Soc. Lond. 43pp.

GEORGE, W. and VINCENT, S. 1976. Some river exposures of London Clay in Suffolk and Essex. Tertiary Res. 1:25-8.

GEORGE, W. and VINCENT, S. 1977. Report of field meeting to Walton-on-the-Naze and Wrabness, Essex 2.X.1976 with notes on the London Clay of Walton. Tertiary Res. 1:83-90.

GOSSELT, M.J. 1874. L'etage eocene inferieur dans le Nord de la France et en Belgique. Bull. Soc. Geol. France 3(2):598-616.

HAILWOOD, E.A. 1977. Configuration of the geomagnetic field in early Tertiary times. J. Geol. Soc. Lond. 133:23-36.

HAILWOOD, E.A. (in press). The role of magnetostratigraphy in the development of geological time-scales. Palaeoceanography.

HAQ, B.U., HAREDENBOL, J. and VAIL, P.R. 1987. Chronology of fluctuating sea levels since the Triassic. Science. 235:1156-67.

HARDENBOL, J. and BERGGREN, W.A. 1978. A new Paleogene numerical time-scale. Am. Assoc. Petrol. Geol. Bull. 6:213-34.

HEDBERG, H.D. 1976. International stratigraphic guide: a guide to stratigraphic classification, terminology and procedure. Wiley, New York. 200pp.

HEILMANN-CLAUSEN, C. 1982. The Palaeocene-Eocene boundary in Denmark. Newsl. Stratigr. 11(2):55-63.

HEILMANN-CLAUSEN, C., NIELSEN, O.B. and GERSNER, F. 1985. Lithostratigraphy and depositional environments in the Upper Palaeocene and Eocene of Denmark. Bull. Geol. Soc. Denmark 33:287-323.

HEIRTZLER, J.R., DICKSON, G.O., HERON, E.M., PITMAN, W.C.,III., and LE PICHON, X. 1968. Marine magnetic anomalies, geomagnetic field reversals and motions of the ocean-floor and continents. J. Geophys. Res. 73:2119-36.

HOTTINGER, L. and SCHAUB, H. 1960. Zur stufeneinteilung des Palaeocaens und des Eocaens. Einfuhrung der stufen Illerdian und Biarritzien. Eclog. geol. Helv. 53:453-80.

HUDDLESTUN, P.F., MARSALIS, W.E. and PICKERING, S.M. Jr. 1982. Tertiary stratigraphy of the central Georgia Coastal Plain. Geol. Soc. Am. southeast section, Georgia Geol. Soc. Guidebook. 12:2.1-2.13.

IRVING, E. and MAJOR, A. 1964. Post-depositional detrital remanent magnetisation in a synthetic sediment. Sedimentology 3:135-43.

ISLAM, M.A. 1983a. Dinoflagellate cyst taxonomy and biostratigraphy of the Eocene Bracklesham Group in southern England. Micropalaeontology. 29:328-53.

ISLAM, M.A. 1983b. Dinoflagellate cysts from the Eocene cliff sections of the Isle of Sheppey, southeast England. Revue Micropalaeontology. 25:231-50.

JOHNSTON, N. 1983. Magnetostratigraphic study of Palaeogene sediments from SE England. Unpubl. MSc dissertation. University of Southampton.

KAPPELOS, C. and SCHAUB, H. 1973. Zur korrelation von biozonnierung mit grossforaminiferen und nannoplankton im Palaeogen der Pyrenaen. Eclog. geol. Helv. 66:687-727.

KAPPELOS, C. and SCHAUB, H. 1975. L'Illerdian dans les Alpes, dans le Pyrenees et en Crimee. Correlation de zones a grands foraminiferes et a nannoplankton. Bull. Soc. Geol. Fr. 17(7):148-61.

KING, C. 1981. The stratigraphy of the London Clay and associated deposits. Tertiary Res. Spec. Paper No.6. 158pp.

KING, C. 1983. Cenozoic micropalaeontological biostratigraphy of the North Sea. Rep. Inst. Geol. Sci. No. 82/7.

KING, C. 1984. The stratigraphy of the London Clay Formation and Virginia Water Formation in the coastal sections of the Isle of Sheppey (Kent, England). Tertiary Res. 5(3):121-60.

KING, R.F. 1955. The remanent magnetisation of some artificially deposited sediments. Mon. Not. Roy. Astr. Soc. Geophys. supplement. 7:15-34.

KNOX, R.W.O'B. 1983. Volcanic ash in the Oldhaven Beds of SE England, and its stratigraphical significance. Proc. Geol. Assoc. 94:245-50.

KNOX. R.W.O'B., HARLAND, R. and KING. C. 1983. Dinoflagellate cyst analysis of the basal London Clay of southern England. Newsl. Stratigr. 12(2):71-4.

KNOX, R.W.O'B. and MORTON, A.C. (1988). The record of early Tertiary volcanism of sediments in the North Sea Basin: In: MORTON, A.C. and PARSONS, L.M. (eds.) Early Tertiary volcanism and the opening of the NE Atlantic. Geol. Soc. Lond. Spec. Pub. No. 39:407-19.

KNOX, R.WO'B., MORTON, A.C. and HARLAND, R. 1981. Stratigraphical relationships of Palaeocene sands in the UK Sector of the Central North Sea. In: Illing, L.V. and HOBSON, G.D. (eds.). Petroleum geology of the continental shelf of North-West Europe. Inst. Petrol. London:267-81.

La BREQUE, J.L., KENT, D.V. and CANDE, S.C. 1977. Revised magnetic polarity time-scale for Late Cretaceous and Cenozoic time. Geology 5:330-5.

LOEBLICH, A.R.Jr. and TAPPAN, H. 1957. Planktonic foraminifers of the Paleocene and Early Eocene age from the Gulf and Atlantic Coastal Plains. US Nat. Mus. Bull. 215:173-98.

LOVLIE, R. 1974. Post-depositional remanent magnetisation in a redeposited deep-sea sediment. Earth Planet. Sci. Letters. 21:315-20.

LUTERBACHER, H.P. 1973. La section tipo del piso Illerdiense. In: Anon.(ed.) XIII coloquio Europeo de micropaleontologia: Espana 1973. Guide book:113-40.

LYELL, C. 1846a. On the new deposits of the southern states of North America. Q. J. Geol. Soc. Lond. 2:405-10.

LYELL, C. 1846b. On the Eocene of Alabama and Georgia. Am. Jour. Sci. ser. 2 1:313-5.

LYELL, C. 1849. A second visit to the United States of North America. 2:37-88. ? New York and London.

LYELL, C. 1852. On the Tertiary strata of Belgium and French Flanders. Q. J. Geol. Soc. Lond. 8:277-368.

MANCINI, E.A. and OLIVER, G.E. 1981. Planktonic foraminifers from the Tuscahoma Sand (upper Paleocene) of southwest Alabama. Micropalaeontology 27: 204-25.

MARTINI, E. 1971. Standard Tertiary and Quaternary calcareous nannoplankton zonation. In: Proceedings of the II Planktonik Conference, Roma, 1970. 2:739-85.

MARTINI, E. and MULLER, C. 1986. Current Tertiary and Quaternary nannoplankton stratigraphy and correlation. Newsl. Stratigr. 16(2):99-112.

MOLYNEUX, L. 1971. A complete result magnetometer for measuring the remanent magnetisation of rocks. Geophys. J. R. Astr. Soc. 24:429-33.

MORTON, A.C., BACKMAN, J. and HARLAND, R. 1983. A reassessment of the stratigraphy of DSDP Hole 117A, Rockall Plateau: implications for the Palaeocene-Eocene boundary in NW Europe. Newsl. Stratigr. 12(2):104-11.

NIELSEN, O.B., BAUMANN, J. DEYU, Z., HEILMANN-CLAUSEN, C. and LARSEN, G. 1986. Tertiary deposits in Store Baelt. In: Moller, J. T. Twentyfive years of geology in Aarhus. Geoskrifter No.24. Geol. Inst. Aarhus. Univ.

NINKOVITCH, D., OPDYKE, N.D., HEEZEN, B.C. FOSTER, J.H. 1966. Palaeomagnetic stratigraphy, rates of deposition and tephrachronology in North Pacific deep sea sediments. Earth Planet. Sci. Letters. 1:476-92.

NOEL, M. and MOLYNEUX, L. 1975. Rapid demagnetisation of palaeomagnetic samples using a rotating magnetic field. Geophys. J. R. Astr. Soc. 43:1017-21.

ODIN, G.S. and CURRY, D. 1985. The Palaeogene time-scale: radiometric-dating versus magnetostratigraphic approach. J. Geol. Soc. Lond. 142:1179-88.

ODIN, G.S. and CURRY, D. and HUNZIKER, J.C. 1978. Radiometric dates from NW European glauconites and the Palaeogene time-scale. J. Geol. Soc. Lond. 135:481-97.

ODUM, H. 1936. Marint Nedre Oligocaen i Danmark. Meddr. Dansk. Geol. Foren. 9(1):88-90.

OKADA, H. and BUKRY, D. 1980. Supplementary modification and introduction of code numbers to the low-latitude coccolith biostratigraphic zonation (Bukry, 1973; 1975). Marine micropal. 5:321-5.

d'OMALIUS d'HALLOY, J.J. 1862. Abrege de geologie, 7th ed. 626pp.

OPDYKE, N.D. and HENRY, K.W. 1969. A test of the dipole hypothesis. Earth Planet. Sci. Letters. 6:139-51.

O'REILLY, W. 1976. Magnetic minerals in the crust of the Earth. Rep. Prog. Phys. 39:857-908.

O'REILLY, W. 1984. Rock and Mineral magnetism. Blackie and Son, Glasgow. 319pp.

ORTLIEB, J. and CHELLONNEIX, E. 1870. Etude geologie des collines tertiares du department du Nord comparees avec celles de la Belgique. ? Lille, 228pp.

PEDERSEN, G.K. and SURLYK, F. 1983. The Fur Formation, a late Palaeocene ash-bearing diatomite from northern Denmark. Bull. Geol. Soc. Denmark. 32:43-65.

PLINT, A.G. 1983. Facies, environments and sedimentary cycles in the Middle Eocene Bracklesham Formation of the Hampshire Basin: evidence for global sea level changes? Sedimentology 30:625-53.

POMEROL, C. 1982. The Cenozoic Era. Ellis Horwood, Chichester, pp 272.

PRESTWICH, J. 1847. On the main points of structure and the probable age of the Bagshot Sands. Q. J. Geol. Soc. Lond. 3:378-409.

PRESTWICH, J. 1854a. On the structure of the strata between the London Clay and the Chalk.... Part ii. The Woolwich and Reading Series. Q. J. Geol. Soc. Lond. 10:75-170.

PRESTWICH, J. 1854b. On the thickness of the London Clay. Q. J. Geol. Soc. Lond. 10:401-19.

PRESTWICH, J. 1855. On the correlation of the Eocene Tertiaries of England, France and Belgium. Q. J. Geol. Soc. Lond. 11:206-46.

PRESTWICH, J. 1888. Further observations on the correlation of the Eocene strata in England, Belgium, and the north of France. Q. J. Geol. Soc. Lond. 44:88-111.

RAVN, J.P.J. 1928. The Tertiary. In: NORDMANN, V. (ed.) Summary of the Geology of Denmark. Danm. Geol. Unders. (5)4:64-77.

REES, A.I. 1961. The effect of water currents on the magnetic remanence and anisotropy of susceptibility of some sediments. Geophys. J. R. Astr. Soc. 5:235-51.

REES, A.I. 1966. The effect of depositional slopes on the anisotropy of magnetic susceptibility of laboratory deposited sands. J. Geol. 74:856-76.

RENEVIER, E. 1873-4. Tableau des terrains sedimentaires (in 4º) plus un texte explicatif. Rouge and Dubois, Lausanne. 34pp.

SHARMA, P.V. 1969. Early Tertiary field reversals recorded in volcanic ash layers of northern Denmark. Bull. Geol. Soc. Denmark. 19(2):218-23.

SHRUBSOLE, W.H. 1878. On the New Town Well at Sheerness. Proc. Geol. Assoc. 5:355-62.

SIESSER, W.G. 1983. Paleogene calcareous nannoplankton biostratigraphy: Mississippi, Alabama and Tennesse. Miss. Bur. Geol. Bull. 125.

SIESSER, W.G., WARD, D.J. and LORD, A.R. 1987. Calcareous nannoplankton biozonation of the Thanetian Stage (Palaeocene) in the type area. J. Micropalaeontol. 6:85-102.

SMITH, E.A., JOHNSON, L.C. and LANGDON, D.W.Jr. 1894. Report on the geology of the Coastal Plain of Alabama. Alabama Geol. Surv. Spec. Rep. No. 6. 759pp.

SOPER, N.J., HIGGINS, A.C., DOWNIE., MATTHEWS, D.W. and BROWN, P.E. 1976. Late Cretaceous-Early Tertiary stratigraphy of the Kangerdlugssuaq area, east Greenland, and the opening of the northeast Atlantic. J. Geol. Soc. Lond. 132:85-104.

STAINFORTH, R.M., LAMB, J.L., LUTERBACHER, H., BEARD, J.H. and JEFFORRDS, R.M. 1975. Cenozoic Planktonic Foraminiferal Zonation and characteristics of index forms. Univ. Kansas Pal. Contr. 62.

STAMP. L.D. 1921a. On cycles of sedimentatation in the Eocene strata of the Anglo-Franco-Belgian Basin. Geol. Mag. 58:108-14,146-57,194-200.

STAMP. L.D. 1921b. On the beds at the base of the Ypresian (London Clay) in the Anglo-Franco-Belgian Basin. Proc. Geol. Assoc. 32:57-108.

STEPHENSEN, A. 1980a. Gyromagnetism and the remanence acquired by rotating a rock in an alternating field. Nature. 284:48.

STEPHENSEN, A. 1980b. A gyroremanent magnetization in anisotropic magnetic material. Nature. 284:49.

STEPHENSON, R.W. 1976. A study of rotational remanent magnetization. Geophys. J. R. Astr. Soc. 47:363-73.

STEURBAUT, E. 1988. New Early and Middle Eocene calcareous nannoplankton events and correlation in middle to high latitudes of the Northern Hemisphere. Newsl. Stratigr. 18(2):99-115.

STEURBAUT, E. and NOLF, D. 1986. Revision of Ypresian stratigraphy of Belgium and northwestern France. Meded. Werkgr. Tert. Kwart. Geol. 23(4):115-72.

STRANGWAY, D.W., HONEA, R.M., McMAHON, B.E. and LARSON, E.E. 1968. The magnetic properties of naturally occuring goethite. Geophys. J. R. Astr. Soc. 15:345-59.

SUMMERHAYES, C.P. 1986. Sea level curves based on seismic stratigraphy: Their chronostratigraphic significance. Palaeogegr., Palaeoclim., Palaeoecol. 57:27-42.

SUTTIL, R. J. 1980. Post-depositional remanent magnetization in Recent tidal-flat sediments. Earth Planet. Sci. Letters. 49:132-40.

TARLING, D.H. 1971. Principles and applications of palaeomagnetism. Chapman and Hall, London. 164pp.

TARLING, D.H. 1983. Paleomagnetism. Chapman and Hall, London, 379pp.

TOULMIN, L.D. and La MOREAUX. 1963. Stratigraphy along the Chattahoochee River connecting link between the Atlantic and Gulf Coast Plains. Am Assoc. Petrol. Geol. Bull. 47:385-404.

TOWNSEND, H.A. 1982. Magnetostratigraphy of Early Palaeogene sediments from southern England. Unpubl. Ph.D. Thesis, University of Southampton.

TOWNSEND, H.A. and HAILWOOD, E.A. 1985. Magnetostratigraphic correlation of Palaeogene sediments in the Hampshire and London Basins, southern UK. J. Geol. Soc. Lond. 142:1-27.

VAIL, P.R. and HARDENBOL, J. 1979. Sea level changes during the Tertiary. Oceanus 22:71-9.

VINE, F.J. and MATTHEWS, D.H. 1963. Magnetic anomalies over ocean ridges. Nature 199:947-9.

VON HILLEBRANDT, A. 1965. Foraminiferen-stratigraphie im Alt-Tertiar von Zummaya (provinz Guipuzcoa, N.W. Spanien) und ein vergleich anderen Tethys-Gebieten. Abh. bayer. Akad. Wiss. math.-nat.Kl., N.F. 123.62pp.

VON HILLEBRANDT, A. 1975. Correlation entre les biozones de grands foraminiferes et de foraminiferes planctoniques de l'Illerdian. Bull. Soc. geol. Fr. 17:162-7.

WARD, D.J. 1972. Report of project meeting to Shelford sand-pit, near Canterbury, Kent. Tertiary Times 1:117-23.

WARD, D.J. 1977. The Thanet Beds exposure at Pegwell Bay, Kent. Tertiary Res. 1:69-76.

WARD, D.J. 1979. The lower London Tertiary (Palaeocene) succession of Herne Bay, Kent. Inst. Geol. Sci. Rep. No. 78/10.

WEBSTER, T. 1814. On the freshwater formations in the Isle of Wight, etc. Trans. geol. soc. Lond. 2:161-254.

WHITAKER, W. 1872. The geology of the London Basin: part 1. Mem. Geol. Surv. U.K.

WHITTAKER, W. 1889. The geology of London:2. Mem. Geol. Surv. U.K.

WILLEMS, W., BIGNOT, G. and MOORKENS, T. 1981. Ypresian. In: POMEROL, C. (ed.) Stratotypes of Palaeogene stages. Bull. Inf. Geol. Bass. Paris. Mem. h.s. 2:267-245.

WILSON, R.L. 1971. Dipole ofset- The time average palaeomagnetic field over the past 25 million years. Geophys. J. R. Astr. Soc. 22:491-504.

WILSON, R.L and ADE-HALL, J.M. 1970. Palaeomagnetic indications of a permanent aspect of the non-dipole field. In: RUNCORN, S.K. (ed.). Palaeogeophysics. Academic Press, London. 307-12.

WILSON, R.L. and LOMAX, R. 1972. Magnetic remanence related to slow rotation of ferromagnetic materials in alternating magnetic fields. Geophys. J. R. Astr. Soc. 30:295-303.

WILSON, R.L. and McELHINNY, M.W. 1974. Investigation of the large scale palaeomagnetic field over the past 25 million years. Eastward shift of the Icelandic Spreading Ridge. Geophys. J. R. Astr. Soc. 39:570-86.

WRIGLEY, A.G. and DAVIS, A.G. 1937. The occurence of Nummulites planulatus in England, with a revised correlation of the strata containing it. Proc. Geol. Assoc. 48:203-28.

ZIEGLER, P.A. 1981. Evolution of sedimentary basins in North-West Europe. In: Illing, L.V. and HOBSON, G.D. (eds.). Petroleum geology of the continental shelf of North-West Europe. Inst. Petrol. Lond. 3-39.

ZIEGLER, P.A. 1982. Geological atlas of western and central Europe. Shell Int. Petrol. Amsterdam.